Investigating the role of *Cryptococcus neoformans*-macrophage interactions on the outcome of cryptococcal infection

The University Of Sheffield.

Katherine Mary Pline

Department of Infection, Immunity & Cardiovascular Disease

School of Medicine, Dentistry & Health

A thesis submitted in partial fulfilment of the requirements for the degree of Doctor of Philosophy

November 2019

Abstract

Cryptococcus neoformans is a pathogenic yeast which causes cryptococcal meningitis in immunocompromised patients, causing heterogeneous infection outcomes in both HIV-positive and HIV-negative patients. Macrophages are known to be important for the control of cryptococcal infection, though *C. neoformans* may manipulate the macrophage intracellular niche to replicate and disseminate infection. Though the interactions between macrophages and cryptococci may determine the course and outcome of infection, few studies to date have examined how individual interactions between cryptococci and macrophages may be heterogeneous, and how these complex interactions contribute to variable infection outcomes *in vivo*. To address this, I used J774 murine macrophages and human monocyte derived macrophages (MDMs) to investigate the effect of fungal dose on macrophage-cryptococcal interactions, and found that increasing burden did not enhance or inhibit phagocytosis or fungal growth. Using a zebrafish model of cryptococcal infection I showed that infection outcome is linearly related to initial fungal burden at high doses, though this is variable and depends on factors besides initial burden. I also showed that *in vitro*, intracellular cryptococcal growth is slowed compared to extracellular growth, highlighting one potential mechanism by which macrophages control cryptococcal infection. Using the measured variability in these macrophage-cryptococcal interactions, I describe how I aided in the production of a computational simulation of cryptococcal infection, highlighting a role for variability in these individual host-pathogen interactions in producing complex infection outcomes *in vivo*. I showed that fungal lipid signalling molecules called prostaglandins are required for parasitism of host macrophages through the activation of host PPAR-γ. Finally, I demonstrated how human PBMCs can be used to model cryptococcal granuloma infection *in vitro*, measuring the formation of swarms and the intracellular and extracellular replication rates. Through considering all these interactions and sources of variability, I have provided insight into how *Cryptococcus* interactions with macrophages affect infection outcomes in cryptococcosis.

Acknowledgements

First of all, thank you to my supervisor Simon Johnston for all the guidance and the support, for being a good role model as well as boss and for understanding what I needed, for being a friend when I needed one. Thank you also to Phil Elks for always answering questions and taking the time to chat and cheer us on.

Thank you to Robbie for helping solve all my problems and showing me the best jumpers, and James for sharing both his brain and sense of humour. Thank you to Aleks for showing me how to begin as a scientist. To Cat for teaching me how to genotype and putting up with my annoying questions, and to everyone in D31 for the friendship and support. Thank you to Rhoda for teaching me to think differently.

Thank you to Hannah, for showing me how to have fun, and for answering all the questions I was too embarrassed to ask anyone else, for helping me laugh and letting me cry.

To Jack, for loving me always and making me feel special, for being my best friend, for giving me Wednesdays and loving me better. To Sara, for being a supportive friend always happy for a chat and a coffee, the kindest person I know. To Rob, one of the funniest people I have had the pleasure of knowing. Thank you, Becky, for the late-night messages, and thank you Dom and Farrah for making me feel like part of the group and for always fighting my corner.

Thank you to my family for missing me while I'm gone, but not asking me to stay. Especially thank you to my sister, who always understands, my mom who gave me love and confidence, and my dad who gives the strongest hugs. To Dan and Steve, thank you for being amazing brothers.

To Karen, thank you for making me feel like I have family when mine is so far away.

And most of all to Samuel – thank you for loving me.

List of abbreviations

15-d-PGJ2 15-Deoxy-Delta-12, 14-prostaglandin J2

AA arachidonic acid

Agr accessory gene regulator

AIDS acquired immune deficiency syndrome

ANOVA analysis of variance

App1 anti-phagocytic protein 1

BBB blood-brain barrier

bp base pair

Cas9 CRIPSR associated protein 9

CD cluster of differentiation

CD4 cluster of differentiation 4

CD8 cluster of differentiation 8

CFU colony forming units

CNS central nervous system

COX cyclooxygenase

CRISPR Clustered Regularly Interspaced Short Palindromic Repeats

CXCL chemokine

CXCR chemokine receptor

DAMP damage associated molecular pattern

DC dendritic cell

DIC differential interference contrast

DMEM Dulbecco's modified eagle's medium

DMSO dimethyl sulfoxide

DNA deoxyribonucleic acid

dpf days post fertilisation

dpi days post infection

E3 embryo medium

ELISA enzyme-linked immunosorbent assay

EP1, EP2, EP3, EP4 prostaglandin E2 receptor 1,2,3,4

FasL FAS receptor ligand

FBS fetal bovine serum

FITC fluorescein isothiocyanate

FSC forward scatter

G-CSF granulocyte-colony stimulating factor

GFP green fluorescent protein

GM-CSF granulocyte macrophage colony-stimulating factor

GPI glycosylphosphatidylinositol

GXM glucuronoxylomannan

GXMGal galactoxylomannan

h hours

H_2O_2 hydrogen peroxide

HIV human immunodeficiency virus

hpi hours post infection

IFN interferon

IFN-γ interferon gamma

Ig immunoglobulin

IL interleukin

IPR intracellular proliferation rate

L-dopa L-3, 4-dihydroxyphenylalanin

Lac laccase

LAMP-1 lysosomal-associated membrane protein 1

LPS lipopolysaccharide

LT leukotriene

mAb monoclonal antibody

MAPK mitogen activated protein kinase

MCP-1 macrophage chemotactic protein 1

MDM monocyte-derived macrophage

MHC-I major-histocompatibility complex class I molecule

MHC-II major-histocompatibility complex class II molecule

MOI multiplicity of infection

MR mannose receptor

mRNA messenger RNA

NADPH nicotinamide adenine dinucleotide phosphate

NF-KB nuclear factor-kappa light chain enhancer of activated B cells

NK natural killer

NLR NOD-like receptors

NO nitric oxide

ns not significant

NSAID non-steroidal anti-inflammatory drug

PAMP pathogen associated molecular pattern

PBMC peripheral blood mononuclear cell

PBS phosphate buffered saline

PCR polymerase chain reaction

PG prostaglandin

PGE_2 prostaglandin E_2

PI3K phosphatidylinositol 3-kinase

PLA_2 phospholipase A_2

Plb1 phospholipase B1

PPAR peroxisome proliferator-activated receptor

PRR pattern recognition receptor

ptges prostaglandin E synthase

RLR RIG-like receptor

RNAseq RNA-sequencing

ROI region of interest

ROS reactive oxygen species

RPMI Rosewell Park Memorial Institute

SD standard deviation

SF serum free

SSC side scatter

Tg transgenic

Th1 T helper cell type 1

Th2 T helper cell type 2

TLR toll-like receptor

TLT troglitazone

Trog troglitazone

TNF tumour necrosis factor

tyro tyrosinase

YPD yeast extract / peptone / dextrose media

Table of Contents

List of figures

Chapter 1. Introduction

The immune system is a complex network of interacting cells, proteins and small molecules that determine the delicate balance between health and illness. One critical component of the immune system involves protecting the body from pathogens, harmful microorganisms that cause disease. The interaction between the host's immune system and the pathogen determines whether the host prevails over disease, or whether it ultimately succumbs to infection. The interplay between host and pathogen, as well as the collaboration of innate and adaptive immune systems, is critical to health. In this chapter I will introduce how the immune system responds to infection, the pathology and virulence of the fungal pathogen *Cryptococcus neoformans*, and how this pathogen interacts with host macrophages to propagate infection.

1.1. The immune system

The human body represents a rich habitat full of nutrients and resources, perfect for colonisation by unwanted trespassers. In order to remain alive and healthy, our bodies deploy a number of defences to protect us from microscopic harm. The body's first line of defence is the epithelium, which acts as a barrier between the inside of the body and the outside world. The epithelial cells of the skin are interconnected by tight junctions, which utilise proteins and the actin cytoskeleton to join adjacent cells in a way that prevents transmission of certain particles while maintaining intercellular signalling. The integrity of these junctions is paramount in protecting the body from invasion, though pathogens have developed ways to breach this barrier (Guttman and Finlay, 2009).

The human body also possesses other anti-microbial defences to prevent invasion. For example the skin, as well as phagocytes and the various epithelia of the body, produces antimicrobial peptides which have potent antimicrobial effects against a wide range of bacteria, viruses, and fungi (Izadpanah and Gallo, 2005). The respiratory tract is protected from invasion by harmful particles and pathogens by

a viscous, carbohydrate-rich layer of mucus. Here, mucin traps inhaled particles and is swept away by the synchronised beating of cilia (Knowles and Boucher, 2002; Tilley et al., 2015). This system of mucociliary clearance prevents epithelial invasion, and 'cough clearance' facilitates the clearance of entrapped particles within the lung. Additional defensive solutions employed by the body include sweat, stomach acid, enzymes, and tears, which function to prevent the body from deposition of harmful particles and pathogens.

Should these inherent defences fail and the body's barrier is breached by invading pathogens, the immune system is tasked with the responsibility of protecting our bodies by preventing the initiation and propagation of infection. The innate immune system is composed of both circulating and tissue-resident cells and molecules which respond to pathogenic insult on contact in a non-specific way, destroying anything that is recognised as 'non-self'. The adaptive immune system, however, responds to infection through activation by specific pathogenic components, and produces a robust response by aiding the activation of the innate immune system while destroying the foreign particles. The collaboration of these systems protects us from the vast repertoire of encountered pathogens which may produce harmful infection.

1.1.1 The innate immune system response to infection

Innate immune cells perform various roles in order to provide the body with protection by providing immediate response to pathogens and specific stimulation of the adaptive immune system. Immediate, nonspecific responses include the release of toxic substances. For example, granulocytes contain and release granules with toxic enzymatic capabilities which destroy pathogens. Many immune cells produce reactive oxygen and nitrogen species which damage invading pathogens. Innate immune cells also interact with pathogens to destroy them. Phagocytic cells of the innate immune system provide methods of directly eliminating microbial threats through phagocytosis of pathogens and infected cells, as well as induction of programmed cell death cascades. Besides the direct killing of pathogens, innate

immune cells also present pathogenic antigens to members of the adaptive immune system to recruit them to sites of infection for activated assistance. The production of cytokines and chemokines by innate immune cells recruits additional cells to sites of infection and stimulates them to respond to infection.

1.1.1.1 Pathogen recognition by innate immune cells

Innate immune cells must discover and combat pathogenic insults as they breach the body's barriers. Epitopes on the surface of pathogens, termed pathogen-associated molecular patterns (PAMPs) are required for survival and pathogenicity, yet may be recognised by immune cells. Damage-associated molecular patterns (DAMPs) are produced by damaged and dying cells, either as a result of injury or pathogen-induced damage. Immune cells recognise these motifs using pattern recognition receptors (PRRs), which include membrane-bound classes of receptors such as RIG-I-like receptors (RLRs), NOD-like receptors (NLRs), C-type lectin receptors (CLRs) and Toll-like receptors (TLRs), though some TLRs are also expressed in endocytic compartments (Kumar et al., 2011).

TLRs are widely studied because they are present and largely homologous across many species, and are well-characterised in flies, mice, and humans (Brubaker et al., 2015). TLR1 and TLR2 recognise a variety of motifs from Gram-positive and Gram-negative bacteria such as lipoproteins and lipomannans, as well as β-glucans and zymosan, which are fungal components. TLR-4 (with MD-2 and CD14) recognises lipopolysaccharide and lipotechoic acid of bacteria, whereas TLR-5 binds flagellin on bacteria. TLR-3, -7, -8, and -9 recognise RNAs and DNAs associated with viral infections. RLRs recognise viral RNA, and NLRs are cytoplasmic receptors which recognise intracellular pathogens. CLRs are phagocytic receptors on specific subsets of innate immune cells, and include receptors such as dectin-1, which recognises β-glucans, and mannose receptors. Scavenger receptors are phagocytic receptors which recognise polymers and acetylated lipoproteins on the surface of particles and pathogens. This robust set of receptors enables the detection of many different

types of pathogenic threat, and induce host signalling cascades to respond to pathogenic insult and receptor activation (Kumar et al., 2011; Murphy et al., 2016).

1.1.1.2 Innate response to pathogens

The innate immune system responds to pathogens in variety of ways to control and prevent their propagation and dissemination. Cells are specialised to perform specific functions, though many immune cells are capable of responding to pathogens in a variety of ways with different effector functions. Granulocytes, for example, possess and release toxic granules containing enzymes and proteins which harm and destroy pathogens. While neutrophils are known for their phagocytic capabilities, they are also potent granulocytes, along with eosinophils and basophils. Granulocytes are important mediators of inflammation, and the appropriate magnitude of response followed by a timely resolution is necessary to prevent chronic inflammation.

Natural killer (NK) cells are also members of the innate immune system which possess granules. NK cell granules contain cytotoxic proteases called granzymes, as well as perforin, a pore-forming protein which forms destructive holes in target cells. NK cells are activated by the absence of self-antigens and major histocompability complex molecules on the surface of cells, nominating these cells as 'non-self' which fail to pacify the destructive actions of NK cells (Lanier, 2005). After contact perforin forms pores in the recipient cell, and proteases are cleaved within the target cell to induce apoptosis. NK cells are most widely known for their ability to recognise and kill cancer cells, though different NK cell phenotypes may support tumour angiogenesis (Bassani et al., 2019; Nicholson et al., 2019).

Besides being involved in normal cellular turnover, phagocytosis is a direct method of eliminating pathogenic threats, a process which involves ingestion and elimination of pathogens by phagocytes. Phagocytes recognise pathogens as discussed above, and internalise them in order to neutralise and destroy the threat. While phagocytes may directly recognise and engulf invading pathogens, methods

which improve pathogen recognition and binding improve phagocytosis (Flannagan et al., 2012; Gordon, 2016). For example, antibody deposition on pathogen surfaces neutralises the pathogen and prevents invasion of host tissues, but also enhances the recognition and engulfment of the pathogen by phagocytes (Wright and Douglas, 1903). Phagocytes possess FcR on their surfaces which recognise the Fc region of antibodies deposited on microbes. Antibody molecules therefore act as adapters which facilitate the uptake of foreign material by phagocytes such as macrophages. The complement system acts in a similar way; through a series of proteolytic cleavages, complement components are created (iC3b) and deposited on the surface of pathogens. The complement receptor on the surface of phagocytes (CR3) recognises this complement, which enhances the binding and uptake of pathogens by the phagocyte (Merle et al., 2015; Sim and Tsiftsoglou, 2004). The complement system may also form pores directly in the pathogen, resulting in their destruction (Bhakdi et al., 1987). Some pathogens possess characteristics which make phagocyte recognition and uptake more difficult; for example, some 'cloak' their surface with capsule and other compounds to prevent recognition and uptake by phagocytes. *Paracoccidioides brasiliensis* is surrounded by melanin which prevents the recognition of cell wall components by phagocytic dectin receptors (da Silva et al., 2006), while *Cryptococcus* capsule helps to prevent phagocytosis (Kozel and Gotschlich, 1982). Interactions between phagocytes and pathogens are discussed in depth in chapter 5.

There are various cells capable of phagocytosis in the human body, including dendritic cells, neutrophils, NK cells, and macrophages. Upon recognition and internalisation of the pathogen by the phagocyte, the pathogen is contained in an endocytic vesicle called a phagosome. The phagosome is acidified and fuses with lysosomes to produce a phagolysosome. The phagocytes create an increasingly microbicidal environment. For example, the production of reactive oxygen species (ROS) by NADPH oxidase damages microbial cells; inducible nitric oxide synthase (iNOS) produces superoxide and nitric oxide to stress the captured pathogens. As the phagolysosome matures it becomes more acidic, and the barrage of lysozymes, proteases, and harmful radical species, combined with the limited nutrient

availability, produces an increasingly microbicidal environment which kills and degrades the pathogen within (Uribe-Querol and Rosales, 2017). Of course, many pathogens are capable of modifying and adapting to the phagosome and the phagolysosome, and possess mechanisms by which they scavenge and detoxify harmful radicals. For example, *Salmonella* employs an arsenal of enzymes to degrade host ROS (Aussel et al., 2011). Pathogenic strategies of intracellular survival and exploitation will be discussed later in chapter 5.

The phagocytosis of pathogens often activates phagocytes to upregulate the expression of many genes which enable the adoption of an anti-microbial, pro-inflammatory phenotype. One study performed DNA microarrays after using different bacterial components to stimulate human macrophages, and showed that after encountering pathogenic material, macrophages upregulated the expression of many pro-inflammatory genes encoding cytokines and chemokines, and induced the enhanced expression of genes relating to receptors, signalling molecules, and transcription factors (Nau et al., 2002). Thus, phagocytosis of pathogens induced expression of genes related to microbicidal effector functions, but also activated the macrophages to be able to potently sense and respond to the environment. Part of the responsibility that comes from phagocytosing pathogenic threats is alerting the immune system to the presence of invading microbes, and to recruit and activate additional immune effector cells to combat infection. As such, phagocytes secrete signalling molecules and may present modified antigenic peptide on their surface via major histocompatibility complex (MHC) molecules, providing stimulation to T cells to induce their activation.

Perhaps one of the most important functions of the innate immune response is the activation of effector cells and the recruitment of a robust immune cell cohort. While the production and response to immune signalling molecules will be discussed later, it is important to mention that innate and adaptive immune systems rely on communication between the two branches to effectively respond to infection, mount an inflammatory response, and maintain homeostasis. The interplay between innate and adaptive immune systems involves many cell types,

including the innate lymphoid cells (ILCs). These cells are derived from lymphoid progenitor cells but lack T cell and B cell receptors. ILCs are important for tissue repair, maintaining epithelial barrier integrity, and are involved in the early immune response to infection. ILCs are categorised based on the transcription factors which induce their development and the cytokines which they produce. These cytokines are roughly analogous to the cytokines produced by the different helper T cell subsets (discussed in the next section); group 1 ILCs produce Th1 cytokines, group 2 ILCs produce Th2 cytokines, and group 3 ILCs produce Th17 cytokines (Spits et al., 2013). ILCs lack antigen receptors but react to cytokines produced by immune cells which are responding to pathogens and allergens, and sense cytokines released by damaged epithelial cells (Eberl et al., 2015). ILCs respond to these cues by releasing cytokines, recruiting effector cells, and inducing the production of mucus and antimicrobial peptides (Walker et al., 2013). There is even evidence that ILCs are capable of immunological memory, as pre-stimulated mice showed ILC retention and enhanced ILC expansion and cytokine production after secondary challenge with allergen (Martinez-Gonzalez et al., 2016, 2017). These immune cells modulate the immune response by presenting antigens to CD4+ T cells to induce activation and by producing cytokines which polarise immune cells and drive effector functions (Sonnenberg and Hepworth, 2019). Thus, by responding to cytokines and producing cytokines in turn, these immune cells aid in the communication and coordination between the innate and adaptive immune systems, enabling robust response to infection.

While the innate and adaptive immune systems are largely separated by activation and specificity of response, these branches are not mutually exclusive, with some innate immune cells performing adaptive functions and vice versa. A prime example of this is dendritic cells (DC), which phagocytose pathogens and present modified pathogenic peptides to T cells to activate them and induce an adaptive immune response. While macrophages and other cell types may perform functions of antigen-presenting cells (APCs), DCs are specialised for this specific function. Thus, while DCs may respond immediately to non-specific pathogenic stimulation, they

are involved in adaptive immune activation and thus bridge the gap between the complementary arms of the immune system.

1.1.2 The adaptive immune system response to infection

1.1.2.1 Pathogen recognition by adaptive immune cells

The adaptive immune system provides pathogen-specific, enduring response to infection, and produces immunological memory to enable the immune system to respond rapidly to threats which have been encountered previously. T cells and B cells compose the adaptive immune response and are derived from lymphoid progenitors, which also give rise to innate lymphoid cells. While innate immune cells can recognise pathogens directly via receptors, T cells require pathogenic antigens to be presented as modified peptides via major histocompatibility complex (MHC) molecules on the surface of antigen-presenting cells (APC), which are received by T cell receptors (TCR) (Birnbaum et al., 2014; Guermonprez et al., 2002). Upon receiving antigen-specific and co-stimulatory signals from APC, T cells clonally expand and differentiate to respond to the specific pathogen matching the received antigen (Curtsinger et al., 2003; Mueller et al., 1989). While B cells may recognise antigen that is presented to them (Heesters et al., 2016), they are also able to recognise soluble antigens via an immunoglobulin molecule attached to their cell surface, which perceives antigen and results in clonal expansion and antibody production. Antibodies bind to pathogens to neutralise them, and also opsonise pathogens to mark them for phagocytosis by phagocytes, or activate the complement system which ruptures cell membranes (Murphy et al., 2016).

1.1.2.2 Adaptive response to pathogens

T cells provide cytotoxic and helper roles, and either directly interact with infected cells, or assist other immune cells to enable them to eliminate threats. T cells are divided by surface marker expression, cytokine production, and associated functions (Mosmann et al., 1986; Tada et al., 1978), producing subsets which are called CD4+ helper T cells, CD8+ cytotoxic T cells, and regulatory T cells. CD4+ helper

T cells are so named because they help to activate other immune cells to respond to infection. For instance, CD4+ T cells and APC co-activate CD8+ T cells, and stimulate the activation of B cells which then mature and produce secreted antibodies (Mitchell and Miller, 1968; Smith et al., 2000). CD4+ T cells can be further subdivided into Th1 and Th17 T cells, which provide cell-mediated immunity mainly against intracellular pathogens, and Th2 cells which provide humoral immunity (Murphy et al., 2016). While CD4+ T cells are broadly categorised into Th1, Th2, Th17 major subtypes, many subtypes exist along a continuum of activation profiles (Raphael et al., 2015). CD8+ cytotoxic T cells induce apoptosis in target pathogenic cells through the release of cytotoxic granules, through activation of FasL to induce apoptosis, and by the production of cytokines (Halle et al., 2017). The role of regulatory T cells is to suppress the activity of other lymphocytes, preventing an over-zealous immune response, especially against the host itself.

The differentiation and development of specific T cell functions is determined by signals received from antigen-presenting cells and from fellow immune cells. These signals represent a crucial mode of communication between the innate and adaptive immune systems, and can modulate the course and outcome of the immune response. This immunological cross-talk forms the basis of the immune response, and is key in mounting a robust response to infection.

1.1.3 Immunological cross-talk

Immune cells produce many signalling molecules to communicate and coordinate actions. Cytokines are diverse protein signalling molecules which are capable of acting in an autocrine, paracrine, and even endocrine manner (Altan-Bonnet and Mukherjee, 2019). The names of cytokines were originally assigned based on the cell type producing them, though the pleiotropic effects and overlapping source of production has rendered these names somewhat arbitrary as the study of these molecules has evolved (Dinarello, 2007). Current classifications are assigned based on the function of the cytokines, structure, and also the inflammatory response elicited. Common classes of cytokines include interleukins (IL-), interferons (IFN-),

tumour necrosis factors (TNF-), lymphokines, growth- and colony-stimulating factors, and the chemoattractant peptides called chemokines. I will refer to the inflammatory effects of the cytokines described as this pertains to my work, but it should be noted that the assignment of 'pro-inflammatory' or 'anti-inflammatory' is not necessarily absolute or mutually exclusive, and context is important in deciding the produced effect. IL-6, for example, induces pro-inflammatory responses in cells when the soluble receptor is bound, but also activates anti-inflammatory cascades when the membrane-bound receptor is activated (Rose-John, 2012).

Cytokines are produced by most immune cells, especially in response to pathogen recognition, though many stimuli may induce the production of cytokines. The ability of immune cells to respond to various cytokines depends on the target cell's developmental state and the ability to recognise the cytokine. Many cell types possess surface receptors which recognise soluble cytokines, though some cytokines bind with extracellular receptors to facilitate access to the target cell to activate a response (Rose-John and Heinrich, 1994)**.** After binding to receptors, activation of intracellular signalling cascades results in the transcriptional regulation of genes. This transcriptional regulation ultimately drives cell action and function, and even affects the production of additional cytokines for secretion. Cytokines may induce or suppress the secretion of cytokines from immune cells, and the interaction of these signalling molecules with effector immune cells largely determines the direction of the immune response.

T cells are important in the activation of specific immune responses, and as such the cytokines they produce drive pro- and anti-inflammatory actions. The presence of IL-12 induces Th1 activation, marked by the production of IFN-γ (Macatonia et al., 1995) which in turn inhibits the proliferation of Th2 cells (Gajewski and Fitch, 1988). IL-4 is secreted by Th2 cells, and results in the upregulation of Th2 cytokines, including IL-4 itself (Swain et al., 1990). In responding to a multitude of different cytokines, T cells and other immune cells are able to communicate and direct immune responses to invading pathogens. While these cytokines may work together to amplify a prescribed course of action, they may also limit one another

to provide a regulated response. For example, IL-4 downregulates the production of TNF-α from IL-2-stimulated murine macrophages (McBride et al., 1990), and IL-10 inhibits the production of pro-inflammatory cytokines by Th1 cells (Fiorentino et al., 1991). A recent study showed the cytokine IL-4 from Th2 T cells induced the expression of IL-10 from activated Th1 T cells to self-regulate the pro-inflammatory Th1 phenotype, limiting the overexpression of cytokines linked to chronic inflammatory immune pathologies (Mitchell et al., 2017). It is the context in which cytokines are produced and which cells are activated that determine whether the immune response is appropriate, or whether it causes critical damage

1.1.4 Macrophages and T cells in infection

Macrophages are particularly important phagocytes because not only do they engulf invading pathogens in the tissues and eliminate infected cells, they collaborate with the adaptive immune system to launch a robust immune response. T cells, along with other immune cells, provide stimuli to macrophages to activate them to perform vital effector functions. Depending on the cytokine produced, macrophages can be induced to respond in a specific way to either drive or dampen an inflammatory response (Duque and Descoteaux, 2014). The type of cytokine produced depends on the phenotype of the T cell. Generally, CD4+ Th1 and Th17 cells produce pro-inflammatory cytokines such as interferon-γ (IFN-γ), tumour necrosis factor-α (TNF-α), and interleukins 6 and 12 (IL-6, IL-12), and induce "classically activated" M1 macrophages with pro-inflammatory responses (Nathan *et al.,* 1983; Erwig *et al.*, 1998). M1 macrophages are associated with enhanced phagocytosis of invading pathogens, production of reactive oxygen and nitrogen species (Ding et al., 1988), and recruitment of microbicidal effector cells. In line with these functions, M1 macrophages are associated with control of intracellular pathogens.

Conversely, CD4+ Th2 cells produce anti-inflammatory cytokines such as interleukin 4 (IL-4), interleukin 10 (IL-10), interleukin 13 (IL-13), and peroxisome proliferator-activated receptor-γ (PPAR-γ), and stimulate "alternatively activated" M2

macrophages (Martinez et al., 2009; McKenzie et al., 1993; Mosmann and Coffman, 1989; Stein et al., 1992). M2 macrophages are anti-inflammatory because they abrogate the inflammatory M1 response (Mosmann and Coffman, 1989) and inhibit the production of reactive species by competing for substrate. For example, L-arginine is a substrate used for the production of either nitric oxide (NO), which is antimicrobial and destructive, versus L-ornithine which is a polyamine needed for cellular processes and tissue repair (Rath et al., 2014), and which is associated anti-inflammatory responses. Furthermore, M2 macrophages have been shown to limit excessive recruitment of inflammatory cells, rather expanding localised immune cells to prevent an excessive immune response (Jenkins et al., 2011), and are associated with clearance of cellular debris and tissue repair.

While these macrophage activation states produce opposing effects, polarisation is not definite and absolute, contrary to what was thought previously (Erwig et al., 1998). Rather, macrophages display a degree of plasticity in activation. Because the physiological environment of infection changes over time from one aimed at attacking invading pathogens to one whose purpose is debris removal and tissue repair, the environmental stimuli change to induce different responses by immune cells. Macrophages are able to adapt to the change in stimuli, enabling the transition from a pro-inflammatory immune state to an anti-inflammatory state that enables the return to tissue homeostasis. Porcheray et al. showed that human macrophages changed their the expression of polarisation markers after sequential stimulation by pro- and anti-inflammatory cytokines, modifying their phenotype to match what was required by the environmental cues (Porcheray et al., 2005). A similar study by Stout et al. showed that depending on the cytokines, pre-treatment of murine macrophages with one cytokine and subsequent administration of an opposing one (i.e. pro- then anti-inflammatory) resulted in the macrophages adopting a phenotype indicative of the most recent cytokine encountered (Stout et al., 2005). However, intermediate phenotypes were also observed, suggesting that while macrophage functional polarisation may shift to adapt to the needs of the changing environment, polarisation states need not be absolute nor extreme (Stout et al., 2005). Similarly, Davis et al. showed that *in vivo* macrophage polarisation changed

during the course of infection with *C. neoformans* in mice (Davis et al., 2013). *In vitro* polarisation was also dynamic, with macrophages altering polarisation markers to reflect the most recent cytokine present and displaying fungicidal capabilities reflective of the cytokine environment (Davis et al., 2013). Thus, macrophage polarisation dynamically changes to reflect the cytokine environment, enabling them to modify their behaviour based on changing environmental stimuli which reflect the inflammatory needs of the host.

In various disease systems cytokines are the major drivers of the outcome of infection. HIV infection is a prime example of how cytokines reflect immune state during infection. At the onset of HIV infection, the host retains a relatively high number of CD4+ T cells, and the cytokine response is largely dominated by Th1 cytokines. However, as the disease progresses and CD4+ T cell count decreases, the cytokine profile shifts from one dominated by IFN-γ and Th1 cytokines, to one where IL-4 and Th2 cytokines prevail (Altfeld et al., 2000; Kedzierska and Crowe, 2001). This impairs cell-mediated immunity and enables opportunistic infectious species to invade. Species of *Cryptococcus* are excellent examples of organisms that cause such infections.

1.2. *Cryptococcus*

1.2.1 Species and lifecycles

Cryptococcus is a genus of facultative intracellular yeasts within the phylum Basidiomycota within the kingdom of Fungi. Previously, *Cryptococcus* was divided into two species: *Cryptococcus neoformans* and *Cryptococcus gattii*. *C. neoformans* encompassed two varietal serotypes, distinguishable by capsular agglutination assays (Franzot *et al.*, 1999): serotype A (var. grubii) and serotype D (var. neoformans) (Kwon-Chung and Varma, 2006). *C. gattii* was recognised as a separate species in 2002 with two serotypes, B and C (Kwon-Chung et al., 2002). Mounting genetic evidence in the recent past has spurred discussion as to whether *Cryptococccus* should be divided based on genotype into distinct species, rather

than relying on 'species complex' to encompass related, though genetically distinct, 'sub-species' (Figure 1.1).

Kwon-Chung has long advised retention of 'species complex' nomenclature, claiming that two species (*Cryptococcus neoformans* and *Cryptococcus gattii*) are sufficient to encompass their biological and ecological differences, while the adoption of species based on different genotypes lacking biological relevance is premature and misleading (Kwon-Chung and Varma, 2006). However, in 2015 seven species were proposed, separating two species from the *C. neoformans* species complex, and five species from the *Cryptococcus gattii* species complex, based on genotypic and phenotypic evidence from clinical isolates (Hagen et al., 2015). A rebuttal headed by Kwon-Chung posed that over 2,606 published strains showed more genotypic variation than could be encompassed by seven separate species, that more strains must be considered using a higher proportion of the genotype for sequencing (Kwon-Chung et al., 2017). Furthermore, Kwon-Chung advocated that recognising many individual species imbues confusion that is unnecessary when the recognition of additional genotypic variants continues to grow, showing that adopting new species names will prove to be temporary, inadequate, and confusing (Kwon-Chung et al., 2017). Despite this, genotypic, phenotypic, ecological, and geographical differences have bolstered the recommendation of adopting the recognition of seven discrete species (Hagen et al., 2017). Both sides of this argument have merit and demonstrate the need for a review of the current standards and limits by which new species are identified and named, particularly as it pertains to the difference between species and clinical isolates. While I believe that the adoption of separate species names is defensible, for the sake of continuity with the existing literature described in this work I will refer to *Cryptococcus* species *neoformans* (formerly var. grubii, serotype A) and species *deneoformans* (formerly var. neoformans, serotype D) as *C. neoformans*, and I will refer to the five nominated species of *Cryptococcus gattii* (formerly serotypes B and C) as *C. gattii*.

Cryptococcus is a basidiomycetous yeast which can produce spores and reproduce sexually as well as asexually. Sexual reproduction occurs by the fusion of haploid

cells of two mating types – a and α. The sexually reproducing forms are named *Filobasidiella neoformans* (serotypes A and D) and *Filobasidiella bacillispora* (serotypes B and C) (Kwon-Chung, 1975, 1976; Kwon-Chung et al., 1982). However, the asexual yeast form is more common and reproduces through budding. It is this form that is isolated from human infection and is considered below. What's more, some serotypes (or newly named species) are capable of hybridisation to form diploid cells. Serotypes A and D (*Cryptococcus neoformans* x *deneoformans*) hybridise to form diploid or aneuploid cells, and while some isolates are self-fertile, most are sterile (Lengeler et al., 2001).

	Species complex serotype	Proposed species
Cryptococcus neoformans	**A) var. grubii**	***Cryptococcus neoformans***
	D) var. neoformans	***Cryptococcus deneoformans***
Cryptococcus gattii	**B) C)**	***Cryptococcus gattii***
		Cryptococcus bacillisporus
		Cryptococcus deuterogattii
		Cryptococcus tetragattii
		Cryptococcus decagattii

Figure 1.1. *Cryptococcus* by species complex serotype and newly proposed species names.

While species complex serotype has long been used to identify the four serotypes of *Cryptococcus*, genotypic evidence proposes the adoption of seven separate species. Adopted from Hagen et al., 2015.

1.2.2 Distribution and human susceptibility

1.2.2.1 Epidemiology

C. neoformans is widely distributed and is associated with bird faeces, bat guano, rotting vegetables, and soil. In fact, *C. neoformans* can colonise birds without apparent symptomatic infection, survive within macrophages, and withstand the high temperature, thus enabling birds to effectively transmit cryptococcal infection (Johnston et al., 2016). C*. gattii* is less widely distributed and is associated with eucalyptus, and is found mainly in the tropics (Chakrabarti *et al.*, 1997; Callejas *et al.*, 1998) but with incidence in British Columbia and the Pacific Northwest (Kidd et al., 2004). *Cryptococcus* has the ability to infect humans with a normally functioning immune system, as evidenced by the *C. gattii* outbreak in British Columbia, Canada from 1999 to 2007 (Kidd et al., 2004; MacDougall et al., 2007). However, the majority of human cryptococcosis cases occur in immunocompromised patients, particularly those infected with strains of *C. neoformans* as opposed to *C. gattii*.

1.2.2.2 *Cryptococcus neoformans* infection susceptibility

Patients infected with *Cryptococcus* can be broadly divided into three groups based on immune status: HIV-associated, non-HIV immunocompromised patients, and otherwise immunocompetent patients (Brizendine et al., 2013; Garelnabi and May, 2018). *Cryptococcus neoformans* is an opportunistic pathogen that mainly infects those with severely compromised immune systems. It is estimated that globally over 223,000 people suffer from cryptococcal meningitis, resulting in 181,000 deaths per year (Rajasingham et al., 2017). This is a lower estimation compared to the nearly 1 million cases estimated in 2009 (Park et al., 2009), likely due to anti-retroviral treatment and current therapies available. 73% of the people who suffer from cryptococcal meningitis are from sub-Saharan Africa (Rajasingham et al., 2017), and in Sub-Saharan Africa *Cryptococcus* is the leading cause of meningitis (Jarvis et al., 2010) and is one of the leading causes of death in people suffering from HIV/AIDS. In fact, cryptococcal meningitis accounts for 15% of AIDS-related deaths worldwide (Rajasingham et al., 2017). Non-HIV immunocompromised patients usually present

with other predisposing factors which render them susceptible to *C. neoformans* infection. These include solid organ transplant (Pappas et al., 2010; Singh et al., 1997), cancer and haematological malignancies (Schmalzle et al., 2016), autoimmune disease, and immunosuppressive treatments (Lin et al., 2015). People who are not immunocompromised may also suffer from cryptococcosis (Chen et al., 2008).

1.2.2.3 *Cryptococcus neoformans* route of infection

While the exact route of cryptococcal infection is not clear, it is believed that cryptococci enter the body through inhalation of spores or yeast cells (Botts and Hull, 2010; Giles et al., 2009; Velagapudi et al., 2009), and then become lodged in the alveoli of the lungs to cause cryptococcosis (Figure 1.2). Because cryptococci can exist as vegetative yeasts or as spores, which form by sexual reproduction, a recent study examined the infection dynamics of yeasts versus spores in a murine model of cryptococcal infection. This study showed that spores were more pathogenic than yeast and resulted in larger lung burden and higher dissemination to the brain (Walsh et al., 2019). Because spores exist within the environment, it is likely that they gain entry into the lung where they germinate to become yeasts, and that these yeasts then propagate infection (Walsh et al., 2019). However, because spores become yeast in the body, and because both yeasts and spores are able to propagate cryptococcal infection, it is difficult to ascertain which actually causes cryptococcal infection. While both are able to cause cryptococcosis, spores appear to be more adept at colonisation and dissemination, meaning that they are likely the infectious propagule that cause systemic cryptococcal infection (Giles et al., 2009; Walsh et al., 2019).

Despite this new evidence for spores as the infectious agents in cryptococcosis, the link between pulmonary infection, widespread fungemia, and CNS invasion remains vague. A study by Davis and colleagues suggested that secondary fungemia, resulting from the germination of spores, was necessary for sustained fungemia, though determination of ‘primary’ versus ‘secondary’ fungemia was not

conclusively shown (Davis et al., 2016). A recent study used bioluminescent imaging in conjunction with magnetic resonance imaging of mice infected with *C. neoformans* expressing luciferase; this enabled spatiotemporal infection progression to be followed in a living animal model of infection (Vanherp et al., 2019). Results from this study suggested that there was a correlation between pulmonary burden and rate of brain dissemination, though widespread fungemia was not noted and a method for CNS invasion was not investigated (Vanherp et al., 2019). However, another study showed that cryptococci were likely to escape the lungs via association with alveolar macrophages, invading the lung draining lymph node whilst inside the immune cells and thus gaining access to the rest of the body (Walsh et al., 2019).

After dissemination from the site of infection, and after a potential, ill-defined phase of widespread fungemia, the CNS may be colonised either by transcellular penetration (Chang et al., 2004), or via a 'trojan horse' mechanism by which macrophages deliver the infectious cells to the CNS (Chretien et al., 2002). Charlier et al. showed that mice which were infected with macrophages containing intracellular cryptococci showed higher fungal burdens in the brain compared to mice infected with free cryptococci (Charlier et al., 2009), demonstrating a role for macrophage in fungal brain colonisation. While evidence for the Trojan-horse method of brain dissemination has been largely based on inference, new studies provide support for the existence of this mode of dissemination. A recent study using a transwell system lined with human cerebral microvascular endothelial cells showed transport of cryptococci across this artificial BBB within human THP-1 monocytes, demonstrating this 'Trojan horse' transportation of cryptococci (Santiago-Tirado et al., 2017). A similar result was produced by Sorrell et al., who showed that macrophages transported *C. neoformans* and *C. gattii* across a monolayer of brain endothelial cells (Sorrell et al., 2016). These studies provide evidence for the mechanism by which cryptococci reach this target site of infection, though dissemination and maintenance of cryptococci within the bloodstream remains unclear. Nonetheless, once cryptococci have breached the central nervous

system, they are able to cause serious health complications such as cryptococcal meningitis and meningoencephalitis.

Because *C. neoformans* is widespread throughout the environment, it is likely that many people encounter this fungus and control the infection, preventing it from disseminating and causing symptomatic cryptococcosis. Evidence suggests that many people are introduced to *C. neoformans* during childhood and are able to control the infection to prevent clinical symptoms (Goldman et al., 2001). Cryptococci may also be contained within the lung, inside of granulomas which are composed of monocytes, multi-nucleated cells, and T cells – though T cells are missing in cryptococcal granulomas in immunocompromised patients, which may account for lack of pulmonary control of infection (Shibuya et al., 2002, 2005). Goldman et al. showed that granulomas in immunocompetent rats controlled infection, while immunosuppressed rats showed aberrant granuloma formation and failure to control infection, demonstrating the need for a robust immune response to induce granuloma formation and infection control (Goldman et al., 2000). Granulomas will be discussed further in chapter 6.

1.2.2.4 *Cryptococcus gattii* susceptibility, route of infection

As mentioned above, *Cryptococcus gattii* is capable of infecting people who are otherwise healthy and immunocompetent, suggesting that it may be a primary pathogen as opposed to an opportunistic pathogen like *C. neoformans*. Unlike *C. neoformans*, which appears to have a high tropism for the CNS, *C. gattii* mainly presents as pulmonary infection and is associated with granulomas (Galanis and MacDougall, 2010). In fact, during the early Vancouver Island outbreak, of those admitted to the hospital for treatment due to *C. gattii* infection, 76% were treated for respiratory treatment, while only 7.8% were treated for CNS pathology (Galanis and MacDougall, 2010). A similar study reported that as many as 30% of patients showed CNS infection (Phillips et al., 2015), still highlighting the lack of CNS involvement compared to *C. neoformans* infection.

Interestingly, after *Cryptococcus* was administered to mice via inhalation, *C. neoformans* was better able to colonise the CNS and brain compared to *C. gattii*, and *C. gattii* was not recovered from the blood (Ngamskulrungroj et al., 2012). However, *C. gattii* proved capable of crossing the blood-brain barrier (BBB) to colonise the CNS when introduced intravenously through the tail vein. This suggests that either some factor in the host blood inhibited *C. gattii* from CNS colonisation, *or* that *C. gattii* was not able to efficiently escape from the lung to colonise the brain and disseminate infection (Ngamskulrungroj et al., 2012). As discussed above, *C. neoformans* likely colonises monocytes and macrophages to escape from the lung environment to disseminate infection (Walsh et al., 2019). While reports comparing the intracellular proliferation rates (IPR) of *C. neoformans* and *C. gattii* disagree about which replicates at a higher rate intracellularly (likely due to differences in isolates), macrophages more readily phagocytose *C. neoformans*, which has a higher intracellular load compared to *C. gattii* (Hansakon et al., 2019; Voelz et al., 2009). If macrophages are the vehicle that cryptococci use to escape the lung environment, and *C. gattii* invades and proliferates less inside of macrophages, the lower number of *C. gattii* inside of macrophages is possibly what produces the lower dissemination into the bloodstream and CNS compared to *C. neoformans*, which readily replicates inside of macrophages. In a study which utilised human THP-1 cells to illustrate the Trojan horse method of transgressing the BBB, *C. gattii* within macrophages crossed the layer of brain endothelial cells significantly less than *C. neoformans* (Sorrell et al., 2016). *C. gattii* inhabited macrophages less than *C. neoformans*, again suggesting that the lower uptake of *C. gattii* may account for its lower dissemination to the CNS.

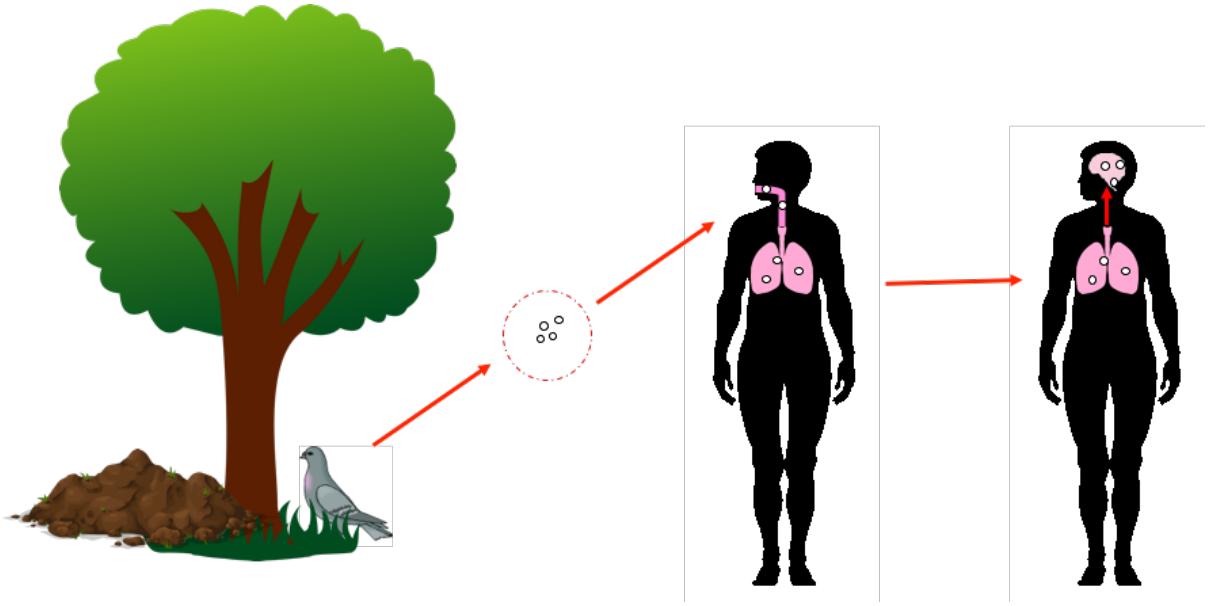

Figure 1.2. Route of *Cryptococcus* infection

Cryptococcus present in the environment is inhaled into the lungs as desiccated spores. Once in the lungs, cryptococci become lodged in the alveoli and alveolar macrophages attempt to clear infection. If they fail and cryptococcosis progresses, cryptococci may eventually transgress the blood-brain barrier and infect the central nervous system, leading to cryptococcal meningitis and cryptococcal meningoencephalitis. Mechanisms of escape from the lung and the induction of widespread fungemia are unclear.

1.2.3 Cryptococcal virulence

Cryptococcus employs various strategies which make it a 'successful' pathogen capable of propagating infection. Cryptococcus is able to avoid capture and destruction by the immune system, and is also able to survive intracellularly if captured to exploit the host intracellular niche. A recurring theme is that the immune system has developed ways to control cryptococcal infection, while the invading pathogen has various adaptations to subvert immune control and to exploit the immune system for virulence and growth (Figure 1.3). I will give a brief overview of cryptococcal survival strategies here, focusing on macrophages as they pertain to my work, saving the finer detail for the introductions to the relative chapters.

1.2.3.1 Phagocytosis by macrophages

Macrophages are a major contributor to control of cryptococcal disease. While macrophages contain various surface receptors for the recognition and phagocytosis of pathogens, antibody opsonisation facilitates enhanced uptake of cryptococci (Levitz and Tabuni, 1991; Mukherjee et al., 1996). Complement-mediated opsonisation is also key for phagocytosis of cryptococci, as antibodies against complement receptors inhibit phagocytosis of opsonised cryptococci (Levitz and Tabuni, 1991). Complement combined with antibody opsonisation further enhances cryptococcal uptake by macrophages (Taborda and Casadevall, 2002). However, *C. neoformans* combats this enhanced macrophage recognition by producing antiphagocytic protein (App1), which binds to the CD11b subunit of CR3 on phagocytes to prevent complement-mediated phagocytosis (Stano et al., 2009). Interestingly, *Cryptococcus* upregulates App1 translation during low glucose conditions representative of conditions in the lung, demonstrating that cryptococci attempt to prevent phagocytosis at the onset of pulmonary infection (Williams and Del Poeta, 2011). Thus, while the immune system employs redundant mechanisms to ensure the neutralisation of this pathogenic threat, the invading pathogen has mechanisms to avoid capture.

Upon inhalation cryptococci enter the lung where they are met with lung surfactant, a layer of lipids and proteins which lines the lungs. Lung surfactant is known to coat inhaled particles to facilitate uptake by resident phagocytes. A study by Geunes-Boyer et al. showed that while surfactant protein-D (SP-D) recognised β-glucan in the cryptococcal cell wall and facilitated enhanced phagocytosis of acapsular cryptococci, it also protected the cryptococci from destruction by macrophages after phagocytosis (Geunes-Boyer et al., 2009). Furthermore, Geunes-Boyer et al. showed that SP-D facilitated the growth and dissemination of cryptococci with intact capsules, and increased fungal survival in the presence of H_2O_2 *ex vivo* (Geunes-Boyer et al., 2012). While surfactant proteins enable the increased phagocytosis of foreign and pathogenic particles, cryptococci utilise this to facilitate resistance to destructive host defence mechanisms, and enhance growth and dissemination.

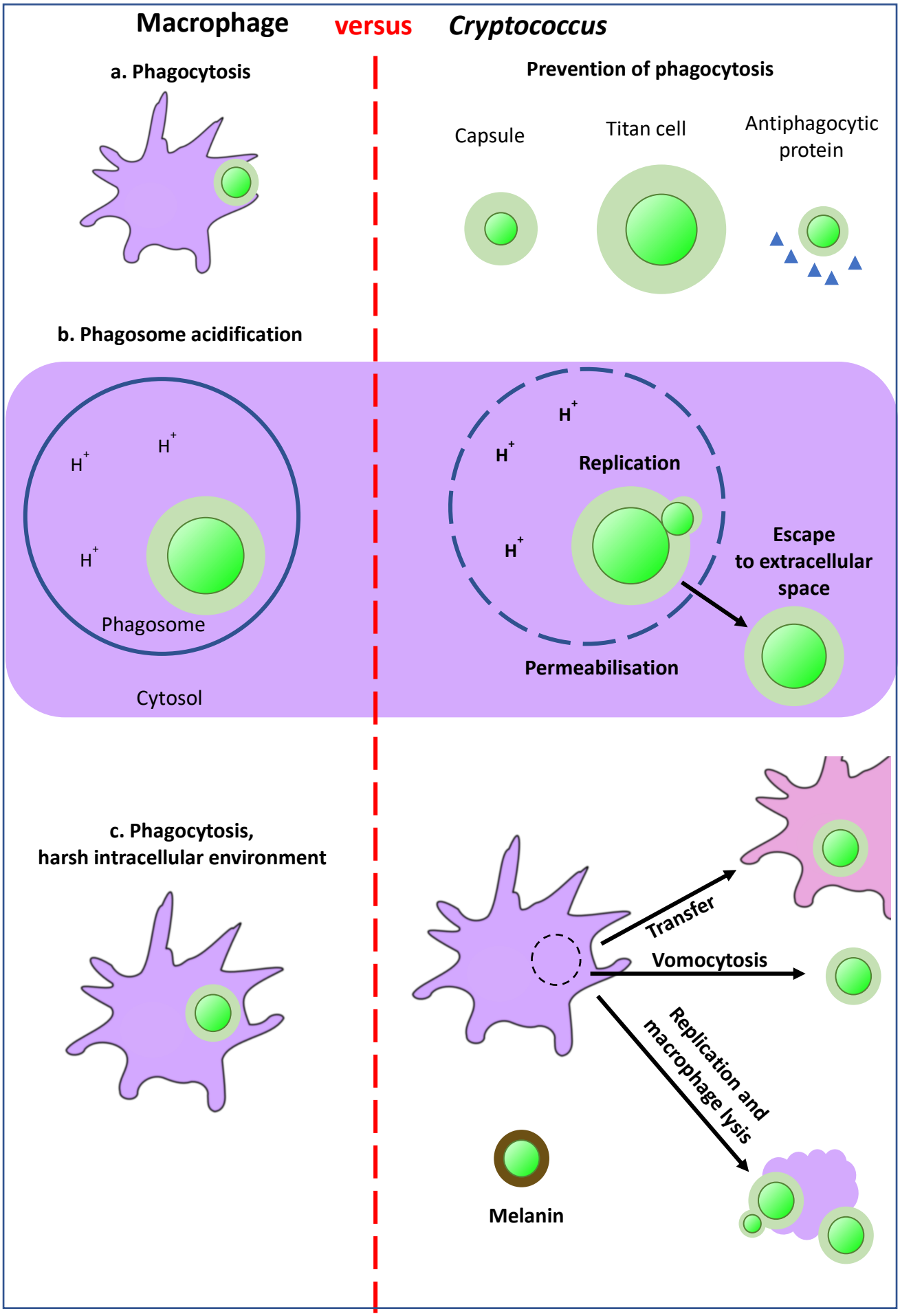
Macrophage
versus
Cryptococcus
a. Phagocytosis
Prevention of phagocytosis
Capsule
Titan cell
Antiphagocytic protein
b. Phagosome acidification
H+
Phagosome
Cytosol
Replication
Escape to extracellular space
Permeabilisation
c. Phagocytosis, harsh intracellular environment
Transfer
Vomocytosis
Replication and macrophage lysis
Melanin

Figure 1.3. The roles of macrophages and cryptococcal responses

As host macrophages attempt to phagocytose cryptococci and destroy them, cryptococci employ strategies to ensure survival and pathogenicity.

a. Phagocytosis. As a phagocyte, macrophages attempt to engulf cryptococci. However, cryptococci have capsules which prevent the recognition of the cell wall by macrophage surface receptors. Cryptococci may also grow to become titan cells which are up to 100 μm in diameter and are difficult to phagocytose, or secrete antiphagocytic proteins which prevent complement receptor recognition and subsequent phagocytosis.
b. Phagosome acidification. After phagocytosis cryptococci are trafficked to the phagosome which fuses with lysosomes and becomes progressively more acidic. However, cryptococci are able to survive and replicate at acidic pH. They are also able to permeabilise the phagosome to escape into the extracellular space.
c. Phagocytosis, intracellular environment. After phagocytosis cryptococci are subjected to the harsh intracellular environment of the macrophage intracellular niche. However, cryptococci are able to transfer to other cells, exit non-lytically via vomocytosis, or induce macrophage lysis and release of intracellular cryptococci. Cryptococci also produce melanin, a dark pigment which scavenges free radicals and toxic reactive species to protect the cryptococci from destruction.

1.2.3.2 Cryptococcal capsule

In addition to opsonic uptake, host macrophages are able to recognise cryptococci via surface receptors. Cryptococci possess a cell wall that is composed of glucan molecules, chitin, chitosan, and mannoproteins which protect the cell from environmental and osmotic stresses. Macrophages possess dectin-1 and mannose receptors on their surface which enable them to recognise β-glucans and mannoproteins on the surface of cryptococci to facilitate phagocytosis (Cross and Bancroft, 1995). Indeed, competitive mannan binding and dectin-1 inhibition assays showed that differentiated human macrophages relied on these receptors for phagocytosis of cryptococci which were not opsonised, as is likely to be the case for cryptococci inhaled into the lung (Lim et al., 2018). However, one distinguishing factor of cryptococci is their capsule which prevents recognition of these epitopes in their cell wall, hindering recognition and uptake by phagocytes (Kozel and Gotschlich, 1982). In fact, the cryptococcal capsule is a major determinant of virulence, representing the interface between the pathogen and immune cells. Because the capsule has been reviewed extensively elsewhere (Bhattacharjee et al., 1984; Bose et al., 2003; Doering, 2009; Wang et al., 2018; Zaragoza et al., 2009), I will give only a brief overview of the structure and focus instead on its relevance to intracellular pathogenicity.

The capsule of *Cryptococcus* is composed of polysaccharides, with the main polysaccharide glucuronoxylomannan (GXM) constituting over 90% of the capsule, and glucuronoxylomannogalactan (GXMGal) constituting the remainder along with mannoproteins (Bose et al., 2003; Doering, 2009; James et al., 1990). This dense capsule prevents recognition of the cryptococcal cell well, 'cloaking' the cell from immune receptors. Many studies have shown that acapsular cryptococci are more readily bound, phagocytosed, and destroyed by macrophages and immune cells compared to encapsulated cryptococci (Chang and Kwon-Chung, 1994; Cross and Bancroft, 1995; Feldmesser et al., 2000; Geunes-Boyer et al., 2009; Levitz and Tabuni, 1991; Siddiqui et al., 2006), illustrating the inhibitory effects of the cryptococcal capsule on immune recognition.

While the cryptococcal capsule represents a barrier between the fungal cell and immune receptors, encapsulated cryptococci may still be phagocytosed. An early study by Levitz et al. claimed that bronchoalveolar macrophage killing of encapsulated cryptococci was greater than for acapsular cells, suggesting that capsule was not a virulence factor early in cryptococcal infection (Levitz and Dibenedetto, 1989). However, in later studies Levitz et al. demonstrated that cryptococci with large capsules were not phagocytosed (Levitz et al., 1997). A study by our group showed that early phagocytosis of cryptococci was necessary for control, as delay in phagocytosis allowed the cryptococci to form large capsules which prevented phagocytosis (Bojarczuk et al., 2016). Thus, while capsule does not fully inhibit early recognition and phagocytosis, growth and extension of cryptococcal capsule prevents further phagocytosis and presents a significant barrier to control of infection.

The early phagocytosis of cryptococci is important for control, as failure to do so allows extracellular growth and production of a thick capsule which interferes with phagocytosis. However, if cryptococci are successfully phagocytosed by macrophages, the pathogen is able to utilise its capsule for intracellular virulence. One study showed that cryptococci with large capsules were more resistant to stress induced by ROS, illustrating that they had the enhanced potential to survive within the destructive macrophage intracellular niche (Zaragoza et al., 2008). Feldmesser et al. showed that only encapsulated cryptococci replicated within murine macrophages which frequently resulted in macrophage cytotoxicity, while acapsular cryptococci failed to proliferate inside of the phagocytes (Feldmesser et al., 2000). Thus, not only does capsule confer prevention of phagocytosis and intracellular resistance to host-induced stressors, it also enables cryptococci to survive and replicate intracellularly, allowing the pathogen to exploit the macrophage intracellular niche.

1.2.3.3 Titan cell formation

Typical *C. neoformans* spores measure 2-3 μm in diameter, while yeast cells are approximately 5 μm in diameter (Velagapudi et al., 2009). This small size allows them to permeate the alveoli of the lung, yet also makes them relatively easy to phagocytose. To compensate for this, cryptococci are able to grow to a larger size, producing titan cells which are 50-100 μm in diameter with thick cell walls and capsules of varying thickness (Zaragoza et al., 2010). Zaragoza showed that these cells are polyploid and divide via budding, and represent up to 10% of the murine lung burden, though at times 70- 90% of cryptococci in the lung had adopted this titan cell morphology when mice were infected with low dose inocula (Zaragoza et al., 2010). Many isolates of *Cryptococcus* are capable of 'titanisation', and recent *in vitro* assays which induced the yeast-to-titan cell switch accurately predicted cryptococcal titanisation of strains *in vivo* (Dambuza et al., 2018). Titan cells resist phagocytosis, and mutant cryptococci which do not form titan cells show reduced dissemination to the brain, illustrating a role for 'titanisation' in dissemination (Crabtree et al., 2012; Okagaki and Nielsen, 2012). Interestingly, titan cells show enhanced resistance to nitrosative and oxidative stress (Gerstein et al., 2015), and the increased stress response and rate of daughter cell formation have been posed as potential mechanisms by which these large cells show augmented dissemination to the CNS (Zhou and Ballou, 2018).

1.2.3.4 Extracellular vesicles

Cryptococcus produces extracellular vesicles which contain capsular components, along with pigments, proteins and lipids. One study showed that uptake of these vesicles by macrophages induced the increased production of NO, TNF-α, TGF-β, and IL-10, suggesting that these vesicles activated macrophages to modulate their activity (Oliveira et al., 2010). Interestingly, vesicles produced by acapsular cryptococci induced stronger macrophage fungicidal activity, suggesting that cryptococcal capsule may produce vesicles which pacify the destructive activity of macrophages (Oliveira et al., 2010). Vesicles have also been shown to induce rapid intracellular proliferation of *C. gattii* within macrophages. The hypervirulent *C. gattii*

outbreak in Vancouver and the Pacific Northwest (PNW) is characterised by increased intracellular replication associated with an upregulation of mitochondrial genes, resulting in the cryptococcal mitochondria appearing tubular (Ma et al., 2009). *C. gattii* of this phenotype participate in 'division of labour' in which some intracellular cryptococci respond to the host phagosome by 'tubularising' their mitochondria to resist stress in a quiescent state, yet conferring enhanced proliferative ability to other cryptococci during co-infection (Voelz et al., 2014). These hypervirulent *C. gattii* secrete extracellular vesicles which traffic to the phagosome and induce increased proliferation, dependent upon RNA and proteins contained within an intact vesicle (Bielska et al., 2018). Thus, while extracellular vesicles induce macrophage activation and modulation in *C. neoformans* infection, they are secreted by the hypervirulent outbreak *C. gattii* to enact a 'division of labour' program to enhance intracellular proliferation.

2.3.5 Additional virulence factors

Cryptococcus has developed additional virulence factors which are important for its survival in the stressful host environment. Melanin is a pigment produced by *C. neoformans* in the presence of L-dopa. A melanin-deficient mutant of *C. neoformans* was more susceptible to killing by oxygen- and nitrogen radicals, demonstrating the role for melanin in scavenging radicals to protect the fungal cells from host-induced damage (Wang et al., 1995). Cryptococcal laccase oxidises L- and D-DOPA to produce melanin, thus contributing to protection from stress (Eisenman et al., 2007), and is also involved in the production of fungal eicosanoids, lipid signalling molecules which *Cryptococcus* produces to interfere with host macrophage signalling and enhance intracellular parasitism (Chapter 3). Phospholipase B is also involved in the production of cryptococcal eicosanoids (Chen et al., 1997b, 1997a), and is associated with virulence (Cox et al., 2001), dissemination (Chen et al., 1997a; Santangelo et al., 2004a), and intracellular parasitism (Evans et al., 2015, 2019). Urease is involved in transgression of the blood-brain barrier and requires a functional calcium transporter to transmigrate across the BBB and survive within the brain parenchyma (Shi et al., 2010; Squizani et al., 2018). While there are more

factors and strategies which enable the pathogenicity of *Cryptococcus neoformans*, the effective virulence of this pathogen largely relies on its relationship with the host immune system.

1.3. Immune response to cryptococcal infection

1.3.1 Immune cells during *Cryptococcus* infection

As *Cryptococcus* causes such devastating disease it is important to understand the roles that immune cells play in limiting infection. Because I will discuss the roles of different immune cells in fighting cryptococcal disease in depth in chapter 6, I will mention them only briefly here. Studies which produce immune cell-deficient models have enabled the elucidation of the relative contribution of different cell types to fighting cryptococcal infection. For example, *C. neoformans* infection in B cell-deficient mice showed that these mice were able to contain infection (Wozniak et al., 2009), and mice lacking neutrophils showed no change in pulmonary fungal burden compared to wild type (Wozniak *et al.*, 2012), indicating that these cells do not significantly control fungal load or contribute to clearance of *C. neoformans*. Mice infected with *C. neoformans* after NK cell depletion showed survival similar to control mice, even though initial fungal burden was higher in NK cell-depleted mice which were infected intravenously (Lipscomb et al., 1987). However, NK cells have improved degranulation in the acidic environment of *Cryptococcus* aggregates, suggesting a role in the active clearance of both *C. neoformans* and *C. gattii*, even when aggregated into cryptococcomas (Islam et al., 2013). Finally, studies have shown that dendritic cells phagocytosed and killed opsonised cryptococci, and also presented cryptococcal antigen on their surface after TLR9-activation, thus facilitating further immune activation (Kelly et al., 2005; Nakamura et al., 2008).

The high incidence of cryptococcal infections in people diagnosed with HIV/AIDS points to a requirement for T cells for control. An early study showed that mice lacking CD4+ T cells had increased brain colonisation, and in mice immunised with cryptococcal antigen the most common immune cells in the brain were CD4+ T lymphocytes and macrophages (Buchanan and Doyle, 2000). A similar study challenged T cell-deficient mice with cryptococcal infection, and resulted in 100% mortality; conversely, immunised mice which survived secondary challenge showed an associated increase in CD4+ T cells in the lungs (Wozniak et al., 2009). This suggests that T cells are required for an effective immune response against

cryptococcal infection. However, a more recent study showed that while CD4+ T cells produce cytokines important for the control of cryptococcal infection, they also contribute CNS immunopathology, demonstrating the requirement for the tight control over the T cells in response to infection (Neal et al., 2017). While CD4+ T cells provide activation stimuli to several immune cells, perhaps one of the most important roles that they play during control of cryptococcal infection is the activation of macrophages, the primary phagocytes which respond to cryptococcal threat.

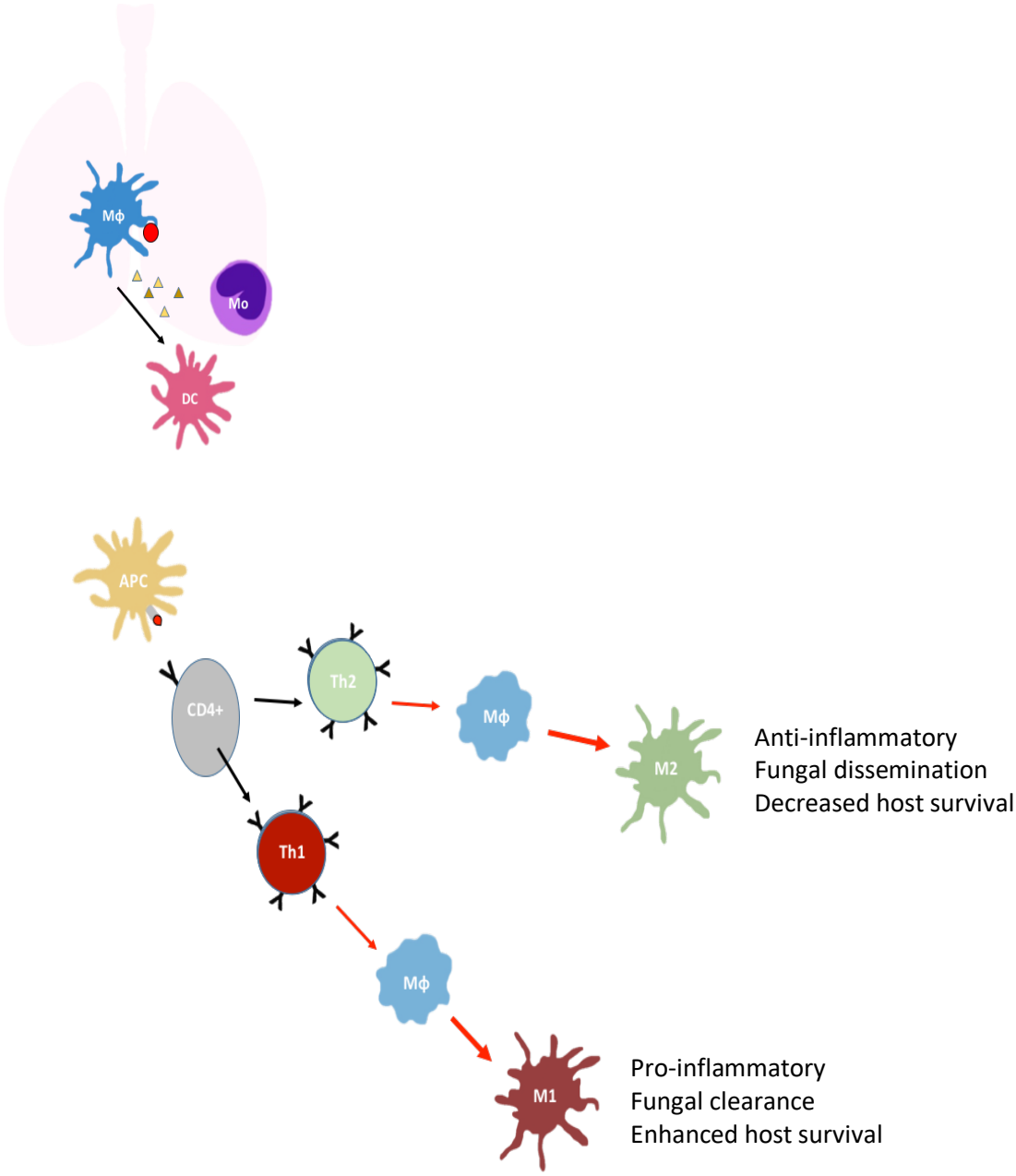

Figure 1.4. Immune cell interaction and activation during *Cryptococcus* infection

Once in the lung, cryptococci (red circle) are met by alveolar macrophages (Mϕ) which are thought to engulf them in immunocompetent hosts. Upon the release of chemokines and cytokines (triangles), additional innate immune cells such as dendritic cells (DC) and monocytes (Mo) are recruited to process and present antigens to the adaptive immune system. Eventually, adaptive immune cells such as B cells and T cells are recruited. After CD4+ T cells (CD4+) are activated by antigen presenting cells (APC) via presentation of pathogenic antigen and stimulation by costimulatory molecules, CD4+ T cells adopt a Th1/Th17 (here just represented as Th1 for simplicity) or a Th2 phenotype. Th1 and Th2 cells stimulate naïve macrophages to become M1 or M2 macrophages, respectively.

1.3.2 Cytokines during *Cryptococcus* infection

As cytokines are important in driving the immune response, I will now discuss their relevance to the infection progression during cryptococcal infection. I will then describe how cytokine profiles differentially activate macrophages, and how these different polarisation states impact the control of cryptococcal infection.

1.3.2.1 Th1 Cytokines

With evidence supporting the requirement for CD4+ T cells in combatting cryptococcal infection, knowing the CD4+ cytokines involved is critical for understanding of immune interactions and infection outcomes in cryptococcosis. The adoption of a Th1 versus a Th2 phenotype during infection determines if the immune response will be pro- or anti-inflammatory, respectively (Figure 1.4). In cryptococcal infection a Th1 response is advantageous for the development of a robust pro-inflammatory immune response and host survival. After 'immunising' mice with cryptococci which produced IFN-γ (H99γ), Wozniak and colleagues showed that pro-inflammatory Th1 cytokines and chemokines were increased in the lungs of these protected mice; these mice survived a secondary challenge with the pathogen, and showed reduced production of Th2 cytokines and chemokines (Wozniak et al., 2009). A later study showed that mice immunised with H99γ and subsequently challenged with *Cryptococcus* had increased levels of Th1 (IFN-γ, IL-2, IL-12) and pro-inflammatory (IL-1, IL-17, TNF-α) cytokines compared to non-protected mice, and that protected mice had increased survival and reduced fungal load in the brain and lungs (Van Dyke et al., 2017). In looking at cytokines and chemokines in the CSF of immune and non-immune mice, Uicker et al. showed that CD4+ T cells, and other cells that produce IFN-γ, were present at higher levels in mice immune to cryptococcal infection, suggesting a role for IFN-γ in the protective immunity against *C. neoformans* (Uicker *et al.*, 2005). Furthermore, in depleting CD4+ T cells, IFN-γ levels declined, suggesting that the source of IFN-γ in CSF infiltrates in infected mice was mainly CD4+ T cells. In these studies, immunisation with a cryptococcal strain that produced a pro-inflammatory cytokine resulted in

the adoption of a pro-inflammatory cytokine profile which was associated with the enhanced the survival of infected mice.

Additional Th1 and pro-inflammatory cytokines are also important in combatting *Cryptococcus*. For example, early studies showed that administration of exogenous TNF-α lengthened survival of mice infected with *C. neoformans*, (Kawakami et al., 1996), and neutralising TNF-α hindered both brain and pulmonary fungal clearance (Aguirre *et al.*, 1995; Herring *et al.*, 2002). Furthermore, mice treated with anti-TNF-α antibodies showed reduced levels of IFN-γ and IL-12, illustrating the effect of individual cytokines on the development of a robust immune response (Herring et al., 2002). Similarly, treatment with anti-IL-12 antibodies in a murine model of *C. neoformans* resulted in failure to clear pulmonary cryptococci and reduced Th1 marker expression (Hoag et al., 1997). Administration of Th1 cytokines such as IL-12 are capable of rescuing mice from fatal cryptococcal infections (Koguchi and Kawakami, 2002), and loss of Th1 response results in the induction of a damaging Th2 response instead (Decken et al., 1998).

Cytokine profiles are also associated with survival and clearance in human cryptococcosis patients. A study by Jarvis et al. examined the cytokine profiles of 90 human patients with HIV-associated cryptococcal meningitis. Jarvis found that patients with increased CSF levels of Th1 cytokines IFN-γ and IL-6 not only had increased survival, but produced more robust inflammatory responses and had more rapid clearance of cryptococci from the CSF (Jarvis et al., 2015, 2013). A similar study examining the baseline CSF cytokine levels in AIDS patients infected with *Cryptococcus* associated survival with a Th1 cytokine profile (Mora et al., 2015). Thus, pro-inflammatory cytokines, especially IFN-γ, are important in clearance of cryptococcal infection.

As Th1 cytokines are required for the control and clearance of cryptococcal infection both in murine and human infections, it is necessary to discern how these cytokines modulate and coordinate the protective immune response. Leukocyte recruitment

is one key component of an effective immune response against *Cryptococcus neoformans*. CD4+ T cells are important for immune cell recruitment to infected sites, especially macrophages (Buchanan and Doyle, 2000; Uicker *et al.*, 2006). The expression of IFN-γ is associated with early recruitment of leukocytes (Wozniak et al., 2009) and improved clinical outcomes. IL-12 is involved in leukocyte trafficking early in infection, and also upregulates the levels of IFN-γ mRNA in murine infection (Kawakami et al., 1996b), increasing the numbers and inflammatory effects of recruited cells in a positive feedback loop which upregulates the recruitment and expression of pro-inflammatory cells. Additionally, in the brains of immunised mice there is increased monocyte chemotactic protein-1 (MCP-1) transcript levels compared to the brains of non-immune mice; as MCP-1 is important for the infiltration of monocytes and macrophages, this suggests that the recruitment of macrophages is important in the battle against *C. neoformans* (Jarvis et al., 2015).

1.3.2.2 Th2 cytokines

During cryptococcal infection, the anti-inflammatory effects of CD4+ Th2 cells and cytokines elicit a different outcome from that imposed by pro-inflammatory Th1 cytokines – one dominated by cryptococcal survival and dissemination (Figure 1.4). The main Th2 cytokines with identified roles in *Cryptococcus* infection are IL-4, IL-10, and IL-13. Loss of Th2 signalling is protective for the host, as mice deficient in IL-4 and IL-13 receptors showed lower cryptococcal burden in the brain compared to wildtype infected mice (Stenzel et al., 2009), and infection of IL-4-deficient mice with *C. neoformans* resulted in prolonged survival of the host (Decken et al., 1998). Infection of transgenic mice overexpressing IL-13 showed increased susceptibility to *C. neoformans* compared to wild type mice, yet there was 89% survival in mice deficient in IL-13 (Müller et al., 2007), showing that the presence of this cytokine is detrimental for the host, and its absence is largely protective. These studies provide evidence of the negative effects that Th2 cytokine signalling induces in the host during *C. neoformans* infection, especially the persistence and spread of cryptococcal infection at the expense of host survival. This is particularly problematic as components of *Cryptococcus* itself attract a Th2-dominated

response. For example, one recent study showed that lung-resident dendritic cells recognised cleaved chitin, a component of the fungal cell wall, and induced a strong Th2 response (Wiesner et al., 2015).

The cytokine profile is important in the course of cryptococcal infection especially in patients with HIV because the cytokine profile changes throughout the course of HIV infection. As the disease progresses there is increased HIV burden and decreased CD4+ T cell counts, causing the predominance of IL-4 over IFN-γ. This induces the cytokine profile to switch from Th1 to Th2 (Altfeld et al., 2000), which enables the growth and dissemination of cryptococci. However, it is worth noting that in humans the dichotomous relationship between Th1 and Th2 is less pronounced than in mouse models (Jarvis et al., 2015).

1.3.3 Macrophage activation and polarisation in *Cryptococcus* infection

As discussed above, *Cryptococcus* is most likely inhaled as a spore or desiccated yeast cell into the lung where it meets the tissue resident macrophages - alveolar macrophages. Macrophages have been shown to be important in the control of cryptococcal infection, as macrophage ablation in murine and zebrafish models of *C. neoformans* infection results in the loss of control of cryptococcal growth (Bojarczuk et al., 2016; Shao et al., 2005). However, the interactions between macrophages and cryptococci are complex and can help resolve cryptococcal infection, or lead to its dissemination (Johnston and May, 2013; Mansour et al., 2014; Rudman et al., 2019; Voelz and May, 2010).

The cytokines that a macrophage is introduced to strongly impact the role of the macrophage during infection. Th1 cytokines IFN-γ, TNF-α, IL-12, and IL-6 induce a pro-inflammatory M1 phenotype. The intracellular replication of cryptococci within macrophages treated with Th1 cytokines is lower than for macrophages treated with Th2 cytokines, illustrating that the macrophage intracellular niche is less permissive in M1 macrophages (Voelz et al., 2009). Again, IFN-γ is a key cytokine in the anti-cryptococcal response, as stimulation of macrophages with IFN-γ produces

an antimicrobial effect, killing pathogens including *C. neoformans* (Nathan *et al.*, 1983). Challenge of mice with H99γ *C. neoformans* results in augmented expression of Th1 cytokines and markers, accompanied by classical M1 macrophage activation and enhanced fungal clearance (Van Dyke et al., 2017; Hardison et al., 2012). Knockout of IFN-γ results in the opposite effect, with alternative M2 macrophage activation and progressive cryptococcal infection (Arora et al., 2005).

Indeed, Th2 cytokines induce macrophages to support the growth and dissemination of cryptococcal infection. For example, mice which showed M2 polarisation markers after infection with *C. neoformans* showed cryptococcal intracellular persistence and replication, as well as the upregulation of Arg-1 over iNOS, lowering the fungicidal activity of macrophages during infection as discussed below (Hardison et al., 2010). As such, these mice showed progressive pulmonary infection. Another study showed that administration of the Th2 cytokine IL-4 to J774 macrophages allowed increased intracellular proliferation of cryptococci compared to untreated and Th1-treated macrophages, demonstrating the permissiveness of M2 macrophages to cryptococcal parasitism (Voelz et al., 2009).

Macrophage polarisation is also associated with cryptococcal uptake. A recent study showed that in mice which were infected with clinical isolates of *C. neoformans* which showed a high rate of uptake, macrophages had enhanced M2 gene expression (Hansakon et al., 2019). Sabiiti et al. showed that clinical isolates of *C. neoformans* with high phagocytic uptake by macrophages were positively correlated with high CNS burden (Sabiiti et al., 2014). As M2 macrophages are associated with dissemination, the high levels of cryptococcal uptake and proliferation present means by which the intracellular niche of M2 macrophages is colonised by cryptococci for the propagation of infection.

The metabolic profile of the macrophage, as determined by the polarisation state, has the ability to destroy cryptococci or to upregulate fungal replication. Of particular importance is arginine metabolism. Macrophages activated by Th1 cytokines (M1 macrophages) upregulate inducible nitric oxide synthase (iNOS)

which produces nitric oxide (NO) from arginine. If stimulated by Th2 cytokines (M2 macrophages), the upregulation of arginase (Arg-1) inhibits NO production (Das et al., 2010) and utilises arginine to produce ornithine and polyamines (Hesse et al., 2001). Pro-inflammatory IFN-γ induces macrophages to produce NO (Mills *et al.* , 2000), which kills pathogens, while anti-inflammatory Th2 cytokines such as IL-4 induce macrophages to upregulate Arg-1 which is beneficial for microbial survival and prevents the production of NO (Sheldon et al., 2013). Macrophages infected with IFN-γ-producing *C. neoformans* or treated with IFN-γ showed upregulated iNOS expression and enhanced macrophage fungicidal activity (Davis et al., 2013; Hardison et al., 2010). Conversely, mice with M2 polarisation markers and Arg-1 activity were associated with cryptococcal intracellular proliferation and pulmonary pathogenesis (Hardison et al., 2010). Thus, Th1 cytokines recruit effector cells and activate macrophages to limit cryptococcal growth and activate fungicidal activities, while Th2 cytokines induce M2 polarisation and are detrimental for the host. As such, expression of iNOS and Arg-1 are frequently used as markers to determine activation state (Arora et al., 2011). Additionally, because NO inhibits cell survival and ornithine stimulates cell division, arginine metabolism strongly affects survival of the pathogen and the availability of metabolites such as polyamines needed for cellular function and tissue repair.

While frequently both Th1 and Th2 cytokines are expressed simultaneously, the proportion of one type over the other determines the overall activation state of the macrophages (Arora et al., 2011). However, macrophage polarisation becomes a bit more complicated when you consider suppressive effects. For example, M2 macrophages produce anti-inflammatory cytokines which suppress the production of Th1 cytokines (Stein et al., 1992), with IL-10 having particularly potent suppressive properties (Couper *et al.*, 2008). Thus, with the adoption of an M2 phenotype it is possible not only to propagate infection, but also to prevent the immune system from steering the immune response back to a protective pro-inflammatory reaction. A similar effect is seen with the prevention of a strong M2 phenotype in the presence of sufficiently high levels of Th1 cytokines.

Furthermore, while macrophage polarisation is critical to the outcome of infection it is not steadfast. Throughout the course of *C. neoformans* infection the macrophage polarisation state changes from being strongly M2 polarised at the onset of infection with high Arg-1 and low iNOS mRNA levels, to strongly M1 polarised around weeks 3 and 4, with high iNOS and reduced Arg-1 mRNA expression levels (Davis et al., 2013). This suggests that either new macrophages are activated to reflect the change in activation state, or existing macrophages change their activation state during the course of the infection. Through initially subjecting macrophages to the M2 cytokine IL-4 *in vitro*, and secondarily introducing the M1 cytokine IFN-γ, Davis observed that the existing macrophages were capable of changing their polarisation to the profile induced by the secondary cytokine, regardless of initial cytokine exposure and activation state (Davis et al., 2013). The reverse, a switch from an M1 profile to an M2 profile, is also possible, demonstrating the plasticity of macrophage polarisation required in a variable, changing environment.

1.3.4 Parasitism of the macrophage intracellular niche by *C. neoformans*

The interactions between cryptococci and the host macrophage are complex and variable. These interactions are the frequent topic of review articles (Johnston and May, 2013; Rudman et al., 2019), and are discussed thoroughly throughout chapter introductions and discussions. As such, I will give only a brief overview of macrophage-*Cryptococcus* interactions here.

C. neoformans is a facultative intracellular pathogen capable of survival both within macrophages and in the extracellular environment (Feldmesser *et al.*, 2000). Cryptococci invade the macrophage intracellular niche as it represents safety from the antimicrobial peptides, enzymes, and granules secreted by various immune cells in the extracellular environment. The cryptococcal capsule and melanin pigment protect cryptococci from harsh stresses imposed by the macrophage intracellular niche (Wang et al., 1995; Zaragoza et al., 2008), and after phagocytosis *C.*

neoformans can survive within the acidic phagolysosome (Levitz et al., 1999). The ability of *Cryptococcus* to proliferate within macrophages has long been recognised (Diamond and Bennett, 1973), and while early in infection the presence of cryptococci inside of macrophages is associated with phagocytosis, after 24h it is associated with replication and cytotoxicity to macrophages (Bojarczuk et al., 2016; Feldmesser et al., 2000).

After exploiting the macrophage intracellular niche for replication, cryptococci are able to exit the macrophage to disseminate infection extracellularly. In a murine macrophage model of infection it was shown that *C. neoformans* can transfer between macrophages, and can extrude from the macrophage in numbers large enough to form a massive vacuole, damaging the macrophage in the process (Alvarez and Casadevall, 2007). Cryptococci can also exit macrophages without killing the host cell even many hours after phagocytic uptake, a phenomenon which has been observed in both murine and human macrophages and has since been termed 'vomocytosis' (Alvarez and Casadevall, 2006; Ma et al., 2006). The host macrophage attempts to combat this escape through the use of actin 'cages' (Johnston & May, 2010), yet *Cryptococcus* is still able to escape the macrophage via fusion between the *Cryptococcus*-containing phagosome with the macrophage cell membrane. Thus, cryptococci replicate within the macrophage intracellular niche, then exit the host cell to propagate infection extracellularly.

Studies have shown that while macrophages may control cryptococcal infection, they may also facilitate the systemic dissemination of *C. neoformans*, especially to the CNS. Charlier et al. showed that there was a higher brain fungal burden in mice inoculated with monocytes infected with *C. neoformans* compared to mice inoculated with free yeast (Charlier et al., 2009). This study suggested the potential for macrophages to carry cryptococci to the CNS to disseminate infection and cause cryptococcal brain pathologies such as meningitis and meningoencephalitis. Furthermore, *Cryptococcus* has been observed in macrophages in the leptomeningeal spaces in mice with cryptococcal fungaemia (Chretien et al., 2002), further condemning macrophages for their involvement in invasion of the blood

brain barrier. However, while macrophages are implicated in dissemination and CNS invasion, they also form protective granulomas around sites of infection (Shibuya et al., 2005), demonstrating the different possible roles that macrophages may play in the outcome of cryptococcal disease.

1.4. Thesis objectives

Cryptococcus neoformans causes devastating infection in humans. As this pathogen is able to both evade and exploit host macrophages, learning how *Cryptococcus* interacts with macrophages, and how it manipulates this host intracellular niche, are key to understanding its pathogenicity and may eventually lead to the development of effective immune therapies which lead to its control. While current studies have examined the relationship between macrophages and cryptococci in detail, there remain specific aspects, particularly detailed quantification, that remain unknown. The effect of fungal dose on macrophage response must be investigated to understand how macrophages respond to infection as the multiplicity increases, illuminating potential activating and inhibitory effects of fungal dose on macrophage behaviour. The rates of cryptococcal intracellular and extracellular replication must be carefully considered, as these rates may affect macrophage-*Cryptococcus* interactions and determine the course and outcome of infection. The mechanisms by which cryptococci manipulate the macrophage intracellular niche must be investigated to understand how this intracellular pathogen is able to exploit the host cells which are tasked with their destruction. And finally, understanding how cryptococci interact with a robust host immune cohort may illuminate the role that phagocytes play in a situation more representative of real-life infection. Understanding how all these factors vary may illuminate how the macrophage intracellular niche produces complex outcomes during *Cryptococcus neoformans* infection.

With the ultimate goal of understanding how the relationship between *C. neoformans* and macrophages guides the progression of infection and produces complex infection outcomes *in vivo*, the aims of my thesis are as follows:

1. To understand the role of lipid mediators in fungal virulence. To investigate this, I used a wild type (H99) and a prostaglandin mutant strain (*Δplb1*) of *Cryptococcus* in order to:
    a. Interfere with host COX signalling to determine if host, or fungal, eicosanoids account for virulence

b. Utilise a CRISPR-Cas9 knockdown to investigate the contribution of host prostaglandins to final fungal burden *in vivo*
c. Investigate the production of PPAR-γ by cells infected with the wild type and mutant strains of *Cryptococcus*

2. To determine if the outcome of macrophage-*Cryptococcus* interactions are affected by varying the multiplicity of infection (MOI):
    a. Determine if increasing MOI affects uptake of cryptococcal cells
    b. Determine if increasing MOI alters the replication of cryptococci
    c. Compare these measures between murine and human macrophages

3. To determine if infection burden relates to infection outcome *in vivo,* and to combine *in vitro*, *in vivo*, and computational models of infection to understand macrophage-pathogen interactions and their contribution to complex infection outcomes:
    a. Perform low fungal burden zebrafish infection assays to simulate early infection
    b. Produce a range of initial infection burdens to understand potential relationships between initial and final infection burden
    c. Use *in vitro* infection to determine the growth rates of cryptococci which are intracellular and extracellular
    d. Aid in the production of a computational model of infection to better understand *Cryptococcus*-macrophage interactions and to understand how the macrophage niche influences infection dynamics

4. To investigate cryptococcal growth in an 'immunocompetent' model of infection using human PBMCs to model immune cell swarm, or granuloma, formation:
    a. Characterise the uptake and replication rates of cryptococci in human PBMC infection
    b. Characterise the swarming of human PBMCs

Chapter 2. Methods

2.1 Ethics Statement

All work on zebrafish was carried out according to legislation and guidelines set by UK law in the Animals (Scientific Procedures) Act 1986 under Project Licenses 40/3574 and P1A4A7A5E.

2.2 *Cryptococcus neoformans*

2.2.1 *Cryptococcus* strains

For examination of the contribution of fungal prostaglandins to macrophage parasitism (Chapter 3) *C. neoformans* var. grubii (serotype A) strain H99 GFP was used (Voelz et al., 2010). For phospholipase B1 mutant experiments, the *PLB1* knockout strain of H99 *Δplb1* GFP was used (Cox et al., 2001), with wildtype H99 used as a control. To examine cryptococcal infection progression (Chapters 4, 5, and 6), *Cryptococcus neoformans* var. grubii, strain KN99 GFP, was used. This strain of *Cryptococcus* is more representative of *C. neoformans* isolates compared to the H99, which is more widely studied but which uniquely has two large genetic translocations that affect glucose metabolism and melanin production, as well as several additional rearrangements resulting from laboratory microevolutionary processes (Janbon et al., 2014; Lam et al., 2016; Morrow et al., 2012).

2.2.2 Storage, rescue, and culture

For long term storage strains were stored in MicroBank vials at -80°C. When needed for use, strains were streaked onto YPD agar plates (YPD 50 g/L Fisher, 2% agar Sigma-Aldrich) and incubated for 48 hours at 28°C to allow the cells to grow and form colonies. These plates were then stored at 5°C until use. The day before injection, cryptococci were scraped from the YPD plate and suspended 2 ml of YPD broth. This was then left overnight at 28°C, rotating horizontally at 20 rpm.

1 ml of KN99 GFP *Cryptococcus neoformans* suspension was removed from the overnight preparation and was washed and pelleted using a centrifuge (3300g for 1

minute). The supernatant of YPD was removed, and cells were resuspended in phosphate buffered saline (PBS). This process of washing was repeated three times. Cells were then diluted 1/20 and counted using a haemocytometer. The number of cryptococci per ml was determined, and cryptococci were diluted to the required concentration (colony forming units per ml (cryptococci/ml)).

2.2.3 Culture viability assays

To determine if *C. neoformans* used for infections were viable, cultures were prepared and washed as above. Cryptococci were diluted to contain 50 cryptococci in 25 μl PBS. 25 μl were then plated on YPD plates, and plates were incubated at 28°C for 48 hours. Colonies were then counted, and the number of colonies was averaged amongst replicates. The percentage of expected colonies which formed was calculated and compared across repeats and between strains.

2.2.4 *Cryptococcus* for *in vivo* infections

For injections, after washing and dilution, cryptococci were resuspended in 10% PVP (polyvinylpyrrolidone, Sigma-Aldrich) in phenol red and diluted to produce the appropriate inoculum. For the *ptges/tyro* assays (Chapter 3) cryptococci were prepared at 500 cryptococci per nl. For low infection clearance assays (Chapter 5), an inoculum of 10 cryptococci per nl was produced. For fungal burden assays 10, 100, 250, 500, and 1000 cryptococci per nl were required. Cells were mixed using a pipette and not through use of a vortex, as vortexing the cryptococci causes damage to the cells. Cells were mixed before loading new needles as cryptococci settle at the bottom of the tube, and mixing allows for injection of consistent numbers of cryptococci.

2.2.5 Opsonisation

For flow cytometry and time lapse experiments the cells were opsonised using 0.1 μl of 18B7 (anti-capsule monoclonal antibody) per 100 μl of *Cryptococcus* and were left to opsonise on a rotator for one hour.

2.2.6 *Cryptococcus* for flow cytometry and time lapse assays

For flow cytometry and time lapse assays 10^2-10^6 cryptococci were required, depending on the assay. Cryptococcal dilutions were prepared at 10x the required concentration, opsonised, then diluted in the required media to 1x required concentration, mixed, and added to cells. This minimised waste of opsonising antibody and ensured cell preparations were homogenous before addition to macrophages.

2.2.7 Growth in media

For comparison to time lapse assays, *Cryptococcus neoformans* was prepared at 10^5 cryptococci/ml in various media and plated in a plastic 24 well plate. Cryptococci were given 1 hour to settle, and were then imaged for 18 hours at x20 magnification, using phase imaging with perfect focus. An image was taken every 2 minutes using both the differential interference contrast (DIC) and GFP channels. The replication of cryptococci was determined by following individual cryptococci over the course of the time lapse, and budding was quantified. Doubling time was calculated by fitting an exponential curve to the data in GraphPad Prism (version 7).

2.3 Zebrafish infections

2.3.1 Husbandry and care of zebrafish embryos

For *ptges* and *tyro* CRISRP/Cas9 experiments, *nacre Danio rerio* (Lister et al., 1999) larvae were used for infection. *Tg(mpeg1:mCherryCAAX)sh378 Danio rerio* embryos (referred to here as mPEG mCherry CAAX) (Bojarczuk et al., 2016) were used for the low dose and high dose clearance assays, as well as for clodronate liposome experiments.

Adult zebrafish were kept in UK Home Office approved facilities in the Bateson Centre aquaria at the University of Sheffield. They were maintained on a 14:10-hour light:dark cycle at 28°C. Larvae were obtained using marbling tanks, and underdeveloped/damaged embryos were disposed of using bleach. Acceptable embryos were stored 60 per plate in E3 (1X E3 with methylene blue to avoid fungal growth in culture) from 0 days post fertilisation (dpf) and stored at 28°C. Embryos were dechorionated 1 dpf. See Figure 2.1 for zebrafish timeline.

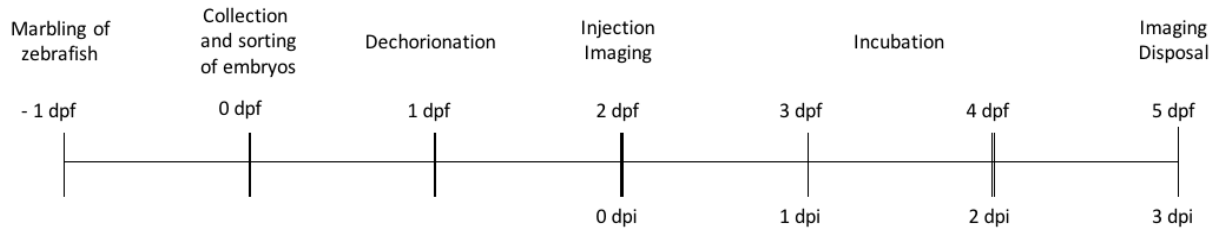

Figure 2.1. Timeline of zebrafish larvae experimental life.

Marbling tanks were placed in the tanks of adult zebrafish in the afternoon, and the embryos were collected the following morning, considered 0 days post fertilisation (dpf). Embryos were dechorionated 1 dpf, and larvae were injected and imaged 2 dpf (0 dpi). Larvae were imaged again 5 dpf (3 dpi) and disposed of in bleach before noon, as larvae may not be used for experiments after day 5.2 when they become protected animals under UK law in the Animals (Scientific Procedures) Act 1986, and a license is required to perform experiments after this point.

2.3.2 Needle and microinjector preparation

Injection needles were prepared by pulling glass capillaries (World Precision Instruments) using an electrode puller (heat 380, pull 200, velocity 199, time 200, pressure 500). Before the time of injection needles were bevelled to produce a fine, sharp point, allowing for the precise injection of infectious agent without causing extraneous harm to the fish. Needles were manually loaded with *Cryptococcus neoformans* and inserted into the microinjector.

Once glass needles were bevelled, loaded, and inserted into the microinjector, the pressure and injection time was calibrated to allow for the injection of a precise volume of *Cryptococcus* cell suspension. Using a graticule slide and mineral oil, the microinjector was calibrated to inject 1 nl of *Cryptococcus* preparation in two pumps to ensure that the correct volume of agent was dispensed without using too much pressure so as to cause unnecessary harm to the fish. Every time a new needle was prepared the calibration step was repeated. This ensured that a consistent volume was dispensed each time and corrected for inconsistencies in the bevelling of the needle.

2.3.3 Infection of zebrafish larvae

CRISPR/Cas9 injections were prepared as stated previously (Loynes et al., 2018). Guide RNA spanning the ATG start codon of zebrafish *ptges* or *tyr* was injected along with Cas9 protein and tracrRNA. CRISPR/Cas9 was injected at the single cell stage at 0 dpf (Evans et al., 2019).

When required, zebrafish larvae were injected with room temperature clodronate or PBS liposomes via the caudal vein at 1 dpf, 24 hours before infection with cryptococci. This ensured that there was time to deplete macrophages before the introduction of infection.

Zebrafish larvae were injected with *C. neoformans* at 2 dpf when blood vessels and circulatory systems had been established. This allowed *Cryptococcus* cells to

disseminate throughout the body of the fish, causing a systemic infection. Larvae were anaesthetised using tricaine (4.2% in E3). Fish were placed on E3 agar plates using a glass pipette. No more than 15 fish were added to a plate at any one time to ensure that they didn't dry out in the time that it took to inject. Larvae were injected via the duct of cuvier and were briefly monitored to ensure that injection was successful and that cryptococci entered the circulation. Larvae which were damaged or mishandled were disposed of in bleach. Minimal handling of the larvae was required.

Where more than one inoculum was injected the order of injection of each of the doses was randomised to ensure the same quality of injection performance across cryptococcal levels and repeats. Larvae were also mixed before plating to ensure no bias in imaging. PVP injections were also performed as an injection control. Once successfully injected, larvae were removed from the injection plate and placed in fresh E3, allowing them to recover from the tricaine. Here they recovered for at least 30 minutes at 28°C. See Figure 2.2 for clarification. Larvae were added to 96 well plates and imaged as described below.

2.3.4 Preparation of zebrafish embryos for imaging

At 2 dpf larvae were anaesthetised using 4.2% tricaine in E3. Injections were performed as described, and infections were followed by imaging of larvae. For low and high dose clearance assays (Chapter 5) a 2% agar (Sigma-Aldrich) was prepared and 100 μl was placed in each well of a glass bottom 96 well plate. After setting, a section of the agar was removed in a rectangular shape to hold each larva in a defined area. This allowed for imaging while reducing potential space for movement, should any larvae awaken from the tricaine. The larvae were then individually placed in the wells of the 96 well plate and positioned. This was achieved using a 20 μl GELloader loading tip. This technique was only utilised for imaging larvae which were 0 days post infection (dpi).

After imaging on 0 dpi, larvae were removed from the glass bottomed 96 well plate and gently washed of tricaine in fresh E3. Larvae were then placed in a fresh plastic 96 well plate in clear E3. Positions and numbers of cryptococci 0 dpi were recorded for each larva, allowing for examination and comparison of infection of known larvae at 3 dpi. Larvae were then kept at 28°C until 3 dpi. Larvae with no confirmed *Cryptococcus* cells were no longer considered and were disposed of in bleach. See Figure 2.2 for clarification.

At 3 dpi a 1% preparation of low gelling agarose and tricaine was prepared and warmed to 37°C. Larvae were anaesthetised and placed into a fresh glass bottom 96 well plate. Excess liquid was removed and the larvae were individually mounted in the low gelling agarose. This technique was used for larvae at 0 and 3 dpi for clodronate liposome assays, as well as for ptges/tyro CRISRP/Cas9 knockdown assays, with a 0.5% agarose solution used on 0 dpi. Larvae were then imaged. Larvae were not kept beyond day 5.2. Larvae were disposed of in bleach at 3 dpi (5 dpf).

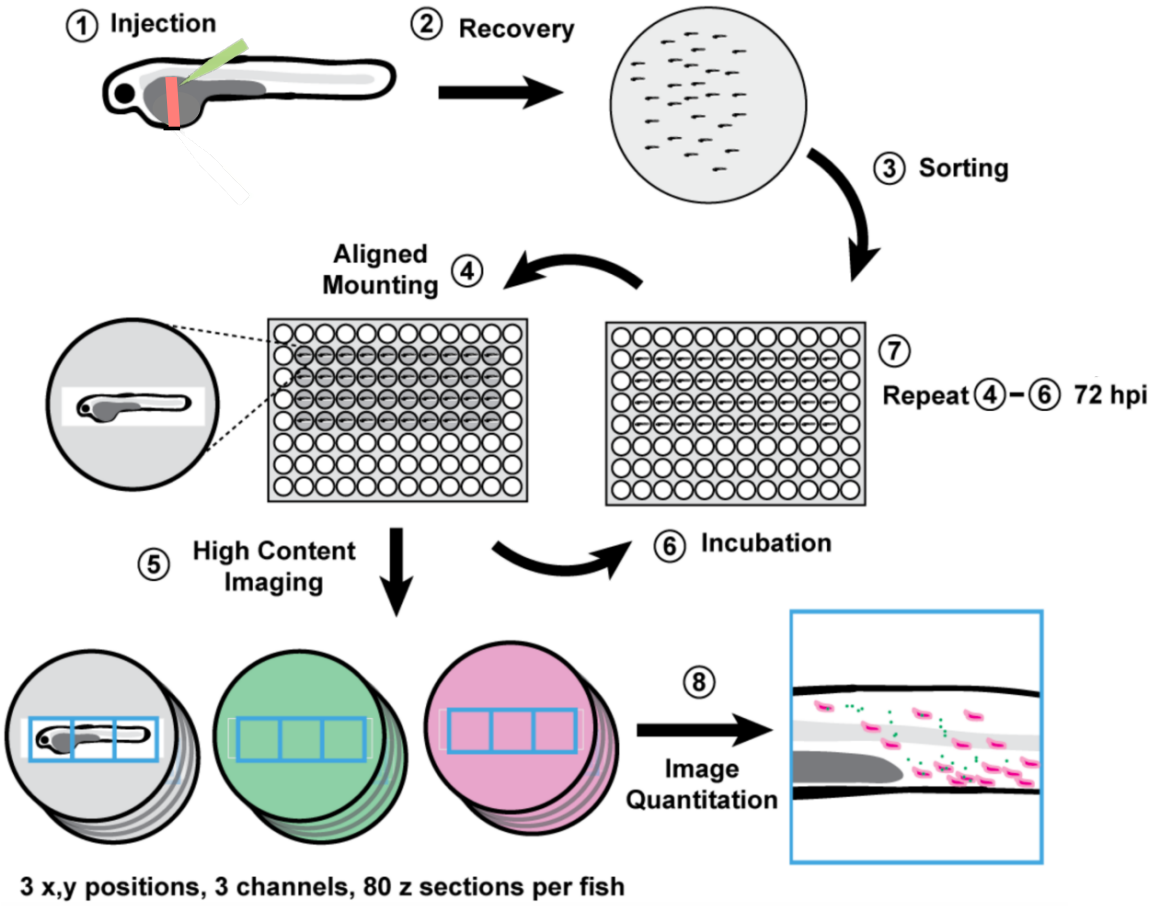

Figure 2.2. Mounting and imaging of zebrafish larvae.

1) Larvae are injected into the duct of Cuvier (pink region).

2) Larvae recover in fresh E3.

3/4) Larvae are loaded into 96 well plates with agar spaces cut to reduce thrashing, or in 0.5% low gelling agarose.

5) Larvae are imaged 0 dpi (fungal burden assays only) with DIC, GFP, and mCherry channels.

6) Larvae are placed in plastic 96 well plate after recovery in fresh E3, kept in incubator.

7) Repeat of mounting in 1% low gelling agarose 3 dpi.

8) Image quantitation and analysis (red are macrophages, green are cryptococci).

Image adapted from Bojarczuk et al., 2016.

2.3.5 Imaging and analysis of zebrafish larvae

Epifluorescence Nikon Eclipse TI microscope and NIS Elements 4.51 analysis software were used to image the larvae.

Larvae were imaged at x2 magnification for *ptges*/*tyro* knockdown (Chapter 3), for high dose fungal infection (Chapter 5), and for clodronate liposome experiments (Chapter 5). DIC and GFP channels were used for these experiments. Images were taken to compare 0 and 3 dpi fungal burdens. A mono image for each channel was produced using NIS Elements 4.11.01 analysis software. GFP mono images were then analysed using FIJI 2.0.0. A threshold was applied to each larva, producing black pixels where green fluorescent pigment is present, including the yolk and frequently the eye. A polygon region of interest was drawn around the total cryptococci per larva, excluding background fluorescence from the yolk and eye. The area of pixels was then measured and compared between 0 and 3 dpi for each larva, providing a relative measure of fungal burden for individual fish between the three days.

Larvae were imaged at x10 magnification for low dose infections (Chapter 5), using DIC, GFP, and mCherry channels, and the entirety of each fish was examined for the presence of cryptococci 0 dpi. The number of *Cryptococcus* cells per fish was recorded. 3 dpi embryos were imaged using DIC, GFP, and mCherry channels. Each individual larva was imaged three times; once in the head region, once in the trunk region, and once in the tail region. This ensured that each portion of the zebrafish was imaged at a magnification sufficient to identify individual cryptococci. Larvae were imaged through the Z plane to image cryptococci throughout the whole depth of the fish. 81 steps were taken every 5 μm to produce a total Z range of 400 μm. No time settings were necessary. Images were analysed in NIS Elements 4.51 analysis software. Utilising the GFP channel images, individual cryptococci were counted manually. The number of cryptococci counted at 0 dpi and 3 dpi were plotted in GraphPad Prism 7.

2.3.6 Zebrafish genotyping

DNA extraction

After completion of imaging zebrafish larvae were anaesthatised with 4.2% tricaine. 100 μl of 50mM NaOH was added at 95°C for 10 minutes in the PCR machine. This was cooled on ice for 5 minutes before the addition of 10 μl of 1M Tris-HCl (pH 8.0). This was vortexed and excess liquid was removed.

PCR

Primers were designed as described previously (Evans et al., 2019; Loynes et al., 2018). Genomic DNA was amplified with primers spanning the ATG site of *ptges*. PCR samples were prepared as follows:

1 μl gDNA (above)

1 μl ptges gRNA F1 forward primer (gccaagtataatgaggaatggg)

1 μl ptges gRNA R1 reverse primer (aatgtttggattaaacgcgact)

4 μl firepol

13 μl water

PCR was run as follows:

Initial denaturation 95°C for 3 minutes

Denaturation 95°C for 30 seconds

Annealing 60°C for 30 seconds

Repeat denaturing and annealing for 39 cycles

Elongation 72°C for 30 seconds

Final elongation 72°C for 5-10 minutes

Digest and electrophoresis

0.5 μl of Mwol was added to digest the PCR product. This was incubated at 60°C for 2 hours. 20 μl of digest products were run in 2.5% agarose gel (see appendix) for 45 minutes at 100 volts. Mwol cleaved DNA at two sites. Wild-type digests produced bands at 184, 109 and 52 bp. Heterozygous (*ptges*$^{+/-}$) produced bands at 293, 184, 109, and 52 bp. Homozygous (*ptges*$^{-/-}$) produced bands at 293 and 52 bp. Gels were then imaged.

2.4 J774 macrophage infection

2.4.1 J774 preparation

J774 murine macrophages were used to study cryptococcal-macrophage interactions because these macrophages are a widely used and robust model for Cryptococcus infection (Alvarez & Casadevall, 2007; Feldmesser et al., 2000; Johnston & May, 2010; Ma, 2009; Voelz et al., 2009; Voelz et al., 2010). Mouse J774 macrophages were prepared in complete medium (see 'freeze down media' in appendix) and kept in liquid nitrogen. For use, J774 cells were brought to 37°C and the complete DMEM was removed. The macrophages were resuspended in fresh complete DMEM that had been brought to 37°C in a T25 flasks and kept in an incubator at 37°C and 5% CO_2. This ensured the proper temperature and pH for macrophage survival and growth. Cells were resuspended and passaged in T75 flasks until at least the third passage when the macrophages were considered healthy and robust enough to be suitable for experiments. Macrophages were no longer utilised after the 14^{th} passage. Cells were checked for contamination and confluence before each passage and during each experiment.

For the experiments described, 10^5 macrophages were used per well, providing enough macrophages to observe a significant number of events without preparing too many as to cause cell death. The media was removed from the macrophages carefully without dislodging any macrophages from the base of the flask. Fresh complete DMEM was added and the macrophages were scraped off from the base of the flask using a cell scraper. Excessive scraping was avoided to prevent damage to the macrophages. Neat macrophages were counted using a haemocytometer, and the number of macrophages per ml was determined. These cells were diluted to 10^5 macrophages/ml, and 1 ml of this preparation was added to each required well of a 24 well plate. Cells were left in the incubator over night for use the following day.

2.4.2 J774 activation and infection

Media was removed from each well and 1 ml of fresh serum free media was added (see appendix). Phorbol myristate acetate (PMA) was diluted 1/100 to produce 0.01mg/ml, and 15 ul of this PMA was added per ml of media in each well. This was left in the incubator for 50 minutes. Macrophages were checked for general health and activation after 50 minutes. Cryptococci were then added at the appropriate concentration, and plates were placed in the incubator to allow infection for 2 hours.

Extracellular *Cryptococcus* were removed so that only engulfed cells were considered. Media was removed from the wells, and 37°C PBS was carefully added to each well to rinse off extracellular cryptococci, removed, and added again. This was done three times. This process was not completely efficient and inevitably left some extracellular cryptococci, but did remove the majority of extracellular cryptococci. Cells were then imaged as prescribed.

2.4.3 J774 harvest for flow cytometry

In the case of flow cytometry experiments the macrophages were harvested from the plate. PBS was removed from the wells after washing, and 200 ul of accutase (Sigma) was added. This was left for 5 minutes, giving the accutase time to dislodge the cells from the wells. 800 μl of PBS was added, and the wells were washed by pipetting the liquid up and down. 1 ml of macrophages was removed from each well. At the end of all macrophage experiments plates were bleached using Rely+On Virkon disinfectant to kill any cryptococci in the wells.

2.4.4 Performance and analysis of flow cytometry

Flow cytometry was performed using Attune™ Nxt acoustic focusing cytometer (Life Technologies and Attune™ NxT Software v2.5). Each sample was prepared and harvested as above. Samples were mixed by hand, and 200 μl was run through the flow cytometer. The macrophage population was determined by known size and complexity characteristics. Macrophages constitute region 1 (R1) in Figure 2.3. From

this population, macrophages with increased GFP fluorescence (BL1A) were determined to be those containing KN99 GFP *Cryptococcus neoformans*. This was designated R3, while those macrophages with lower levels of fluorescence were considered macrophages lacking internalised cryptococci (R2).

To determine *Cryptococcus*-positive and –negative populations, KN99 WT and KN99 GFP *Cryptococcus* were measured without macrophages. In infected macrophage samples a gate was drawn around the positive (GFP) population to provide the total number of GFP-positive macrophages in each sample – the total number of cells containing *Cryptococcus* (R4). See Figure 2.3 for details.

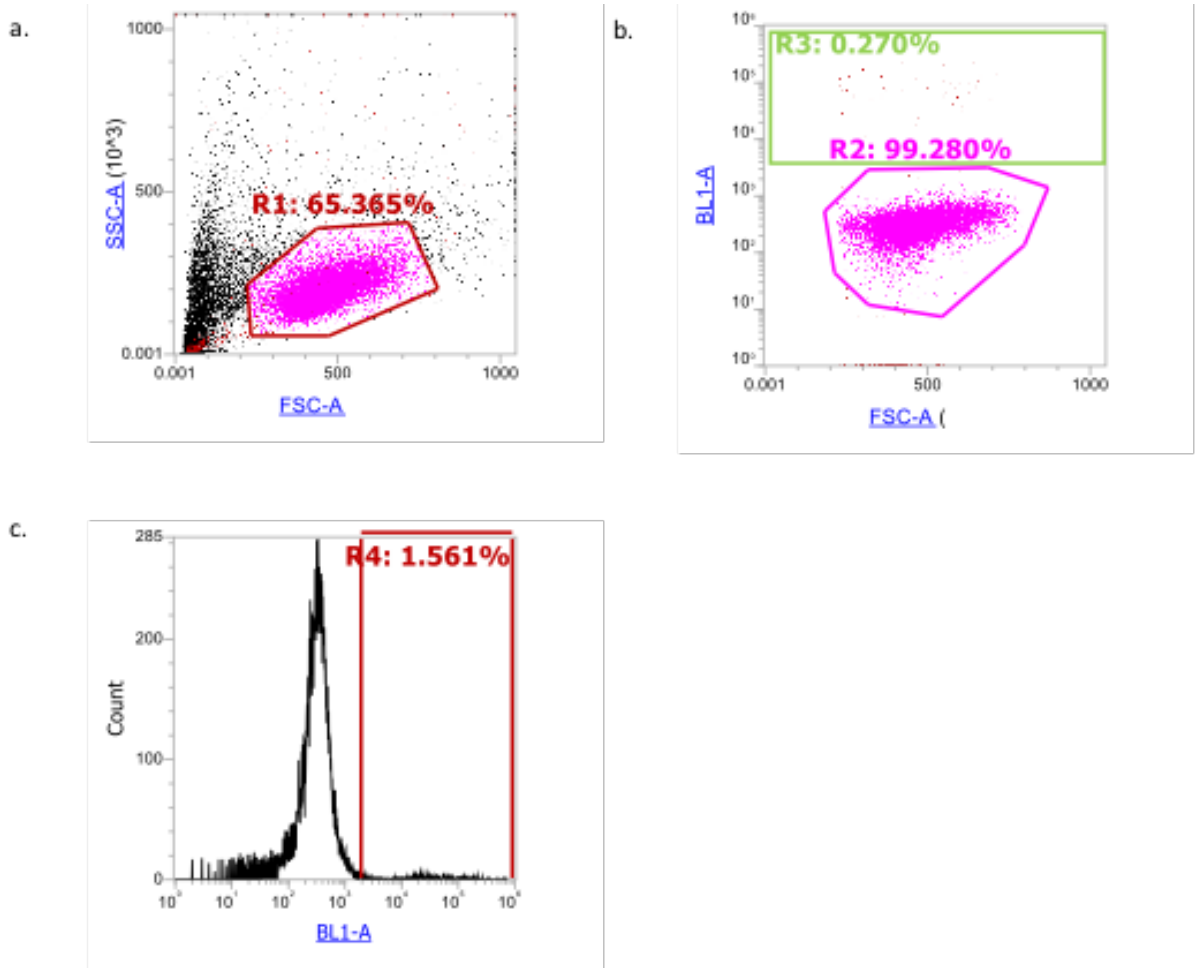

Figure 2.3. Analysis of flow cytometry.

Regions were drawn for all macrophages (R1) based on a sample containing only macrophages. From this region, macrophages were gated according to GFP expression (BL1-A). Those without internal GFP cryptococci and therefore expressing only low background GFP expression (R2) were distinguished from macrophages with internal GFP cryptococci (R3), and all GFP-positive cryptococci (R4). BL1-A measures green fluorescence, FSC-A represents forward scatter, and SSC-A represents side scatter.

2.4.5 J774 time lapse imaging and analysis

After 2 hours of infection extracellular cryptococci were rinsed from the macrophages as described above, and fresh serum free DMEM was added to macrophages (see appendix). Macrophages were imaged as soon as possible after washing. Again, Nikon eClipse TI microscope and NIS Elements 4.51 analysis software were used for imaging. The plate of macrophages was put in the incubation chamber of the Nikon with temperature set to 37°C and CO_2 at 5%. The x20 Phase lens was used in combination with perfect focus to provide high resolution of macrophages and intracellular cryptococci. Images were taken every 2-5 minutes for 18 hours. DIC and GFP channels were used, but GFP channel was used only once every half hour to avoid bleaching and damage to the macrophages. Time lapse images were analysed by performing manual counts.

The percentage of macrophages which contained intracellular cryptococci was determined by counting all of the macrophages in a field of view and determining which contained intracellular cryptococci using the GFP channel. The percentage of infected macrophages per field of view was converted to macrophages per ml based on known size of the field of view and the 24 well plates.

The percentage of the total cryptococci which were intracellular was determined by counting the number of intracellular cryptococci within a field of view, determining the number of intracellular cryptococci in the well, and comparing this to the number of infecting cryptococci administered. The settling rate of cryptococci in different media was calculated by Jaime Cañedo (Johnston lab), and was used as the number of cryptococci which were used to infect.

Intracellular replication of cryptococci was determined by following individual cryptococci using the GFP channel and noting when a fungal cell budded. Extracellular proliferation was quantified in the same way. The number of cryptococci at different times was plotted in GraphPad Prism (versions 7.0c and

8.2.1) and the doubling time was determined by plotting each using an exponential fit.

2.4.6 J774 COX inhibition PGE_2 ELISA

J774 macrophages were seeded 10^5 per ml and left at 37°C, 5 % CO_2 for two hours, allowing the cells to adhere to the base of the plate. Wells requiring aspirin had supernatants removed, and replaced with fresh DMEM containing 1 mM aspirin (Sigma) in 1% DMSO. Cells were left for 24 hours. At 24 hours all wells received fresh serum free media. Wells requiring aspirin for the duration received 1 mM aspirin in DMSO. Arachidonic acid was used to as a positive control for prostaglandin production, as it is the substrate required for the production of prostaglandins and has been shown as necessary for the sufficient production of prostaglandins for detection by ELISA (Noverr et al., 2003a). Aspirin treated cells requiring arachidonic acid were treated with 30 μg per ml arachidonic acid in ethanol. Control wells received the following: either 1% DMSO, 30 μg per ml arachidonic acid, or ethanol. Cells were again left at 37°C, 5 % CO_2 for 18 hours. Supernatants were then removed and frozen at -80°C until use.

Supernatants were analysed as per the PGE_2 EIA ELISA kit instructions (Cayman Chemical, item number 514010). Briefly, ELISA wells were laid out as specified in the instructions, and blanks and standards were prepared as prescribed. A new pipette tip was used to pipette each reagent. J774 supernatants were diluted 1/8 and 1/16 in EIA buffer. Samples were measured in triplicate. After the addition of the appropriate reagents, buffers, and samples plates incubated at 4°C for 18 hours while oscillating. Samples were developed using Ellman's reagent for up to 90 minutes, covering the plates in foil to prevent damage by the light. Plates were read at a wavelength between 405 and 420. Standard curves were prepared using GraphPad prism, and PGE_2 concentrations of each sample were compared to the standard curve. The 1/16 sample dilutions produced values that fell on the standard curve, and were therefore used for analysis.

2.4.7 J774 COX inhibition time lapse

Macrophages were seeded at 10^5 per ml as described above. After two hours cells requiring aspirin were treated with 1 mM aspirin in DMSO in fresh DMEM. Cells were then left overnight for 18 hours. H99 GFP and Δ*plb1* GFP were prepared at 10^6 cells per ml as described above and opsonised with 18B7 for one hour. J774 macrophages were not activated with PMA to avoid any interaction between aspirin and activation on uptake. J774s were then infected with the fungal cells in fresh serum free DMEM for two hours before removing the supernatant, washing three times in PBS, and adding fresh serum free DMEM. Cells requiring aspirin for the duration were administered aspirin (1mM) with the infecting cryptococci and replaced in serum free DMEM after the infection and wash steps of the protocol. Cells were imaged for 18 hours using x20 phase imaging and perfect focus, with a DIC image taken every 2 minutes and a GFP image taken every 30 minutes. Cells were maintained at 37°C, 5% CO_2 throughout the duration of imaging. Analysis was performed by manual counts of intracellular and extracellular cryptococci as described above.

2.4.8 PPAR-γ antibody staining of infected J774 macrophages

J774 cells were prepared as above and seeded 10^5 per ml without activation by PMA to avoid interference with antibody labelling. Wells contained coverslips for imaging. H99 GFP and Δ*plb1* GFP were opsonised with 18B7 for one hour. 18B7 was then removed by centrifugation and fungal cells were suspended in 1 ml of PBS with 1:200 FITC for one hour. FITC staining labelled cryptococcal capsule with green fluorescent protein, allowing them to be easily identified. Supernatant was removed again, cells were resuspended in PBS, and J774 were infected with 10^6 of either H99-GFP or Δ*pbl1* GFP in serum free DMEM. After 2 hours of infection media was removed from macrophages, and the macrophages were washed three times with PBS. 10 μm TLT or DMSO was added to uninfected cells to act as controls. Cells were then left for 18 hours at 37°C, 5 % CO_2.

After 18 hours supernatants were removed and J774s were fixed with cold methanol for 5 minutes at -20^{o}C before washing with PBS three times, leaving PBS for five minutes at room temperature between washes. Coverslips were blocked with 5% sheep serum in 0.1% triton (block solution) for 20 minutes before being transferred into the primary PPAR-γ antibody (1:50, Santa Cruz Biotechnology sc-7273 lot #B1417) with 1:10 human IgG in block solution for one hour. Coverslips were washed 3 times in PBS and incubated with 1:200 anti-mouse TRITC, 1:40 anti-human IgG, and 0.41 μl/ml DAPI in block solution for one hour. Coverslips were then washed three times with PBS, three times with water, and fixed to slides using MOWIOL. Slides were left in the dark overnight and imaged the following day. Cells were imaged at x60 magnification using DIC, DAPI, GFP, and Cy5 channels.

Quantification and analysis was performed using FIJI version 2.0.0. For each cell a line was drawn from the outside of the cell, through the cytoplasm and nucleus, and out of the cytoplasm to the other side of the cell. Nuclear intensity was determined by the plateau that corresponded to the position of the nucleus. For each nuclear plateau the intensity was averaged along the length of the nucleus, and this measurement was used for comparison and analysis.

2.5 Human cell infections

2.5.1 Ethics statement

Informed written consent was obtained before whole blood was collected from healthy human donors. The South Sheffield Research Ethics Committee (REC) provided ethical approval for the collection of blood for the study of monocyte derived macrophages (REC reference 07/Q2305/7).

2.5.2 Cell isolation

(I did not collect or isolate the human blood cells. This work was performed by Jonathan Kilby and his team at the Royal Hallamshire Hospital Medical School. However, the protocol is briefly described here.)

After collection of blood samples, whole blood was added to Ficoll-Paque in a sterile centrifuge tube at a ratio of 1:2 (Ficoll:Blood). This was centrifuged at 1500 rpm for 23 minutes before the plasma layer was discarded. PBS was added to PBMCs, and this was centrifuged at 1000 rpm at 4°C for 13 minutes. Supernatant was removed, pellet was re-suspended in PBS, and was centrifuged again. Pellet was then resuspended in complete RPMI (see appendix) and 1 ml was added per well in a 24 well plate, or 3 ml was added to individual glass-bottomed dishes. Cell count was approximately $2x10^6$ PBMCs per well.

I maintained these cells at 37°C, 5% CO_2. For PBMC assays the cells were infected the following morning using KN99 GFP *C. neoformans* in serum free RPMI (see appendix). If macrophages were required, cells were maintained for 2 weeks to allow macrophage differentiation, and complete RPMI was changed every 3-4 days.

2.5.3 Human cell infection

KN99 GFP *C. neoformans* (var. grubii, serotype A) were used for infection assays. Cryptococci were cultured, washed, diluted, and opsonised as above. For MDM assays, macrophages were infected for 2 hours before removing extracellular cryptococci before imaging. For PBMC assays the cells were infected and imaging commenced immediately to observe the phagocytosis events. MDMs were not activated to provide a baseline for future investigation into the effect of different cytokines. At the end of all experiments, plates were bleached using Rely+On Virkon disinfectant to kill any cryptococci in the wells

2.5.4 Human PBMC antibody staining

To determine the cell subsets present in the human PBMC samples, initially coverslips were added to wells and cells were fixed following infection, and antibody staining was performed. However, as most cells in these subsets did not sufficiently adhere to the coverslip, or were subsequently washed off during the

immunohistochemistry protocol, imaging of live cells in glass-bottomed dishes was performed.

To do this, 2 μl of FITC mouse anti-human CD3 (BD Pharmigen Biosciences), 2 μl mouse anti-human CD14 APC (Invitrogen, MHCD1405), and 20 μg of human IgG were added to glass dishes containing PBMCs. 100 μl of opsonised cryptococci were added. These dishes were either imaged immediately, to represent the PBMCs at the onset of time lapse assays, or were incubated for 24 hours before imaging, to represent the PBMCs at the end of 24-hour time lapse assays. Dishes were imaged at x60 magnification using DIC, DAPI, GFP, and Cy5 channels. The same antibodies were added to dishes used for x20 phase time lapse imaging in attempt to record the formation of PBMC swarms, but continuous imaging and the x20 magnification did not produce usable images, especially as the GFP signal from CD3 cells was dim and the APC signal of monocytes quickly faded.

Special thanks to Dr Helen Marriott for graciously sharing antibodies.

2.5.5 Human cell time lapse Imaging and quantification

For both MDM and PBMC imaging Nikon eClipse TI microscope and NIS Elements 4.51 analysis software were used. x20 phase imaging was performed using perfect focus to maintain clear images throughout the duration of imaging. DIC images were captured every 2-3 minutes, and GFP images were captured every 30 minutes to follow the cryptococci without bleaching or damaging the human cells. Phagocytosis and replication quantification was performed by watching individual cryptococci throughout the course of the time lapse assays and counting events manually.

The percentage of macrophages which contained intracellular cryptococci was determined by counting all macrophages in a field of view and determining how many possessed intracellular cryptococci, as shown by the GFP channel. The percentage of infected macrophages was calculated. The percentage of cryptococci which were internalised was determined by calculating the number of intracellular cryptococci per field of view, using this to determine the number of internalised cryptococci in the whole well, and using the settling rate of *C. neoformans* in the media (as determined by Jaime Cañedo) to ascertain the total number of cryptococci able to settle onto the macrophage layer in the given time frame. This "settling rate" was used as the total number of cryptococci used to infect.

Fungal replication was calculated by counting the budding of individual cryptococci in time. The number of cryptococci was plotted against time for individual starting cryptococci, and doubling time was determined by fitting an exponential curve in GraphPad Prism (version 7.0).

2.6 Statistics

GraphPad Prism versions 7.0c and 8.2.1 were used for statistical analyses. Normality was determined based on adherence to a Gaussian distribution. Normality tests were not performed as they are unreliable (Johnston personal communication). 95% confidence intervals were used to assess statistical significance.

Unpaired two-tailed t-tests were performed to compare the means of conditions. Mann-Whitney tests were performed when data was non-parametric.

Ordinary one-way ANOVAs were performed to compare the means of conditions. Multiple comparisons were performed, using Tukey's test to correct for multiple comparisons. Two-way ANOVAs were performed when necessary, correcting for multiple comparisons using statistical hypothesis testing and no post test.

Chapter 3. The role of fungal-derived prostaglandins in macrophage parasitism

3.1 introduction

3.1.1 Prostaglandin synthesis and interactions with immune cells

Eicosanoids are lipid signalling molecules which, through activation of their receptors, regulate a wide range of physiological effects. In humans, eicosanoids are produced after arachidonic acid is freed from the cell's phospholipid membrane by phospholipases, specifically phospholipase A_2 (PLA_2). Oxidation of arachidonic acid results in the production of prostanoids, leukotrienes, cysteninyl-leukotrienes, lipoxins, hydroxyeicosatetraenoic acids, and epoxides, which are then metabolised into final eicosanoid species by specific synthases. In this chapter I will be discussing prostaglandins, a type of prostanoid, which are oxidized by cyclooxygenase enzymes (COX-1 and COX-2) to produce PGG_2. This is converted to stable PGH_2 before synthases produce distinct prostaglandins: PGE_2, PGD_2, PGI_2, and $PGF_{2\alpha}$ (Figure 3.1). While the various prostaglandins are important in health and disease, I will be mainly discussing PGE_2 as it pertains to my work.

PGE_2 is produced by a variety of immune cells, including B cells (Graf et al., 1999; Ryan et al., 2005), dendritic cells (Harizi and Gualde, 2004; Józefowski et al., 2003), macrophages (Norris et al., 2011; Rouzer et al., 2004; Stafford and Marnett, 2008), and activated T cells (Sreeramkumar et al., 2016). Production of PGE_2 by these cell types elicits a range of actions which modulate immune cell responses (Harizi et al., 2008). PGE_2 signals through four G protein coupled receptors in humans: EP1, EP2, EP3, and EP4 (Sugimoto and Narumiya, 2007). The time and place in which PGE_2 activates its various receptors can produce different effects, illustrating the importance of context on signalling and physiological outcome.

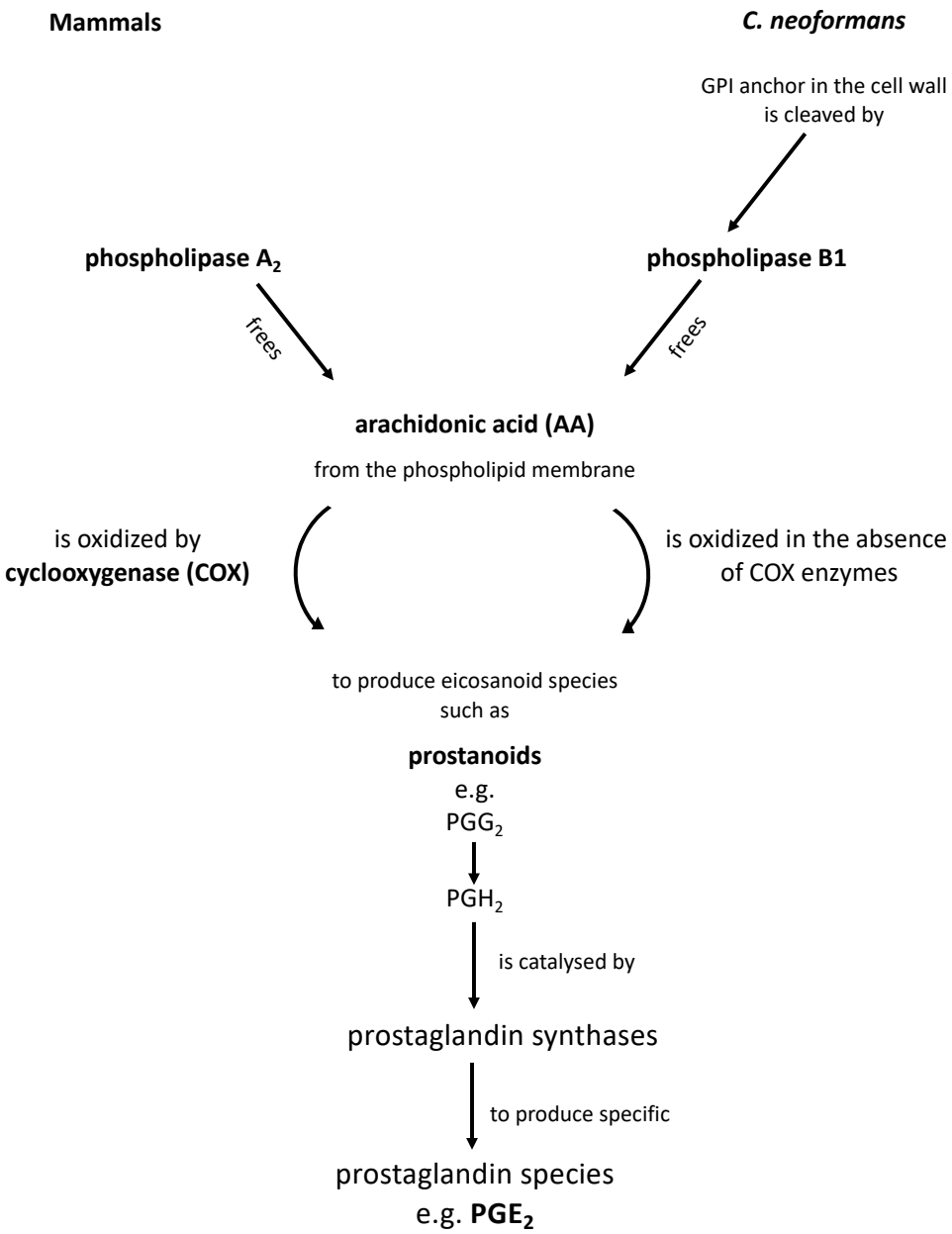

Figure 3.1. The production of prostaglandin E_2

In mammals, phospholipase A_2 frees arachidonic acid from the phospholipid membranes of cells. This is oxidized by cyclooxygenase (COX) enzymes (or lipoxygenase enzymes) to produce prostanoid species such as prostacyclins, thromboxanes, and *prostaglandins.* These are further catalysed by specific enzymes to produce different species, including PGE_2. *C. neoformans* utilizes phospholipase B1 to free arachidonic acid from membranes, which is catalysed in the absence of COX enzymes to produce prostanoids, including the eventual production of PGE_2.

For example, PGE_2 has contradictory effects on T cells. In *in vitro* T cell clone assays, PGE_2 exerted anti-inflammatory effects through inhibition of pro-inflammatory Th1 cytokine production, and increased anti-inflammatory Th2 cytokine production (Betz and Fox, 1991; Gold et al., 1994; Hilkens et al., 1995). Interestingly, more recent studies have pointed to a pro-inflammatory role for PGE_2 with regard to T cells. *In vitro* and *in vivo* studies examining the outcomes of EP4 receptor stimulation by PGE_2 have shown this this prostaglandin induced Th1 differentiation of CD4+ T cells, and increased the amount of IFN-γ-producing T cells at nanomolar concentrations through PI3K signalling (Chen et al., 2010; Yao et al., 2009). Additionally, *in vivo* studies on knockout mice which lacked PGE_2 receptors showed that the mice had reduced surface expression of CD69, CD25, and CD71 T cell activation markers, demonstrating that PGE_2 was required for Th1 and regulatory T cell activation (Sreeramkumar et al., 2016). Crucially, the pro-inflammatory effects were seen only at low concentrations while the anti-inflammatory effects were seen at higher concentrations (Yao et al., 2009), indicating the possibility that PGE_2 may elicit different effects at different times during inflammation. Discrepancies in these effects of PGE_2 on T cell activation and action may also be due to the cell types and stage of PGE_2 treatment considered.

Macrophages also produce and respond to PGE_2. Norris et al. analysed the production of prostaglandins by different murine macrophage cells, and showed that not only did macrophages produce prostaglandins in response to microbial infection, but that the phenotype of the macrophages affected the production of prostaglandins, with cells from different models producing different levels of prostaglandins at different times after stimulation (Norris et al., 2011). Prostaglandins produced by macrophages are important as they can induce cascades which stimulate or suppress activation of immune cells. Multiple studies have demonstrated that prostaglandins produced by macrophages have the potential to act in an autocrine manner, modulating the macrophage products and hence the action of immune cells in different settings. For example, after stimulation with LPS, mouse resident peritoneal macrophages showed increased COX-1 and prostaglandin synthase levels, leading to an increase in prostacyclin and PGE_2

secretion (Rouzer et al., 2004). However, inhibition of COX-1 increased TNF-α secretion. This is important, since this pro-inflammatory cytokine is produced by macrophages during infection and inflammation, and functions by modulating immune cell responses, including those of the macrophages themselves. This finding was corroborated in Raw 264.7 macrophage-like cells, where LPS-induced TNF-α mRNA transcription was abruptly halted by addition of exogenous PGE_2 (Stafford and Marnett, 2008). Thus, macrophage prostaglandin synthesis affects macrophage function and the secretion of cytokines which have the potential to modulate the immune response.

During the course of inflammation and infection, the different roles of prostaglandins in modulating immune response in different contexts are important in determining the outcome of host immune cell interactions. The roles that prostaglandins play in specific immune pathologies have been reviewed in great detail elsewhere (Belley and Chadee, 1995; Harizi et al., 2008; Smyth et al., 2009). Here I will focus on prostaglandins in inflammation and infection.

3.1.2 Prostaglandins in inflammation

Prostaglandins elicit a wide range of effects in the body. As introduced previously, they are involved in the balance of inflammatory responses (Higgs, 1986; Ricciotti and Fitzgerald, 2011), often in association with cyclooxygenase activity. While COX-1 is constitutively expressed in most cells, COX-2 is expressed especially in response to inflammatory signals (Crofford, 1997; Dubois et al., 1998).

COX-2 activation and the resulting production of PGE_2 is associated with inflammation in some chronic inflammatory disorders, especially arthritis. In models of human *ex vivo* osteoarthritis and rat adjuvant-induced arthritis, COX-2 expression was upregulated in areas of high inflammation (Anderson et al., 1996; Kang et al., 1996). Indeed, the amount of PGE_2 spontaneously produced due to overstimulation of COX-2 in osteoarthritic cartilage was up to ten times higher than the level released in non-affected cartilage (Amin et al., 1997). Anderson et al. suggested that

high expression of PGE_2 in the rat arthritis model induced the production of pro-inflammatory cytokines, which in turn upregulated COX-2, increasing the inflammatory effects of the condition in a positive feedback loop (Anderson et al., 1996). The involvement of prostaglandins in inflammation is underpinned by the ability of nonsteroidal anti-inflammatory drugs, such as aspirin and ibuprofen, to reduce inflammation through preventing the production of prostaglandins by COX inhibition (Vane, 1971).

Prostaglandins can also have anti-inflammatory effects, and are important for the resolution of inflammation. While PGE_2 is upregulated in the rat model of adjuvant-induced arthritis above (Anderson et al., 1996), the PPAR-γ ligand 15d-PGJ_2 (a derivative of PGD_2) suppressed the progression of clinical arthritis in the same model (Kawahito et al., 2000a). The roles of PGD_2 and 15d-PGJ_2 in modulating pro- and anti-inflammatory cytokine production during acute inflammation were also shown in a mouse model of peritonitis (Rajakariar et al., 2007). These prostaglandins influenced the production of pro- and anti-inflammatory cytokines, which encouraged the influx and efflux of immune cell such as macrophages.

Interestingly, in a rat model of inflammation, PGE_2 production dominated the early inflammation phase of lesion formation, while PGD_2 and 15d-PGJ_2 dominated the later inflammation resolution phase (Gilroy et al., 1999). This suggests roles for prostaglandins in both the production, and the resolution, of an inflammatory response. Indeed, even PGE_2 has been shown to play different roles during different stages of the inflammatory response by acting on different subunits of NFκB – a transcription factor important in inducing inflammatory cascades. In synovial fibroblasts harvested from human patients with rheumatoid arthritis, treatment with PGE_2 inhibited the heterodimerization necessary for NFκB transcription at 6h post treatment, but not at 1h, demonstrating different effects of PGE_2 at different time points in inflammation (Gomez et al., 2005). Taken together, these studies describe how different prostaglandins can be upregulated and active at different points during inflammation; this enables appropriate actions necessary for the different phases of the inflammatory immune response.

3.1.3 Prostaglandins in infection

The role of prostaglandins in infection is fascinating because they can be protective for either host or pathogen. Host cells produce prostaglandins upon detection of pathogenic material; for example, murine macrophages produce prostaglandins through COX-2 activation after TLR-4 stimulation (Norris et al., 2011) – a pattern recognition receptor best known for its activation by bacterial lipopolysaccharide. Indeed, macrophages produce a vast milieu of prostaglandins in response to LPS and LPS-agonists (Gupta et al., 2009).

While host cells are capable of producing prostaglandins in response to infection, the same prostaglandins produced in response to different infections can have opposing effects – enabling the control of infection, or facilitating microbial survival and proliferation. Mayer-Barber et al. studied the effect of cytokine-prostaglandin cross-talk in an *in vivo* model of *Mycobacterium tuberculosis*. In this infection, limiting the production of type-I interferons is important for the control of infection. Here, *Mtb* infection induced the production of IL-1 by host myeloid cells, which induced production of PGE_2; PGE_2 helped control bacterial infection through limiting production of type-I IFNs. Addition of type-I IFNs antagonised this process and enabled bacterial growth, as did inhibition of host prostaglandin production (Mayer-Barber et al., 2014).Thus, in this model of infection, host prostaglandins led to the control of bacterial growth.

In the context of viral infection, PGE_2 can have the opposite effect, enabling the propagation of microbial infection. During influenza infection, type-I IFNs are important for control of viral growth, and are therefore necessary for host protection. Using a murine model of influenza infection, Coulombe et al. demonstrated that production of PGE_2 by host macrophages decreased the production of type-I IFNs, which led to increased viral load (Coulombe et al., 2014). Here, PGE_2 impaired type-I IFN production as it did above during *Mtb* infection, but this was detrimental for the host during influenza infection. Thus, the differential

regulation of host prostaglandin production is important in determining the outcome of different infections.

Many microbes and parasites are also capable of producing a vast variety of prostaglandins (Noverr et al., 2003b); in fact, production of these lipid mediators is extremely advantageous in aiding some microbes to induce and propagate infection. For example, utilisation of host fatty acids by *Schistosoma mansoni* enables the production of eicosanoids by cercariae, the free-swimming life stage of the parasite which infect humans through skin penetration. Eicosanoid production by these parasites promotes host penetration and transformation of the cercariae into mature parasitic worms (Fusco et al., 1986). The malarial parasite *Plasmodium falciparum* produces various prostaglandins from exogenous arachidonic acid (Kubata et al., 1998). *P. falciparum* produces prostaglandins to inhibit host TNF-α production, which in turn limits host immune activation and enables successful growth of the parasite (Kubata et al., 1998). Several pathogenic fungi such as *C. albicans* and *C. neoformans* also produce eicosanoids and prostaglandins, which may be employed by the fungi to mediate host immune modulation and promote infection (Noverr et al., 2001, 2002).

Because prostaglandins can have pro- and anti-microbial effects, it is important to discern the source of the effective prostaglandins during infection, as well as the factors controlling their production. This is crucial – is the host producing prostaglandins to control infection? Or is the pathogen manipulating host prostaglandin production in order to evade destruction and propagate infection? In human macrophages, *E. coli* induces distinct eicosanoid and cytokine production by differentially-polarised macrophages; infection results in upregulation of pro-inflammatory cyclooxygenase activity and PGE_2 production in M1 macrophages, and production of pro-resolution lipid mediators by M2 macrophages (Werz et al., 2018). Thus, the modulation of prostaglandins which affect the production of cytokines must be carefully considered, and vice versa, as these factors have the potential to drive infection outcomes.

3.1.4 Cryptococcal prostaglandins

As discussed in the main introduction, *Cryptococcus neoformans* is a pathogenic fungus which is successful in propagating human infection through a number of effective strategies and adaptations which promote its virulence. One such strategy is its ability to synthesise eicosanoids and prostaglandins which are indistinguishable from those made by vertebrates (Noverr et al., 2001, 2002). So far, only two enzymes have been conclusively linked to prostaglandin production by *Cryptococcus neoformans* – phospholipase B1 (Plb1) and laccase.

Phospholipase B

Cryptococcal phospholipase B1 is well characterised (Chen et al., 1997b, 1997a, 2000a; Vidotto et al., 1996), and appears analogous to mammalian phospholipase A_2 (Noverr et al., 2003a), freeing arachidonic acid from phospholipid membranes (Chen et al., 2000a) for incorporation into lipid signalling molecules (Figure 3.1). Though Plb1 may remain cell-wall associated to perform its functions, it can also be released and secreted from the fungal cell (Chayakulkeeree et al., 2011; Djordjevic et al., 2005; Siafakas et al., 2007). Prostaglandin production is reduced in a phospholipase B mutant strain of H99 *C. neoformans*, though this defect is rescued upon the addition of exogenous arachidonic acid (Noverr et al., 2003a).

Though Plb1 enables *Cryptococcus* access to the arachidonic acid necessary for prostaglandin synthesis, there is some debate as to whether *Cryptococcus* possesses cyclooxygenase enzymes. While Noverr et al. demonstrated that COX inhibition with indomethacin decreased fungal prostaglandin production (Noverr et al., 2001), Erb-Downward et al. showed that COX inhibition had no effect on prostaglandin production, and suggested that the reduced prostaglandin production shown by Noverr was actually as due to reduced cell viability (Erb-Downward and Huffnagle, 2007). Regardless, *Cryptococcus neoformans* retains the ability to produce prostaglandins *de novo*, or with addition of exogenous arachidonic acid (Erb-Downward and Huffnagle, 2007; Noverr et al., 2001).

Phospholipase B has long been associated with cryptococcal virulence. Infection of BALB/c mice with isolates of *Cryptococcus* which produce high levels of Plb1 induced higher levels of infection in the lung and brain compared to strains which produced less Plb1 (Chen et al., 1997a). Furthermore, murine infection with a phospholipase B-deficient mutant (*Δplb1*) resulted in significantly longer host survival compared to the H99 parental strain, and the *Δplb1* strain showed markedly lower survival in the cerebrospinal fluid in a rabbit meningitis model of infection (Cox et al., 2001). Both of these studies suggest that phospholipase B is important for cryptococcal survival and dissemination – hallmarks of virulence.

One way in which *Cryptococcus* utilises phospholipase B for virulence is through intracellular parasitism of host cells. Infection of murine J774 macrophage-like cells *in vitro* with *Δplb1* H99 *C. neoformans* showed that this mutant initiated budding later and more slowly than the parental H99 strain (Cox et al., 2001). Furthermore, *in vitro* infection of macrophages with the Δ*plb1* mutant resulted in reduced intracellular fungal replication and increased fungal killing within the host phagosome compared to the wildtype parental strain (Evans et al., 2015). These studies illustrate that fungal Plb1 is required for effective intracellular parasitism of the host macrophage niche.

While a role for cryptococcal Plb1 in intracellular survival and proliferation has been shown, the role it plays in fungal dissemination remains up for debate. Chen et al. showed that strains of *Cryptococcus neoformans* which produced low levels of phospholipase B failed to establish CNS infection and showed reduced dissemination to the brain (Chen et al., 1997a), suggesting that Plb1 may be necessary for dissemination. In using the *Δplb1* strain in a murine model of infection, Santangelo et al. showed that phospholipase B was necessary for dissemination of cryptococci from the lung into the bloodstream (Santangelo et al., 2004b). However, they claimed that dissemination to the brain may occur through a phospholipase-independent mechanism, suggesting that the reduced intracellular proliferation of the phospholipase-deficient mutant strain resulted in monocytes delivering fewer fungi to the CNS (Santangelo et al., 2004b). If true, this means that dissemination to

the brain may not be a direct result of a mechanism induced by phospholipase activity, and may merely exist as a by-product of the intracellular parasitism conferred by phospholipase (Santangelo et al., 2004b). Finally, escape from host phagocytes is important for dissemination to the CNS in the Trojan-horse method of transgressing the blood-brain barrier; however, vomocytic escape of cryptococci was dependent on fungal Plb1, meaning that phospholipase B may be important in enabling CNS dissemination through macrophage escape (Chayakulkeeree et al., 2011). While the exact role for phospholipase B in fungal dissemination remains elusive, further investigation into the effect of prostaglandins on the propagation infection may illuminate the relationship between intracellular parasitism and fungal dissemination.

Laccase

Laccase, encoded by the genes *lac1* and *lac2* in *Cryptococcus*, is the second enzyme associated with cryptococcal prostaglandin production (Erb-Downward et al., 2008). Laccase was originally shown to be involved in cryptococcal melanin production (Williamson et al., 1998). Later, however, laccase became associated with cryptococcal survival in human CSF, independent of melanin production (Sabiiti et al., 2014). Microarray analysis showed that upon phagocytosis by J774 cells, both *lac1* and *lac2* were upregulated; measurement of a GFP-reporter line of *C. neoformans* confirmed that it was indeed the cryptococcal cells that upregulated expression of this enzyme, indicating a role for laccase in response to interaction with the host immune system (Fan et al., 2005a). Using cryptococcal cell lysates, Erb-Downward et al. demonstrated that antibody inhibition and genetic deletion of laccase resulted in the loss of cryptococcal prostaglandin production (Erb-Downward et al., 2008). They also showed that laccase did not perform cyclooxygenase activity, but rather catalysed PGE_2 and 15-keto- PGE_2 from PGG_2 (Erb-Downward et al., 2008). Thus, cryptococci utilise the laccase enzymes to catalyse E prostaglandins.

It is hypothesised that prostaglandins produced by cryptococci exert immune modulation and promote fungal virulence. In a murine pulmonary model of

infection, deletion of cryptococcal laccase genes resulted in decreased pulmonary burden and decreased dissemination to the CNS (Qiu et al., 2012a), highlighting the role of laccase in cryptococcal virulence and dissemination. Additionally, laccase has been shown to promote fungal virulence through modulation of host immune cell polarisation. ELISA analysis and intracellular cytokine staining of murine lung leukocytes revealed that cryptococcal laccase promoted Th2 cytokine production, reduced Th1/Th17 cytokine production and the frequency of IFN-γ and IL-17-producing CD4+ T cells during infection. Cryptococcal laccase modulated the immune response to infection by shifting the T cell polarisation state away from a Th1/Th17 clearance phenotype toward a non-protective Th2 phenotype (Qiu et al., 2012), resulting in alternative macrophage activation and enhancement of propagation infection.

Taken together, these studies demonstrate that the presence of prostaglandins during infection is beneficial for the *Cryptococcus* while being detrimental for the host. However, it is important to discern the source, the form, and the action of these lipid mediators when attempting to understand their role in infection pathogenesis and disease progression.

3.1.5 Derivation and function of eicosanoids in cryptococcosis

The context and form in which physiological mediators are produced have the potential to affect host-pathogen interactions in different ways. In a setting of cryptococcal infection, it is important to discern not only how prostaglandins impact the progression of infection, but also which form they take and the mechanisms by which they exert their effects. As both host and pathogen are capable of producing prostaglandins during infection, it is also important to discover the source of the eicosanoids, and how they may interact when derived from competing sources.

For example, a study by Shen and Liu (2015) examined the effect of blocking PGE_2 signalling through EP2 and EP4 receptor blockade in a murine model of cryptococcal infection. Treating mice with EP2 and EP4 receptor antagonists (both alone, and in

combination) prior to infection with *C. neoformans* resulted in lower lung burden compared to untreated control mice (Shen and Liu, 2015). Additionally, measurement of cytokine mRNA levels produced by infected mice treated with the receptor antagonists resulted in the upregulation of IFN-γ, TNF-α, IL-17, and IL-22 mRNAs in M1 macrophages – cytokines which are typically associated with a protective, pro-inflammatory host response. PGE_2 signalling blockade also upregulated the number of cells producing these cytokines (Shen and Liu, 2015). While these results suggest that one way in which PGE_2 signalling operates during cryptococcal infection is through the downregulation of M1 cytokine production, this study failed to determine if the active prostaglandins were produced by the host or by the fungus. Indeed, while blocking the host PGE_2 receptor is a sufficient way to determine the effect of prostaglandins on infection burden and cytokine signalling, the prostaglandins whose signalling was prohibited could have come from the host or from the *Cryptococcus*.

Additionally, current studies often neglect to consider which form of PGE_2 is responsible for the prescribed effects on infection. This is an important consideration, as PGE_2 can be dehydrogenated to 15-keto-PGE_2, metabolised to $PGF_{2\alpha}$, or dehydrated to PGA_2. These different derivations of one compound have different properties and react differently in diverse settings (Gupta et al., 2009). This is particularly important to understand, as differential metabolite production may activate either pathogen or host signalling cascades, which in turn have the potential to produce varied downstream effects on infection outcome.

While many effects of EP2 and EP4 activation by PGE_2 are known, less is known about the activation of the PPAR-γ receptor by PGE_2 metabolites. The activation of PPAR-γ by other eicosanoids is understood to some extent. For example, Kawahito et al. showed that 15d-PGJ_2 treatment of synoviocytes resulted in the nuclear translocation of PPAR-γ, and treatment with this prostaglandin suppressed the progression of clinical arthritis in a rat adjuvant-induced model of arthritis (Kawahito et al., 2000a). 15d-PGJ_2 treatment of Raw 264.7 macrophage-like cells resulted in an anti-inflammatory phenotype, inhibiting LPS-induced nitrite production, IL-1

release, and COX-2 expression - actions which were attributed to the binding of PPAR-γ (Maggi et al., 2000). Alleva et al. showed that pro-inflammatory cytokine production in LPS-induced macrophages was strongly downregulated when PPAR-γ was activated by 15d-PGJ_2 (Alleva et al., 2002). While the interplay between 15d-PGJ_2 and PPAR-γ is broadly understood, the relationship between PGE_2 and PPAR-γ remains unclear. It is important to discern the potential interplay between PGE_2 and PPAR-γ, as PGE_2 affects the course of cryptococcosis, and PPAR-γ signalling cascades have the potential to mediate many downstream effects which could determine the outcome of infection.

As described extensively throughout this chapter, PGE_2 plays important roles in immune cell activation, inflammatory cascades, and infection progression. While the blockade of PGE_2 receptor signalling has been shown to result in reduced fungal burden and promotion of protective M1 macrophage cytokine production in cryptococcal infection (Shen and Liu, 2015), studies to date have neglected to investigate the source of the prostaglandins, as well as the active metabolite form and the direct action on immune cells. Here, I will describe results of the experiments I performed in contribution as second author to the paper '15-keto-prostaglandin E2 activates host peroxisome proliferator-activated receptor gamma (PPAR-γ) to promote Cryptococcus neoformans growth during infection' (Evans et al., 2019). I show that inhibition of host prostaglandin synthesis *in vitro* through host COX inhibition, and *in vivo* by CRISPR/Cas9 knockdown of host prostaglandin synthase, bear little effect on fungal burden. I show, through time lapse experiments and ELISA analysis, that crucial prostaglandins produced in *C. neoformans* infection are fungal-derived. Finally, I demonstrate that Cryptococcus neoformans manipulates host immune cell behaviour through activation of host PPAR-γ, and that fungal eicosanoids are required to do so. In doing so, I illustrate the importance of fungal-derived prostaglandins in affecting the outcome of *Cryptococcus* infection.

3.2 Aspirin treatment of J774 macrophages reduces PGE_2 production

To begin, it was important to discern if inhibition of host prostaglandin synthesis was possible. Future experiments would involve inhibiting the action of COX enzymes through the use of aspirin, an irreversible COX inhibitor. To confirm that host prostaglandin production was inhibited upon treatment with this irreversible COX inhibitor, J774 murine macrophage-like cells were treated with aspirin and PGE_2 production was measured using a PGE_2 monoclonal ELISA. PGE_2 production was measured after 18 hours of treatment as this was the ending time point to be used in the time lapse experiments. PGE_2 production by COX-inhibited macrophages was compared with PGE_2 production by untreated macrophages, and those treated with arachidonic acid (AA), which is necessary for cells to produce appreciable amounts of prostaglandins for detection by ELISA (Noverr et al., 2003a). Prostaglandin production with DMSO and ethanol treatment were also compared, as these were used to prepare aspirin and arachidonic acid, respectively.

As expected, arachidonic acid increased the amount of PGE_2 produced by J774 macrophages compared to untreated macrophages (Figures 3.2a and 3.2b; means 55.28 and 23.87 pg/ml, respectively). Aspirin treatment reduced the amount of PGE_2 produced compared to untreated macrophages, both when administered as a pre-treatment (pt aspirin, mean 6.71 pg/ml), and when administered to macrophages for the additional 18 hours (aspirin, mean 1.62 pg/ml); however, COX inhibition for the duration of the experiment more potently inhibited PGE_2 production by macrophages. Administration of arachidonic acid with a pre-treatment of aspirin, as well as with prolonged aspirin exposure for the duration of the 18 hours, resulted in an intermediate level of PGE_2 produced (means 20 and 14.88 pg/ml, respectively). The same was true for J774 macrophages with added DMSO and ethanol (means 32.93 and 12.14 pg/ml, respectively). These results showed that administration of aspirin reduced the amount of PGE_2 produced by J774 macrophages. While aspirin treatment did permit some prostaglandin production, the amount was greatly reduced compared to that produced by macrophages alone. In fact, because PGE_2 production was enhanced in macrophages treated with DMSO compared to cells

alone, the PGE_2 levels detected by the ELISA may have been a by-product of DMSO treatment in aspirin administration. While aspirin treatment did permit some PGE_2 production by macrophages this was much lower than production by aspirin treated-macrophages.

Due to a shortage of ELISA kits and reagents only two repeats were considered performed. As such, one-way ANOVAs produced no statistical significance in PGE_2 production between conditions considered. For stronger statistical analysis, a third repeat should be performed and quantified.

a.

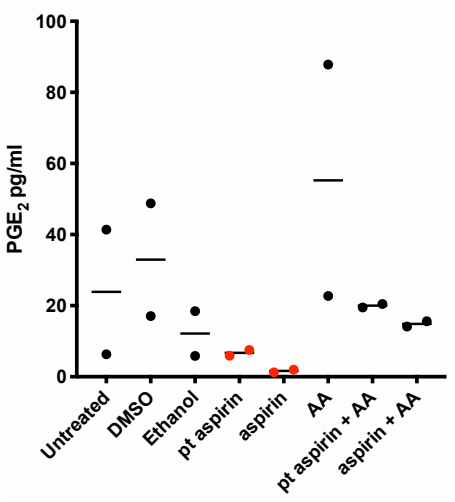

b.

Condition	Kit 1 PGE_2/ml	Kit 2 PGE_2/ml	Mean PGE_2/ml	SD
Untreated	41.42	6.33	23.87	24.81
DMSO	48.77	17.08	32.93	22.40
Ethanol	18.44	5.84	12.14	8.92
pt aspirin	5.90	7.53	6.71	1.15
aspirin	2.02	1.23	1.62	0.56
AA	87.34	22.72	55.28	46.04
pt aspirin + AA	19.49	20.51	20.00	0.72
aspirin + AA	15.65	14.12	14.88	1.08

Figure 3.2. Administration of the irreversible COX inhibitor aspirin reduced PGE_2 production by J774 macrophages

a. Amount of PGE_2 produced by J774 macrophages under various treatment conditions after 18 hours, as measured by ELISA. Levels of PGE_2 were measured for untreated J774 macrophages, or after treatment with arachidonic acid (AA), aspirin 1h pre-treatment (pt), 1h pre-treatment plus the full 18h (aspirin), and vehicle controls. 2 repeats are shown, with 3 replicates considered per condition for each repeat. One-way ANOVA comparing the mean PGE_2 produced by untreated macrophages to other conditions showed no significance, though overall $p < 0.001$.

b. Descriptive statistics showing the amount of PGE_2 produced by J774 macrophages after 18 hours with different treatments. Two repeats were performed with different ELISA kits as shown above.

3.3 Fungal-derived prostaglandins impact cryptococcal parasitism of host macrophages

To ascertain if the effective prostaglandins in infection are produced by host macrophages or by the cryptococci themselves, I treated J774 murine macrophage-like cells with 1 mM aspirin, an irreversible COX inhibitor, to prevent host prostaglandin production. I then performed time lapse analysis of opsonised H99 and *Δplb1* GFP *C. neoformans* infection (Figures 3.3 and 3.4). I reasoned that if the prostaglandins promoting virulence were indeed from the fungi, then blocking host prostaglandin synthesis would bear no effect on fungal proliferation; conversely, if host prostaglandins affected fungal virulence, inhibiting their production would affect fungal proliferation. Treatment with aspirin does not affect cryptococcal prostaglandin production, as BLAST sequence searching and treatment with indomethacin suggest that *Cryptococcus neoformans* does not possess cyclooxygenase enzymes (Erb-Downward and Huffnagle, 2007). For the infection I used both the wild-type H99 *Cryptococcus*, as well as the phospholipase deficient mutant *Δplb1*. This was to confirm that fungal prostaglandins were required for intracellular growth; if fungal prostaglandins were indeed responsible for fungal virulence, removing the ability to synthesise them would reduce fungal intracellular proliferation, and would not be affected by the inhibition of host COX. Macrophages were not activated to investigate only the effect of prostaglandins on uptake, avoiding contribution to phagocytosis from activation.

Treatment of J774 macrophages with a COX inhibitor did not alter the ability of the cryptococci to replicate intracellularly (Figures 3.5a). The intracellular proliferation of the cryptococci remained constant when macrophages were untreated, pre-treated with aspirin, or were treated with aspirin for the duration of the infection, illustrating that inhibiting host prostaglandin synthesis did not appear to affect cryptococcal replication (Figure 3.5a relative fold change two-way ANOVA comparing aspirin treatments $p = 0.9750$ with no pairwise significance amongst aspirin treatments for each strain). As previously described (Evans et al., 2015), the *Δplb1* mutant showed reduced intracellular proliferation compared to the

phospholipase B-containing wild-type H99 strain (Figure 3.5a two-way ANOVA comparing relative fold change between fungal strains p = 0.0010, pairwise significance between H99 and *Δplb1* only). Furthermore, not only did the prostaglandin mutant strain show reduced intracellular proliferation, it also displayed reduced survival, as fungal replication was below zero. This showed that there was no evidence for the ability of host prostaglandins to affect the ability of cryptococci to replicate intracellularly, and that fungal prostaglandins were required for effective intracellular parasitism of host macrophages in a phospholipase B-dependent manner.

I also compared the proportion of macrophages which contained intracellular cryptococci. I did this to determine if host or fungal prostaglandins impacted phagocytic uptake of cryptococci and subsequent infection of macrophages. Treatment with aspirin did not appear to alter the percentage of macrophages which phagocytosed cryptococci for each strain (Figure 3.5b two-way ANOVA for comparing the effect of COX inhibition on uptake p = 0.6502). Here, there was no evidence that host prostaglandin production increased phagocytosis of cryptococci, or impaired the ability of cryptococci to inhabit the macrophage intracellular niche. While aspirin treatment appeared to have no effect on the percentage of macrophages which contained intracellular cryptococci, macrophage uptake was affected by the fungal strain (Figure 3.5b two-way ANOVA comparing effect of fungal strain on uptake p = 0.0037). Here, the percentage of macrophages which contained *Δplb1* was lower than those which contained the parental H99 strain. This may have been due to decreased survival of the phospholipase mutant strain within macrophages, as described previously (Evans et al., 2015); it is possible that increased killing of *Δplb1* cryptococci during the 2 hour infection window before quantification omitted them from detection and quantification.

Phagocytic index (PI; the number of cryptococci on average contained within each infected macrophage) was calculated and compared across strains and treatments. There was no evidence of a significant difference in PI amongst aspirin treatment conditions at the start of infection (Figure 3.5c two-way ANOVA comparing effect of

host prostaglandins on phagocytic index p = 0.2582). This suggests that host prostaglandins did not appear to affect the number of cryptococci per macrophage. However, the number of cryptococci within each macrophage was lower after infection with the phospholipase-deficient mutant (Figure 3.5c two-way ANOVA comparing effect of fungal prostaglandins on phagocytic index p = 0.0278, no pairwise significance).

Taken together, these data show no evidence of host prostaglandins affecting intracellular fungal proliferation, phagocytosis of fungi, or the number of cryptococci which were phagocytosed to infect each macrophage (Figure 3.5d). These results did, however, suggest that fungal prostaglandins were important for intracellular fungal replication and were likely important for habitation of macrophages. It should be noted that only two repeats were considered here and statistical analyses should be considered with caution and viewed as illustrative. The analysis of a third repeat may provide a more accurate representation of the effect of COX inhibition and phospholipase B deficiency on fungal growth and infection.

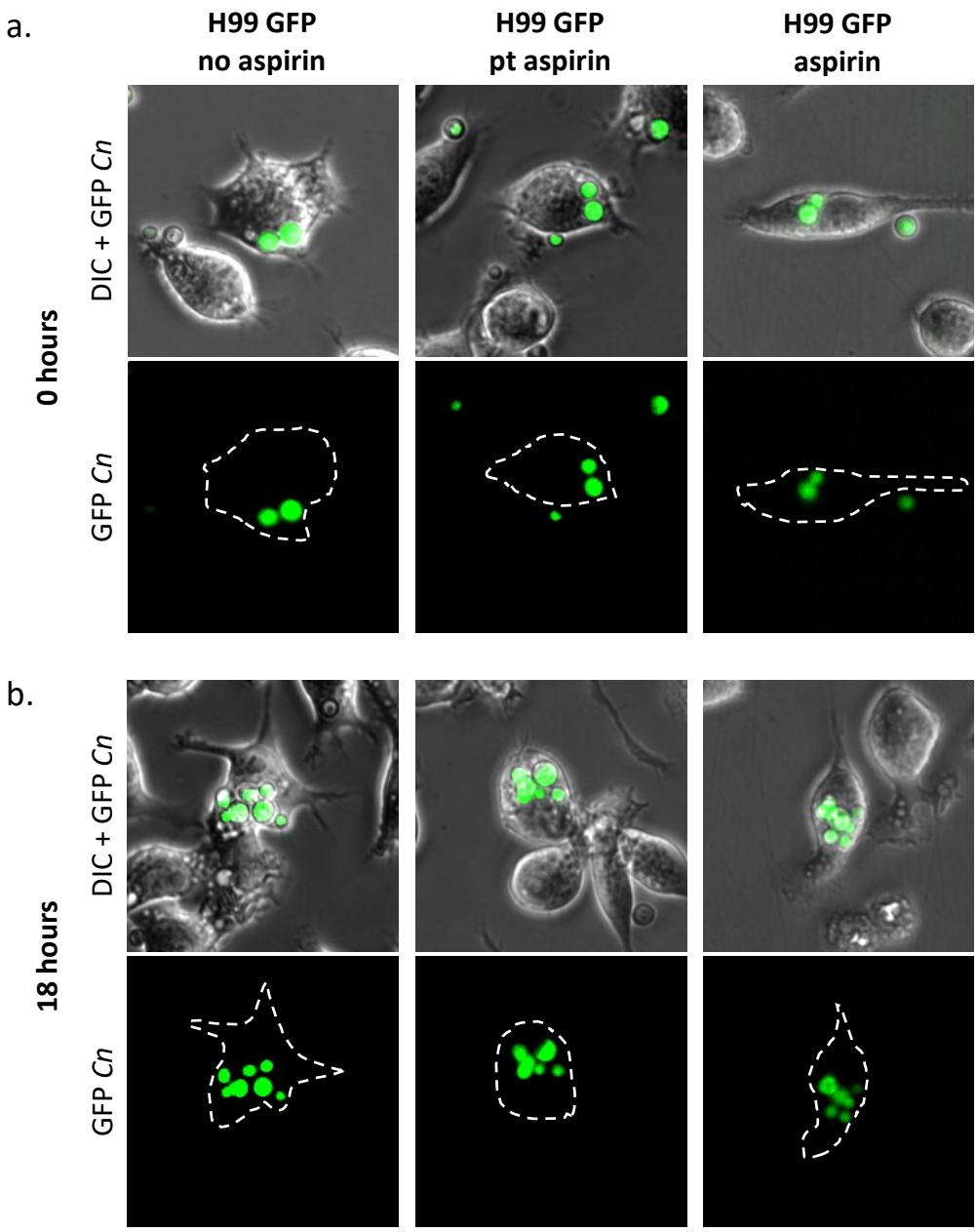

Figure 3.3. Inhibition of host prostaglandins during H99 infection

J774 murine macrophages were left untreated, were pre-treated with aspirin (pt), or were administered with aspirin for the duration of 18 hours (aspirin) to inhibit cyclooxygenase from producing prostaglandins. Images show intracellular cryptococci within macrophages at 0 hours (a) and 18 hours (b). Aspirin treatments are shown along the top. H99 GFP *C. neoformans* are in green, and white dashed lines mark the outlines of the infected macrophages.

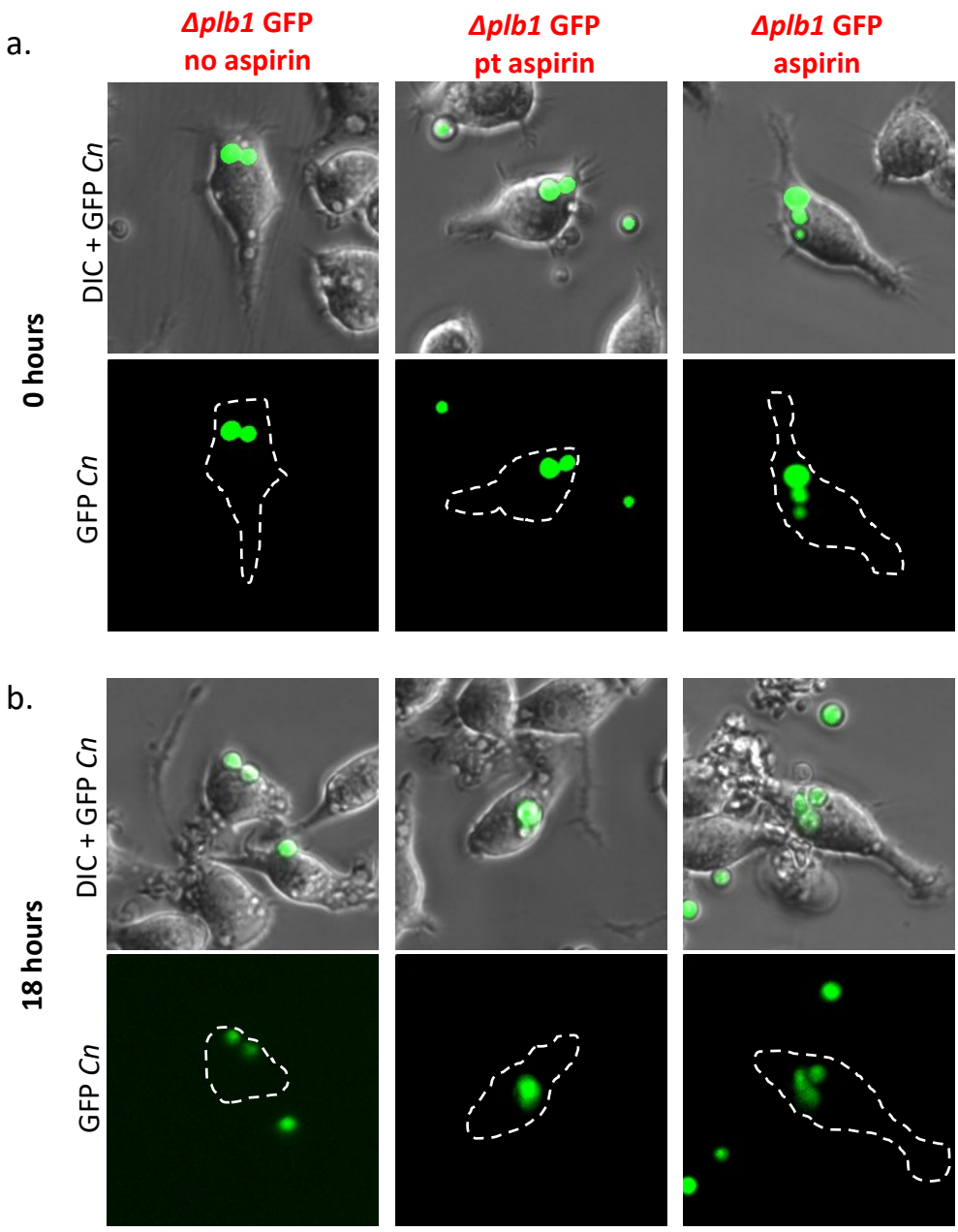

Figure 3.4. Inhibition of host prostaglandins during *Δplb1* infection

J774 murine macrophages were left untreated, were pre-treated with aspirin (pt), or were administered with aspirin for the duration of 18 hours (aspirin) to inhibit cyclooxygenase from producing prostaglandins. Images show intracellular cryptococci within macrophages at 0 hours (a) and 18 hours (b). Aspirin treatments are shown along the top. *Δplb1* GFP *C. neoformans* are in green, and white dashed lines mark the outlines of the infected macrophages.

a.

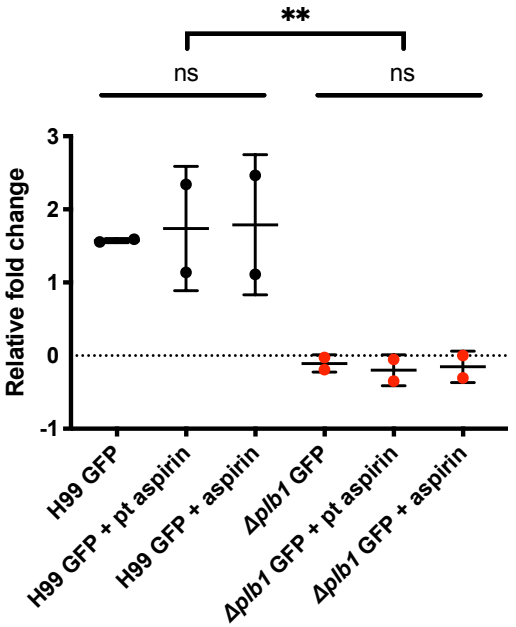

b.

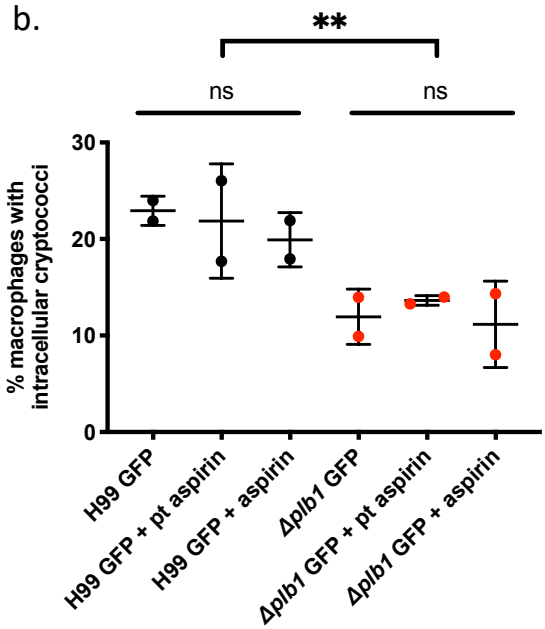

c.

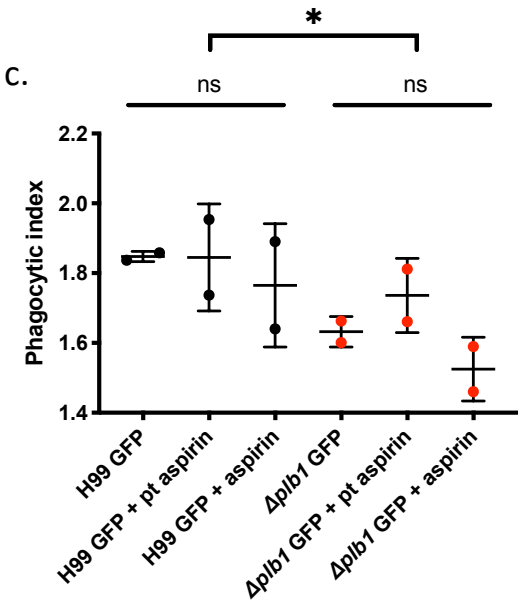

d.

Condition	n	Average fold change		% mac with IC *Cn*		PI	
		Mean	SD	Mean	SD	Mean	SD
H99 GFP	2	1.57	0.03	23.14	5.54	1.85	0.01
H99 GFP + pt aspirin	2	1.74	0.85	21.86	5.61	1.85	0.15
H99 GFP + aspirin	2	1.80	0.95	20.32	7.02	1.77	0.18
Δplb1 GFP	2	-0.11	0.12	12.34	3.87	1.63	0.04
Δplb1 GFP + pt aspirin	2	-0.20	0.21	13.64	3.41	1.74	0.11
Δplb1 GFP + aspirin	2	-0.15	0.22	11.80	5.16	1.53	0.09

Figure 3.5. Host cyclooxygenase inhibition does not affect fungal replication or phagocytosis

J774 murine macrophages were pre-treated (pt) with 1mM aspirin in DMSO for 1h, were pre-treated with aspirin then left in aspirin for the duration of 18h (aspirin), or were left untreated. The macrophages were infected with opsonised H99 or *Δplb1* GFP *C. neoformans* for 2h, washed of extracellular cryptococci, and infection was followed for 18h using time lapse imaging. Mean and standard deviation are displayed for each condition. 2 repeats are represented, with 2 or 3 replicates per condition averaged for each repeat. MOI is 10:1 (10 cryptococcal cells : 1 macrophage). Wells infected with H99 GFP are the points in black and wells infected with *Δplb1* GFP are the points in red. It should be noted that because only two repeats were quantified here, statistics shown here are for illustration only.

a. Fold change for cryptococci which were intracellular, relative to initial number of intracellular cryptococci. Aspirin treatment did not appear to alter relative fungal fold change for H99 or for *Δplb1*, though relative intracellular fold change appeared to be higher for H99 than for *Δplb1* (two-way ANOVA comparing effect of aspirin treatment p = 0.9750, comparing the effect of cryptococcal strain p = 0.0010, pairwise significance only amongst the different strains and not between aspirin treatments).
b. Percentage of macrophages which contained intracellular cryptococci at the commencement of time lapse imaging. Aspirin treatment did not appear to alter the phagocytic uptake of cryptococci, though a higher proportion of macrophages appeared to contain intracellular H99 than *Δplb1* (two-way ANOVA comparing the effect of aspirin treatment on uptake p = 0.6502, comparing the effect of fungal strain p = 0.0037).
c. Phagocytic index (the number of cryptococci contained per macrophage) at the start of time lapse imaging. Aspirin treatment did not appear to affect the number of cryptococci contained within macrophages, though PI appeared to be lower for macrophages infected with *Δplb1* compared to H99 (two-way ANOVA comparing effect of host prostaglandins p = 0.2582, comparing the effect fungal prostaglandins p = 0.0278, no pairwise significance).

d. Descriptive statistics comparing the intracellular proliferation (IPR), the percentage of macrophages within intracellular cryptococci at the commencement of time lapse imaging, and the phagocytic index (PI).

3.4 Inhibition of host prostaglandin synthesis *in vivo* does not affect fungal replication in prostaglandin-deficient *C. neoformans*

To confirm that it was fungal- rather than host-derived prostaglandins that conferred fungal virulence *in vivo*, I aimed to treat zebrafish larvae with aspirin to inhibit host COX activity, and therefore host prostaglandin synthesis. Unfortunately, treatment of zebrafish larvae with aspirin over a broad range of concentrations resulted in severe developmental defects and frequent zebrafish mortality (data not shown). It is possible that aspirin affects more than cyclooxygenase activity in the larvae, and has potential downstream effects that sacrifice fish larva development and overall health.

To circumvent the negative effects of aspirin on zebrafish larva development and survival, I utilised CRISPR/Cas9-mediated knockdown of the PGE_2 synthase gene (*ptges*) in the zebrafish larva model of infection (Loynes et al., 2018)[1]. In utilising this knockdown technology, the effect that host prostaglandins had on cryptococcal virulence and fungal burden *in vivo* could be determined. Based on my *in vitro* assays where host prostaglandin production was inhibited, I hypothesised that inhibition of host prostaglandin synthesis *in vivo* would not affect the ability of cryptococci to replicate, and fungal burden would not be affected.

Zebrafish larvae were injected with CRIPSR/Cas9 directed against prostaglandin synthase (*ptges*$^{-/-}$) at the single cell stage at 0 days post fertilization (dpf). As a control for the introduction of CRISPR/Cas9, we performed CRISPR/Cas9 knockdown of tyrosinase (*tyro*$^{-/-}$), as knockdown of this gene affects only pigmentation of CRISPants and does not alter prostaglandin production in zebrafish. Larvae were genotyped after the duration of the experiments (Figures 3.6b and 3.6d), and any larvae in which CRISPR/Cas9 was unsuccessful were omitted from analysis.

[1] Catherine Loynes in the Renshaw lab performed the CRISPR/Cas9 knockdown assays, while I performed the infection, infection quantification, and PCR analysis.

At 2 dpf larvae were infected with H99 GFP or *Δplb1* GFP *C. neoformans*. Fungal burdens were compared at 0 and 3 days post infection (dpi), as measured by GFP+ pixels per fish (Figures 3.6a and 3.6c). This allowed me to compare fungal burdens at both timepoints for individual larvae. At 0 dpi, control *tyro*$^{-/-}$ larvae were infected with a higher inoculum of *Δplb1* GFP cells (Figures 3.7a and 3.7d; two-way ANOVA for each condition compared to *Δplb1*+tyro$^{-/-}$ $p < 0.0001$). While two-way ANOVA suggested that both host prostaglandin synthase and cryptococcal phospholipase B contributed to the mean fungal burden at 0 dpi, this was actually just due to higher doses of cryptococci being injected during infection. This was not intentional and had no effect on zebrafish survival (data not shown).

After infection, I compared the fungal burdens at 3 dpi between zebrafish larvae which did (*tyro*$^{-/-}$) or did not (*ptges*$^{-/-}$*)* contain prostaglandin synthase, and were infected with either H99 or *Δplb1 C. neoformans* (Figures 3.7b and 3.7d). If host COX inhibition failed to affect fungal burden *in vivo* as it did *in vitro*, you would expect no difference in fungal burden between larvae which were *ptges*$^{-/-}$ and *tyro*$^{-/-}$ infected with the same strain of *Cryptococcus*. If cryptococcal prostaglandins affected fungal burden *in vivo* as they did *in vitro*, you would expect that larvae infected with H99 would have a higher fungal burden than larvae infected with *Δplb1*, regardless of host prostaglandin synthase.

At 3 dpi there was no difference in fungal burden between *ptges*$^{-/-}$ and *tyro*$^{-/-}$ larvae infected with *Δplb1 C. neoformans*, suggesting that knockdown of host prostaglandin synthase did not affect *Δplb1* fungal growth (Figure 3.7b; two-way ANOVA, $p = 0.838$). However, *ptges*$^{-/-}$ larvae infected with H99 showed increased fungal burden compared to *tyro*$^{-/-}$ larvae infected with H99 *C. neoformans* (Figure 3.7b; two-way ANOVA $p = 0.0055$, see figure for additional ANOVA comparisons). These results are conflicting, suggesting that host prostaglandins did not affect fungal burden when fungi were incapable of producing prostaglandins (*Δplb1*), but that they did affect fungal burden when the pathogen was able to synthesise prostaglandins (H99). This may suggest that active host prostaglandin synthase actually helped to control cryptococcal infection when fungal prostaglandins were

produced. It is also possible that host prostaglandins did not affect fungal burden but that some off-target effect of tyrosinase knockdown conferred resistance to the host to reduce fungal burden compared to *ptges*$^{-/-}$ larvae. In fact, tyrosine is oxidised to melanin, and melanin enhances fungal survival in response to host defence mechanisms, enabling survival and growth. Therefore, inhibition of tyrosinase could theoretically lower fungal survival and replication, producing the results reported. However, this would show an identical effect in larvae infected with *Δplb1*, yet tyrosinase ablation did not result in decreased fungal burden in larvae infected with *Δplb1 C. neoformans*. Analysis showed that only fungal phospholipase B, not host prostaglandin synthase, affected the mean fungal burden at 3 dpi (two-way ANOVA; effect of host prostaglandin synthase on fungal burden p = 0.1353, the effect of fungal phospholipase B1 on fungal burden p = 0.0044).

Interestingly, fungal burden was not significantly different at 3 dpi between tyrosinase knockdown larvae infected with H99 and *Δplb1* (Figure 3.7b; two-way ANOVA p = 0.9669). The previous result may hint that loss of tyrosinase decreased H99 fungal burden, which would hinder H99 growth and allow the fungal burden *Δplb1*-infected larvae to 'catch up'. However, since these control larvae were injected with a higher dose of *Δplb1* than H99 at 0 dpi it is possible that H99 proliferated better than *Δplb1* to reach a similar fungal burden at 3 dpi. However, relative fungal fold change was not significantly higher in *tyro*$^{-/-}$ larvae infected with H99 GFP cryptococci (Figures 3.7c and 3.7d; two-way ANOVA comparing relative fold change in H99- and *Δplb1*-infected tyrosinase knockdown larvae p = 0.967).

Finally, at 3 dpi the fungal burden of *ptges*$^{-/-}$ larvae infected with H99 was higher than for those infected with *Δplb1* (Figure 3.7b; two-way ANOVA p < 0.0001), as you would expect if cryptococcal prostaglandins affected fungal burden but host prostaglandins did not. It is possible that ablation of host prostaglandin synthase affected cell types other than macrophages, and that inhibition of host prostaglandins may have reduced control of fungal infection by acting on these cell types. However, as macrophages are the main cells to respond to and phagocytose cryptococci in the zebrafish larva model of infection this seems unlikely (Bojarczuk

et al., 2016; Davis et al., 2016). Again, analysis showed that fungal phospholipase B contributed to the final fungal burden, while host prostaglandin synthase had no effect (two-way ANOVA; host prostaglandin synthase $p = 0.1353$, fungal phospholipase B $p = 0.0044$). Thus, in a zebrafish larva model of cryptococcal infection, fungal-derived prostaglandins affect the fungal burden at 3 dpi.

(page intentionally left blank for figures + legends on following pages)

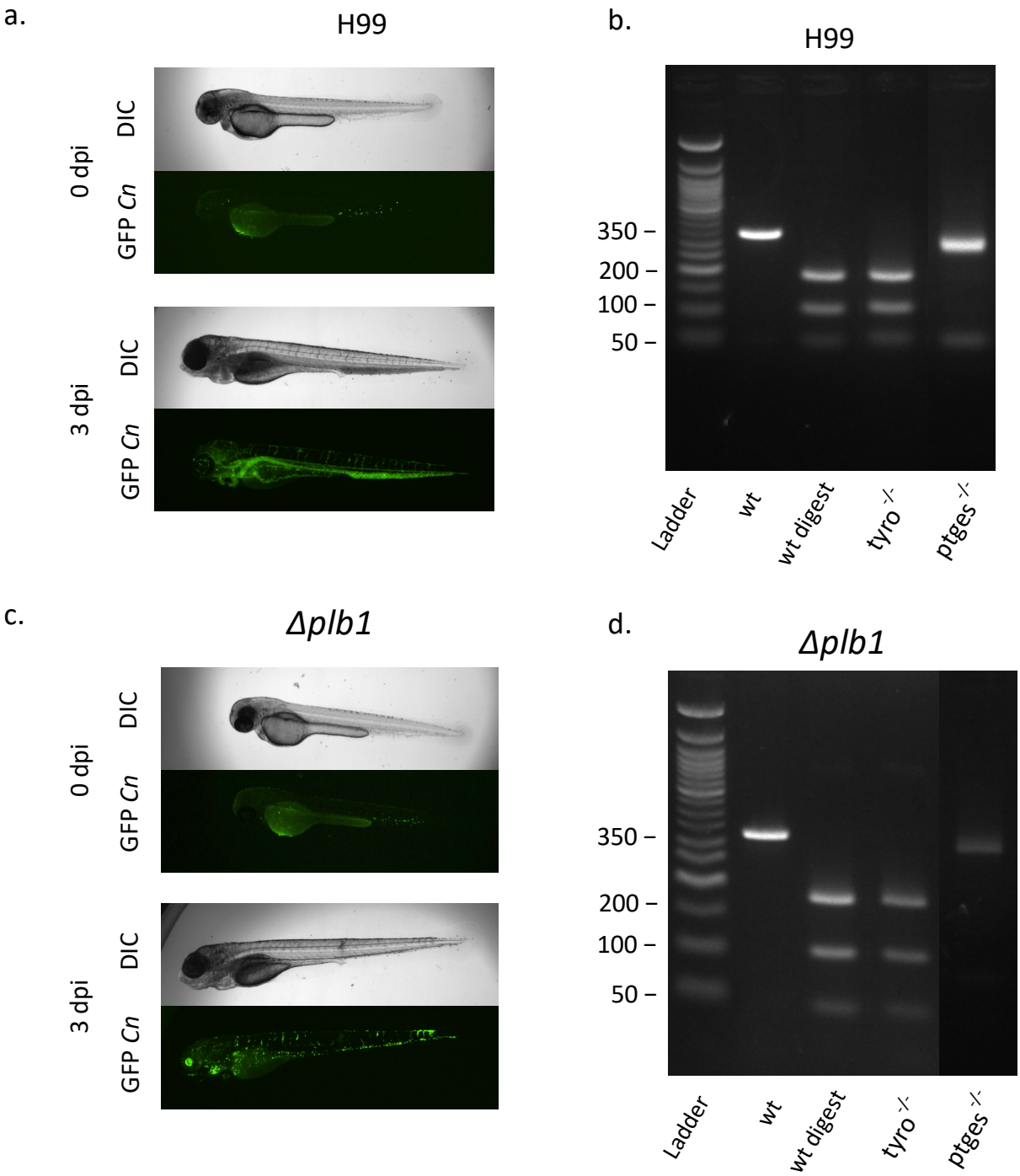

Figure 3.6. Knockdown of zebrafish prostaglandin synthase

To inhibit host prostaglandin synthesis, a guide RNA was designed to target the ATG sequence of *ptges*, the zebrafish prostaglandin synthase gene. Tyrosinase knockdown was used as a control. CRISPR/Cas9 knockdown was performed when zebrafish larvae were at the single cell stage. Larvae were then infected with H99

GFP or *Δplb1* GFP *C. neoformans* at 2 days post fertilization (0 days post injection - dpi), and infections were quantified at 0 and 3 dpi for each larva. Larvae were genotyped at 3 dpi. Cas9 mutation deletes an Mwol restriction site so that when digested, successful knockdown prevents the cleavage of genomic DNA. PCR amplification produced a 345 bp product. Digestion of wildtype DNA produced 184, 109, and 52 bp bands. Heterozygous (*ptges*$^{+/-}$) produced bands at 293, 184, 109, and 52 bp. Homozygous (*ptges*$^{-/-}$) produced bands at 293 and 52 bp. 3 repeats were performed.

a. 0 and 3 dpi infection of *ptges*$^{-/-}$ larva with H99 GFP *C. neoformans*.
b. Representative electrophoresis of CRISPant zebrafish larvae infected with H99 *C. neoformans*. Lanes show the NEB 50 bp ladder, wildtype undigested PCR product, fully cut wildtype PCR product, and the Mwol digested genomic DNA from *tyro*$^{-/-}$ and *ptges*$^{-/-}$ CRISPant zebrafish larvae.
c. 0 and 3 dpi infection of *ptges*$^{-/-}$ larva with *Δplb1* GFP *C. neoformans*.
d. Representative electrophoresis of CRISPant zebrafish larvae infected with Δ*plb1 C. neoformans*. Lanes show the NEB 50 bp ladder, wildtype undigested PCR product, fully cut wildtype PCR product, and the Mwol digested genomic DNA from *tyro*$^{-/-}$ and *ptges*$^{-/-}$ CRISPant zebrafish larvae.

a.

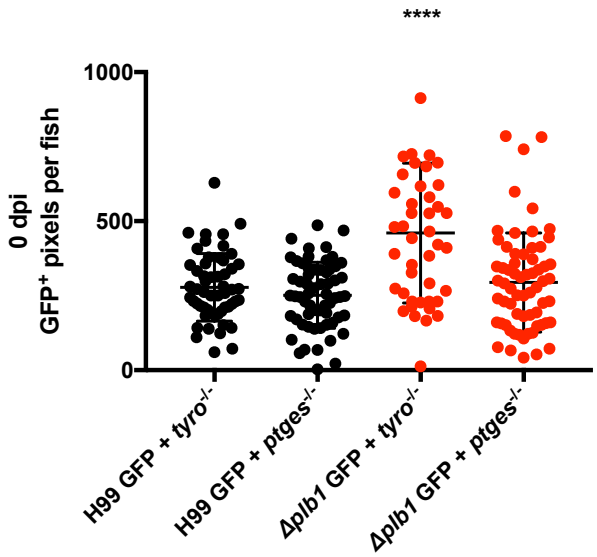

b.

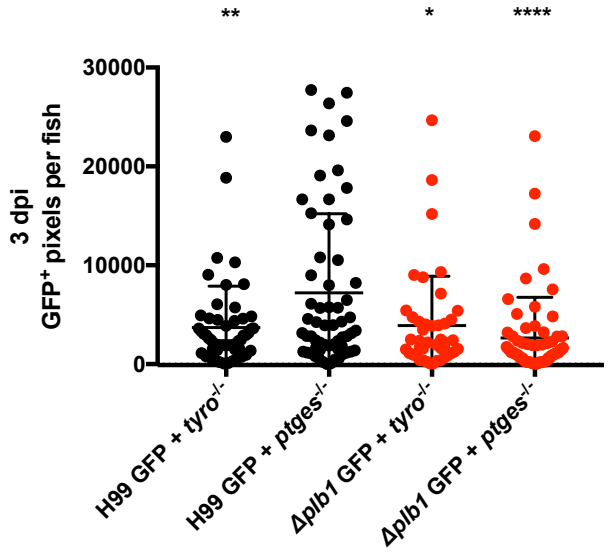

C.

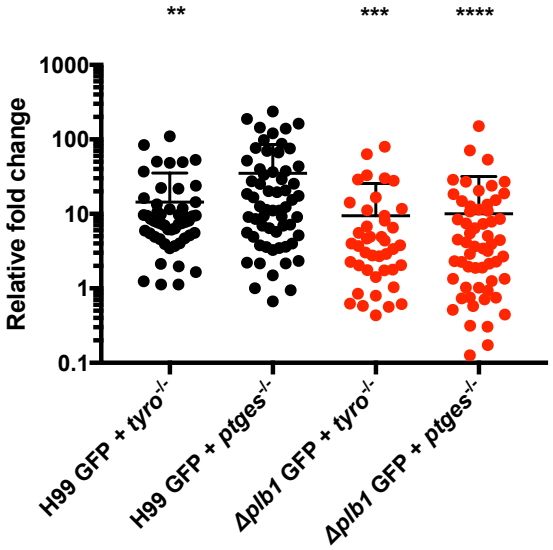

d.

Condition	n	larvae	0 dpi GFP+		3 dpi GFP+		Rel. fold change	
			Mean	SD	Mean	SD	Mean	SD
H99 GFP + *tyro*$^{-/-}$	3	55	278.0	113.0	3698	4196	14.5	20.8
H99 GFP + *ptges*$^{-/-}$	3	61	251.2	111.0	7212	8013	35.0	50.6
Δplb1 GFP + *tyro*$^{-/-}$	3	44	460.2	234.4	3890	4996	9.5	16.2
Δplb1 GFP + *ptges*$^{-/-}$	3	64	294.2	166.3	2651	4120	10.0	21.8

Figure 3.7. Knockdown of host prostaglandin synthase does not affect fungal replication when infected with *Δplb1*, but affects replication in H99 infection

Using CRISPR/Cas-9 technology, prostaglandin synthase and tyrosinase genes were mutated in zebrafish larvae (*ptges*$^{-/-}$ and *tyro*$^{-/-}$, respectively). Wildtype zebrafish larvae were infected with H99 and *Δplb1* GFP *C. neoformans* at 2 dpf (0 dpi). Fungal

burden was measured as GFP+ pixels per fish. Data from 3 separate repeats are shown, with no less than 12 larvae considered per condition for each repeat. Each point is a zebrafish larva, and the mean and standard deviation are represented. Larvae infected with H99 GFP *C. neoformans* are in black, and larvae infected with *Δplb1* GFP *C. neoformans* are in red.

a. Comparison of H99 and *Δplb1* fungal burden at 0 dpi in *tyro*$^{-/-}$ and *ptges*$^{-/-}$ zebrafish larvae. *Tyro*$^{-/-}$ larvae infected with *Δplb1* had the highest fungal burden (two-way ANOVA, $p < 0.0001$ for each condition compared to *tyro*$^{-/-}$ infected with *Δplb1*), and no other larvae showed significantly different levels of fungal infection. While both the CRISPR knockdown and the *Cryptococcus* strain contributed to this difference (two-way ANOVA $p < 0.0001$ for host prostaglandin synthase knockdown, $p < 0.0001$ for cryptococcal phospholipase B), the higher level of cryptococcal infection here reflects that more cryptococci injected during infection.
b. Comparison of fungal burden at 3 dpi. *Ptges*$^{-/-}$ larvae infected with H99 *C. neoformans* showed significantly higher fungal burden compared to other conditions (two-way ANOVA, for H99 + *ptges*$^{-/-}$ compared to: H99 + *tyro*$^{-/-}$ $p = 0.0055$, *Δplb1* + *tyro*$^{-/-}$ $p = 0.0186$, and *Δplb1 + ptges*$^{-/-}$ $p < 0.0001$). There was no other pairwise significance, and while knockdown of host prostaglandin synthase had no effect on final fungal burden (two-way ANOVA $p = 0.1353$), the absence of fungal Plb affected final fungal burden (two-way ANOVA $p = 0.0044$).
c. Relative fold change compared to fungal burden at 0 dpi. H99 infection of *ptges*$^{-/-}$ larvae yielded a higher relative fold change compared to other conditions (two-way ANOVA, H99 + *ptges*$^{-/-}$ compared to: H99 + *tyro*$^{-/-}$ $p = 0.0033$, *Δplb1* + *tyro*$^{-/-}$ $p = 0.0004$, *Δplb1 + ptges*$^{-/-}$ $p < 0.0001$). There was no other pairwise significance between conditions. However, host prostaglandin synthase and fungal phospholipase B both contributed to differences in mean fold change (two-way ANOVA; host prostaglandin synthase $p = 0.0139$, *Cryptococcus* strain $p = 0.0005$, interaction $p = 0.0200$).
d. Descriptive statistics comparing the GFP+ fungal burdens of larvae at 0 and 3 days post infection, and the relative fold change in fungal burdens for larvae under the different conditions.

3.5 *Cryptococcus* induces host PPAR-γ nuclear translocation in a phospholipase B-dependent manner

Having established that *Cryptococcus* produces prostaglandins that confer fungal virulence, I examined the effect of fungal prostaglandins on host cell signalling. *Cryptococcus* produces prostaglandins which are indistinguishable from host prostaglandins; it has therefore been suggested that it is possible for cryptococcal prostaglandins to interfere with host signalling to manipulate the host immune cell responses (Noverr et al., 2001). For example, a study showed that activation of PPAR-γ by 15d-PGJ2 resulted in dampening of macrophage activation and inhibition of induction of the iNOS promoter – activity which is important for the clearance of microorganisms (Ricote et al., 1998). While this study showed that PGE_2 did not affect iNOS promoter activity when transfected with a PPAR-γ expression plasmid, it did not examine how PGE_2 affects PPAR-γ expression.

Recently, we showed that PGE_2 produced by *Cryptococcus* must be dehydrogenated to 15-keto-PGE_2 to enhance fungal virulence (Evans et al., 2019). 15-keto- PGE_2 potently binds PPAR-γ in competitive ligand binding assays in preadipocyte cells (Chou et al., 2007), and while this cell type is not relevant to my work, it demonstrates that 15-keto- PGE_2 is capable of inducing PPAR-γ receptor activation, which in turn may induce transcription in affected cells. Because *Cryptococcus* produces PGE_2 which is dehydrogenated to 15-keto-PGE_2, it is important to discern the potential impact this has on host PPAR-γ signalling, as this could affect the outcome of infection.

To determine how fungal-derived prostaglandins affect host PPAR-γ activation, I infected J774 murine macrophages with H99 GFP and *Δplb1* GFP *C. neoformans* for 18 hours. Troglitazone, a potent agonist of PPAR-γ, was used as a positive control as it has been shown to activate PPAR-γ in a zebrafish model (Tiefenbach et al., 2010). DMSO was used as a negative control. I then performed immunohistochemistry to determine if PPAR-γ was activated in host cells, inducing its translocation to the nucleus (Figure 3.8a). Upon ligand binding and activation, cytosolic PPAR-γ

translocates to the nucleus, and activation therefore results in higher nuclear PPAR-γ staining compared to the cytosol.

Quantification of mean nuclear staining revealed that infection with H99 *Cryptococcus* significantly increased PPAR-γ nuclear staining compared to both the uninfected DMSO and troglitazone controls, inducing its translocation to the nucleus during infection (Figures 3.8b, 3.8c, and 3.8d; H99 GFP compared to each other condition by one-way ANOVA $p < 0.0001$). Furthermore, nuclear translocation was significantly higher in wildtype H99 infection compared to the phospholipase-deficient mutant, confirming that *C. neoformans* activates PPAR-γ in a phospholipase B1-dependent manner (Figures 3.8b and 3.8c; one-way ANOVA comparing H99 and *Δplb1* $p < 0.0001$). Nuclear staining for PPAR-γ in *Δplb1*-infected macrophages was not significantly different compared to DMSO when repeats were combined, (Figure 3.8b; one-way ANOVA $p = 0.0647$), though translocation was lower than DMSO in individual repeats (Figure 3.8c; one-way ANOVA $p < 0.0001$). This suggests that infection with *Δplb1 C. neoformans* did not activate host PPAR-γ. Alternatively, DMSO may have interfered with labelling, or may have induced some PPAR-γ translocation. Nonetheless, *Δplb1*-deficient *C. neoformans* did not induce the activation of PPAR-γ compared to wildtype *C. neoformans* or uninfected controls. Thus, fungal prostaglandins are required to activate host PPAR-γ immune signalling.

a.

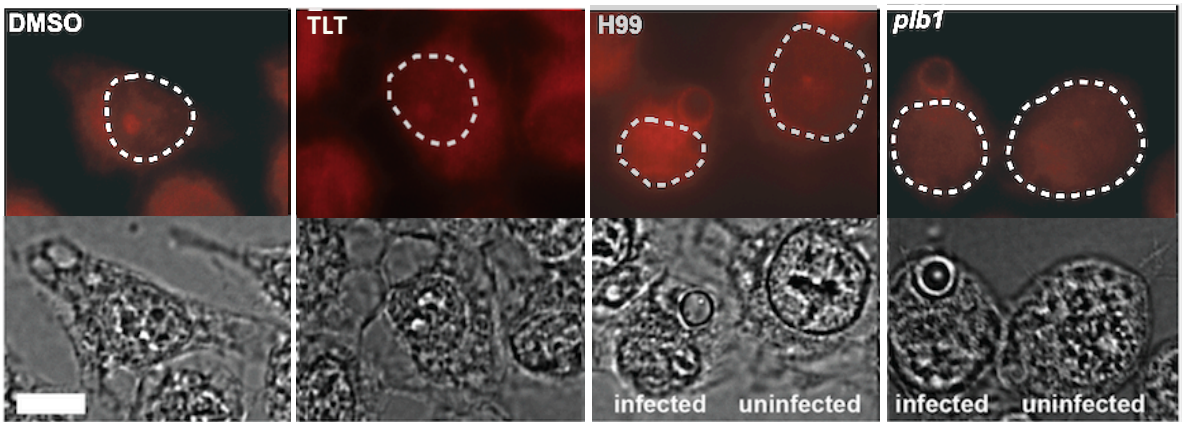

b.

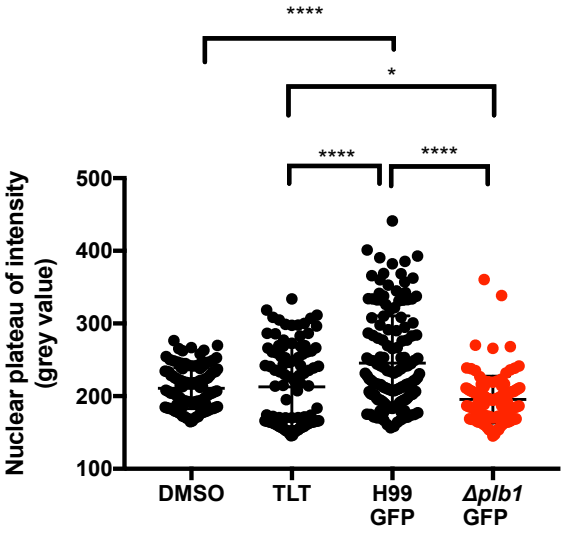

c.

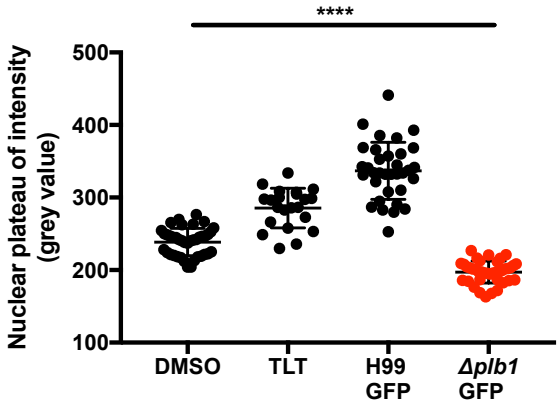

d.

Condition	3 repeats n	cells	Mean	SD	Representative n	cells	Mean	SD
DMSO	3	115	211.00	28.21	3	40	238.60	18.73
TLT	3	102	212.90	54.78	3	22	285.50	27.22
H99 GFP	3	151	245.50	65.02	3	34	336.70	39.39
Δplb1 GFP	3	123	195.30	32.05	3	39	197.20	15.19

Figure 3.8. Cryptococcal activation of host PPAR-γ results in nuclear translocation and is phospholipase B-dependent

J774 macrophages were infected with opsonised H99 GFP or *Δplb1* GFP *C. neoformans* for 18 hours, or were treated with a vehicle control (DMSO) or a positive control (troglitazone – trog, TLT). Cells were then washed and stained with PPAR-γ antibody, then imaged. Nuclear grey value represents the fluorescence of the PPAR-γ antibody localised to the macrophage nucleus. 3 repeats are shown, with no fewer than 102 cells total considered per treatment. Red points are cells infected with *Δplb1* GFP *C. neoformans*. Means and standard deviations are shown.

a. Example images of immunofluorescence experiments in J774 macrophages staining for PPAR-γ nuclear localization. Images provided are from the Cy3 channel (PPAR-γ) and the corresponding cell in DIC. The area of the nuclei is marked with a white dotted line. Cells were imaged at x60 magnification, and scale bar is 10 µM.
b. Quantification of mean nuclear grey value of J774 macrophages treated with DMSO or troglitazone (TLT – a PPAR-γ agonist), or infected with H99 GFP or *Δplb1* GFP *C. neoformans*. Three repeats are shown, with n = 115, 102, 151, and 123 cells quantified for each respective condition. Pairwise significance as calculated by one-way ANOVA is illustrated (DMSO v H99 GFP $p < 0.0001$, TLT vs H99 GFP $p < 0.0001$, TLT vs *Δplb1* GFP $p = 0.0367$, H99 GFP v *Δplb1* GFP $p < 0.0001$). When repeats were grouped there was no significant difference between DMSO and the TLT positive control, but there was a significant increase in nuclear grey value for TLT in individual repeats as shown in (c) below.
c. Nuclear intensity of one repeat as a representative to demonstrate that TLT does in fact induce PPAR-γ translocation to the nucleus. No less than 22 cells were quantified for each condition. One-way ANOVA determined $p < 0.0001$ for each pairwise comparison.
d. Descriptive statistics showing the mean nuclear intensity for individual J774 macrophages under each condition over all three repeats, and for the representative repeat.

3.6 Discussion

3.6.1 The effects of prostaglandins on cryptococcal proliferation

Many microbes produce prostaglandins which may affect the interactions between the host and the pathogen, whether through modulation of virulence factors or modification of the host immune response. For example, *C. albicans* and *C. neoformans* both produce prostaglandins which impair lymphocyte proliferation, reduce macrophage chemokine IL-8 and TNF-α production, and promote IL-10 expression in murine splenocytes (Noverr et al., 2001), demonstrating a potential role for fungal-derived prostaglandins in modification of the host immune response. Alternatively, one study showed that *A. fumigatus* prostaglandins were beneficial for host survival, reducing fungal survival in response to oxidative stress and suggesting a role for host-pathogen crosstalk in determining infection outcome (Tsitsigiannis et al., 2005). Interestingly, while hosts produce prostaglandins in response to infection, they may be exploited by the pathogen to produce detrimental infection outcomes. For example, overexpression of host COX-2 by airway epithelial cells in transgenic mice resulted in reduced *Pseudomonas aeruginosa* clearance (Park et al., 2007), where inhibition of host COX-2 resulted in enhanced clearance during murine lung infection (Sadikot et al., 2007). Here, over-expression of host prostaglandins, either through the use of transgenic models or in response to bacterial infection, was beneficial for the invading pathogen and led to increased infection burden. Because both pathogens and hosts produce prostaglandins which may affect the progression of infection, determining the source and the targets of these signalling molecules is important in understanding host-pathogen interactions.

Cryptococcus neoformans produces prostaglandins which are indistinguishable from those produced by host cells (Noverr et al., 2001). This means that this devastating pathogen may produce lipid mediators which are capable of interfering with host signalling, potentially enabling pathogenic immune evasion and host immune manipulation. As such, it is important to determine the source of prostaglandins during infection; are these mediators produced by the host to

control infection? Or are they are produced by the pathogen to impair host immunity and affect virulence?

To determine if host prostaglandins affected fungal virulence in cryptococcal infection, I used aspirin to irreversibly inhibit host prostaglandin synthesis, leaving fungal prostaglandin production intact and enabling me to discern the contribution of each source of eicosanoids. Inhibiting prostaglandin production by J774 macrophages failed to produce an increase in fungal intracellular replication when compared to untreated control macrophages. As the loss of host prostaglandins did not induce enhanced fungal proliferation, this suggested that the presence of host prostaglandins did not act to inhibit intracellular cryptococcal growth during infection, and that inhibition of host prostaglandin synthesis did not affect cryptococcal proliferation *in vitro*. Furthermore, no reduction in cryptococcal replication was seen after COX inhibition of J774 macrophages, showing that host prostaglandins were also not required by the cryptococci for growth *in vitro*. Indeed, if host prostaglandins were beneficial to cryptococci for growth then the loss of this resource would impair cryptococcal growth. During a murine infection with *Histoplasma capsulatum*, inhibition of host prostaglandin synthesis resulted in reduced fungal burden and increased host survival (Aparecida et al., 2013), demonstrating how host prostaglandin production supported fungal growth in the absence of COX inhibition during *H. capsulatum* infection. However, while macrophage prostaglandins did not affect fungal growth during cryptococcal infection, infection with phospholipase-deficient strain of *Cryptococcus neoformans* resulted in lower intracellular proliferation, as shown previously (Evans et al., 2015). Here, fungal prostaglandin production was required for effective intracellular parasitism of host macrophages by cryptococci.

3.6.2 The effect of prostaglandins on occupation of macrophages

As phagocytosis is important for host control of infection, I also quantified the effect of prostaglandins on phagocytosis. I found that inhibition of host COX also did not affect the phagocytosis of cryptococci. The proportion of macrophages which

contained intracellular cryptococci was not affected by lack of host prostaglandins, but was instead lowered by the deficiency of fungal phospholipase. Since *Cryptococcus* uses host macrophages as an intracellular niche to evade killing and safely replicate, considering the proportion of macrophages which contain intracellular cryptococci may also be used as a measurement of cryptococcal parasitism of host macrophages. After COX inhibition of J774 macrophages, phagocytic index was not significantly different between host COX inhibition conditions, showing that macrophages were equally capable of phagocytosing similar numbers of cryptococci and that host prostaglandin production did not affect this. However, fewer macrophages engulfed the phospholipase-deficient mutant, and the PI was lower between cryptococcal strains. This lower level of invasion of host macrophages by the *Δplb1* strain may suggest that *Δplb1* fungi were less successful at invading the host intracellular niche, and this may account in part for the reduced virulence of this strain. Taken together, the results of this *in vitro* assay showed that host prostaglandin synthesis was not a determinant of fungal replication or successful parasitism of host macrophages, and that fungal phospholipase activity was important to confer fungal virulence.

These results contrast with a previous study by Evans et al. showing that while the percentage of macrophages which phagocytosed cryptococci was not significantly different between macrophages infected with wildtype H99 and *Δplb1* cryptococci, the total number of cryptococci ingested was higher for *Δplb1* mutant cryptococci (Evans et al., 2015). While this may suggest that fungal phospholipase B deficiency led to greater uptake by macrophages, Evans et al. relied on fixation of macrophages and imaging of coverslips; the imaging process in this case may have washed away some of the H99-infected macrophages, inflating the measured uptake of *Δplb1* by macrophages. In my assays, performing time lapse imaging prevented the removal of any infected cells and allowed me quantify fungal uptake in living macrophages. Furthermore, I did not activate macrophages to avoid drawing conclusions based on any factor other than phagocytic uptake in different host COX conditions; this may have contributed to the differences in reported results, as activation may affect differential uptake between strains. Alternatively, uptake of the less virulent *Δplb1*

strain may have induced individual macrophages to phagocytose successive cryptococci; however, I did not observe this during time lapse analysis. Nonetheless, Evans similarly showed that the IPR was lower for the mutant cryptococci, a result mirrored in my experiments. This reduced replication within the host niche again shows that *Δplb1* cryptococci were less able to exploit the host macrophage intracellular niche for replication.

While host COX inhibition in my J774 macrophage model of infection did not affect cryptococcal uptake or intracellular proliferation, fungal prostaglandins affected the ability of cryptococci to parasitize macrophages, both in terms of macrophage invasion (percentage of macrophages with intracellular cryptococci), and replication within the macrophage intracellular niche. This suggests not only that cryptococcal prostaglandins enabled successful colonization of host immune cells, but that their absence may have failed to attenuate the macrophage permissiveness to intracellular infection, thus hindering the ability of the cryptococci to replicate within the hostile macrophage intracellular niche. In fact, one study showed that administration of PGE_2 to murine BMDMs reduced superoxide production by the macrophages in response to *P. aeruginosa* infection, demonstrating that prostaglandins may attenuate the microbicidal activity of macrophages (Sadikot et al., 2007). Indeed, bacterial virulence factors regulate macrophage COX-2 activity and subsequent PGE_2 production in order to modulate macrophage polarisation and subsequent microbicidal activity in *Salmonella* Thyphimurium and *Yersinia enterocolitica* infections (Sheppe et al., 2018). Thus, the reduced parasitism of the *Δplb1* strain of *C. neoformans* may be due to the failure of the cryptococci to temper the polarisation of macrophages, hindering the ability of *Δplb1* cryptococci to thrive and replicate within the macrophage intracellular niche.

3.6.3 Fungal prostaglandins confer virulence *in vivo*

To determine the effect of prostaglandins on *in vivo* cryptococcal infection, I specifically inhibited host prostaglandin synthesis in a zebrafish model of infection. CRISPR/Cas9 knockdown of host prostaglandin synthase in a zebrafish lava model of

infection showed that H99 infection of *ptges*$^{-/-}$ larvae resulted in increased fungal burden at 3 dpi compared to the *tyro*$^{-/-}$ control. This suggests that host prostaglandins may have actually inhibited fungal growth to some extent in an *in vivo* model of infection, similar to how PGE_2 induces *Y. enterocolitica* clearance *in vitro* (Sheppe et al., 2018). A similar increase in burden has previously been reported for prostaglandin synthase knockout mice infected with *S. pneumoniae*, where host PGE_2 was necessary for control of bacterial growth (Dolan et al., 2016). However, because host prostaglandin inhibition *in vitro* (via COX inhibition of J774 macrophages) had no effect on cryptococcal growth within macrophages, it is possible that *in vivo* knockdown of host prostaglandin synthase may have affected cells beyond macrophages. Other immune cells such as neutrophils are likely involved in the control of cryptococcal infection in larvae (Davis et al., 2016), and inhibition of PGE_2 production by these cells in the *ptges*$^{-/-}$ fish may have enabled the uncontrolled growth of the cryptococci compared to control larvae. Furthermore, knockdown of prostaglandin synthase in mice not only inhibited PGE_2 production, but also induced alternative prostaglandin production in response to bacterial infection (Dolan et al., 2016). If alternative anti-microbial prostaglandins were produced in *ptges*$^{-/-}$ larvae in response to cryptococcal infection, these may have affected the fungal burden in *ptges*$^{-/-}$ larvae. Finally, the increased burden in ptges$^{-/-}$ zebrafish may reflect a reduced virulence of H99 larvae in zebrafish lacking tyrosinase. Because tyrosinase is involved in melanin production, and melanin confers virulence to cryptococci, the loss of this resource in the tyro$^{-/-}$ larvae may have lowered the resistance of fungi to host stressors and resulted in less fungal growth (or higher fungal killing by host cells) in the tyrosinase mutant.

However*, in vivo* knockdown of host prostaglandin synthase had no effect on *Δplb1* infection burden at 3 dpi, suggesting that host prostaglandins had no effect on fungal virulence during *Δplb1* infection. It is interesting that there was no increase in fungal burden in the *ptges*$^{-/-}$ larvae compared to the *tyro*$^{-/-}$ control larvae when infected with the phospholipase-deficient strain, as was the case in the wildtype H99 strain. This suggests that the ability of the host to produce PGE_2 did not affect cryptococcal growth *in vivo*, and while host prostaglandins were not important for

the control of *Δplb1* infection, they may have been when infected with prostaglandin-producing cryptococci. Here, there may be some cross-talk between host and cryptococcal cells which involved fungal-derived prostaglandins. During *in vitro* macrophage infection fungal prostaglandins were important for intracellular replication within host macrophages with no apparent effect of host prostaglandins; however, host prostaglandins produced by cells other than macrophages may have aided in the control of fungal infection *in vivo*.

While the evidence suggests that host prostaglandin production may not be critical in affecting *Cryptococcus* infection, again fungal prostaglandins affected fungal growth. When comparing *ptges*$^{-/-}$ larvae infected with H99 and *Δplb1*, fungal prostaglandin production resulted in higher fungal burden. Relative fungal fold change, representing overall growth per fungal cell over the 3 days, was higher for H99 compared to *Δplb1* cryptococci in *ptges*$^{-/-}$ larvae. While 3 dpi fungal burden and relative fungal fold change were not significantly different between H99 and *Δplb1* in *tyro*$^{-/-}$ larvae, the fact that there was a higher fungal burden of *Δplb1* at 0 dpi and the fungal burdens were not significantly different 3 days later suggests that H99 fungi replicated more efficiently than *Δplb1* in the *tyro-/-* larvae, though statistical significance was not achieved. This again suggests that fungal-derived prostaglandins were important for fungal virulence *in vivo*.

3.6.4 Downstream effects of prostaglandin signalling on immune polarisation

The effects of prostaglandin production must be considered carefully, especially as they can have an immunomodulatory effect on host immune response. The pathogenic fungus *Paracoccidioides brasiliensis*, for example, produces prostaglandins which confer viability in culture (Biondo et al., 2010; Bordon et al., 2007). Interestingly, Soares et al. treated monocytes with indomethacin to prevent prostaglandin production, which induced the monocytes to kill the *P. brasiliensis* cells (Soares et al., 2001). While the source of prostaglandins was not specifically investigated, inhibition of prostaglandin production induced fungicidal activation by

the phagocytes, suggesting that during this infection prostaglandins were beneficial for the pathogen and detrimental for the phagocytes. Furthermore, killing of the fungi required only low levels of TNF-α production when prostaglandin production was inhibited, where the immune response required both high levels of TNF-α and IFN-γ when prostaglandin production was allowed; this suggests that immune modulation in the presence of prostaglandins inhibited activation and killing of fungi by monocytes (Soares et al., 2001). Thus, modulation of immune signalling and activation represents a potential source of immune interference induced by prostaglandins, which may act similarly during cryptococcal infection.

As modulation of host immune response by pathogens can affect infection progression, determining the effect of fungal prostaglandins on immune signalling and polarisation may illuminate the mechanism by which *Cryptococcus* utilises prostaglandins to enhance intracellular parasitism. Another eicosanoid species, 15d-PGJ_2, modulates the cytokine profile in the onset of inflammation, as well as the influx and efflux of immune cells from sites of inflammation (Rajakariar et al., 2007). 15d-PGJ_2 signalling can shift cytokine secretion from the pro-inflammatory Th1 (TNF-α) profile toward a more anti-inflammatory, Th2 (IL-10) profile – which in turn has the ability to affect macrophage polarisation. Indeed, 15d-PGJ_2 activates host PPAR-γ and produces an anti-inflammatory phenotype during inflammation (Alleva et al., 2002; Kawahito et al., 2000b; Maggi et al., 2000). 15d-PGJ_2 has been shown to repress inflammatory response genes in mouse macrophages (Pascual et al., 2005), especially iNOS mRNA transcription and gene expression (Ricote et al., 1998). iNOS expression is important in the pro-inflammatory M1 response against *Cryptococcus*, and as such, host PPAR-γ activation has the potential to influence macrophage defence against cryptococcal infection. As such, I investigated the effect of fungal prostaglandins on host PPAR-γ activation.

In performing PPAR-γ antibody staining after cryptococcal infection of J774 macrophages, I showed that infection with wildtype *C. neoformans* induced host PPAR-γ activation and nuclear translocation. Phospholipase-deficient *C. neoformans* infection resulted in a much lower level of PPAR-γ activation compared to infection

with H99, showing that fungal prostaglandin production was required for efficient activation of macrophage PPAR-γ. These results are interesting because they showed that fungal prostaglandins have the capability to interfere with host immune signalling. While the specific molecular effects of fungal activation of host PPAR-γ were not determined here, this experiment showed that *Cryptococcus* is capable of manipulating host immune signalling and, thus, the outcome of infection. For example, in down-regulating host iNOS activity through PPAR-γ activation as shown with 15d-PGJ_2 (Ricote et al., 1998), *Cryptococcus* may prevent its own destruction, enhancing intracellular proliferation and overall virulence.

Through further experiments utilising a PPAR-γ reporter zebrafish line, fungal prostaglandins were shown to activate host PPAR-γ, and this enhanced the growth of the fungi *in vivo* (Evans et al., 2019). These results showed that fungal prostaglandins enhanced growth in a zebrafish model of infection, and this was related to PPAR-γ activation by fungal the fungal eicosanoid 15-keto-PGE_2, a derivative of PGE_2. While 15-keto-PGE_2 has previously been shown to act as a PPAR-γ ligand, (Chou et al., 2007), these combined results presented a novel mechanism by which cryptococcal prostaglandins, specifically 15-keto-PGE_2, promote fungal virulence through PPAR-γ activation (Evans et al., 2019). As PGE_2 metabolites are capable of activating macrophage PPAR-γ, potentially tempering the host intracellular environment to one permissive to intracellular growth, failure to do so by the phospholipase mutant of *C. neoformans* may be one way in which it fails to successfully exploit the macrophage intracellular niche.

3.7 Conclusions and future work

Altogether, I have demonstrated that host-derived prostaglandins are not required for successful cryptococcal parasitism of macrophages, that they may play some role in controlling fungal infection through actions outside of macrophage control, and that fungal-derived eicosanoids can manipulate macrophage signalling to promote virulence. Various pathogenic fungi are capable of not only altering host prostaglandin production and downstream immune response, but also produce

functional prostaglandins which may interfere with control of infection and promote virulence (Noverr et al., 2001). While the direct molecular mechanisms by which fungal prostaglandins promote intracellular parasitism of host macrophages is yet to be completely understood, we know that cryptococcal prostaglandin production is important for intracellular replication and PPAR-γ activation (Evans et al., 2015, 2019). Future experiments should explore the specific effects that macrophage PPAR-γ activation has on the polarisation of infected macrophages and how this affects cryptococcal intracellular parasitism, potentially through the use of single-cell RNA-sequencing and cytokine secretion assays.

Through inhibition of host prostaglandin production *in vitro*, I showed that host eicosanoids did not affect fungal replication within the macrophage intracellular niche. However, specific PGE_2 inhibition via prostaglandin synthase knockdown *in vivo* provided less clear results; this suggested that other host-derived eicosanoids may have affected cryptococcal virulence, or that host- and pathogen-derived prostaglandins may interact to produce conflicting or intermediate effects. As such, the potential eicosanoid cross-talk between invading pathogen and defending host should be investigated in finer detail to discern exactly how host and pathogenic prostaglandins interact, and what factors drive their action in different cell types.

While there are persisting questions into how prostaglandins affect cryptococcal virulence and intracellular parasitism, the work I have done provides further evidence that cryptococcal prostaglandins enhance cryptococcal exploitation of the host macrophage intracellular niche and subsequent fungal pathogenic success.

Chapter 4. *Cryptococcus*-macrophage interactions are not affected by the multiplicity of infection

4.1 Introduction

The study of infectious diseases has progressed over the years as technology has improved our ability to image, quantify, and produce experimentally-determined evidence from models that previously produced only broad understanding into how pathogens interact with the host immune system. Still, current modes of studying infection provide insight into the pathogenicity of disease, but fail to determine the effect of host-pathogen interactions on disease progression and outcome. While correlations are drawn between the level of infection and the outcome, often studies neglect to address the effect of infection dose on interactions between pathogens and phagocytes – interactions which can be crucial in deciding the fates of both the pathogen and the host. In this chapter I will address how cryptococcal infection burden affects interactions with host macrophages.

4.1.1 The effects of population density on pathogen survival

The relationship between microbial density and physiological action has long been recognized, and largely began with study of *S. pneumoniae* competence (Tomasz, 1965) and the discovery of density-dependent autoinduction of luminescence in marine bacteria (Kempner and Hanson, 1968; Nealson et al., 1970). Today, many bacteria are known to possess mechanisms of sensing culture density, and the production of 'quorum sensing' (QS) molecules enables the expression of genes which enhance cooperative survival, fitness, and pathogenicity of some pathogens in response to population density and environmental cues (Antunes and Ferreira, 2009; Bassler and Losick, 2006; Caetano et al., 2010; Castillo-Juárez et al., 2015; Li and Nair, 2012).

In order to survive and grow, whether in nature or in a host, pathogens must possess the ability to sense and respond to the environment. To ensure endurance of the population at levels that enable survival and eventually active infection, they must

also retain the ability to signal amongst members of the group. In many cases, pathogens can sense population density and coordinate a group response to ensure survival in adverse conditions. One way in which bacteria do this is by limiting exhaustion of nutrients, sacrificing members of the group if necessary. In utilising a glucose starvation model of *Escherichia coli*, Takano et al. found that *E. coli* not only recycled nutrients from dead cells, but that the bacteria purposely aimed to produce a high cell density during exponential growth in order to harvest nutrients from cells which they sacrificed in times of nutrient scarcity (Takano et al., 2017). In doing so, *E. coli* ensured that there was a reserve of nutrients among the group from which they could draw sustenance in times of stress. Interestingly, the population growth rate of the bacteria in starvation conditions decreased with increasing inoculum, but not due to nutrient availability. Instead, the bacteria stopped growing at a density that allowed the same number of cells to grow again if the supernatant was used for growing *E. coli* from the start of the death phase. This suggests that these bacteria sensed the population density of viable cells and adjusted their growth accordingly to allow the long-term survival of the population in a feedback-type manner. While this study did not identify the molecular mechanisms employed by *E. coli* to regulate population density, it is known that *E. coli* possesses homoserine lactone – a molecule related to acylated homoserine lactones, quorum sensing molecules of bacteria – which lowers population density of *E. coli* during starvation (Huisman and Kolter, 1995; Phaiboun et al., 2015). Though these experiments were not performed *in vivo*, and the density-dependent phenomenon discussed here was not present during nutrient-rich growth conditions, they demonstrate a change in growth phenotype in response to environmental and population cues to enable microbial survival.

Another way in which a subpopulation of microbes sacrifice for the survival of the population as a whole is the density-dependent-signalling which prevents population phage infection. *E. coli* utilises a toxin-antitoxin mechanism to induce, or repress, cell death through the *mazEF* operon. In times of stress, transcription of the antitoxin (mazE) is inhibited, resulting in accumulation of the toxin (mazF) and leading to bacterial cell death. An extracellular death factor is required to initiate

the process; this factor is produced in a density-dependent manner in *E. coli*, and acts as a quorum sensing autoinducer that is effective at threshold concentrations (Kolodkin-Gal et al., 2007). The induction of this process is associated with stresses such as infection by phages, which pose a threat to the bacterial community (Hazan and Engelberg-Kulka, 2004). The prevention of antitoxin transcription, and thus cell 'suicide' by toxin production, prevents the growth of the phage within the infected cell, and also inhibits phage spread to the bacterial population as a whole, leading to phage exclusion and survival of the *E. coli* population (Hazan and Engelberg-Kulka, 2004).

While the ability to perceive microbial population density enables the efficient use of available nutrients, and may protect the population from harm by phages, all microbes in a population do not need to possess the ability to sense and respond to density. In fact, sensing population density often leads to the production of excreted products for use by the group – a task which involves the expenditure of energy. To cope with this, some microbes "cheat" and utilise the products produced by fellow microbes within the population without producing any themselves. In a wax moth model of *S. aureus* infection, density-dependent response is a cooperative social trait that promotes staphylococcal virulence. For example, a quorum-sensing mutant *S. aureus* is less virulent than the wild type strain, and causes less wax moth death compared to the wild type (Pollitt et al., 2014). However, mutant quorum sensing staphylococci "cheat" and exhibit increased fitness when in a mixed population with staphylococci which are capable of producing quorum sensing molecules. This is possible as long as the bacteria with are capable of producing quorum sensing molecules remain the majority (Pollitt *et al.*, 2014). Here, involuntary sacrifice by some bacteria for the exploitation of others is beneficial to the population as a whole.

Fungi also utilise density-dependent cues to enhance survival. *C. albicans* utilises density-dependent signalling to protect itself from oxidative stress through the production of the quorum sensing molecule farnesol (Deveau et al., 2010). With the increase of population density, *C. albicans* becomes more resistant to hydrogen

peroxide. Suspension of *C. albicans* in conditioned media from stationary-phase culture results in greater resistance to oxidative stress, suggesting a possible role for a density-dependent secreted factor, such as farnesol, in *C. albicans* survival (Westwater et al., 2005). However, the addition of farnesol does not completely recapitulate the resistance to oxidative stress provided by conditioned medium; indeed, addition of farnesol to fresh media results in resistance above that of fresh media alone, but fails to achieve survival upon oxidative threat similar to *C. albicans* suspended in conditioned media, even when farnesol production is enhanced (Westwater et al., 2005). This suggests that farnesol may not be the only extracellular factor to confer protection against reactive oxygen species. However, upregulation of farnesol production does increase survival during oxidative stress, implicating that this quorum sensing molecule is produced by *C. albicans* in a dose-dependent manner that confers some enhanced survival in harsh circumstances.

Interestingly, Shirtliff et al. have shown that *C. albicans* produces ROS which can result in fungal cell death; however, they have suggested this as a potential mechanism to regulate apoptosis in order to reduce cell number and therefore strain on nutrients in high-density biofilms (Shirtliff et al., 2009). To further aid in the survival of the population during times of stress, it has also been shown that quorum sensing, especially through farnesol, inhibits gene translation and protein synthesis in *C. albicans* and *S. cerevisiae* (Egbe et al., 2017; Shirtliff et al., 2009). By inhibiting translation of genes related to growth and filamentation, less energy is spent on morphological development, a frugal tactic which is useful in times of stress and nutrient starvation. As discussed with bacteria above, fungi are able to sacrifice some of their population for the good of the population as a whole.

4.1.2 Density-dependent pathogen morphology

Beyond survival, density-dependent quorum signalling within bacterial populations has other effects on the community. For example, many bacteria receive signals from fellow cells and the environment to induce morphological changes. These changes serve the purpose of enabling microbial penetration and pathogenic

dissemination, enhancing the fitness of the group as a whole. One important example of this is when bacteria utilise population density cues to release DNA from cells, aiding in successful biofilm formation. Competence is the process by which bacteria take up extracellular DNA from their environment through transformation – a process which first requires DNA to be released from donor cells. In *Streptococcus pneumoniae*, competence is cell density-dependent and requires 'macromolecular' pheromones, or quorum sensing molecules, to induce release of DNA (Sigve Havarstein et al., 1995; Tomasz, 1965; Tomasz and Hotchkiss, 1964). Competence-induced streptococcal lysis and DNA release via quorum sensing is important for *S. pneumoniae* biofilm formation, which is beneficial for bacterial survival and virulence (Moscoso et al., 2006). Interestingly, this lysis and release of DNA occurs only in a fraction of bacterial cells (Steinmoen et al., 2002), enabling the remaining cells within the biofilm to aggregate and survive within the biofilm colony.

Pathogenic fungi also possess the ability to sense population density and coordinate morphological responses within the population. In fact, multiple quorum sensing molecules have been discovered that are produced by fungi, with farnesol and tyrosol being the most widely studied. *C. albicans* is a dimorphic fungus that displays an "inoculum size effect", where it switches from filamentous, hyphal form to a budding yeast phenotype as population size increases to a threshold of 10^6 cells/ml. Hornby and colleagues discovered that if *C. albicans* was cultured in spent, conditioned media, a secreted factor within the media induced a morphology change from a hyphal form to yeast; here, the quorum sensing molecule farnesol was found to be responsible for this effect (Hornby et al., 2001). In fact, treatment of *C. albicans* with commercially purified farnesol produced the same morphology switch that is observed at 10^6 cells/ml (Hornby et al., 2001).

This density-dependent effect is interesting because germ tube formation leading to a hyphal morphology is important in producing architecturally complex, stable biofilms. However, farnesol disables *C. albicans* biofilm development through inhibition of hyphae formation in a dose-dependent manner (Ramage et al., 2002). Biofilms are employed by microbes not only to enable group cooperation, but also

typically provide protection from adverse conditions, including administration of pharmaceutical medications. Yet, one study showed that farnesol production by *C. albicans* resulted in thinner biofilms which lowered resistance to the antifungal drug fluconazole, compared to *C. albicans* in the absence of farnesol (Yu et al., 2012). However, to understand the role of farnesol in hyphae and biofilm development, it is also important to consider the actions of tyrosol.

Shortly after Hornby isolated farnesol as a quorum sensing molecule in *C. albicans*, Chen et al. found that conditioned media from high density cultures shortened the lag phase of growth in low density *C. albicans* cultures, and found tyrosol to be partially responsible for the effects seen (Chen et al., 2004). Indeed, when exogenous tyrosol was added to low density cultures, the *C. albicans* abolished the lag phase and initiated exponential growth (Chen et al., 2004). However, tyrosol was not the only compound responsible for the resumption of exponential growth, as the concentration of tyrosol added exogenously was much higher than concentrations detected in conditioned media, illustrating the need for additional quorum sensing molecules – potentially farnesol.

As with farnesol, the presence of tyrosol at specific population densities induces morphological effects. In the experiment above, addition of exogenous tyrosol prompted the switch from a yeast morphology to the induction of hyphal growth (Chen et al., 2004). However, at high cell densities *C. albicans* switched from a hyphal form to a free yeast morphology through the action of farnesol, suggesting that farnesol prevailed over tyrosol in determining phenotypes at high cell concentrations (Hornby et al., 2001). Indeed, work carried out by Alem et al. showed that tyrosol and farnesol were important during different phases of biofilm development. During early phases of biofilm development, tyrosol increased hyphae formation, especially between 2 and 6 hours. However, later during biofilm formation farnesol was produced at higher concentrations, and promoted the planktonic yeast morphology over a hyphal form, enabling the release of yeast from the biofilm and promoting the dispersal of the fungus (Alem et al., 2006). Here, fungi were able to signal within a densely packed community to sense population density

and promote different phenotypes at different cell concentrations. This enabled the production of a structure that was advantageous for survival, followed by the release of yeast to propagate infection and develop new biofilms in areas where there was higher nutrient availability (Alem et al., 2006; Ramage et al., 2002). The ability to switch between yeast and hyphal forms is useful for *C. albicans* pathogenicity, as the hyphal form is more invasive, and the small size of the yeast form is especially advantageous for dissemination. As such, density-dependent morphological changes in pathogenic fungi also impact fungal virulence.

In a similar manner, the bacterium *Vibrio cholerae* utilises quorum sensing to suppress thick biofilm formation (Zhu and Mekalanos, 2003). The formation of biofilms of appropriate thickness enables individual bacteria within to detach from the biofilm and colonise target tissue in the planktonic form. The ability to perceive culture density and respond in a way that prioritises group phenotypic coordination is so crucial in *V. cholerae* infection that redundant, robust quorum sensing mechanisms are employed by this bacterium (Jung et al., 2015). Thus, while the ability to form biofilms is important for many infectious pathogens because it affords the cells within protection, biofilms must be properly structured in order to confer any advantage. Quorum sensing systems within populations support the switches necessary for the adoption of appropriate phenotypes and group morphologies.

4.1.3 Density-dependent microbial virulence

While population density detection and response certainly affect survival and phenotype, an important factor in infection is virulence. In fact, in many bacterial quorum sensing systems are strongly linked to virulence. *P. aeruginosa*, for example, contains multiple systems which enable the detection of cell density and in turn upregulate the expression of virulence genes (Gambello and Iglewski, 1991; Passador et al., 1993; Pearson et al., 1994, 1995). The *las* and *rhl* quorum sensing systems lead to the production of autoinducers which ultimately target the promoters of various genes once threshold concentrations are achieved. A screen

of 7,000 *P. aeruginosa* mutants revealed that the expression of 270 genes were upregulated in response to autoinducer stimulation, many of which were involved in virulence (Whiteley et al., 1999). What's more, blocking bacterial population signalling through quorum sensing inhibitors down-regulated the expression of *P. aeruginosa* virulence-related genes *in vitro* (Ahmed et al., 2019; O'loughlin et al., 2013), illustrating the necessity for population cues to propagate an effective infection. A key example of how density-dependent gene regulation is involved in *P. aeruginosa* virulence is the production of autoinducer molecules which induce the expression of the *lasB* gene (Gambello and Iglewski, 1991; Passador et al., 1993; Pearson et al., 1994). This gene encodes elastase, which is a potent virulence factor for *P. aeruginosa* and is associated with lung health and pseudomonal virulence in human clinical cystic fibrosis (Jazayeri et al., 2016).

Interestingly, inhibiting quorum sensing receptors directly relates to virulence and survival during some infections *in vivo*. For example, O'Loughlin et al. showed that infection of *C. elegans* with a *las* receptor mutant strain of *P. aeruginosa* resulted in greater *C. elegans* survival compared to nematodes infected with wild-type strains (O'loughlin et al., 2013). Through preventing the activation of the *las* receptor by density-dependent cues, the virulence of this bacteria was attenuated, illustrating the direct effects of density-dependent cues on pathogen virulence and host survival.

Staphylococcus aureus also produces an autoinducing peptide, Agr, in response to staphylococcal cell density. Ultimately, this autoinduction peptide induces the transcription of an effector RNA molecule, which upregulates the transcription of genes associated with virulence (George and Muir, 2007; Ji et al., 1995; Novick and Geisinger, 2008). Interestingly, *S. aureus* quorum sensing induces the context-dependent alteration of behaviour and gene expression. RNA transcription profiling of *S. aureus* showed that many virulence genes were upregulated by the autoinducer at different phases of infection through density-dependent regulation (Dunman et al., 2001). This expression of different genes at different times during

infection ensured that specific genes are upregulated to best suit a specific phase of infection.

4.1.4 The effect of microbial density on host-pathogen interactions

Thus far I have described how pathogens draw cues from the population to coordinate responses which promote survival and virulence. However, it is also important to consider how pathogens interact with host immune cells, as these interactions often mean the difference between eradication of infection and microbial success. Indeed, individual host-pathogen interactions are important in events such as immune evasion, antimicrobial resistance, and dissemination of infection. Unfortunately, most studies consider either host-pathogen interactions during phagocytosis and pathogen elimination, *or* the effect of pathogen population density on infection outcome. To truly understand how pathogen interactions with host immune cells impact the outcome of infection, the effects of pathogen dose on host response must also be considered.

Interestingly, the few studies that have examined the impact that pathogen density has on phagocyte activity mostly focus on the effect of quorum sensing molecules and autoinducers on phagocytosis. Vikström and colleagues investigated the effect of *P. aeruginosa* quorum sensing molecules on human macrophage phagocytosis (Vikström et al., 2005). They claimed that treatment of human MDMs with *P. aeruginosa* QS molecules upregulated phagocytosis when the QS signal was present at high concentrations early in infection, suggesting that enhancement of phagocytosis was time- and concentration-dependent, and depended on sensing of bacterial signalling molecules. Interestingly, in this study macrophages were stimulated with *P. aeruginosa* signalling molecules, yet the phagocytosis assay involved phagocytosis of dead *S. cerevisiae* yeast, even though fungi produce different quorum sensing molecules from bacteria. However, when considering phagocytosis in general, the presence of quorum sensing molecules induced increased phagocytosis by human macrophages. Here, perception of microbial

density signals by macrophages enhanced phagocytosis of particles which were perceived as a threat by the phagocyte.

A study by Mahamad and colleagues examined not the effect of quorum sensing molecules on infection dynamics, but rather investigated the effect of phagocytic load on phagocyte viability – a factor of great importance in determining the outcome of host-pathogen interactions. In examining the effect of phagocytic uptake load of *Mycobacterium tuberculosis* on human monocyte derived macrophage viability, Mahamad et al. found that large phagocytic load increased the probability of macrophage death, especially when a large number of *Mtb* were phagocytosed at once as an aggregate (Mahamed et al., 2017). In fact, the probability of macrophage death increased with multiplicity of infection; the phagocytes became overwhelmed and underwent apoptotic cell death which was advantageous for *Mtb* growth. Indeed, death of the phagocyte and subsequent phagocytosis by a second macrophage induced the *Mtb* to grow faster upon death of the second phagocyte, producing positive feedback whereby bacterial load serially increased upon additional macrophage death and subsequent phagocytosis. Here, the dose of pathogen phagocytosed impacted the phagocytic response, and manipulation of the dead macrophage niche for replication by the *Mycobacterium* resulted in a faster rate of replication compared to extracellular bacteria (Mahamed et al., 2017).

Jubrail et al. investigated the interaction between the macrophage intracellular niche and pathogenic success in *S. aureus* infection. They found that as the multiplicity of infection (MOI) increased, human THP-1 macrophages became overwhelmed and failed to effectively kill intracellular bacteria (Jubrail et al., 2016). Furthermore, as the MOI increased, the number of bacterial cells per macrophage failed to increase in proportion with infection. This suggested that macrophages may have shown a density-dependent decrease in phagocytic ability with increasing bacterial burden. Conversely, it may have also demonstrated that as the bacterial load increased, staphylococci show decreased ability to successfully occupy the host intracellular niche.

This study also examined the effect of infection burden on host survival with an *in vivo* murine model of *S. aureus* infection. At low levels of infection, bacterial cells were successfully cleared by 72 hours, despite some persistence within host macrophages early in infection, as showed by bronchoalveolar lavage. However, when infected with a high dose of bacterial cells the infection persisted, with 78% of mice failing to clear infection by 72 hours despite neutrophil recruitment (Jubrail et al., 2016). Lavage showed that macrophages had a higher proportion of intracellular bacteria compared to levels measured when infected with the lower doses, suggesting that as the infection burden increased macrophages were less effective in killing intracellular bacteria. Here, the level of infection affected the ability of macrophages to phagocytose bacterial cells, impaired the ability of macrophages to kill the bacteria, and illustrates how interactions with host cells at different levels of infection has consequences on infection outcome. Interestingly, failure to kill intracellular bacteria resulted in phagocyte lysis, bacterial reuptake, and subsequent macrophage death, effectively propagating infection at the expense of host cells. This is a good example of how pathogen interactions with individual host cells have the ability to impact the entire course of infection.

An interesting potential quorum sensing system exists within the fungus *Histoplasma capsulatum* and may directly relate to interactions between the pathogen and the host. This fungus normally resides within soil where it exists in the form of a mould. However, when inhaled, it undergoes a morphological switch to a yeast form, which is an effective intracellular parasite. When grown in culture the yeasts produce α-(1,3)-glucan, a cell wall polysaccharide. However, this only occurs when the culture reaches sufficiently high density during the stationary growth phase. Interestingly, the addition of conditioned media from high density culture induces synthesis of this polysaccharide in low density cultures, suggesting that a potential secreted factor may stimulate the production of this polysaccharide (Kügler et al., 2000). This is important for the survival and pathogenicity of the yeast cells, as this cell wall component prevents efficient recognition of the yeast cells by dectin-1 on host macrophages, and thus may prevent phagocytosis when yeast cells

are present at high density (Rappleye et al., 2007). Furthermore, *H. capsulatum* yeasts produce α-(1,3)-glucan when they are replicating within host macrophages. Kügler and colleagues have suggested that because this polysaccharide is produced by the yeast while replicating within host macrophages, when intraphagosomal concentration of the signalling molecule is likely to be high, it may be a potential mechanism by which the pathogen uses quorum sensing to detect when it is in a phagosome (Kügler et al., 2000). This signalling may induce the expression of virulence factors by the yeasts, and result in the enhanced parasitism of the host macrophage. Additionally, cell wall polysaccharides provide many fungi with protection from harsh environments; the density-dependent production of α-(1,3)-glucan by *H. capsulatum* within the phagosome may therefore protect the yeasts from destruction by the host phagocytes. Thus, this polysaccharide may be produced in a density-dependent fashion by the yeast both to prevent phagocytosis, and as a signalling molecule utilised whilst parasitising host macrophages; this represents an important mechanism by which a pathogenic fungus uses quorum sensing to modulate interactions with host macrophages.

The ability of host cells to phagocytose pathogens and effectively eliminate them is important in the fight between pathogenic success and destruction. While pathogenic quorum sensing molecules may have the ability to affect phagocytosis and thus impair the implementation of microbial virulence strategies, microbial load may also hinder the ability of host cells to neutralise pathogenic threats. Indeed, pathogens may exploit the phagocyte intracellular niche for their own gain. Because *Cryptococcus neoformans* capitalises on the host intracellular niche, it is important to consider the effect of cryptococcal dose on interactions with host immune cells.

4.1.5 Host response to cryptococcal density

The presence and action of quorum sensing molecules in *Cryptococcus* infection has not been extensively studied, and as such remains unclear. After the observation that growth of a *Δtup1* mutant *C. neoformans* showed a density-dependent defect in colony growth *in vitro* at densities less than 1000 cells, Lee and colleagues isolated

an 11-amino acid oligopeptide with apparent quorum sensing-like attributes, termed CQS1 (Lee et al., 2007). Addition of culture filtrates from *Δtup1* cells grown at high density to low density culture resulted in the growth of colonies at low densities which previously failed to produce colonies. This suggests that the conditioned media from *Δtup1* high density cultures contained a molecule capable of affecting density-dependent growth, as with many other quorum sensing molecules discussed previously. However, this density-dependent growth defect was not observed in wild type cryptococcal cells, and transcription of TUP1 does not decrease to levels low enough to be comparable to the *Δtup1* mutant. Furthermore, transcripts of this proposed quorum sensing molecule were detectible in the wild type strain, yet the wild type strain grew normally at most densities, suggesting that the effects seen in this mutant may be irrelevant to cryptococcal growth (Lee et al., 2007).

Interestingly, further work by the same group showed that the density-dependent growth retardation discussed here in *Cryptococcus neoformans* serotype D was not recapitulated by serotype A *in vitro* (Lee et al., 2009a). Instead, *Δtup1* serotype A mutants presented with enlarged capsules and reduced melanin production. While the density-dependent growth defects seen in serotype D were not recapitulated by serotype A *in vitro*, mouse infection with the *Δtup1* mutant of serotype A showed greatly attenuated virulence *in vivo*, with 80-fold lower fungal burden in mice on the day of death (Lee et al., 2009a). While it is interesting that deletion of this gene resulted in reduced fungal burden *in vivo*, this may be due to the effects of the gene on virulence factors and may not bear strict relevance to a density-dependent response.

Interestingly, the peptide termed CQS1 identified by the studies above as the cryptococcal quorum sensing-like peptide, has been found to be involved in cryptococcal mating. Tian et al. found that cryptococcal cell density was related to filamentation and the induction of unisexual mating in *C. neoformans* (Tian et al., 2018). Indeed, disruption of the gene encoding this peptide resulted in inhibition of unisexual filament formation, and was rescued by the addition of exogenous

quorum sensing peptide. Furthermore, deletion of the CQS1 gene inhibited meiotic sporulation and bisexual filamentation, demonstrating the role for density-dependent signalling in cryptococcal reproduction (Tian *et al.*, 2018).

Further work by Albuquerque et al. has attempted to elucidate potential quorum sensing effects in *C. neoformans*. Adding conditioned media from stationary phase cryptococci to low density culture produced a density-dependent increase in *C. neoformans* growth (Albuquerque et al., 2014). This phenomenon has been observed during quorum sensing responses in many bacteria, though similar effects may be achieved through the production of extracellular growth factors. Interestingly, known fungal quorum sensing molecules such as farnesol and tyrosol were unable to produce the results achieved by the addition of conditioned media, though commercial pantothenic acid managed to recapitulate some of the observed effects. Unfortunately, this study failed to address the contribution of host immune cells to the control of cryptococcal infection, neglecting to address the possibility of quorum sensing in an infection situation. Nevertheless, it points to the potential for a density-dependent growth response in *C. neoformans* in culture.

Work done in our lab has investigated the interaction between cryptococcal burden and infection in a zebrafish host. After stratifying infection burden and analysing the fungal growth after a period of three days, the increase in fungal burden was proportional compared to the initial fungal burden (Bojarczuk et al., 2016), suggesting lack of cooperation amongst cryptococci to enhance proliferation. Interestingly, when considering the role of macrophages over an increasing fungal burden, there was no decrease of the macrophages' ability to respond to increasing fungal burden, suggesting that macrophages did not become overwhelmed under the conditions and doses tested (Bojarczuk et al., 2016), and illustrating that host-pathogen interactions were maintained over increasing fungal burdens during *C. neoformans* infection.

While studies into the presence of cryptococcal dose-dependent responses through the activity of specific molecules are beginning to illuminate potential physiological

and infection-specific effects, many of the current studies have neglected to investigate the effect of cryptococcal dose on individual host-pathogen interactions. While work by Sabiiti examined correlations between phagocytosis and replication of different clinical strains with patient outcomes (Sabiiti et al., 2014), the effect of fungal dose on uptake and proliferation remains unclear. As discussed in the introduction, *Cryptococcus*-macrophage interactions are complex; macrophages can phagocytose and kill the cryptococci, or the cryptococci can replicate within the macrophage niche and disseminate infection, exiting through vomocytosis and even transferring between cells (Johnston and May, 2013). These interactions can ultimately decide whether the host succumbs to infection or prevails over cryptococcal disease. Because patient outcomes in human cryptococcosis are variable and stochastic (Jarvis et al., 2014), and with macrophages playing such important, varied roles in cryptococcosis, it is important that we understand how the level of infection affects interactions between cryptococcal cells and host macrophages and how this contributes to complex infection outcomes. As such, in this chapter I will describe experiments I performed in effort to understand how increasing the multiplicity of infection affects the interaction between macrophages and cryptococcal cells. Here, I will show evidence supporting the idea that that increasing fungal burden affects neither uptake by macrophages nor replication by *Cryptococcus*, and that each *Cryptococcus*-macrophage interaction should be considered an individual encounter.

4.2 There is no dose activation or inhibition of phagocytosis of *C. neoformans* by J774 macrophages

To determine if the level of fungal infection affects the ability of macrophages to phagocytose cryptococci, I infected murine macrophage-like J774 cells with an increasing inoculum of cryptococcal cells (Ma et al., 2009). 100,000 activated J774 cells were infected with 10^2-10^5 opsonised KN99 GFP *C. neoformans* (a multiplicity of infection (MOI) of 0.001-1). This timepoint was 0 hours, and infection continued for 18 hours. I then quantified the proportion of the total macrophages which contained intracellular cryptococci over increasing levels of fungal burden using both flow cytometry (Evans et al., 2017; Voelz et al., 2010) and time lapse analysis. I reasoned that if increasing fungal burden overwhelmed the macrophages' ability to phagocytose cryptococci, as fungal burden increased the proportion of macrophages that contained cryptococci would plateau or decrease. Alternatively, if an increasing level of cryptococci resulted in an enhanced phagocytic activation of macrophages, the proportion of macrophages containing intracellular cryptococci would increase disproportionately to the level of fungal infection. Finally, if the level of fungal infection considered here bore no effect on macrophage phagocytosis, the proportion of infected macrophages would increase linearly with fungal dose.

At 0 hours, flow cytometry showed that the proportion of macrophages containing intracellular cryptococci increased linearly with dose (Figure 4.1a linear regression $p = 0.0093$, $R^2 = 0.3933$; nonlinear regression $R^2 = 0.3936$). A similar trend was observed at 18 hours with a linear relationship between fungal burden and the percentage of macrophages infected (Figure 4.1b linear regression $p = 0.0104$, $R^2 = 0.3841$; nonlinear regression $R^2 = 0.3842$). Time lapse also revealed a linear relationship between infection burden and the proportion of macrophages containing intracellular cryptococci, both at 0 hours (Figures 4.1d linear regression $p = < 0.0001$, $R^2 = 0.8916$; nonlinear regression $R^2 = 0.8790$) and at 18 hours (Figure 4.1e linear regression $p < 0.0001$, $R^2 = 0.8598$; nonlinear regression $R^2 = 0.8518$). This suggests that uptake by macrophages increased linearly with dose, and that level of fungal infection did not enhance or inhibit phagocytosis by macrophages.

Furthermore, as phagocytosis increased linearly with dose, it is likely that uptake by macrophages was due to the chance of the macrophages encountering cryptococci.

Interestingly, flow cytometry showed that over 18 hours, the proportion of macrophages which contained intracellular cryptococci decreased, though this was not a significant decrease (Figure 4.1c). Because the same effect was not produced by time lapse analysis (Figure 4.1f), the decrease shown by flow cytometry was likely due to the loss of infected macrophages in the washing stage prior to removing macrophages from the well plates.

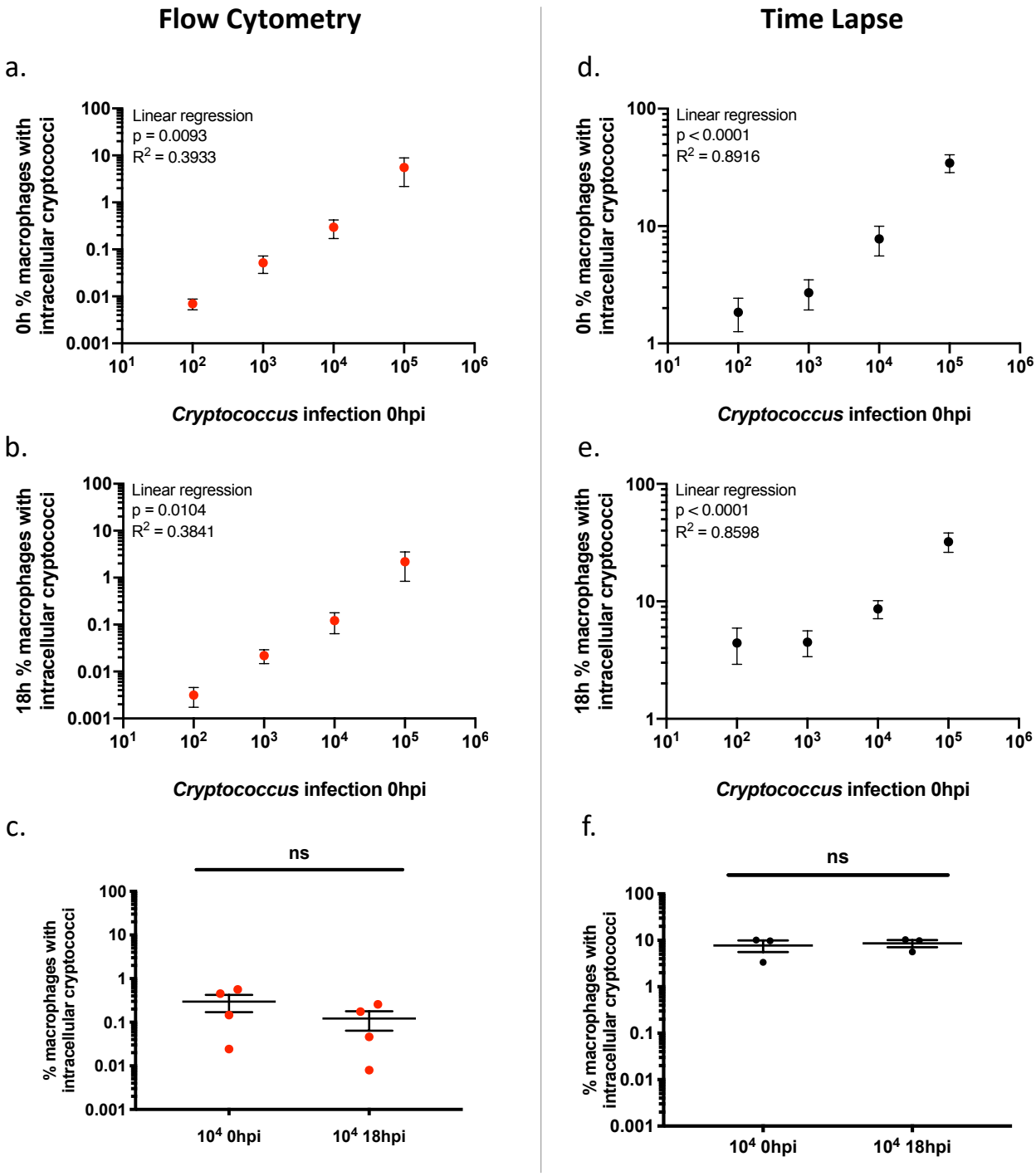

Figure 4.1. The proportion of J774 macrophages which phagocytosed cryptococci increased with initial fungal dose

After 18 hours of infection with KN99 GFP *C. neoformans*, the percentage of J774 macrophages containing intracellular cryptococci was determined by flow cytometry (red panel, left) and time lapse analysis (black panel, right). Calculations account for the total macrophages within each well. 4 repeats were performed for flow cytometry assays, with 4-6 replicates per condition averaged for each repeat.

3 repeats were performed for time lapse assays, with no less than 250 macrophages considered per condition. Means and standard errors are shown.

a. The percentage of macrophages which contained intracellular cryptococci at 0h as determined by flow cytometry. There was a linear increase in the percentage of macrophages which contained intracellular cryptococci as fungal burden increased (linear regression $p = 0.0093$, $R^2 = 0.3933$; nonlinear regression $R^2 = 0.3936$).
b. The percentage of macrophages which contained intracellular cryptococci at 18h as determined by flow cytometry. There was a linear increase in the percentage of macrophages which contained intracellular cryptococci as fungal burden increased (linear regression $p = 0.0104$, $R^2 = 0.3841$; nonlinear regression $R^2 = 0.3842$).
c. Comparison of the percentage of infected macrophages between 0h and 18h. Only one initial fungal dose is shown here for the sake of clarity, but results were the same for each comparison. The proportion of macrophages containing cryptococci decreased over 18 hours, though this decrease was not significant (Mann-Whitney test $p = 0.4857$).
d. The proportion of macrophages which contained intracellular cryptococci at 0h as determined by time lapse analysis. There was a linear increase in the percentage of macrophages which contained intracellular cryptococci as fungal burden increased (linear regression $p = < 0.0001$, $R^2 = 0.8916$; nonlinear regression $R^2 = 0.8790$).
e. The proportion of macrophages which contained intracellular cryptococci at 18h as determined by time lapse analysis. There was a linear increase in the percentage of macrophages which contained intracellular cryptococci as fungal burden increased (linear regression $p < 0.0001$, $R^2 = 0.8598$; nonlinear regression $R^2 = 0.8518$).
f. There was no significant difference between the proportion of macrophages containing intracellular cryptococci at 0h and 18h when compared by time lapse analysis (Mann-Whitney test $p = 0.700$). Only one initial fungal dose shown here for clarity, but results were similarly non-significant in each comparison.

To compare the two methods, I plotted the measured percentage of macrophages containing intracellular cryptococci as determined by flow cytometry and time lapse analysis on the same graph. Interestingly, fungal uptake was higher when calculated by time lapse analysis compared to flow cytometry (Figures 4.2a and 4.2c; unpaired t-test p = 0.0130, 0.0095, 0.0098, and 0.0061 when comparing the two methods for infection with 10^2, 10^3, 10^4, 10^5 cryptococci, respectively). As the data collected by time lapse analysis included manual counting of individual fluorescent cryptococci where flow cytometry relied on the detection of fluorescent fungi after a step to remove adherent cells, it is likely that infected cells were lost during the flow cytometry protocol or that the flow cytometer failed to detect cryptococci which were less fluorescent. As such, it is likely that the flow cytometry underestimates the infection and results should be interpreted with caution. For most of the remainder of this thesis the preferred methodology for infection quantification was time lapse analysis.

To determine if increasing cryptococcal burden induced an immune-dampening effect, I measured macrophage replication over an increasing fungal burden. I hypothesised that if the presence of high levels of cryptococci suppressed immune response by hindering e.g. macrophage expansion, then macrophage fold change should decrease with increasing fungal burden. If the presence of pathogenic cryptococci induced macrophage expansion, fold change would increase with burden. Finally, if cryptococcal density had no effect, macrophage fold change should remain the same with increasing fungal dose. As shown by both flow cytometry and time lapse imaging, the macrophage fold change neither increased nor decreased with growing fungal inoculum (Figure 4.2b and 4.2c). Indeed, there was no dose activation or inhibition of macrophage replication between experiments, or amongst inocula. This suggests that the presence of increasing numbers of cryptococcal cells does not induce macrophages to enhance proliferation, or overwhelm them to reduce replication, producing neither an immune enhancing nor an immune inhibitory effect in the conditions tested here.

(page intentionally left blank for figures + legends on following pages)

a.

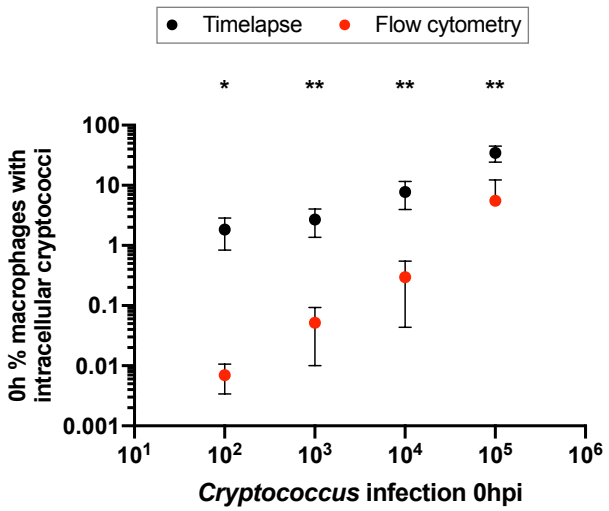

b.

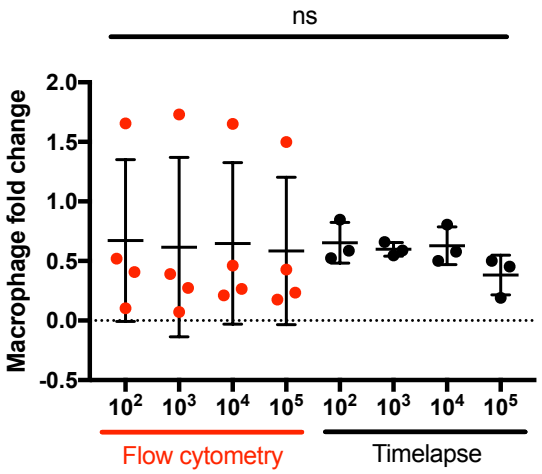

c.

0h *Cn*	n	Flow cytometry Mean % infected	SD % infected	Mean MΦ fold change	SD MΦ fold change
10^2	19	0.01	0.01	0.67	0.68
10^3	20	0.05	0.05	0.62	0.75
10^4	20	0.28	0.22	0.65	0.68
10^5	20	4.84	5.64	0.58	0.62
0h *Cn*	**n**	**Timelapse Mean % infected**	**SD % infected**	**Mean MΦ fold change**	**SD MΦ fold change**
10^2	3	4.42	2.61	0.65	0.17
10^3	3	4.49	1.93	0.60	0.06
10^4	3	10.34	4.95	0.63	0.16
10^5	3	32.23	10.50	0.38	0.17

Figure 4.2. There was no dose activation or inhibition of J774 macrophages to phagocytose cryptococci, or to replicate, with increasing fungal burden

After 18 hours of infection with KN99 GFP *C. neoformans*, the percentage of J774 macrophages which contained intracellular cryptococci, and the macrophage fold change, were determined by flow cytometry (red points) and time lapse analysis (black points). Calculations account for the total macrophages within each well. N represents the number of replicates; flow cytometry was analysed by 3 repeats, with 4-6 replicates averaged per condition, and time lapse analysis three replicates per condition were considered. Means and standard deviations are shown.

a. The percentage of macrophages at 0h which contained intracellular increased linearly with dose (linear regression flow cytometry p = 0.0093, R^2 = 0.3933; linear regression time lapse p = <0.0001, R^2 = 0.8917). Similar results were achieved for 18h (linear regression flow cytometry p = 0.0104, R^2 = 0.3841; linear regression time lapse p < 0.0001, R^2 = 0.8598). The percentage of infected macrophages calculated by time lapse analysis was significantly higher than when calculated by flow cytometry (unpaired t-test p = 0.0130, 0.0095, 0.0098, and 0.0061 when comparing the two methods for each dose at 0 hours, and p = 0.0173, 0.0048, 0.0011, 0.0024 when comparing methods at 18 hours). The SD at the highest fungal burden for flow cytometry is not shown because it is too close to the point to see.
b. The relative macrophage fold change was not affected by increasing fungal dose, with no significant difference between assays or amongst doses (one-way ANOVA considering all p = 0.9983; flow cytometry one-way ANOVA p = 0.9980; time lapse one-way ANOVA p = 0.1692). If the flow cytometry repeat which produced significantly higher macrophage fold change is excluded from analysis there is still no significant difference between fungal doses (not shown; flow cytometry one-way ANOVA p = 0.8933).
c. Descriptive statistics for flow cytometry (top) and time lapse analysis (bottom) comparing the percentage of macrophages infected and the macrophage fold change over an increasing fungal dose. MΦ refers to macrophages and SD refers to standard deviation.

4.3 The multiplicity of *C. neoformans* infection does not enhance or inhibit the ability of cryptococci to replicate intracellularly within murine macrophages

To determine if fungal burden affects intracellular cryptococcal replication, I quantified the number of cryptococcal cells within macrophages at 0h and 18h using flow cytometry, and later confirmed the results through time lapse imaging. I reasoned that if cryptococci cooperated to enhance replication as fungal burden increased, as seen in many examples of quorum sensing, that the fold change relative to initial burden would increase with dose. Alternatively, if increasing burden induced cryptococci to slow growth, the relative fold change would decrease as fungal burden increased. Finally, if the cryptococci did not display a density-dependent growth phenotype, there would be no difference in the relative fold change as fungal burden increased.

Comparing cryptococcal fold change relative to initial intracellular fungal burden revealed that increasing fungal burden did not enhance or inhibit the ability of intracellular cryptococci to replicate (Figure 4.3; relative fold change by flow cytometry one-way ANOVA $p = 0.892$, by time lapse one-way ANOVA $p = 0.475$). Furthermore, while the relative fold change as ascertained by flow cytometry was consistently higher than that calculated by time lapse analysis, there was no significant difference in relative fold change between the two assays (data not shown, one-way ANOVA $p = 0.753$, no pairwise significance). However, the standard deviation of relative fold change was smaller in the time lapse calculations, suggesting that time lapse analysis was a more consistent form of measurement.

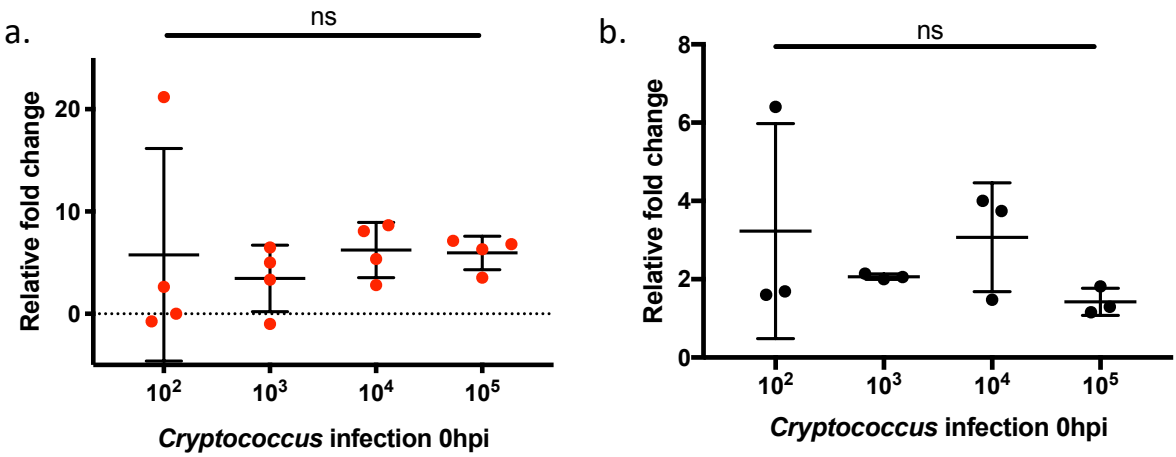

c.

0h *Cn*	Flow Cytometry Fold change n	Mean	SD	Timelapse Fold change n	Mean	SD
10^2	4	5.77	10.38	3	3.23	2.75
10^3	4	3.46	3.24	3	2.07	0.07
10^4	4	6.23	2.70	3	3.07	1.39
10^5	4	5.95	1.65	3	1.43	0.35

Figure 4.3. MOI did not alter cryptococcal replication within J774 macrophages

100,000 J774 murine macrophage-like cells were infected with an increasing number of KN99 GFP cryptococcal cells for 18 hours. Only intracellular cryptococci are shown here. Fold change relative to the initial inoculum was calculated for the fungal cells after 18 hours. Means and standard deviations are shown.

a. Flow cytometry analysis of the relative fold change in cryptococcal cells within macrophages. Four repeats were performed, and points represent the average of 6 replicates per condition. There was no significant difference in fold change over increasing levels of initial cryptococcal infection (one-way ANOVA p = 0.892).

b. Time lapse analysis of the relative fold change in cryptococcal cells after 18 hours of infection over three repeats. There was no significant difference in the ability of the cryptococci to divide over an increasing initial fungal burden (one-way ANOVA p = 0.475).

c. Descriptive statistics of fold change after 18 hours of infection for both flow cytometry and time lapse assays. N represents the number of repeats, SD is standard deviation.

4.4 Doubling time of *C. neoformans* is not affected by fungal dose

While calculating fungal fold change is a good indicator of the ability of *Cryptococcus* to proliferate at increasing levels of fungal burden, it does not provide a specific estimate of the rate of replication. As such, I performed the same infection assay as above and quantified the growth of individual cryptococcal cells within macrophages, outside of macrophages, and after vomocytosis from macrophages. I infected 100,000 activated J774 murine macrophages with 10^4-10^6 opsonised KN99 GFP *C. neoformans* for two hours before the extracellular cryptococci were washed away. A higher initial dose of cryptococci was used for this assay because not enough cryptococci were phagocytosed when the macrophages were infected with only 10^2 cryptococci to provide a sufficient number of intracellular cryptococci to follow. I then followed the infection for 24 hours using time lapse imaging to monitor the growth of individual cryptococci. A longer time frame was considered here to give the cryptococci ample opportunity to replicate within the imposed time limit. I reasoned that if cryptococci cooperated to enhance replication, doubling time would decrease as fungal burden increased. If the opposite was true, and the presence of increasing numbers of cryptococcal cells induced the fungi to slow fungal growth, that doubling time would increase with burden. Finally, if there was no effect of fungal dose on replication in the conditions tested here, doubling time would remain constant as cryptococcal burden increased.

I followed the intracellular proliferation of over 30 cells for each initial fungal dose. As the initial fungal burden increased, the mean doubling time of individual cryptococci (or mother-daughter groups) neither increased nor decreased (Figures 4.4a and 4.4e; one-way ANOVA $p = 0.3724$). Additionally, as the number of cryptococci within each macrophage increased, the doubling time of the cryptococci did not significantly increase (Figure 4.4b; one-way ANOVA no significance for each initial fungal dose). The doubling time of extracellular cryptococci also failed to increase with fungal burden (Figures 4.4c and 4.4e; one-way ANOVA $p = 0.6348$), as did those which exited non-lytically from macrophages via vomocytosis (Figures 4.4d and 4.4e; one-way ANOVA $p = 0.6899$). In each case, as the fungal burden

increased the mean doubling time of the population of individual cryptococci remained constant, meaning that the presence of more cryptococci within the population did not increase individual cell replication. Therefore, over the time tested here, replication rate was not affected by fungal burden.

a.

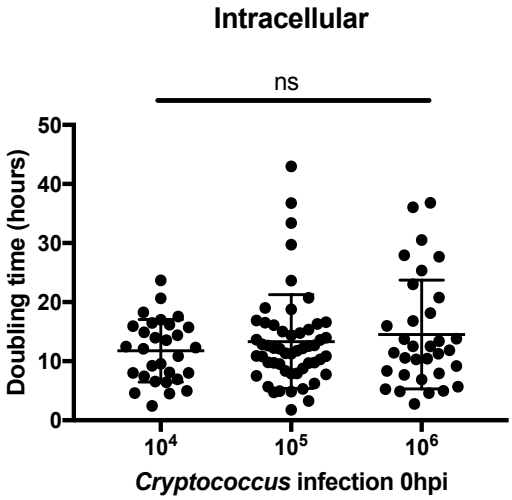

b.

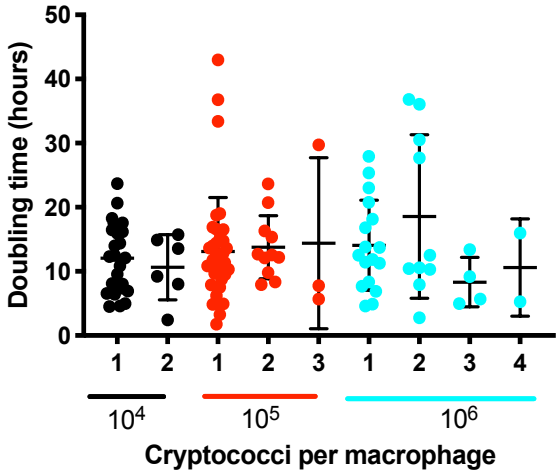

c.

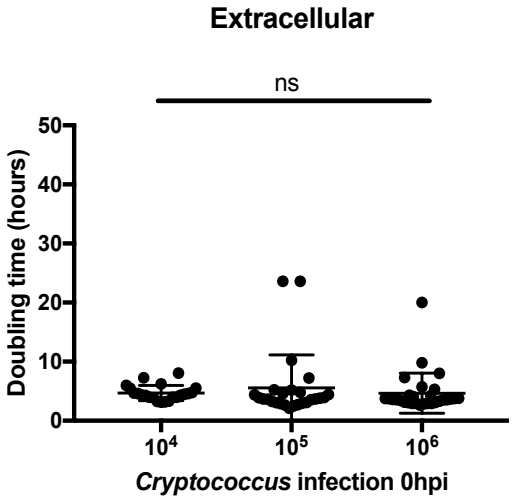

d.

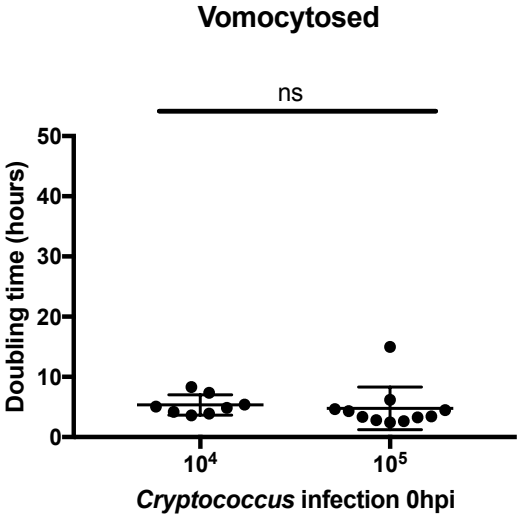

e.

	Intracellular doubling time			Extracellular doubling time			Vomocytosed doubling time		
0h *Cn*	n	Mean	SD	n	Mean	SD	n	Mean	SD
10^4	30	11.76	5.29	22	4.70	1.29	8	5.33	1.68
10^5	53	13.33	7.95	26	5.58	5.56	11	4.78	3.55
10^6	33	14.52	9.19	29	4.66	3.39	-	-	-

Figure 4.4. Increasing fungal burden did not affect cryptococcal doubling time

Murine J774 macrophages were infected with an increasing inoculum of KN99 GFP *C. neoformans*, and individual cryptococcal cells were followed for up to 24 hours to quantify doubling time. Intracellular (a, b), extracellular (c), and vomocytosed (d) cells were followed over 3 repeats. 3 replicates per repeat were considered, with up

to 11 cells followed in each replicate. Points represent individual cryptococci, and mean and standard deviation are shown.

a. Doubling time of intracellular cryptococci was not affected by initial fungal dose (one-way ANOVA p = 0.3724, no pairwise significance).
b. Comparison of intracellular doubling times stratified by the initial number of phagocytosed cryptococci within each macrophage. There was no significant difference in doubling time as the number of cryptococci within each macrophage increased (no significance by t-test of ANOVA for each dose).
c. Doubling time of extracellular cryptococci (in the presence of J774 cells, but not within them) was not significantly different between doses (one-way ANOVA p = 0.6348).
d. Doubling time of cryptococci which were inside of macrophages but were expelled non-lytically was not significantly different across doses (only 2 levels of infection considered due to the difficulty in following vomocytosed cells late in infection at the highest fungal burden; unpaired t-test p = 0.6899).
e. Descriptive statistics comparing the doubling times of cryptococci in each condition over increasing initial inocula of *C. neoformans*. N is the total number of cells followed over the three repeats, SD is standard deviation.

4.5 There is no dose activation or inhibition of phagocytosis of cryptococci by MDMs

While J774 macrophages are a good model for *C. neoformans* phagocytosis and intracellular proliferation (Johnston and May, 2010; Ma et al., 2009; Voelz et al., 2009), there are differences between human cells and murine cells which means that the interaction between cryptococci and murine macrophages may not fully capture the nature of interactions between human macrophages and cryptococci (Ingersoll et al., 2010). I therefore chose to infect human monocyte-derived macrophages (MDMs) to see if human macrophages controlled cryptococcal infection in a similar way to the murine macrophages. To determine if the effects of infection dose on macrophage phagocytosis and fungal replication observed in the presence of murine macrophages were similar for human cells, I performed the assays described above in the presence of human monocyte derived macrophages (MDMs) (Voelz et al., 2009). I infected 100,000 activated MDMs with 10^3-10^6 opsonised KN99 GFP *C. neoformans* for 2 hours, washed off extracellular cryptococci, and continued infection for 18 hours. To discern if fungal dose affected the ability of human macrophages to phagocytose cryptococci, I quantified the proportion of macrophages with intracellular cryptococci over 18 hours of infection. The number of infected macrophages was only quantified at fungal burdens up to 10^5 because phagocytosis was difficult to quantify at the highest dose. Though not directly quantified, the number of infected macrophages appeared to increase proportionally with fungal dose (i.e. the proportion of infected macrophages did not seem disproportionally small or large compared to what was expected based on the next highest fungal dose). Here I hypothesised that if increasing fungal burden induced macrophages to enhance phagocytosis, the percentage of macrophages possessing intracellular cryptococci would increase with initial fungal dose. Alternatively, if an increase in fungal burden overwhelmed macrophages, the percent of infected macrophages would decrease with initial fungal dose.

At 0h, while the percentage of infected macrophages increased with fungal dose, there was no significant difference in the percentage of MDMs which had

phagocytosed cryptococci (Figures 4.5a and 4.5e; one-way ANOVA p = 0.163, no pairwise significance). Interestingly, linear regression analysis showed that there was no significant linear relationship between initial fungal burden and the proportion of MDMs with intracellular cryptococci (Figure 4.5a; linear regression p = 0.135). Similar results were achieved after 18 hours of infection; despite the increase in the proportion of macrophages containing intracellular cryptococci, there was no significant difference in the proportion of MDMs which contained intracellular cryptococci over an increasing fungal dose (Figure 4.5b and 4.5e; one-way ANOVA p = 0.303, no pairwise significance). There was also no linear relationship between the initial fungal burden and the percentage of infected MDMs at 18h (linear regression p = 0.135). These results suggest that increasing the number of cryptococci within the environment potentially overwhelmed macrophage phagocytic activity, as the percentage of macrophages with intracellular cryptococci at the highest fungal dose was less than what would be expected if there was a linear relationship between fungal burden and phagocytic uptake. However, it is likely that stochastic interactions between cryptococci and macrophages may have contributed to the high standard deviation in the percent of infected macrophages, failing to produce a linear relationship. However, the mean proportion of infected macrophages did increase proportionally with initial fungal burden (Figure 4.5c). Considering only the mean percent of macrophages infected without this variation shows that there was an increase in uptake with fungal dose, though this was not significantly linear (Figure 4.5c; linear regression p = 0.1214 for 0h, p = 0.1159 for 18h). As with the J774 time lapse analysis, the percentage of macrophages with intracellular cryptococci did not significantly change over 18 hours (Figures 4.5d and 4.5e; unpaired t-test p > 0.99, non-significant difference for each dose considered).

a.

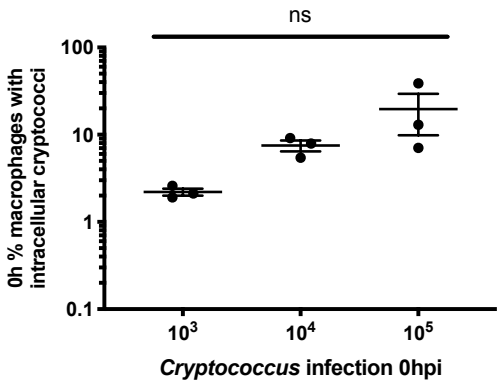

b.

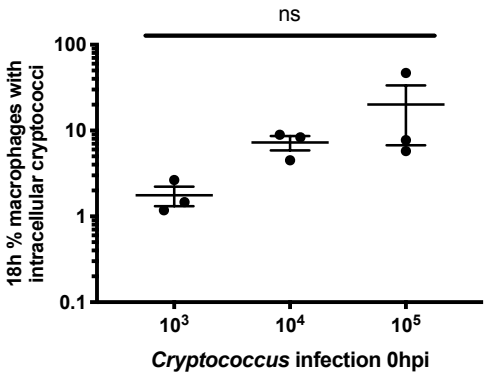

c.

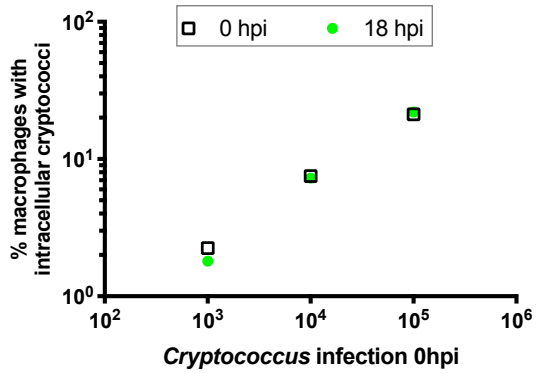

d.

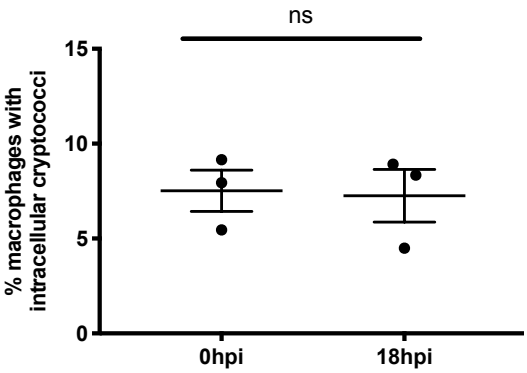

e.

0h Cn	0h % Infected			18h % Infected			Macrophage Fold Change		
	n	Mean	SEM	n	Mean	SEM	n	Mean	SEM
10^3	3	2.20	0.20	3	1.76	0.45	3	0.99	0.05
10^4	3	7.52	1.09	3	7.25	1.39	3	1.87	1.53
10^5	3	19.63	16.88	3	20.17	13.43	3	0.97	0.14

Figure 4.5. Fungal burden did not enhance or inhibit phagocytosis of cryptococci by human monocyte derived macrophages

Human MDMs were infected for 24h. The percentage of macrophages which contained intracellular cryptococci was measured at 0h. For comparison with J774 data, the percentage of macrophages infected at 18h was quantified. 3 repeats were performed, with the mean of 2-3 replicates per initial fungal dose represented as points. Means and standard errors are shown.

a. At the start of infection, the proportion of MDMs which contained intracellular cryptococci was not significantly different between initial fungal

doses (one-way ANOVA p = 0.1634, no pairwise significance). There was no significant linear relationship between infection burden and percentage of infected macrophages (linear regression, p = 0.1399).

b. At 18h the proportion of macrophages which contained intracellular cryptococci was not significantly different as initial fungal burden increased (one-way ANOVA p = 0.3029, no pairwise significance). There was no significant linear relationship between infection burden and percentage of infected macrophages (linear regression p = 0.1352).
c. A comparison of only the mean percentage of macrophages containing intracellular cryptococci at 0 and 18 hours (i.e. just the means depicted in (a) and (b)). Transparent squares represent the mean percent of infected macrophages across repeats at 0 hpi, and green circles represent 18h. The mean percentage of macrophages with intracellular cryptococci increased with dose, though this increase was not linear (linear regression for 0h p = 0.1214, for 18h p = 0.1159).
d. The proportion of macrophages which contained intracellular cryptococci did not change significantly after 18h (unpaired t-test p > 0.999, one dose shown for clarity, no significant difference for each fungal dose).
e. Descriptive statistics comparing the percentage of macrophages which were infected after 0h and 18h of infection. N represents number of repeats considered, SEM is standard error of the mean.

4.6 In human MDMs the level of fungal burden does not affect cryptococcal replication

Because cryptococcal replication is important for pathogenicity, I again measured the replication of cryptococci to determine how fungal dose affects their proliferation in the presence of human MDMs. To calculate the intracellular cryptococcal fold change, I quantified the total number of intracellular cryptococci at 0 and 18h. As before, I hypothesised that if an increase in the number of cryptococci induced fungal cooperation and upregulation of replication, relative fold change would increase with fungal dose. If increasing fungal dose resulted in a downregulation of replication, relative fold change would decrease with fungal dose. As the initial fungal burden increased, there was no increase or decrease in the relative fungal fold change (Figure 4.6a and 4.6e; one-way ANOVA $p = 0.696$, no pairwise significance). This suggests that as the initial cryptococcal inoculum increased, the cryptococci did not cooperate within the population to either enhance or inhibit replication in the presence of human MDMs.

To determine if the level of cryptococcal infection had any effect on the replication rate of cryptococci, I followed individual intracellular and extracellular cryptococcal cells for up to 24 hours to allow time for doubling time to be determined. I then quantified the replication of individual cryptococci. Within MDMs, as initial fungal burden increased there was no increase or decrease in doubling time of intracellular cryptococci (Figure 4.6b and 4.6e; one-way ANOVA $p = 0.264$, no pairwise significance). This suggests that the presence of additional cryptococci did not result in signalling amongst the fungal population that induced individual fungal cells to replicate at a faster rate. Interestingly, as the number of cryptococci inside of separate macrophages increased (i.e. starting intracellular cryptococci within each macrophage), the doubling time of the intracellular cryptococci increased, irrespective of initial infection dose (Figure 4.6c). This suggests that the increased starting number of cryptococci inside of macrophages induced the cryptococci to divide more slowly. Finally, as initial fungal burden increased there was no effect of dose on the extracellular doubling rate (Figure 4.6d and 4.6e; one-way ANOVA p =

0.844, no pairwise significance). This suggests that increasing fungal load did not induce extracellular cryptococci to downregulate replication rate in a dose-dependent manner. Taken together these results indicate that as the initial fungal inocula increased, the cryptococci may cooperate amongst one another to downregulate replication rate, but only within subpopulations inside of individual MDMs.

a.

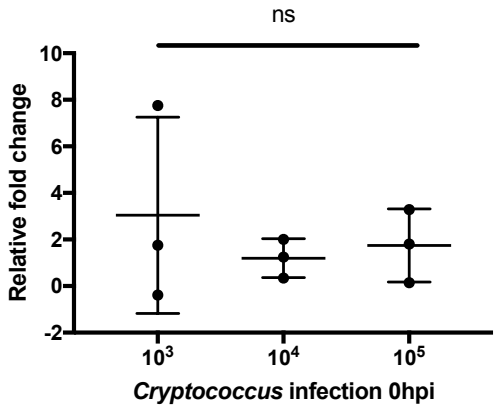

b.

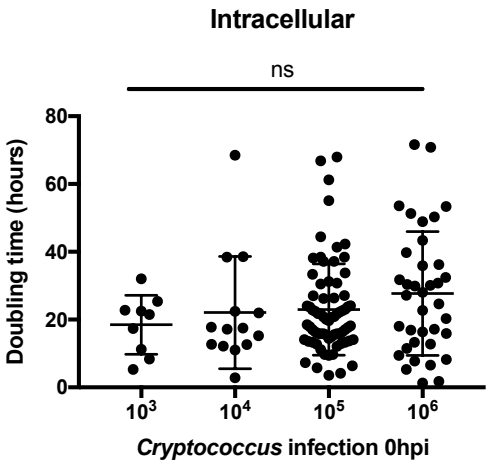

c.

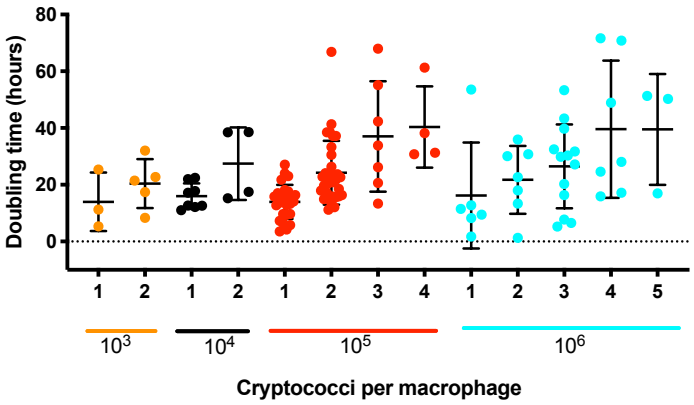

d.

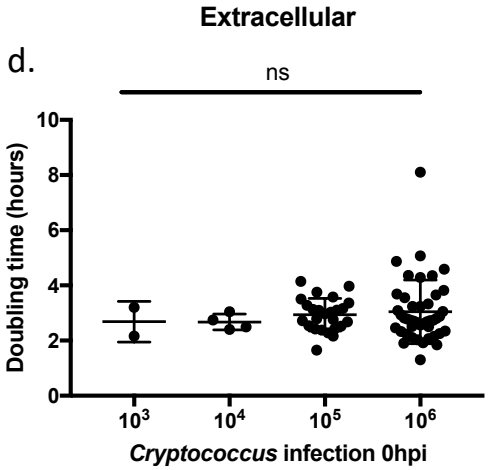

e.

0h Cn	Relative fold change			Intracellular doubling time			Extracellular doubling time		
	n	Mean	SD	n	Mean	SD	n	Mean	SD
10^3	3	3.04	4.22	9	18.49	8.69	2	2.69	0.74
10^4	3	1.20	0.83	14	22.07	16.58	4	2.67	0.29
10^5	3	1.75	1.57	73	22.97	13.47	25	2.94	0.59
10^6	-	-	-	37	27.72	18.28	44	3.04	1.16

Figure 4.6. Increasing fungal burden did not affect cryptococcal replication or doubling time in the presence of human MDMs

100,000 human monocyte derived macrophages (MDMs) were infected with an increasing number of opsonised KN99 GFP cryptococcal cells for 24 hours. The number of intracellular cryptococcal cells was measured at 0h and 18h to determine fold change and to enable comparison to J774 data. Individual cryptococcal cells were followed throughout the full 24h of infection to quantify doubling time over 3 repeats, with 3 replicates per repeat, and up to 13 cryptococci followed per

replicate. Doubling times were determined by fit of an exponential growth model. Means and standard deviations are shown.

a. The relative cryptococcal fold change was not significantly different as starting fungal burden increased (one-way ANOVA p = 0.696, no pairwise significance). Three repeats were performed, with the average of 2-3 replicates per dose for each repeat represented as points.
b. As fungal burden increased, the doubling time of individual cryptococci which were intracellular within MDMs did not significantly increase or decrease (one-way ANOVA p = 0.264, no pairwise significance).
c. The starting number of intracellular cryptococci was determined for each macrophage. Then, the doubling time was compared for these stratified intracellular doses. As the number of phagocytosed cryptococci for each macrophage increased (i.e. starting intracellular cryptococci within each macrophage = 1, 2, …), the doubling time of the cryptococci also increased. However, only cryptococci within macrophages infected with 10^5 cryptococci showed significantly different doubling times (among only red points; one-way ANOVA p <0.0001).
d. As fungal burden increased, the doubling time of individual cryptococci which were extracellular did not significantly increase or decrease (one-way ANOVA p = 0.844, no pairwise significance).
e. Descriptive statistics comparing relative fold change, intracellular and extracellular doubling time, over increasing initial fungal doses. N represents repeats for fold change and cells followed for doubling times. SD is standard deviation.

4.7 Comparing murine J774 macrophage and human MDM infection

To assess the usefulness of the two models, I compared the infection of J774 macrophages and MDMs. For each initial fungal dose, there was no difference in the percentage of macrophages which contained cryptococci between J774 cells and MDMs at both 0h (Figure 4.7a; Mann-Whitney test; 10^3 $p > 0.999$, 10^4 $p = 0.700$, 10^5 $p = 0.200$) and 18h (Figure 4.7b; Mann-Whitney test; 10^3 $p = 0.100$, 10^4 $p = 0.400$, 10^5 $p = 0.700$). This suggests that J774 macrophages and human MDMs showed similar abilities to phagocytose cryptococci over increasing fungal burdens.

There was also no difference in intracellular cryptococcal fold change (Figure 4.7c cryptococcal fold change, Mann-Whitney test: 10^3 $p = 0.700$, 10^4 $p = 0.200$, 10^5 $p > 0.999$), though J774 macrophages divided and human MDMs did not (Figure 4.7d macrophage fold change, Mann-Whitney tests; 10^3 $p = 0.0002$, 10^4 $p = 0.0184$, 10^5 $p = 0.031$). The doubling time of cryptococci was significantly higher for cryptococci within human MDMs (Figure 4.7e; Mann-Whitney test; 10^4 $p = 0.008$, $10^5 = 0.0002$), suggesting increased control over cryptococcal proliferation rate within human MDMs. Additionally, extracellular proliferation was faster in the presence of human MDMs (Figure 4.7f; Mann-Whitney test 10^4 $p = 0.0001$, 10^5 $p = 0.0005$). This was likely due to faster cryptococcal growth in RPMI, the media used for human MDM assays, compared to DMEM which is used for J774 cells (data not shown; doubling time of cryptococci in SF RPMI = 3.15 hours, in SF DMEM 5.88 hours; Mann-Whitney test $p < 0.0001$; at least 79 cryptococci considered for each media). Only two fungal doses are considered here, as three different fungal doses were considered for each assay, with only two comparable. The difference in cryptococcal doubling times between the two models suggest that human MDMs enforced stronger control over intracellular replication rate.

(page intentionally left blank for figures + legends on following pages)

a.

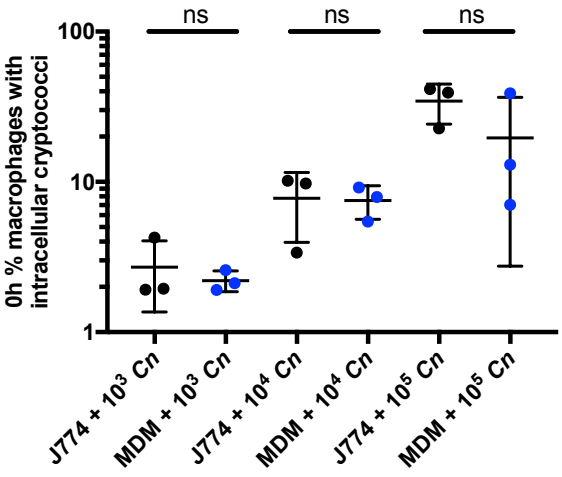
0h % macrophages with intracellular cryptococci
100
10
1
ns
ns
ns
J774 + 10^3 Cn
MDM + 10^3 Cn
J774 + 10^4 Cn
MDM + 10^4 Cn
J774 + 10^5 Cn
MDM + 10^5 Cn

b.

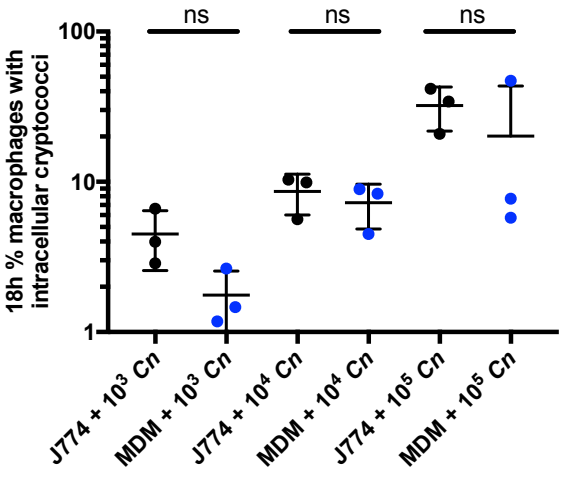
18h % macrophages with intracellular cryptococci
100
10
1
ns
ns
ns
J774 + 10^3 Cn
MDM + 10^3 Cn
J774 + 10^4 Cn
MDM + 10^4 Cn
J774 + 10^5 Cn
MDM + 10^5 Cn

c.

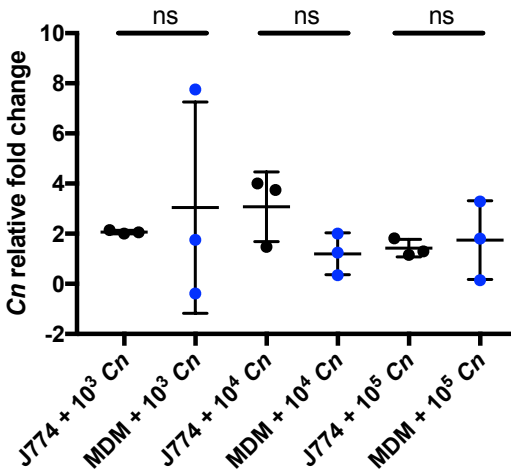
Cn relative fold change
10
8
6
4
2
0
-2
ns
ns
ns
J774 + 10^3 Cn
MDM + 10^3 Cn
J774 + 10^4 Cn
MDM + 10^4 Cn
J774 + 10^5 Cn
MDM + 10^5 Cn

d.

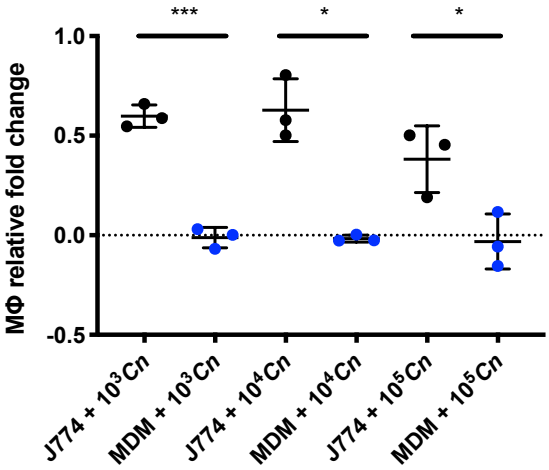
MΦ relative fold change
1.0
0.5
0.0
-0.5
***
*
*
J774 + 10^3Cn
MDM + 10^3Cn
J774 + 10^4Cn
MDM + 10^4Cn
J774 + 10^5Cn
MDM + 10^5Cn

e.

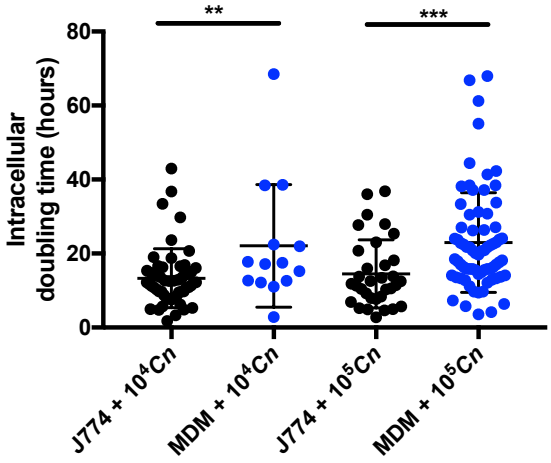
Intracellular doubling time (hours)
80
60
40
20
0
**
***
J774 + 10^4Cn
MDM + 10^4Cn
J774 + 10^5Cn
MDM + 10^5Cn

f.

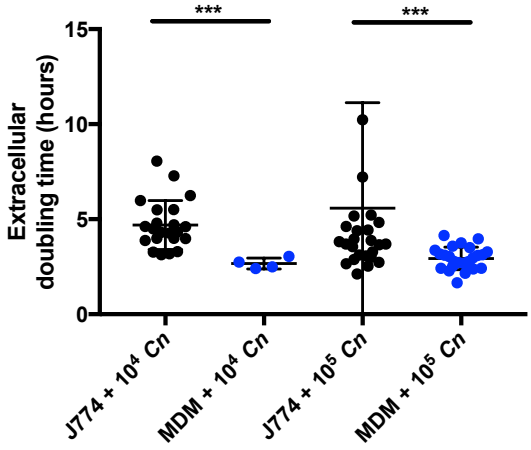
Extracellular doubling time (hours)
15
10
5
0
***
***
J774 + 10^4 Cn
MDM + 10^4 Cn
J774 + 10^5 Cn
MDM + 10^5 Cn

Figure 4.7. Comparing response to increasing fungal dose by J774 macrophages and human MDMs

J774 murine macrophages and human MDMs were infected with KN99 GFP *C. neoformans* for 18 hours. Analyses and quantifications are compared here. 3 repeats were performed for each, with 2-3 replicates per repeat. For a, b, c, and d the means of each replicate are displayed as points, and means and standard deviations shown. For e and f points represent individual cryptococci. The level of initial cryptococcal infection is labelled on the x-axis. J774 data points are in black, while MDM data points are in blue.

a. At 0h the percentage of macrophages which contained intracellular cryptococci over increasing initial fungal burdens was not significantly different between J774 macrophages and MDMs (Mann-Whitney test; 10^3 $p > 0.999$, 10^4 $p = 0.700$, 10^5 $p = 0.200$).
b. At 18h the percentage of macrophages which contained intracellular cryptococci over increasing initial fungal burdens was not significantly different between J774 macrophages and MDMs (Mann-Whitney test; 10^3 $p = 0.100$, 10^4 $p = 0.400$, 10^5 $p = 0.700$).
c. There was no significant difference in intracellular fungal fold change between J774 and MDM infection (Mann-Whitney test; 10^3 $p = 0.700$, 10^4 $p = 0.200$, 10^5 $p > 0.999$).
d. J774 macrophages replicated more than human MDMs after infection with each respective fungal dose (Mann-Whitney tests; 10^3 $p = 0.0002$, 10^4 $p = 0.081$, 10^5 $p = 0.031$).
e. Intracellular doubling time for cryptococci within MDMs was significantly higher than for cryptococci within J774 macrophages (Mann-Whitney test; 10^4 $p = 0.008$, $10^5 = 0.0002$).
f. Doubling time for cryptococci outside of macrophages is significantly lower in the presence of human MDMs compared to J774 macrophages (Mann-Whitney test; 10^4 $p = 0.0001$, 10^5 $p = 0.0005$).

4.8 Discussion

During infection, many pathogens possess the ability to signal within the population once a specific population density, and signalling molecule threshold, is reached. This quorum sensing phenomenon results in coordinated gene expression and group response, and can affect virulence and pathogen interactions with host cells. Understanding of microbial quorum sensing largely began with photoluminescence in *Photobacteirum fischeri* (Kempner and Hanson, 1968) and bacterial competence *Streptococcus pneumoniae* (Tomasz, 1965; Tomasz and Hotchkiss, 1964), but has since grown to include many microbial species which utilise density-dependent population signalling to initiate different functions. For example, *Escherichia coli* and *Salmonella enterica* var. typhimirium produce quorum sensing molecules to sense and respond to cell density and environmental metabolic products (Pearson et al., 1994; Surette and Bassler, 1998), ensuring growth induction when the environment is suitable and when population density warrants collective growth. *Pseudomonas aeruginosa* and *Staphylococcus aureus* use density-dependent signalling to produce virulence factors to enhance pathogenicity (Gambello and Iglewski, 1991; Ji et al., 1995). In sensing the presence and density of fellow cells, *S. aureus* cooperate as a population to enhance their virulence potential, especially through cell wall associated factors and associated exoproteins which enhance virulence (Novick, 2003). The yeast *Histoplasma capsulatum* produces cell wall polysaccahrides in response to population density which affects phagocytosis and survival with phagosomes (Kügler et al., 2000; Rappleye et al., 2007). Microbes also utilise concerted signalling and regulation of gene expression to induce phenotypic changes which enhance survival and pathogenicity. *P. aeruginosa* and *S. aureus* induce density-dependent lysis of some cells within the population to incorporate extracellular DNA into biofilms (Allesen-Holm et al., 2006; Rice et al., 2007), and *C. albicans* modulates morphology and biofilm development in response to population density (Hornby et al., 2001; Ramage et al., 2002). *Myxococcus xanthus* utilises population signalling to sense cell density and nutrient limitation, developing into multicellular fruiting bodies once a minimal population density is reached (Kaplan and Plamann, 1996; Kuspa et al., 1992). The wide utilisation of density-dependent

communication in microbial populations is versatile, serving many different purposes to increase the survival and pathogenicity of the population as a whole.

Several studies have shown that *C. neoformans* may also possess quorum sensing capabilities in which genes related to population density affect fungal growth in culture (Lee et al., 2007, 2009b), filamentation in unisexual mating (Tian et al., 2018), as well as melanisation and biofilm formation (Albuquerque et al., 2014). While phagocytosis and intracellular replication have been related to patient CSF burden (Sabiiti et al., 2014), no studies have closely looked at the effect of cryptococcal density on individual interactions between cryptococci and macrophages. Because interactions between *C. neoformans* and host macrophages are pivotal in deciding the outcome of cryptococcosis, I investigated the effect of cryptococcal density on fungal replication and phagocytosis, and found that fungal density induced no dose-dependent activation or inhibition of phagocytosis by macrophages, or replication by cryptococci.

4.8.1 Infection dose and macrophage phagocytosis

Host response and phagocytosis

During infection, it is important to consider the effect of pathogen density on phagocyte viability and effectiveness. As pathogen density increases, phagocytes may become overwhelmed and fail to phagocytose and kill invading pathogens. For example, when C57BL/6 mice were infected with *S. pneumoniae*, there was a clear relationship between bacterial load and infection outcome; infection with 10^4 pneumococci resulted in bacterial clearance in both the lungs and the blood, associated with killing by alveolar macrophages, while infection with 10^7 bacteria resulted in loss of bacterial control by macrophages (Dockrell et al., 2003; Preston et al., 2019). *H. influenzae* was also shown to overwhelm alveolar macrophages at high doses as infection resulted in a loss of control by macrophages and subsequent onset of pneumonia in infected mice (Preston et al., 2019). Further studies showed that phagocytes became overwhelmed by increasing burden during *S. aureus* and *M. tuberculosis* infections which resulted in immune cell death and consequent

pathogen survival (Jubrail et al., 2016; Mahamed et al., 2017). With macrophage phagocytosis and viability being so important during cryptococcal infection, it is important to understand how increasing burden affects macrophage behaviour.

In the infection assays described in this chapter, cryptococcal phagocytosis by macrophages was linearly related to initial fungal burden during J774 infection, as the proportion of macrophages containing intracellular cryptococci increased with the rise in cryptococcal infection. The percentage of macrophages with intracellular cryptococcal cells did not increase or decrease disproportionately with level of infection, suggesting that macrophages neither upregulated phagocytosis nor became overwhelmed by the larger number of cryptococci in the extracellular environment. Some studies have suggested that quorum sensing molecules produced by *P. aeruginosa* induce human polymorphonuclear chemotaxis and receptor expression (Wagner et al., 2007; Zimmermann et al., 2006), and that quorum sensing molecules induce macrophage phagocytosis of yeasts (Vikström et al., 2005). However, here there was no dose-dependent enhancement or inhibition of phagocytosis, suggesting that the presence of higher doses of cryptococci and related population density signalling molecules did not induce macrophages to upregulate phagocytosis. Because the percentage of macrophages which contained intracellular cryptococci increased with burden, as seen with increasing multiplicity of infection in *Candida albicans* infection (Rudkin et al., 2013), the relationship was likely determined by the probability of macrophages encountering cryptococci, suggesting that each macrophage-*Cryptococcus* interaction was an independent infection. This is in agreement with a previous study from our lab, showing that macrophage phagocytosis of cryptococci is proportional to fungal dose in a zebrafish mode of cryptococcal infection (Bojarczuk et al., 2016).

Immune cell invasion by cryptococci

Alternatively, the percentage of macrophages which successfully phagocytosed cryptococci may be seen as the proportion of macrophages which were parasitised by cryptococci (Feldmesser et al., 2000; Ma et al., 2009; Voelz et al., 2009). It is important to consider intracellular parasitism as many pathogens, including

Salmonella Typhimurium, *Leishmania*, and *Mycobacterium* species, exploit the relative safety of the host intracellular niche, replicating within host cells as a key component of their pathogenesis (Bermudez et al., 1995; Chang, 1980; Leung and Finlay, 1991; Mirkovich et al., 1986). During the *Cryptococcus* infection here, as the initial fungal burden increased a greater number of cryptococci came into contact with J774 macrophages and were able to successfully invade and occupy the macrophage intracellular niche. Because the relationship between burden and macrophage infection was linear, just as the macrophages did not upregulate phagocytic uptake in response to fungal dose, cryptococci did not cooperate to induce higher frequency of macrophage infiltration in response to population density– unlike *S. enterica*, which use QS signals to express genes required for host cell invasion (Choi et al., 2012). In J774 macrophage infection, density-dependent quorum sensing between cryptococci does not seem to enhance macrophage parasitism by cryptococci, or induce an enhanced or attenuated macrophage response.

It has previously been reported that cryptococcal uptake by J774 macrophages correlates with phagocytosis by human MDMs (Sabiiti et al., 2014). In my assays, while the proportion of macrophages containing intracellular cryptococci was not significantly different between J774 macrophages and MDM cells at each initial fungal dose, the percentage of MDMs which contained intracellular cryptococci did not increase *linearly* with fungal burden as it did during J774 infection. However, linear regression assesses how closely a dataset adheres to the classic linear equation, taking the variability in the data points into account. While uptake by MDMs did not fit this linear equation, the mean percentage of infected macrophages did increase with dose. The failure to achieve a linear relationship was due to the high standard deviation, which was likely due to stochastic interactions between cryptococci and macrophages during infection, causing a variable level of macrophage infection.

However, at the highest level of fungal infection there was a lower percentage of MDMs which successfully phagocytosed cryptococci. This was not likely due to

killing of fungal cells by MDMs at the highest fungal dose, lowering the percentage of macrophages which contained live cryptococci, as fungal death was not seen during time lapse imaging. It is possible that as fungal dose increased MDMs became overwhelmed and failed to phagocytose cryptococci at a level proportional to dose. Alternatively, cryptococci may have cooperated at higher fungal doses to evade immune capture or to escape from the phagocyte. This is possible, as it has been suggested that the *S. aureus agr* locus, which encodes the *Staphylococcus* quorum sensing system, is associated with endosome escape (Shompole et al., 2003). Alternatively, just as *H. capsulatum* yeasts produce cell wall factors at high density which prevent efficient phagocytosis (Rappleye et al., 2007), it is possible that cryptococci upregulated capsule production at the higher fungal doses considered here to evade phagocytosis. However, the most likely explanation for the reduced phagocytosis by MDMs is the high variation in uptake between donors at the highest level of fungal infection. While it is possible that the ability of MDMs to phagocytose cryptococci plateaued at higher doses, MDMs from more donors would need to be considered before accepting that no linear relationship existed between cryptococcal infection dose and uptake by MDMs. It is known that there is high donor variation in MDM control of intracellular cryptococcal proliferation (Garelnabi et al., 2018), and it stands to reason that phagocytosis may be similarly affected.

4.8.2 Infection dose and cryptococcal replication

Cryptococcal replication in response to extracellular fungal density

To understand the effect of fungal density on interactions with macrophages it is also important to discern how infection density affects cryptococcal replication. Microbes such as *C. albicans* take advantage of density-dependent cues within their environment to shift the growth phase, reducing the time spent in lag phase (Chen et al., 2004), whereas *E. coli* can negatively regulate their population density (Takano et al., 2017). Because cryptococci can utilise the macrophage niche to replicate and disseminate infection (Charlier et al., 2009; Chretien et al., 2002;

Feldmesser et al., 2000), I examined how the initial fungal dose affected the ability of cryptococci to proliferate within macrophages.

I have shown that as the level of infection increased, the relative fold change of cryptococci within J774 macrophages and human MDMs neither increased nor decreased significantly, indicating that fungal replication was not affected by initial fungal burden. Furthermore, as the initial fungal inoculum increased, the doubling time of intracellular cryptococci with J774 macrophages and MDMs failed to significantly increase. This suggests that over 18 hours of infection cryptococci did not coordinate within the population to increase intracellular replication in a dose-dependent manner. Of course, the inability of cryptococcal dose to affect intracellular proliferation may have been due to the fact that the cryptococci were within a confined niche inside of the macrophage, and therefore may have been impervious to extracellular signalling molecules. Yet, while the phagosome presents a defined area within the host cell, cryptococci are able to permeabilise the phagosome, removing potential barriers to communication (Johnston and May, 2010; Tucker and Casadevall, 2002). Thus, because sequestration within host cells is unlikely to affect cryptococcal signalling, it is clear that the level of fungal burden did not alter the ability of the fungi to replicate intracellularly.

Cryptococcal replication in response to intracellular fungal density

Interestingly, as the number of starting intracellular cryptococci per macrophage increased (i.e. the number of cryptococci per phagosome), the intracellular doubling time of cryptococci within J774 macrophages did not decrease. This suggests that not only did initial extracellular cryptococcal density fail to induce increased replication of cryptococci within J774 macrophages as discussed above, the intracellular population density failed to produce a density-dependent enhancement of replication as well. This is interesting, as quorum sensing may be seen as a possible method of sensing diffusion gradients (Redfield, 2002). Signal diffusion and subsequent cooperation within the macrophage niche does occur; macrophage co-infection with wildtype and a phospholipase B1 mutant of H99 *C. neoformans* at a ratio of 2:1 increased the intracellular proliferation of the mutant

strain (Evans et al., 2019), showing that the phospholipase B1 produced by the wildtype strain was sufficient to rescue the growth of the mutant strain. This illustrates that fungal signalling, or perhaps proximity to necessary molecules, can induce increased growth within J774 cells. With cryptococci in such close proximity within the host cell, diffusion gradients and quorum signalling would be strong within the confined space, further suggesting the lack of quorum sensing between cryptococci in this system.

Additionally, as the number of cryptococci within each phagosome increased, the doubling time of the fungi did not increase, showing that the fungi did not replicate *slower* in response to intracellular population density. Here, the cryptococci did not limit growth as population density within each J774 macrophage increased. This suggests that after phagocytosis by J774 macrophages, cryptococci did not inhibit growth in order to limit consumption of nutrients and occupation of limited niche space based on cues from population density. In fact, while nutrient starvation is an important consideration, *Cryptococcus* has specific adaptations which enable survival within phagocytes during nutrient scarcity associated with intracellular infection. As mentioned above, *C. neoformans* can damage the phagosomal membrane and gain access to the nutrients within the cytosol (Johnston and May, 2010; Tucker and Casadevall, 2002). Additionally, phagocytosis of H99 *C. neoformans* by J774 macrophages induces expression of genes encoding carbohydrate and iron transporters (Fan et al., 2005b), and cryptococci phagocytosed by J774 cells also express copper transport receptors within the phagolysosome (Waterman et al., 2007), enabling the consumption of valuable nutrients. Furthermore, intracellular *C. neoformans* is able to 'scavenge' and store lipid droplets from murine BMDM (Nolan et al., 2017), from which cryptococci obtain carbon during infection by β-oxidation (Kretschmer et al., 2012). Finally, cellular autophagy by cryptococci within J774 macrophages provides nutrients and enables survival of intracellular cryptococci (Hu et al., 2008). Thus, nutrient starvation was unlikely to be a limiting factor with increasing fungal dose within macrophages during the infection time considered here. As such, because cryptococci did not limit replication due to nutrient limitation, cryptococcal

replication was not affected by intracellular population density, suggesting that there was no effective quorum sensing occurring within the population in these conditions.

Macrophage control of intracellular replication

While investigating the effect of pathogen density on infection progression, it is important not only to consider the potential for signalling and coordination amongst cryptococci, but also the possible change in macrophage control as infection dose increases. Recent studies have shown that macrophages and pathogens simultaneously alter their gene expression after interaction (Tierney et al., 2012), and as such the potential for macrophages to alter their behaviour on cryptococcal encounter is important in determining the outcome of the individual interactions. Given that the intracellular fold change of cryptococci did not change with increasing fungal burden, as the fungal dose increased macrophages did not increase or decrease their control over intracellular fungal replication. Indeed, if macrophages perceived a high level of pathogenic threat, they may have regulated their response to actively reduce pathogenic replication, and the cryptococcal fold change would decrease with increasing burden – an effect that was not observed over the concentrations and time limits imposed in these assays.

Furthermore, during J774 infection intracellular doubling time of cryptococci did not increase with the rise in initial fungal burden within the well, or with the increase in initial number of phagocytosed cryptococci within each macrophage. While this may suggest that cryptococci were not cooperating to enhance replication, it may also suggest that macrophages did not increase their control over intracellular pathogen replication as the fungal burden increased. Additionally, because the intracellular cryptococci did not replicate faster with increasing burden, macrophages did not become overwhelmed to relinquish control of fungal replication with higher fungal doses, as is seen in *S. aureus* infection (Jubrail et al., 2016). Because there was no significant increase or decrease in the doubling time of the cryptococci as the initial cryptococcal dose increased, cryptococci did not cooperate to enhance

proliferation, and macrophages did not exert increased control over cryptococci intracellularly.

Interestingly, during human MDM infection as the initial level of cryptococcal infection within the well increased the intracellular doubling time also increased, though this was not statistically significant. What's more, as the number of intracellular cryptococci within each macrophage increased, the intracellular doubling time increased. Potentially, cryptococci sensed the density of fungal cells within the macrophage intracellular niche and coordinated the slowing of replication to prevent depleting space, enabling continued survival within the haven of the intracellular niche. A possible advantage of this is the continued, low-level infection associated with cryptococcal latency which allows fungal cells to safely remain in the host without causing acute infection and subsequent immune response (Garcia-Hermoso et al., 1999; Goldman et al., 2000).

Alternatively, as the initial fungal burden increased, both within the well and within individual macrophages, MDMs may have exerted stronger control over cryptococcal intracellular proliferation, sensing the increase in threat and acting to slow pathogenic replication intracellularly. This is possible, as we know that cryptococcal dose has the ability to affect macrophage cytokine secretion; in fact, the level of TNF-α production increases with the multiplicity of infection when human monocytes are infected with *C. neoformans* (Levitz et al., 1994). During human MDM infection, the dose-dependent production of phagocytic cytokines may induce surrounding immune cells to produce effector cytokines which affect immune activation state and result in stronger control over cryptococcal proliferation.

4.8.3 Comparison of models

While comparable in many respects, the main difference between J774 macrophage and MDM infection was the replication rate of cryptococci. In fact, the mean doubling time of intracellular cryptococci (averaged across doses) was roughly 9.6 hours longer within MDMs compared to the murine macrophages. Interestingly, extracellular doubling time was faster in the presence of MDMs, though this was due to the different media. Nonetheless, cryptococcal replication was much slower within human MDMs, suggesting that these cells more effectively suppressed the cryptococcal growth rate – providing extra incentive to cryptococci to remain extracellular. However, caution is warranted when drawing conclusions by comparing different models, as human MDMs and murine J774 macrophages do not necessarily exhibit identical activation state (Lacey et al., 2012; Levitz and Farrell, 1990). It is also important to consider that the human MDMs may have shown bias in polarisation; human MDMs are typically classified as being M2-polarised (Bazzi et al., 2017), which is permissive to intracellular cryptococcal growth. However, it is possible for the macrophages to shift their polarisation state, especially after introduction of infection or cytokines (Davis et al., 2013; Lacey et al., 2012).

4.8.4 Conclusions and future work

The results discussed in this chapter indicate that as initial fungal dose increases, quorum sensing is not employed by *Cryptococcus neoformans* to upregulate proliferation during macrophage infection. This contradicts work by Albuquerque et al. who claimed that cryptococcal growth in culture showed a density-dependent response (Albuquerque et al., 2014), though this was not show during macrophage infection. Furthermore, increasing fungal burden does not affect phagocytosis by J774 macrophages, yet may result in decreased phagocytosis by MDMs at high levels of fungal burden. This decrease in phagocytosis was not observed during zebrafish infection with H99 *C. neoformans*, where there was a linear relationship between infection burden and the number of infected macrophages (Bojarczuk et al., 2016). During MDM infection, this is likely due to donor variation which is known to contribute to differences in control of intracellular cryptococcal infection (Garelnabi

et al., 2018). I have also shown that intracellular and extracellular replication is not affected by increasing fungal dose in J774s, but intracellular density induces an increase in doubling time within MDMs. Taken together, these results indicate that fungal burden does not affect interactions with murine macrophages, yet may influence interactions with human MDMs.

Cryptococcal killing was not observed in the time lapse experiments, and this represents a significant drawback of these experiments – as reported in similar assays previously (Bojarczuk et al., 2016; Diamond and Bennett, 1973; Levitz and Farrell, 1990). While macrophages may phagocytose cryptococcal cells in the absence of stimulatory CD4+ T cell cytokines, the lack of these cytokines reduces anticryptococcal responses (Jarvis et al., 2013; Voelz et al., 2009). While cytokines and additional immune cell subsets were not included in order to test the effect of fungal dose on macrophage-specific responses, utilising these in future experiments may illuminate the effect of fungal dose on killing by macrophages in a more robust infection situation. Future work should also attempt to recapitulate the environment of real-life infections, introducing cytokines, chemokines, nutrients, and effector cells likely to be encountered in different infection situations.

Another consideration for future work is the amount of infection time given to observe the potential effects of fungal dose on replication. Work by our lab has shown that most phagocytosis in an *in vivo* zebrafish model of infection occurs within the first 24 hours, with a significant amount in the first 2 hours (Bojarczuk et al., 2016). In both J774 and human MDM assays, I incubated macrophages with cryptococcal cells for 2 hours before washing away extracellular cryptococci. While infection continued for 18 hours after this point, I saw no additional phagocytosis throughout the time lapse videos, suggesting that in these models phagocytosis of opsonised cryptococci occurs only within the first 2 hours. As such, it was not strictly necessary to allow more than two hours of infection to determine if fungal dose impacts phagocytosis. However, if conditions requiring coordination and cooperation amongst the population are not met, density-dependent effects may not be observed. In this case, it may be interesting to follow this set of experiments

over a longer time frame to determine if fungal quorum sensing does in fact affect cryptococcal replication, and to test the effect of the addition of conditioned media. Albuquerque showed that conditioned media from stationary phase cryptococci induced the most growth 36-48 hours after introduction to low density culture (Albuquerque et al., 2014), though my experiments ceased after 18 hours – a timepoint which may have been too early for the accumulation of potential quorum signalling molecules to elicit effect. However, to consider this a continuous flow of media would be required to ensure the health of the cryptococci, though would likely remove QS molecules present. Interestingly, it is worth noting that quorum sensing in bacteria doesn't just increase the number of microbes, but rather affects the growth phase by shortening the amount of time spent in the lag phase. Addition of conditioned media may merely increase the number of cryptococcal cells, affecting the number of cryptococci rather than the stage of growth, and may suggest the presence of an excreted growth factor rather than a quorum sensing molecule. It would be interesting to add conditioned media from cryptococcal cultures and observe the effect on phagocytosis and replication.

Another interesting point for future consideration is the effect of intracellular fungal density on the induction of unisexual and bisexual mating. CQS1, a proposed quorum sensing peptide of *Cryptococcus*, is present at high population density; Tian et al. showed that at high fungal densities there is induction of unisexual and bisexual mating amongst cryptococci associated with this peptide (Tian et al., 2018). As the fungal density within the confined space of the phagosome or macrophage intracellular niche is high, especially compared to the extracellular environment, it would be interesting to see if fungal dose affected cryptococcal mating intracellularly. This would potentially require longer time frames, but could suggest intracellular signalling amongst cryptococci within the host niche as has been suggested for *Histoplasma capsulatum* (Kügler et al., 2000).

Finally, while flow cytometry is well characterised for analysis of phagocytosis and intracellular proliferation of *C. neoformans* (Evans et al., 2017; Voelz et al., 2010), it resulted in significantly lower proportions of infected macrophages compared to

time lapse analysis. I believe that this was due to macrophages becoming round and less adherent to the plate during cryptococcal infection, resulting in infected macrophages being removed during the washing step of the assay. Alternatively, time lapse analysis may overestimate the number of infected macrophages, though care was taken to avoid experimental bias in choosing the fields of view for time lapse imaging. Regardless, even though flow cytometry analysis produced trends similar to those achieved through time lapse imaging, analysis of time lapse videos allowed the determination of individual cryptococcal doubling times and as such remains the main method for probing cryptococcal-macrophage interactions throughout the remainder of this thesis.

Chapter 5. Macrophage control of cryptococcal infection

5.1 Introduction

5.1.1 Host cell exploitation in infection

Classical nomenclature of invading microorganisms has relied on identifying the necessity of intracellular versus extracellular lifestyles for survival, replication, and dissemination. Traditionally, extracellular pathogens included those which existed outside of host cells, such as *Staphylococcus aureus, Streptococcus pyogenes, Pseudomonas aeruginosa,* and *Escherichia coli*, though the obligation for extracellularity for many is under debate. Intracellular pathogens were labelled as either obligate (such as *Chlamydia*, *Anaplasma, Ehrlichia*, *Rickettsia and Microsporidia*) or facultative (such as *Brucella, Shigella,* and *L. monocytogenes, Candida and Cryptococcus*) based on whether an intracellular phase was necessary or 'optional', respectively (Moulder, 1985). Objections to this system have been raised on the basis that many obligate intracellular pathogens have an extracellular phase necessary for transmission between cells and hosts, and that extracellular pathogens may have an intracellular phase necessary for initiation of extracellular life (Silva, 2012). While numerous microbes are extracellular and reside outside of host cells, I will be focusing on pathogens which are capable of survival and replication within host cells, as exploitation of the host niche represents a source of complexity and potential heterogeneity of outcome in host-pathogen interactions.

Pathogens utilise of many methods of evading immune cell capture and destruction (described in detail in Uribe-Querol and Rosales, 2017). *Staphylococcus aureus* employs several effective strategies for evading phagocytosis and destruction by host immune cells. For example, staphylokinase inhibits antibody opsonisation and complement deposition by the degradation of opsonins, which in turn reduces phagocytic uptake of bacteria (Rooijakkers et al., 2005). *S. aureus* also produces leukotoxins which 'intoxicate' host immune cells, forming pores in the target cells and inducing lysis, thus preventing phagocytosis and facilitating escape from phagocytes should uptake occur (Alonzo and Torres, 2014). *Clostridium difficile* produces toxins which inhibit phagocytosis by inhibiting proteins which modulate

actin polymerisation (Jank et al., 2007). The exotoxins enter host phagocytes via endocytosis, then form pores in the endosomal compartment to gain access to the cytosol and subsequently glycosylate Rho proteins. This inactivates Rho proteins which results in disorganised actin polymerisation, inhibiting phagocytosis. Thus, inhibition of phagocytosis is a potent mechanism by which pathogens subvert immune control.

Another effective method of evading phagocytosis is through preventing the binding of immune receptors. Pathogenic fungi mask immunogenic motifs on their surface to prevent recognition by immune cells. *Aspergillus fumigatus* is a commonly inhaled fungus which fails to elicit an immune response upon dormant spore inhalation. The surface of *A. fumigatus* is covered with a layer of hydrophobic RodA proteins. Stimulation of human DCs with this protein failed to induce DC maturation, cytokine production, and pathogen-specific T cell cytokine production; however, mutant conidia lacking this rodlet layer induced expression of DC maturation markers and cytokines, chemokines, and ROS (Aimanianda et al., 2009). This pathogen uses a surface rodlet layer to cloak its immunogenic surface and prevent immune activation. Interestingly, Luther and colleagues showed swelling induced by germination exposed β1-3 glucan on the cell surface which was recognised by dectin-1, leading to phagocytosis (Luther et al., 2007). Thus, while cloaking mechanisms efficiently prevent phagocytosis, this is not fail-proof, though germination and hypha formation are often associated with escape from phagocytes. Cryptococcal capsule also prevents phagocytosis (Kozel, 1977), and the anti-fungal drug caspofungin reveals β-glucans on filamentous *C. albicans* as a mechanism to facilitate clearance (Wheeler et al., 2008).

While pathogens may evade recognition by immune cells, perhaps more intriguing is the exploitation of host cells by microbes during infection. One potential benefit of the host intracellular niche is the relative safety from extracellular antimicrobial effector molecules produced by host immune cells such as reactive oxygen and nitrogen species, antimicrobial peptides, granular contents, complement, and neutralising antibodies. For example, the safety of the naïve phagocyte intracellular

environment is a proposed advantage for the intracellular life of *Leishmania major* infection (Mirkovich et al., 1986).

Intracellular pathogens may also exploit the host cell for the gain of nutrients in "nutritional virulence" (Abu Kwaik and Bumann, 2013). *Listeria monocytogenes* utilises host-derived glycerol and glucose-6P as its main carbon sources (Grubmüller et al., 2014). In fact, not only does this intracellular parasite exploit host metabolism, but because it uses two host-derived carbon sources, there is less nutrient strain on the host than would be imposed by utilisation a single host-derived carbon source. This means that there is less stress on the host, ensuring the endurance of both the host cell and the intracellular pathogen within (Grubmüller et al., 2014). In fact, *Salmonella* colonisation of host tissues is dependent on a diverse repertoire of host-derived nutrients and metabolites as well as robust microbial metabolism, with dependence on host resources distributed amongst diverse pathways so that scarcity or defective metabolic capabilities do not result in immediate peril for the intracellular pathogen (Steeb et al., 2013). Intracellular pathogens not only catabolise host-derived nutrients, but can trigger host protein degradation, raid host lysosomes, and manipulate host autophagy pathways to gain access to nutrients whilst inside host cells. With access to nutrients and safety, intracellular pathogenesis is attractive for many microbes.

While many pathogens are capable of thriving within host cells, they may survive in different environments within the cells – within vacuoles, the phagosome, or the cytosol. Upon entry into epithelial cells or macrophages, *Salmonella enterica* serovar Typhimurium becomes encased in a *Salmonella*-containing vacuole, which acidifies and acquires characteristics of late endosomes. At acidic pH, *Salmonella* utilises a type III secretion system (T3SS) to produce a needle which it uses to eject effector molecules outside of the vacuole to the host cell cytoplasm (Chakravortty et al., 2005). These molecules manipulate host processes and machinery to produce an environment that is favourable for the intracellular bacteria (Figueira and Holden, 2012). *Legionella* and *Chlamydia* also escape destruction and reside within

the host intracellular niche through the modification of host vacuoles, a common strategy employed by pathogens for successful inhabitation of host cells.

The ability to adapt to the host environment and exploit the intracellular niche for replication is an important pathogenicity mechanism for intracellular microbes. *Mycobacterium tuberculosis* (Mtb), for example, is capable of intracellular proliferation within the macrophage phagosome after ingestion. Evidence of host macrophage manipulation by live Mtb has long been recognised, with the discovery that intact bacilli inhibit lysosome fusion with the phagosome, though inhibition is not evident in structurally damaged bacilli (Armstrong and Hart, 1971). Live bacteria inhibit acidification of the macrophage phagosome by inhibiting accumulation of V-ATPases on the phagosome membrane (Sturgill-Koszycki et al., 1994), enabling the survival of the bacteria within the phagosome itself. This bacterium parasitises the macrophage intracellular niche to facilitate replication, even killing host macrophages to infect subsequent macrophages in a positive-feedback manner, leading to exponential bacterial growth and concurrent death of host macrophages (Mahamed et al., 2017).

Pathogenic fungi also manipulate phagosome maturation. One study showed that through a similar survival strategy, *Aspergillus fumigatus* conidia inhibited host phagolysosome acidification. This inhibition was dependent on intact DHN-melanin on the surface which loosened during germination, and the inhibition of acidification varied between different species (Thywißen et al., 2011). Fungal cell wall components have been shown to be involved in the modulation of phagosome maturation. One study showed that a *Candida albicans* mutant with truncated O-mannan failed to slow phagosome maturation compared to wildtype fungi. Here, wild-type *Candida* containing functional O-mannan masked β-glucan in the cell wall, which not only prevented immune recognition, but slowed rapid phagosome maturation (Bain et al., 2014). *Candida albicans* also inhibits phagosome acidification, especially the filamentous form (Fernández-Arenas et al., 2009). Thus, manipulation of harsh host environments enables the defensive strategy of pathogenic fungi.

Conversely, *Listeria monocytogenes* escapes from the phagosome to the host cytoplasm where it resides and replicates. Indeed, in an early study non-haemolytic mutants of this bacterium failed to escape the phagosome, and showed extremely impaired intracellular replication within human enterocyte-like cells compared to the wildtype strain (Gaillard et al., 1987), illustrating the requirement for cytoplasmic residence for the successful replication of this bacterium. *L. monocytogenes* accomplishes phagosomal escape through the use of a haemolysin, listeriolysin O, with loss of function in this gene producing an avirulent phenotype *in vivo* (Cossart et al., 1989). Other factors contribute to the intracellular growth and pathogenicity of *L. monocytogenes* (Portnoy et al., 1992), but cytoplasmic proliferation is a key component of the lifecycle of this bacterium. *Shigella*, *Rickettsia,* and *Burkholderia* also reside within the host cytosol.

While pathogens are capable of colonising various different host cell types, interactions between pathogens and macrophages are of particular interest because macrophages, along with neutrophils, are among the first cells to meet invading pathogens in the tissues. While macrophages may engulf and destroy pathogens, invading microbes may also exploit the macrophage niche, taking advantage of a cell type that is ubiquitous throughout the host and therefore likely to be encountered. The ability of many microbes to replicate within amoebae has led to the idea that macrophages represent a similar niche as amoebae, which are colonised by various pathogens (Casadevall, 2012; Price and Vance, 2014). This therefore enables the survival of pathogens within macrophages which act as a "host", and is one suggested solution to the so-called "macrophage paradox" where macrophages are commonly exploited by invading microorganisms as a niche, rather than acting as executioner (Price and Vance, 2014). Determining the role of the intracellular niche, and the effects of exploitation and modulation by pathogens, is important in understanding pathogenicity and infection dynamics.

5.1.2 Immune modulation by intracellular pathogens

When considering intracellular pathogens it is important to understand how the pathogen affects the immune cells it inhabits. The resulting effects on immune activation state and the production of effector molecules may modulate the immune response and the outcome of infection. A study investigating macrophage gene expression profiles after infection with *Brucella melitensis* showed that *Brucella* infection down-regulated mitochondrial gene expression associated with cytochrome c release and ROS production, preventing apoptosis of infected macrophages and bacterial destruction by ROS (He et al., 2006). Furthermore, macrophage gene expression was temporally regulated, enabling the survival of some 'precious' *Brucella* within macrophages after an initial stage of bactericidal activity (He et al., 2006). The directed effects that the invading bacteria exerted over the macrophage host not only tempered the antimicrobial processes performed by the phagocytes, but also allowed the continued persistence of a subset of intracellular pathogens within the intracellular niche with limited arousal of the host cells, enabling the bacteria to cleverly hide and initiate successful infection.

A study by Seider and colleagues demonstrated that interference with ROS production is another type of immune interference employed by intracellular fungal pathogens, including *Candida glabrata* and *Candida albicans* which showed a dose-dependent inhibition of ROS production by human MDMs (Seider et al., 2011). *C. glabrata* infected human MDMs while stimulating limited immune activation, inducing less pro- (TNF-α, IL-1β, IL-6, IL-8, and IFN-γ) and anti-inflammatory (IL-10) cytokine production by MDMs than even the non-pathogenic *Saccharomyces cerevisiae* control. *C. glabrata* was readily phagocytosed by human MDMs, then resided in a non-acidic phagosome, where it proliferated whilst inducing minimal macrophage damage until excessive intracellular proliferation caused the *C. glabrata* to lyse the MDMs and proliferate extracellularly (Seider et al., 2011). Here, the fungal cells inhabited a modified host intracellular niche and modulated the host immune response by not raising suspicions, replicating intracellularly without

inducing host cell apoptosis or microbial destruction before escaping from the host cell to propagate infection extracellularly.

Mycobacterium tuberculosis (Mtb), as mentioned above, is a persistent pathogen that not only possesses an arsenal of techniques to enable survival within the host intracellular niche, but also employs strategies to modulate the host immune response to enable the propagation of infection. A study by Rajaram and colleagues showed that Mtb induced PPAR-γ expression and subsequent IL-8 production in human MDMs (Rajaram et al., 2010). This process contributed to intracellular proliferation within host macrophages in part through control of MDM pro-inflammatory cytokine production, as blocking of this process through inhibitors against PPAR-γ resulted in reduced intracellular growth and increased pro-inflammatory cytokine production by the macrophages (Rajaram et al., 2010). Recently, the virulence-associated *mce2* operon was linked to inhibition of ERK and MAPK signalling pathways in macrophages during *Mycobacterium* infection, with effects on macrophage activation and immune response (Qiang et al., 2019). Indeed, infection of C57BL/6 mice with *Δmce2 Mycobacterium* strains induced pro-inflammatory TNF and IL-6 production, and even reduced bacterial burden and dissemination (Qiang et al., 2019). Here, not only did the pathogen survive within the host phagosome, it modified the macrophage cytokine profile, thus affecting immune activation state.

Francisella tularensis, the gram-negative bacterium which causes tularemia, has even been weaponised in the past due to its ability to subvert the host immune system and propagate fatal infection. A study investigating J774 infection with *F. tularensis* showed that during infection of TLR-activated J774 murine macrophages, the macrophages not only failed to inhibit intracellular proliferation of *F. tularensis*, but infection with this bacterium inhibited pro-inflammatory cytokine production by the macrophages and inhibited intracellular signalling pathways involving NFkB, p38, and c-Jun (Telepnev et al., 2003). Recent studies suggests that *F. tularensis* antioxidant enzymes prevent the accumulation of ROS in the macrophage, which prevents MAPK signalling and NFκB activation, suppressing pro-inflammatory

cytokine production by infected macrophages (Rabadi et al., 2015). The antioxidant activity performed by *F. tularensis* may even prevent macrophage autophagy, enabling the intracellular survival of this pathogen (Rabadi et al., 2015). There is also evidence that *F. tularensis* induces macrophages to switch from an initially pro-inflammatory activation state early in infection to an anti-inflammatory state 24 hours later, both *in vitro* and during *in vivo* murine infection, to facilitate its intracellular survival within the host (Shirey et al., 2008). As such, there are many ways in which an intracellular pathogen may mitigate and modulate the host immune response to ensure survival and pathogenic success.

Interestingly, the specific state of the invading pathogen can affect the host phagocyte response and downstream immune cell activation. Using a mouse BMM model of *Salmonella enterica* serovar Typhimurium and single-cell RNA-seq, Avraham and colleagues found that there was substantial variation in the host translational response to infection (Avraham et al., 2015). Indeed, immune cell gene expression showed consistently high variance throughout infection in what is normally considered a "homogenous" macrophage population, and was associated with variable cues received from the intracellular bacteria. Modification of bacterial LPS induced differential Type-I IFN response in individual mouse immortalised BMMs, and *Salmonella* genes required for intracellular survival after ingestion showed a great degree of variability, contributing to the heterogeneity in macrophage activation state and response. In this study the differences in the state of ingested pathogen induced differential macrophage responses, illustrating the importance of considering the effect of individual pathogenic cells on host response (Avraham et al., 2015). The interaction of diverse and heterogeneous pathogens with host phagocytes, and the subsequent effects these interactions have on immune activation state and infection outcome, represent a wide network of interconnected possibilities and heterogeneity in the conflict between host and invading enemies.

5.1.3 The use of simulations in the study of infection

With there being so many pathogens with varied responses to host immune cells, displaying complex infection outcomes, the use of *in silico* computational simulations in infection modelling has proven highly informative. Computational simulations of *in vivo* infections have allowed the contribution of different infection variables to be considered independently based on experimental measurements of immune parameters. Applying measured variables to computational simulations enables the examination of different infection pathways and outcomes at a level that is not plausible *in vivo*. Using *in silico* modelling to understand how the immune system responds to different infections and host conditions can illuminate how infection progresses and produces different outcomes amongst individuals.

For example, application of an evolutionary game theory approach to *Aspergillus fumigatus* infection within the alveolar sacs of the lung examined the balance between pathogen-induced infection and host-driven inflammation, and the effect this balance has on fungal morphotype and consequent persistence (Pollmächer et al., 2016). In utilising what is known about *A. fumigatus* infection from *in vitro* and *in vivo* experiments, the application of spatially-restricted interactions (i.e. likelihood of interactions amongst conidia within each alveolar sac) and different stages of infection, Pollmächer et al. investigated the progression of the immune response. In doing so, the production of stochastic *in silico* simulations showed how each step of the immune response induced different magnitudes of successive immune processes, resulting in either clearance or persistence of the fungal cells within the defined lung. Interestingly, the combined simulations in this study showed that alveolar macrophages are successful in clearing lung conidia when the fungi are present at low doses, but at high doses polymorphonuclear cells are required to clear infection, especially with the onset of hyphal morphology (Pollmächer et al., 2016). Here, application of known values and interactions from *in vitro* and *in vivo* studies to the hierarchical structure of the immune system illuminated relationships between infection dose and strength of immune response in the defence against a widespread fungus.

Another type of infection model, designed by Carbo and colleagues, looked at *Helicobacter pylori* infection in the gut mucosa (Carbo et al., 2013). This system took advantage of layering different types of models to replicate spatial organisation of the gut, activation and actions of different types of immune cells, and the potential effect that invading bacteria elicit as they move through the layers of the gut. Calibration for this model came from determining levels of immune cells in different areas of infected C57BL/6 mice over 60 days of infection, using *in vivo* infection data to inform a computational simulation. Interestingly, this model enabled the prediction of the effect of removing specific stimuli to the cells – specifically PPAR-γ – which was done by altering the activation states of the immune cells in the system based on the known effects of PPAR-γ. This simulation was also used to estimate whether the damage caused to the intestinal mucosa was caused by the invading bacteria or the force of the immune response, and found that the blame shifts from the bacteria to the immune cells – a result that was corroborated by using a mouse model to measure the relative effects. While this model is limited based on what is currently known about infection progression, the approach to this model combined known relationships, spatio-temporal dynamics of interacting immune cells, and built in stochasticity. Amazingly, the use of *in silico* knockouts allowed determination of the effects of individual components on the system as a whole.

Another simulation fit a computational model of whole blood *Candida albicans* infection to existing experimental datasets (Lehnert et al., 2015). Using random transitions between *Candida* cell states which included intracellular, extracellular, phagocytosis-resistant, and phagocytosis-susceptible *C. albicans* during spatial migration, this model built stepwise simulations to look at phagocytosis and killing of *Candida* during bloodstream infection. In all of these simulations, computational parameters were defined by what is known about real life infections, and though the constant flux of *in vivo* disease cannot be completely captured, *in silico* modelling of infection dynamics enables deeper understanding of *in vivo* infections than is possible with current imaging technologies. Despite the need for defined

assumptions, fitting models to our current knowledge base may help to explain the progression and variability of infection, and may reveal potential therapeutic strategies which may require less sacrifice of experimental animals.

5.1.4 Exploitation of host macrophages by *Cryptococcus neoformans*

Cryptococcus neoformans is a pathogen that is capable of invading the host macrophage and exploiting this intracellular niche for safety, replication, and dissemination. *C. neoformans* has an arsenal of strategies which enable it to survive within host macrophages, conquering it as a replicative niche (see in-depth review - Johnston and May, 2013). *C. neoformans* has a capsule composed mainly of polysaccharides which is an important component of its defence. In murine infection, capsule prevents efficient phagocytosis by macrophages because capsule components block mannose and β-glucan receptors on the phagocyte from access to surface carbohydrates on the fungi (Cross and Bancroft, 1995). Indeed, at high inocula murine bronchoalveolar macrophages phagocytose more acapsular than encapsulated cryptococci (Levitz and Dibenedetto, 1989), and a large capsule strain of *Cryptococcus* shows markedly reduced uptake by phagocytes (Levitz et al., 1997). What's more, capsule growth in time prevents phagocytosis by macrophages in a zebrafish model of cryptococcal infection (Bojarczuk et al., 2016).

While the cryptococcal capsule is a potent anti-phagocytic defence of cryptococci, it also enables intracellular survival. For example, cryptococci with larger capsules grow better in oxidative environments than cryptococci with smaller capsules, and are better at surviving within the stressful intracellular environment during infection. Cryptococci with large capsules recovered from the lungs of mice even showed enhanced survival during H_2O_2 insult compared to cryptococci with small capsules grown in culture (Zaragoza et al., 2008). Indeed, the capsule is associated with intracellular survival and replication within macrophages (Feldmesser et al., 2000), demonstrating a role for the capsule in intracellular parasitism. Furthermore, *Cryptococcus* melanin (secreted, and as a component of its cell wall) protects against microbicidal peptides such as defensins, protegrins, and magainin (Doering et al.,

1999). Because cryptococci are likely to encounter these antimicrobial peptides produced by phagocytic cells, this is one mechanism which protects the fungal cells from harm by the host whilst occupying the intracellular niche. Thus, cryptococci utilise the capsule and cell-wall components to protect itself from harmful microbicidal effectors produced by host immune cells.

Perhaps one of the most notable adaptations *C. neoformans* has developed to survive within the macrophage intracellular niche is its ability to reside within the phagosome (recently reviewed by DeLeon-Rodriguez and Casadevall, 2016). Once phagocytosed, lysosomes fuse with the cryptococcal phagosome, as revealed by LAMP-1 staining (Alvarez and Casadevall, 2006; Levitz et al., 1999). Currently, however, the acidification of *Cryptococccus*-containing phagosomes is debated. It is known that cryptococci prefer an acidic environment for growth as there is an inverse relationship between cryptococcal growth and pH in cell free culture (Levitz et al., 1997). The addition of weak bases like chloroquine and quinacrine increase MDM control and killing of intracellular cryptococci by alkalinising the intracellular niche occupied by the cryptococcal cells (Harrison et al., 2002), though anti-cryptococcal activity is dependent on temperature and pH (Harrison et al., 2000). However, the decrease in intracellular cryptococcal numbers may in fact be due to cryptococcal escape of the host cell (Ma et al., 2006). Nonetheless, cryptococci reside within an acidic phagosome, and based on the effects of chloroquine and quinacrine, it appears that acidity is a crucial component for fungal survival. While early reports claimed that *Cryptococcus* does not significantly alter the pH of the phagosome (Levitz et al., 1999), a recent study showed that infection of J774 murine macrophages and human MDMs with live H99 *C. neoformans* resulted in failure of the phagosome to acidify compared to infection with heat killed fungal cells. This interference with phagosomal acidification was accomplished through the manipulation of Rab GTPases by live fungi (Smith et al., 2015). Thus, it appears that cryptococci inhibit phagosomal acidification. However, while this study showed that the fungus manipulated maturation of the host phagosome and subsequent acidification, it is possible that the phagosome remained acidic but that cryptococci rather prevented further acidification. The prevention of the infected phagosome

to reach maximal levels of acidification may be a strategy of the fungus to prevent sufficient antimicrobial protease activity by the host cell.

Interestingly, cryptococci induce permeabilisation of the phagosome and may escape into the cytosol. In J774 murine macrophages the phagosome reliably contains cryptococci until 3 hours, at which time point the phagosome becomes "leaky" as shown by the diffusion of fluorescently-labelled dextran away from the infected phagosome (Johnston and May, 2010; Tucker and Casadevall, 2002). Inducing phagosome permeabilisation allows the dilution of phagosomal pH, rendering host proteases less effective (Tucker and Casadevall, 2002). Escape form the phagosome into the cytosol may also enable the cryptococci to take advantage of cytosolic nutrients, as described in the previous chapter discussion. Interestingly, cryptococci can scavenge cytosolic lipids from host macrophages, and high lipid availability is associated with cryptococcal escape from the host macrophage, suggesting a further possible advantage of escaping to the cytosol (Nolan et al., 2017).

The resistance to macrophage fungicidal activity enables cryptococci to not only survive within the intracellular niche, but also to replicate within it. In 1973 Diamond noted that not only did human MDMs fail to kill cryptococci, but they provided a suitable environment for intracellular proliferation (Diamond and Bennett, 1973). Intracellular cryptococcal replication occurs as early as 2 hours after phagocytosis (Tucker and Casadevall, 2002), and replication depends on various fungal factors, including phospholipase B1 (Evans et al., 2015). The passivity of macrophages to permit cryptococcal intracellular replication also relies on macrophage activation state; indeed, a study examining the effects of cytokine polarisation of macrophages showed that activation of macrophages with Th2 cytokines IL-4 and IL-13 increased intracellular proliferation of *C. neoformans*, while TFN-α and IL-17 had no effect on fungal IPR (Voelz et al., 2009). Furthermore, murine BMDMs which were activated with IFN-γ more potently inhibited cryptococcal growth than those treated with IL-4, though the macrophage activation displayed plasticity and growth inhibition was dependent upon final activating conditions (Davis et al., 2013).

Cryptococcal intracellular replication occurs within different cell types representative of the different intracellular niches the fungi occupy to effectively propagate infection. Cryptococcal spores or desiccated yeast cells are inhaled into the lung and are thought to be the infectious agent of cryptococcosis (Velagapudi et al., 2009). Examination of murine alveolar macrophages by electron microscopy showed the presence of intracellular cryptococci with excessive intracellular growth which resulted in macrophage cytotoxicity (Feldmesser et al., 2000). Hence, cryptococci are able to colonise and replicate within the first immune cells they encounter. Microglia, the resident immune cells of the brain, phagocytose cryptococci and maintain them within a phagosome, where the presence of budding cells and an increase in intracellular cryptococci over 24 hours showed that the cryptococci replicate intracellularly in this niche (Lee et al., 1995). This is interesting as cryptococci traffic to the brain in humans, producing cryptococcal meningitis and meningoencephalitis. The ability of cryptococci to reside and replicate within microglia suggests that cryptococci not only traffic to the host CNS, but develop an intracellular niche within the CNS to safely proliferate and disseminate infection.

While cryptococci may proliferate so extensively within macrophages that the phagocyte bursts (Feldmesser et al., 2000; Voelz et al., 2009), cryptococci can also exit macrophages without lysing the cell through a type of phagosomal extrusion termed ‘vomocytosis’. Phagosomes attempt to contain intracellular cryptococci by producing actin cages, though when these cages fail the phagosome fuses with the phagocytic cell membrane and cryptococci are able to exit the macrophage (Johnston and May, 2010). Again, differences in macrophage activation state affect the rate of vomocytosis, with Th1-activated macrophages allowing less cryptococcal escape than Th2-activated macrophages (Voelz et al., 2009). This is important, as it suggests that classically activated pro-inflammatory macrophages help to control cryptococcal infection in part through limiting the escape of cryptococci into the extracellular environment. Differences in cell type also produce different vomocytosis phenotypes, with cryptococci escaping more readily from human primary macrophages than murine J774 macrophages (Ma et al., 2006).

Vomocytosis is a useful mechanism by which cryptococci are able to escape the host cell without triggering inflammatory cascades associated with host cell lysis, and is a possible mechanism for fungal dissemination after entry to the central nervous system.

Macrophages not only provide a replicative niche for cryptococci, but they have also been proposed as the vehicle which delivers cryptococci across the blood-brain barrier to infect the central nervous system, eventually causing cryptococcal meningitis and meningoencephalitis. In a murine model of cryptococcal infection, mice inoculated with infected murine BMDM showed increased brain fungal burden at 24h than mice infected with free cryptococci (Charlier et al., 2009), suggesting that macrophages were used to deliver cryptococci to the murine CNS. Furthermore, ablation of macrophages using clodronate in mice led to reduced fungal burden in the brain compared to control mice, further supporting the idea that macrophages can be exploited by cryptococci to disseminate infection (Charlier et al., 2009). Again, macrophage polarisation may play a part in dissemination, as a study which treated mice with the Th1 cytokine IL-12 for the first 7 days of cryptococcal infection showed reduced brain colony formation (Kawakami et al., 1996b). Here, while macrophage contribution was not specifically examined, infiltration of mononuclear cells into the brain was observed and associated with increased fungal load in brains of untreated mice, suggesting the lack of IL-12 modulation of immune response led to greater brain colonisation (Kawakami et al., 1996b). Furthermore, the fungal virulence factor laccase was required for dissemination to the brain in a murine model of infection (Qiu et al., 2012a); cryptococcal laccase expression induces enzymatic activity and surface marker expression characteristic of a Th2 immune response, suggesting that alternative activation of macrophages contributes to the dissemination of cryptococci to the CNS in murine infection (Qiu et al., 2012a). Finally, a recent study investigating the link between different virulence parameters and infection outcome of clinical isolates showed that murine infection with high uptake strains of *C. neoformans* was positively correlated with brain dissemination, connecting uptake with CNS infection *in vivo* (Hansakon et al., 2019). Sabiiti also demonstrated that high CNS

burden was correlated not with high intracellular proliferation of cryptococci, but was rather associated with high cryptococcal uptake by J774 macrophages (Sabiiti et al., 2014). All of these studies provide evidence supporting the idea that cryptococci not only survive and replicate within host macrophages, but that they exploit the host intracellular niche to traffic to the CNS.

5.1.5 Macrophage control of cryptococcal infection

While *Cryptococcus neoformans* has many mechanisms for exploiting the macrophage intracellular niche, it is also important to consider macrophage control of cryptococcosis. A study from our lab looked at the effect of depleting macrophages from the zebrafish model using clodronate liposomes, and found that in the absence of macrophages cryptococcal growth was uncontrolled (Bojarczuk et al., 2016). Macrophage depletion produced a larger fungal burden at 48 and 72 hours post infection, showing macrophage control is essential in containing *C. neoformans* early in infection *in vivo* (Bojarczuk et al., 2016).

As before, the activation state of the macrophages is important; activation of an M1 phenotype induces anti-cryptococcal action, whereas M2 activation promotes cryptococcal growth and dissemination. For example, studies which looked at the effect of the loss of the Th1 cytokine, IFN-γ, on murine infection showed that the lungs of IFN-$\gamma^{-/-}$ mice infected with *C. neoformans* had not only increased burden and more intracellular yeast cells within macrophages, but also expressed markers for alternative macrophage activation and severe inflammation (Arora et al., 2005, 2011). Here, loss of M1 activation induced M2 macrophage activation and resulted in the loss of control of infection. Another study showed that overexpression of the Th2 cytokine IL-13 increased alternative macrophage activation, produced high fungal burden, widespread dissemination, and resulted in high mortality in infected mice (Müller et al., 2007). While classical pro-inflammatory macrophage activation was not specifically shown in this study, the control of infection in IL-$13^{-/-}$ mice compared to the aberrant growth of cryptococci in the presence of strong Th2 cytokine activation suggested that classical macrophage activation, or at least

absence of alternative macrophage activation, is sufficient to drive fungal clearance by the host macrophages, and is similarly corroborated in IL-4 receptor-ablated mice (Müller et al., 2013).

Classical pro-inflammatory cytokine stimulation has shown to be highly advantageous in the control of *C. neoformans* infection. Indeed, Flesch et al. showed that stimulation of murine MDMs with IFN-γ reduced cryptococcal growth (Flesch et al., 1989). Furthermore, a study which infected mice with IFN-γ-producing *C. neoformans* showed that the Th1 cytokine produced a protective response associated with lung and brain clearance. Here, the strong induction of a Th1 response proved necessary for survival (Hardison et al., 2010; Wozniak et al., 2009). This is interesting as high CSF IFN-γ concentration is associated with clearance rate in human cryptococcosis (Jarvis et al., 2014), possibly linking infection control with classical macrophage activation and a Th1 immune response in human cryptococcosis. Thus, while cryptococci are certainly capable of macrophage exploitation, macrophages are likewise able to control cryptococcal infection, though appropriate activation is required.

With the wide variety of possible interactions between macrophages and cryptococci representing many possible outcomes of individual interactions, it is important to consider the consequence of macrophage control and parasitism on the outcome of cryptococcosis. Avraham has discussed how heterogeneity in microbial populations contributes to heterogeneity in host-pathogen interactions, and therefore affects the outcome of infection (Avraham and Hung, 2016). This is important especially in cryptococcosis, as disease progression and response to antifungal treatment is incredibly variable both in HIV-negative (Pappas et al., 2001), and HIV-positive patients (Lee et al., 2011). Immune status (Brizendine et al., 2013), underlying conditions (Kiertiburanakul et al., 2006), and organ transplant status (Gassiep et al., 2017) affect the susceptibility and outcome of patients, and while variables associated with different outcomes have arisen from large-scale human cryptococcosis studies (Jarvis et al., 2014), infection outcome and response to treatment are still variable and somewhat upredictable. With this in mind, gaining

a deeper understanding into macrophage control of *Cryptococcus* infection may provide insight into the heterogeneity in infection outcome.

As discussed above, Avraham et al. have shown that murine BMDMs may vary in their ability to phagocytose threats despite belonging to a supposedly "homogeneous" phagocyte population, with some cells more actively responding to pathogenic cues than others (Avraham et al., 2015). However, while host responses were heterogeneous, this was attributed to differences in the bacterial population, namely activation of regulators associated with intramacrophage survival, LPS modification, and the Type I IFN response (Avraham et al., 2015). Thus, pathogenic heterogeneity induced a highly stochastic host response. It is this variability in host-pathogen interactions that remains largely unstudied in cryptococcal infection. While host cytokine production has been correlated with cryptococcal meningitis outcome (Jarvis et al., 2015), and host variation in response has been quantified (Garelnabi et al., 2018), the impact of variability on *Cryptococcus*-macrophages interactions on infection outcome remains vague.

In this chapter, I will describe experiments I performed to understand the variability in cryptococcal behaviour and how this impacts interactions with macrophages. The data gathered from these experiments have been used to produce an *in silico* model of zebrafish cryptococcal infection. As described above, the production of computational simulations of infection allow us to understand the contribution of individual variables to infection outcome, and thus provide insight that is lacking from current modes of scientific investigation. I will describe the collection of data and how these data have been used to inform the production of the computational simulation, though the simulation was created by James Bradford and Dr Rhoda Hawkins, and will therefore not be shown in this thesis. The utilisation of several models of cryptococcal infection have illustrated the importance of individual host-pathogen interactions in cryptococcal infection, and will eventually be used to produce a computational simulation of human *Cryptococcus* infection, enabling us to understand the contribution of macrophages to the complex infection outcomes in human cryptococcosis. I also provide evidence showing that cryptococcal

proliferation occurs at a faster rate when cryptococci are in the extracellular environment, and that the slow growth of intracellular cryptococci suggests a role for macrophage control of intracellular proliferation.

5.2 The outcome of infection is stochastic at low levels in zebrafish

As shown in the previous chapter, phagocytosis increases linearly with dose, and fungal replication remains constant over increasing inocula *in vitro*. To test if there was a linear relationship between initial fungal burden and final outcome *in vivo*, I used a zebrafish model of cryptococcal infection. This model is useful for studying macrophage-*Cryptococcus* interactions *in vivo* because zebrafish larvae have functional macrophages capable of phagocytosis as early as 30 hours post fertilisation (hpf), clearing *E. coli* from circulation at this timepoint (Herbomel et al., 1999), and were thus able to respond to cryptococcal threat after infection at ~48 hpf here. Furthermore, a functional adaptive immune system is not present until 4-6 weeks post fertilisation (Lam et al., 2004), and is representative of the immunocompromised state that renders many *C. neoformans* patients susceptible to infection. While neutrophils are present at 48 hpf (Lieschke et al., 2008), phagocytosis of cryptococci is largely performed by macrophages in zebrafish (Tenor et al., 2015). Alveolar macrophages are the main innate effector cells to respond to cryptococci during murine infection (Feldmesser et al., 2000), and are believed to be the initial phagocyte involved in phagocytosis of cryptococci in human cryptococcosis. Thus, using a zebrafish larva model of infection allowed me not only to follow hundreds of individual infections, but enabled me to study the role of macrophages in the absence of an adaptive immune response.

At 2 days post fertilisation (dpf) I injected zebrafish larvae with KN99 GFP *Cryptococcus neoformans* into the circulation; this represented 0 days post infection (0 dpi). I counted the number of cryptococci injected for each larva manually. The same larvae were imaged three days later at 3 dpi, and the fungal burdens for each individual larva was compared at 0 and 3 dpi. In attempt to capture what happens at the onset of cryptococcal infection, I only considered larvae with between 1 and 10 cryptococci at 0 dpi; as with many infections, cryptococcosis is likely initiated by one or a few infectious propagules. Additionally, because counting was done by eye and overlapping cryptococci were difficult to count at high burdens, I stopped

counting once the fungal burden at 3 dpi exceeded 100, and these were classified as “high burden” for categorical analysis.

Over the initial levels of fungal burden considered here the final fungal burden was incredibly variable; some larvae controlled infection and showed a decrease in burden, while most failed to control infection and produced an increased fungal burden at 3 dpi (Figure 5.1a). In general, there was an increase in fungal burden with increasing 0 dpi infection burden, though this was variable. To determine if there was a relationship between the initial fungal burden and the outcome of infection three days later I performed linear regression analysis comparing initial and final fungal burdens for all larvae. While there was a linear relationship between fungal burdens a low R^2 value was produced, indicating that the linear relationship was largely explained by factors other than initial fungal burden (Figure 5.1a; linear regression $p = 0.0437$, $R^2 = 0.0197$). Omitting larvae with ‘high burdens’ at 3 dpi where counting of fungal cells was ceased did not produce a linear relationship (linear regression; $p = 0.1970$, $R^2 = 0.0086$). As such, the outcome of these individual infections was variable based on initial fungal burden, with a high degree of stochasticity in final fungal outcome. Indeed, while the mean fungal burden at 3 dpi showed a small increase, it failed to increase in line with 0 dpi fungal burden and instead increased and decreased between each initial fungal dose (Figure 5.1b and 5.1c). Thus, it is likely that factors beyond initial fungal burden decide outcome at this low level of infection, and are likely related to stochastic interactions with the host.

a.

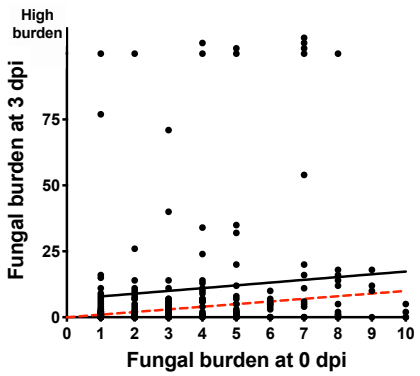

b.

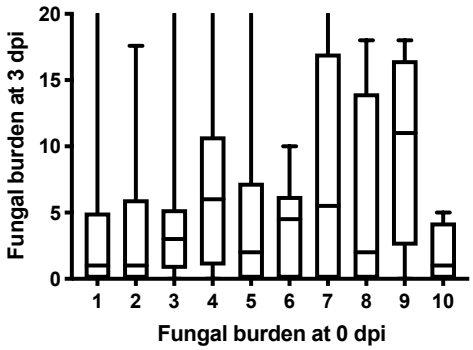

c.

Fungal burden at 0 dpi	Fungal burden at 3 dpi			
	n	Mean	Median	SD
1	35	5.1	1.0	13.2
2	33	3.5	1.0	5.6
3	34	6.4	3.0	13.4
4	20	7.9	6.0	8.6
5	22	6.2	2.0	10.1
6	10	4.0	4.5	3.3
7	10	11.6	5.5	16.4
8	11	6.3	2.0	7.2
9	4	10.0	11.0	7.5
10	4	1.8	1.0	2.4

Figure 5.1. At low initial levels of infection, outcome of cryptococcal infection is variable *in vivo*

Zebrafish larvae were infected with between 1 and 10 cryptococci at 0 dpi. At 3 dpi, the fungal burden for each individual larva was calculated. 4 repeats were considered, with no less than 32 larvae per repeat.

a. Comparison of fungal burden at 0 and 3 dpi. Each point represents one zebrafish larva. The hashed red line represents a line with a slope of 1 to help visualise increased/decreased fungal burden; points above are zebrafish larvae which showed an increase in burden, and those below are larvae which showed a decrease in burden. The black line shows linear regression ($p = 0.0437$, $R^2 = 0.0197$).
b. Box and whisker plot of fungal burdens at 3 dpi. Median, 5^{th}, and 95^{th} percentile compose the box, and whiskers are the maximum and minimum number of cryptococci counted per larva at 3 dpi.
c. Descriptive statistics of fungal burdens of individual infected larvae, separated by initial burden at 0 dpi.

5.3 At high initial fungal burdens, the outcome of infection is linearly related to initial dose in zebrafish

To determine if the same variable infection outcome was observed in zebrafish larvae infected with a higher initial inoculum, I infected zebrafish larvae with up to 600 KN99 GFP *C. neoformans* at 2 dpf (0 dpi). Larvae were imaged and infections were quantified at 0 and 3 dpi for each larva (Figures 5.2a and 5.2b). Because larvae were infected with between 1 and 600 cryptococci at 0 dpi, fungal burden was quantified by determining the pixel area of the GFP+ cryptococci at both times. This is a well-characterised method of quantifying fungal burdens at high doses, and each pixel is ~ 1 cfu (Bojarczuk et al., 2016; Evans et al., 2015).

In zebrafish larvae there was a linear relationship between initial and final fungal burdens over a range of high starting burdens (Figure 5.2c; linear regression $p < 0.0001$, $R^2 = 0.1913$). The mean fungal burden at 3 dpi increased with initial fungal burden, except at the highest initial dose where only 4 larvae were considered (Figures 5.2 d and 5.2e). Here, there was a strong linear relationship between initial and final fungal burdens. This suggests that infection outcome was related to initial infection burden at higher burdens representative of late infection. However, while there was a linear relationship between fungal burden at 0 and 3 dpi, there was still a high degree of variability in infection outcome (linear regression $R^2 = 0.1913$).

a.

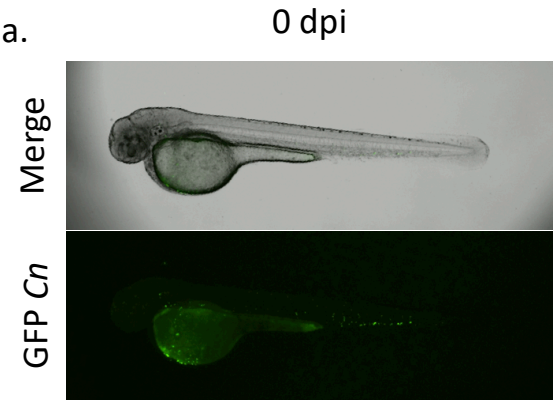

b.

c.

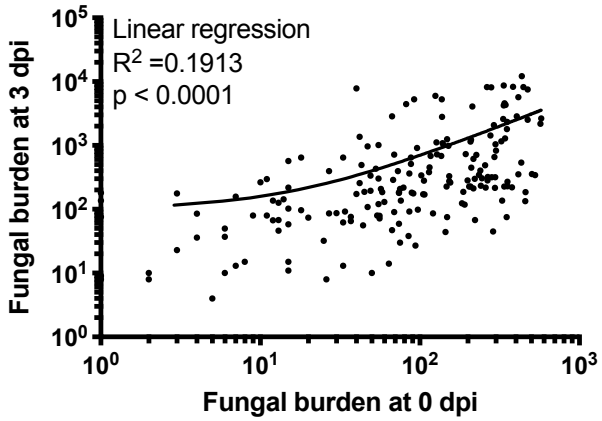

d.

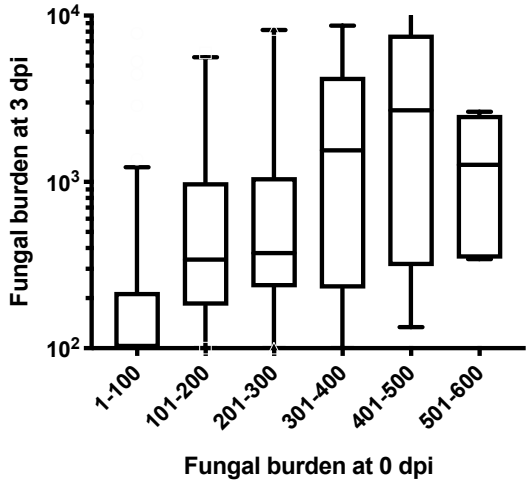

e.

Fungal burden pixel area 0dpi	Fungal burden pixel area 3 dpi			
	n	Mean	Median	SD
1-100	107	360.8	90	1030
101-200	29	901.5	341	1426
201-300	30	1173	374	2063
301-400	16	2530	1548	2810
401-500	10	4023	2699	4192
501-600	4	1380	1267	1205

Figure 5.2. Over a high range of initial fungal burdens there was a linear relationship between fungal burden at 0 and 3 dpi

Individual zebrafish larvae were infected with up to 600 KN99 GFP *C. neoformans* at 0 dpi. Fungal burdens were quantified at 0 and 3 dpi by quantifying GFP+ pixel counts. 196 larvae were infected over three repeats, with no less than 52 larvae considered for each repeat.

a. Zebrafish larva infected with GFP *C. neoformans* at 0 dpi.
b. Zebrafish larva infected with GFP *C. neoformans* at 3 dpi.
c. Comparison of fungal burdens by pixel area at 0 and 3 dpi. Each point represents one individual larva. Linear regression $p < 0.0001$, R^2 0.1913.
d. Comparison of final fungal burden at 3 dpi, separated by initial inoculum at 0 dpi. Mean, 5^{th}, and 95^{th} percentiles compose the box, while whiskers are maximum and minimum number of pixels per larva.
e. Descriptive statistics of GFP+ pixel area at 3 dpi, separated by initial fungal burden.

5.4 Macrophages help control cryptococcal growth during zebrafish infection

As it is known that macrophages interact with cryptococci in a variety of ways, and with the ultimate goal of understanding how these diverse interactions produce variable infection outcomes *in vivo*, I used clodronate liposomes to deplete macrophages from the zebrafish larvae to determine if macrophages help to control infection in this system. Clodronate liposomes reliably deplete macrophages from the zebrafish host while leaving the neutrophilic population intact (Bernut et al., 2014; Bojarczuk et al., 2016). I injected clodronate liposomes into the circulation via the caudal vein at 1 dpf to allow the cytotoxic effects to deplete macrophages before the initiation of infection. PBS liposomes were injected in the same way into control larvae. I then infected zebrafish larvae with KN99 GFP *C. neoformans* via the duct of cuvier at 2 dpf (0 dpi), and quantified fungal burden for each individual larva at 0 and 3 dpi (Figures 5.3a-c, g).

Comparing the fungal burdens of larvae treated with PBS and clodronate liposomes showed that while the fungal burdens were comparable at 0 dpi (Figure 5.3d; Mann-Whitney test $p = 0.4678$, means = 14.27 and 14.25 pixels for larvae treated with PBS and clodronate liposomes, respectively), fungal burdens was significantly higher at 3 dpi in larvae treated with clodronate liposomes (Figure 5.3e; Mann-Whitney test $p = 0.0015$, means = 767.9 and 4263 pixels for PBS and clodronate liposomes, respectively). Furthermore, the relative cryptococcal fold change was significantly higher in larvae treated with clodronate liposomes (Figure 5.3f; Mann-Whitney test $p = 0.0019$, means = 186.5 and 643.7 for larvae treated with PBS and clodronate liposomes, respectively). These results are comparable to those published previously using H99 *C. neoformans* (Bojarczuk et al., 2016). Collectively, these data suggest that cryptococci replicated more in the absence of macrophages, since depletion of macrophages resulted in loss of control of fungal infection compared to control larvae. While the presence of macrophages did not result in the clearance of cryptococci at the doses tested here, macrophages were necessary for control of cryptococcal infection, and loss of this phagocyte produced uncontrolled growth.

(page intentionally left blank for figures + legends on following pages)

a.

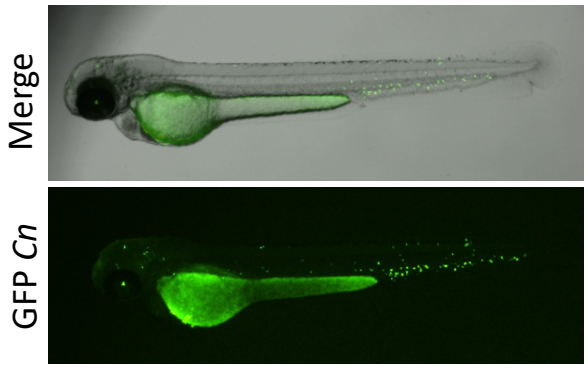

b.

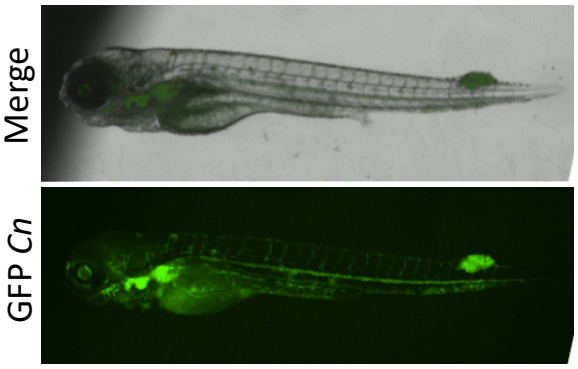

c.

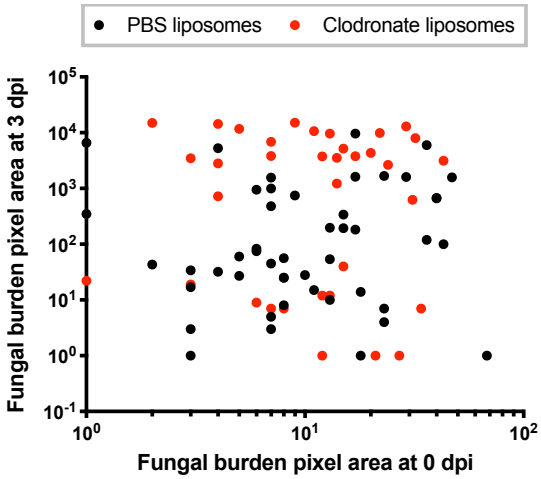

d.

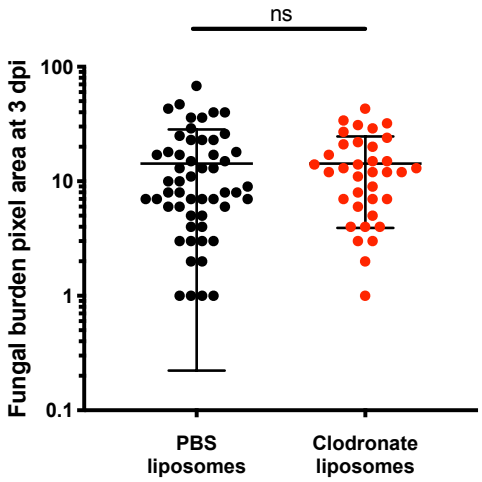

e.

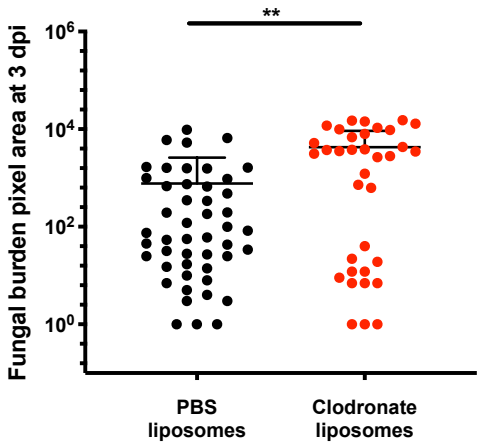

f.

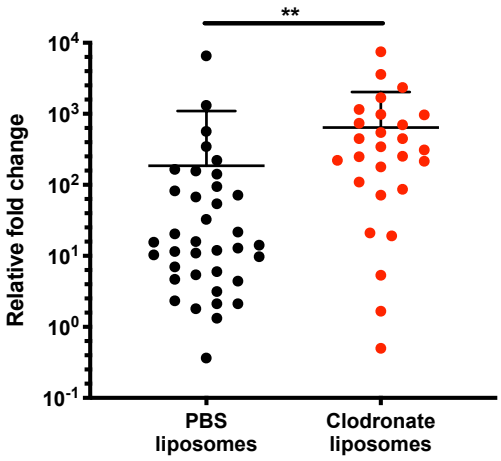

g.

Liposomes	n	0 dpi pixel area		3 dpi pixel area		Relative fold change	
		Mean	SD	Mean	SD	Mean	SD
PBS	55	14.27	14.05	767.9	1851	186.5	906.1
Clodronate	36	14.25	10.34	4263	4981	643.7	1391

Figure 5.3. Macrophages help to control cryptococcal infection in zebrafish larvae

Zebrafish larvae were treated with either PBS or clodronate liposomes at 1 dpf, and infected with KN99 GFP *C. neoformans* at 2 dpf (0 dpi). Fungal burdens for each larva at 0 and 3 dpi are shown. 3 repeats were performed with no less than 11 larvae considered for each condition per repeat. Larvae treated with PBS liposomes are represented by black points and those treated with clodronate liposomes are in red.

a. 3 dpi zebrafish larva treated with PBS liposomes. Cryptococci are shown in green.
b. 3 dpi zebrafish larva treated with clodronate liposomes with the same initial fungal burden as (a) at 0 dpi. Cryptococci are shown in green.
c. Comparison of fungal burdens for individual larvae at 0 and 3 dpi.
d. Comparison of fungal burdens at 0 dpi between larvae treated with PBS or clodronate liposomes (Mann-Whitney test $p = 0.4678$). Each point represents one zebrafish larva. Mean and standard deviation shown.
e. Comparison of fungal burdens at 3 dpi between larvae treated with PBS or clodronate liposomes (Mann-Whitney test $p = 0.0015$). Each point represents one zebrafish larva. Mean and standard deviation shown.
f. Relative fold change of larvae treated with PBS or clodronate liposomes (Mann-Whitney test $p = 0.0019$). Each point represents one zebrafish larva. Mean and standard deviation shown.
g. Descriptive statistics of d-f. N is number of larvae considered, SD represents standard deviation.

5.5 *In silico* modelling

From the results described so far, we know that at high fungal burdens there is a linear relationship between initial fungal burden and infection outcome 3 days later in a zebrafish model of *C. neoformans* infection. However, the outcome is stochastic and variable, with factors besides initial burden contributing to the relationship between burdens. We also know that macrophages help to control fungal growth in this infection model, though clearance of infection is rare over three days. Cryptococci can interact with macrophages in multiple ways, and can evade phagocytosis and killing, or can replicate intracellularly within the macrophage niche (Johnston and May, 2013). As such, I wanted to investigate the role of the macrophage intracellular niche in cryptococcosis and to understand how it contributes to the variable infection outcomes seen *in vivo*. As discussed previously, *in silico* computational simulations can be useful tools to study infection as they allow for the testing of the effects of individual variables on infection dynamics and outcomes. Therefore, I partnered with James Bradford and Dr Rhoda Hawkins (Department of Physics and Astronomy, University of Sheffield) to produce a computational simulation of *in vivo* cryptococcal infection. With the goal of understanding how cryptococcal interactions with host macrophages produce complex infection outcomes *in vivo*, we used my zebrafish infection data to produce a computational model of real life cryptococcal infection. *In vitro* measurements of cryptococcal interactions with macrophages could then be added to the simulation to determine their relative effects on infection outcome.

To simulate the relationship between initial and final fungal burdens, a model was fit to the zebrafish infection dataset in Figure 5.2c. Based on the zebrafish infection data and the estimated doubling time of cryptococci *in vivo*, different combinations of fungal replication and death rates were modelled to produce a spread similar to that seen in my zebrafish infection. This provided a baseline to allow us to test the effect of different variables. I then performed various *in vitro* assays to measure different aspects of *Cryptococcus*-macrophage interactions using a J774 macrophage infection model.

To understand macrophage-*Cryptococcus* interactions I measured the following variables:

1. The viability of KN99 GFP *C. neoformans* cultures
2. The proportion of total cryptococci which were phagocytosed by macrophages
3. The percentage of total macrophages which phagocytosed cryptococci
4. The intracellular proliferation rate of cryptococci
5. The extracellular proliferation rate of cryptococci
6. The proportion of cryptococci which showed exponential growth
7. The proportion of cryptococci which failed to proliferate intracellularly and extracellularly

5.6 The proportion of cryptococci which are phagocytosed is dependent upon infecting inoculum

When performing an infection it is important to think about the microbe's viability, as infecting with cells which are not viable can indicate the presence of a relationship when there is none, or can instead report no correlation when one exists. Therefore, I performed a culture viability assay to determine if the cryptococcal cells used were likely to be viable at the time of infection. To do so, I cultured KN99 GFP *C. neoformans* overnight. After culturing, I washed the cells as I normally would have to perform an infection and plated a volume containing a known number of cells on YPD agar (here, 25 μl containing a calculated 50 cryptococci). After incubating for 48 hours, I counted the number of colonies formed on each plate and calculated the percentage of viable colonies from the number of cryptococci plated. After six repeats containing 29 plates total for each strain, approximately 100% of the cryptococci were shown to be viable, with no difference between the wild-type and GFP-expressing KN99 strains of *C. neoformans* (Figures 5.4a and 5.4b; unpaired t-test $p = 0.6438$). This suggested that at the time of infection, the cryptococci injected were likely to be viable. However, there was some variability in the percentage of viable cryptococci; this was likely due to

counting error. If this was due to differences in viability it was unlikely to affect my assays; in zebrafish infections I counted the number of viable GFP-expressing cells, and I measured the proportion of cryptococci which grew in macrophage infection assays. Therefore, variability in cryptococcal viability in culture should not affect the results.

In the previous chapter I showed that the proportion of macrophages which phagocytosed cryptococci increased linearly with the initial fungal burden in both J774 macrophages and MDMs. However, this does not necessarily reflect the proportion of the cryptococcal culture which is phagocytosed. As this is important to uncover how cryptococcal uptake affects disease outcome, I performed time lapse imaging of J774 macrophage infection with opsonised KN99 GFP *C. neoformans*. After infecting the macrophages for 2 hours and subsequently washing away the extracellular fungi, I counted how many cryptococci were intracellular at 0 hours. To determine how many of the introduced cryptococci were phagocytosed, first the settling rate of the cryptococci in serum free DMEM (media used for J774 time lapse imaging) was calculated (with Jaime Cañedo, Johnston lab). The settling rate represented the number or proportion of cryptococci that sedimented during the allocated 2-hour time frame and therefore had the chance to be phagocytosed. This represents a realistic approximation of the number of cells able to interact with macrophages. I then used this to calculate the percentage of the settled cryptococci which were phagocytosed.

Here, the percentage of cryptococci which were successfully taken up decreased with fungal dose (Figures 5.4c and 5.4e; linear regression $p = 0.3839$). While the percentage of phagocytosed cells decreased, the absolute number of internalised cryptococci increased with initial dose (Figures 5.4d and 5.4e; linear regression $p = 0.0022$, $R^2 = 0.9957$). This reflected the proportion of macrophages within the population which met a fungal cell and were able to phagocytose it; when more cryptococci were present there was a greater likelihood of an activated macrophage encountering a cryptococcal cell, and the number of phagocytosed cryptococci increased.

(page intentionally left blank for figures + legends on following pages)

a.

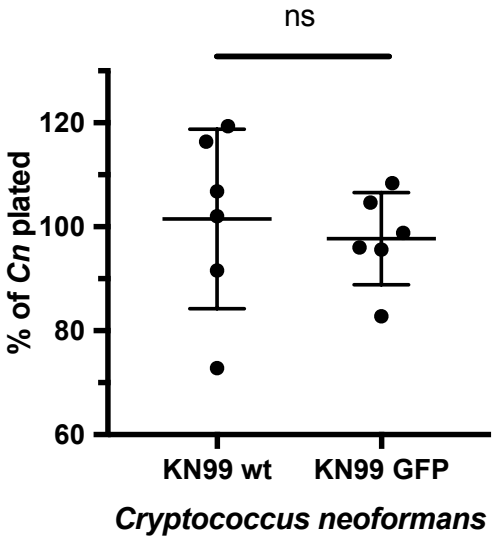

b.

	% *Cn* viable		
Cn	n	Mean	SD
KN99 WT	29	101.5	17.26
KN99 GFP	29	97.71	8.872

c.

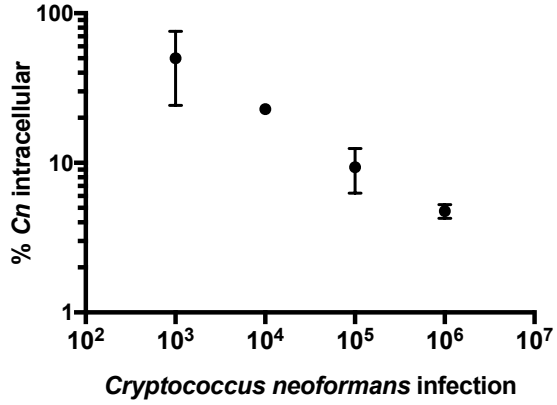

d.

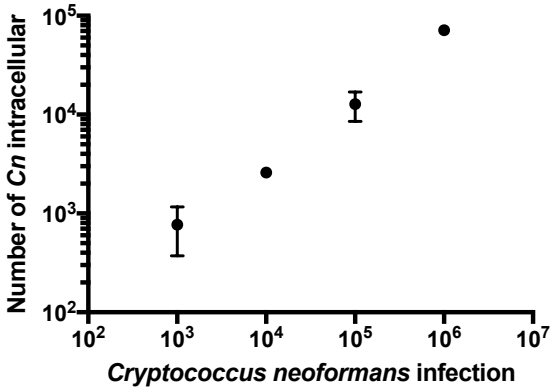

e.

		% Cn phagocytosed		number Cn phagocytosed	
Cn dose	n	Mean	SD	Mean	SD
10^3	8	50	25.81	770	397.5
10^4	9	22.87	1.41	2590	160.4
10^5	9	9.354	3.09	12,740	4211
10^6	9	4.764	0.503	71,400	7534

Figure 5.4. Uptake of cryptococci by macrophages is related to the initial fungal burden

a. The percentage of total plated cryptococci from overnight cultures which produced colonies after 48 hours. 50 cfu were plated on YPD agar and the percentage of the expected number of cryptococci was calculated over 6 repeats. Unpaired t-test p = 0.6438. Mean and standard deviation are shown. Replicates for each repeat were averaged.
b. Descriptive statistics of the percentage of viable cfu plated over 6 repeats.
c. J774 murine macrophages were infected with an increasing dose of KN99 GFP *C. neoformans*. The settling rate of cryptococci was calculated and used to determine what proportion of cryptococci were phagocytosed after 2 hours (the time considered the start of *in vitro* infection throughout). The percentage of phagocytosed cryptococci was not linearly related to initial fungal burden (linear regression p = 0.3839). Mean and standard deviation are shown. 3 repeats with 2-3 replicates per condition were considered. Replicates for each condition were averaged.
d. J774 macrophages were infected with KN99 GFP *C. neoformans* and the number of intracellular cryptococci per well was quantified after 2 hours. There was a linear relationship between initial inoculum and the number of phagocytosed cryptococci (linear regression p = 0.0022, R^2 = 0.9957). Mean and standard deviation are shown. 3 repeats with 2-3 replicates per condition were considered. Replicates for each repeat were averaged.
e. Descriptive statistics of percent and number of cryptococci were phagocytosed.

5.7 Macrophages control infection by reducing the replication rate of intracellular cryptococci

As shown in Figure 5.3, macrophages helped to control cryptococcal infection *in vivo* in zebrafish. However, cryptococci are able to replicate within macrophages, complicating the macrophage-*Cryptococcus* relationship. Cryptococci also replicate extracellularly and may escape the host macrophage to do so. Therefore, to gain a deeper understanding into the variation in macrophage-*Cryptococcus* interactions, I quantified replication rates of individual cryptococci inside and outside of J774 macrophages. To do this, I performed 24 hour time lapse imaging of J774 macrophage infection with 10^5 KN99 GFP *C. neoformans*, as this fungal dose produced a sufficiently high number of intracellular cryptococci without excessive extracellular growth. Here, I followed individual intracellular and extracellular cryptococci throughout the course of infection and quantified the replication of fungal cells when budding occurred. I also quantified the doubling times of cryptococci which were previously intracellular but had been vomocytosed from the macrophages. Doubling time was calculated assuming non-linear, exponential growth.

Comparing the growth curves of intracellular and extracellular cryptococci, the cryptococci that were extracellular showed faster growth, with those which were intracellular showing a more gradual increase in numbers (Figures 5.5a and 5.5b). Cryptococci which escaped from J774 macrophages similarly displayed exponential growth, except those which had vomocytosed late in infection and therefore had little time to replicate (Figure 5.5c). The slower growth of intracellular cryptococci was further confirmed when comparing doubling times; indeed, the mean intracellular doubling time of *Cryptococcus* was 12.76 hours, compared to 5.21 and 5.02 hours for extracellular and vomocytosed cryptococci, respectively (Figures 5.5d and 5.5e, one-way ANOVA $p = 0.0006$, pairwise comparison $p < 0.0001$ when comparing intracellular doubling time to that of extracellular, vomocytosed, and KN99 alone in culture). These results suggest that macrophages controlled intracellular replication, though replication was not completely halted.

Furthermore, comparing extracellular and vomocytosed doubling times to those of individual cryptococci alone in media (in the absence of macrophages) revealed that there was no difference in doubling time between these conditions, suggesting that macrophage extracellular factors did not help to control extracellular fungal growth in these conditions (one-way ANOVA p = 0.896 and 0.937 for extracellular and vomocytosed cryptococci compared to *Cryptococcus* in media alone, respectively).

Finally, because there is the possibility for heterogeneity in microbial populations, even from individual cultures, it is important to consider the differences in growth potential. One measure of this is the standard deviation of the doubling times of individual microbial cells. However, it is also useful to know what proportion of the fungal population fails to replicate, and what proportion are less successful at exponential growth. To quantify this, I set a threshold for minimal degree of exponential growth ($R^2 < 0.7$). Cryptococci whose growth curves fell below this threshold either failed to replicate, or replicated at a rate so slowly that the growth curves appeared to be flat rather than exponential. Of 118 intracellular cryptococci, only 19 showed growth below the exponential cut-off (16.1%). Of the 83 extracellular cryptococci followed, 77 showed sufficiently high growth rates (7.2% below exponential growth threshold). As a final measure of cryptococcal viability, I quantified the proportion of cryptococci which failed to replicate in the allotted 24 hours. Of 151 cryptococci followed in the presence of J774 macrophages, only 3 failed to replicate (1.99%), suggesting that ~2% of cryptococci were dead or in a quiescent, non-replicating state for the duration of the time lapse. Collectively, these results provide evidence about cryptococcal growth in the presence of macrophages, and illustrate variability in growth which may affect *Cryptococcus* interactions with macrophages.

a.

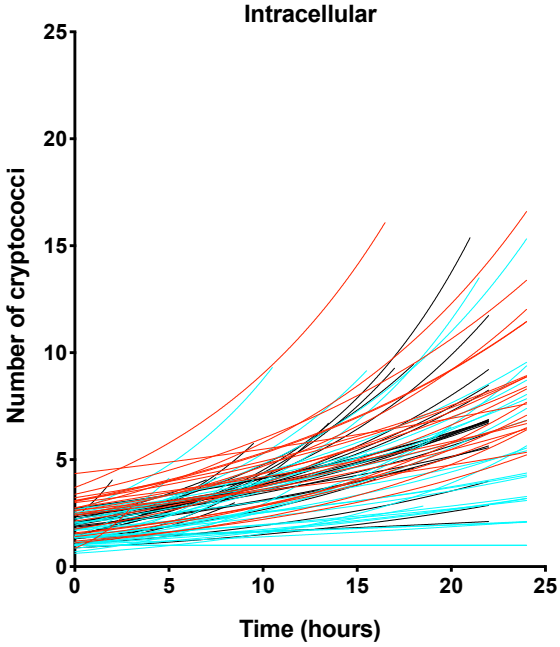

b.

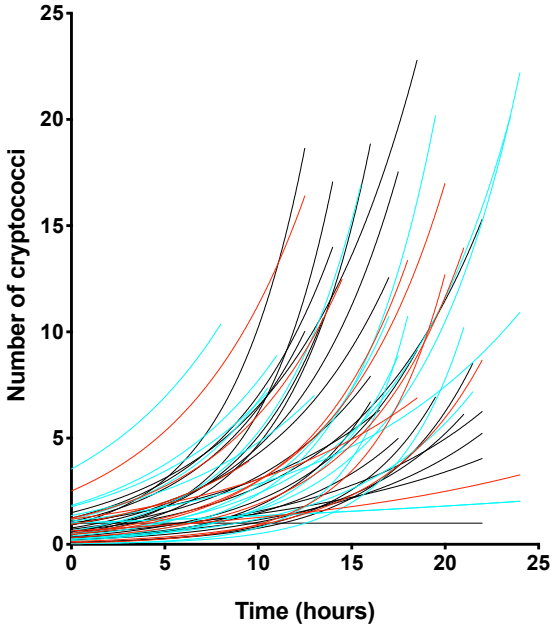

c.

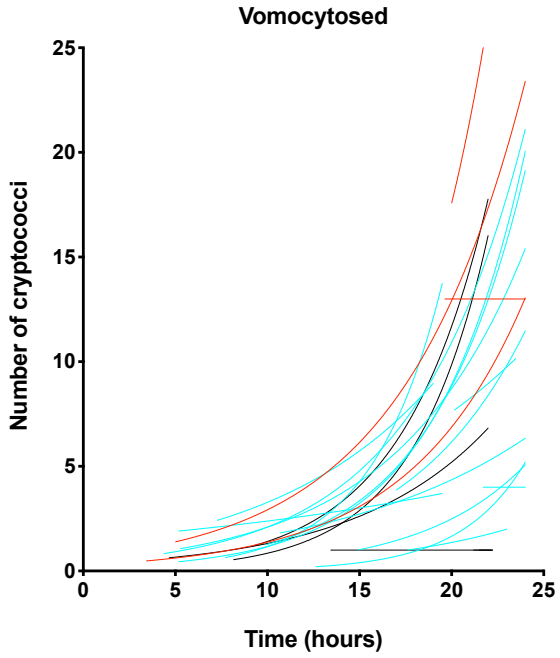

d.

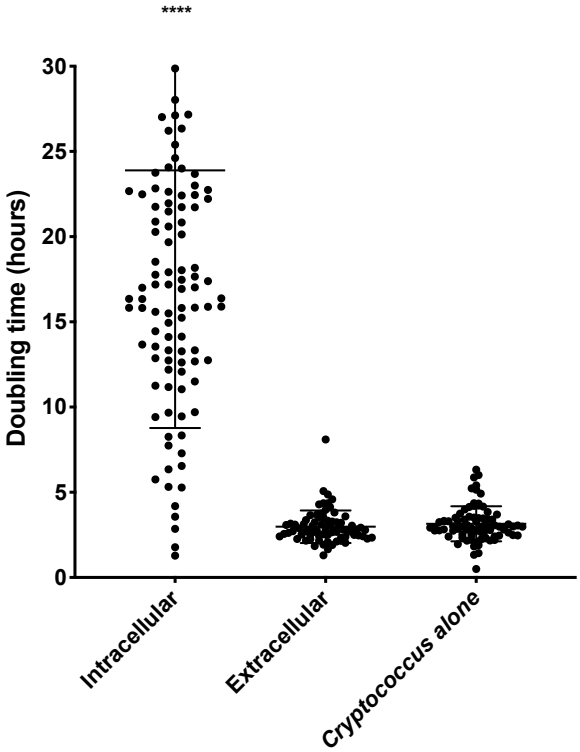

e.

Cryptococci	Doubling time		
	n	Mean	SD
Intracellular	83	12.76	7.11
Extracellular	67	5.21	4.11
Vomocytosed	19	5.02	2.86
Cryptococcus alone	83	5.88	6.04

Figure 5.5. Growth of intracellular, extracellular, and vomocytosed cryptococci during J774 macrophage infection

J774 murine macrophages were infected with 10^5 KN99 GFP for 2 hours, extracellular cryptococci were washed off, and infection was followed for 24 hours using time lapse imaging. Phase x20 imaging was used to take an image every 2 minutes. Replication of individual cryptococci was followed in time.

a. Intracellular proliferation of KN99 GFP within J774 macrophages during 24 hours of infection. Colours represent different donors.
b. Proliferation of cryptococci which were extracellular during J774 macrophage infection over 24 hours. Colours represent different donors.
c. Replication of cryptococci which were vomocytosed from J774 macrophages. Colours represent different donors.
d. Doubling time of cryptococci which were intracellular, extracellular, vomocytosed, or in media alone without J774 macrophages. Each point represents the doubling time of an individual starting *Cryptococcus* cell. Mean and standard deviation are shown, with 3 repeats represented. One-way ANOVA $p = 0.0006$; multiple comparisons $p < 0.0001$ when comparing intracellular doubling time to each of the other conditions.
e. Descriptive statistics of growth rates over three repeats.

5.8 Human MDMs control cryptococcal infection by inhibiting intracellular fungal growth

With the ultimate goal of applying this data and the resulting simulation to human cryptococcosis infection, and using it to understand how the interactions between *C. neoformans* and macrophages produce variable infection outcomes, I performed the same assays as above using human monocyte derived macrophages. As shown in chapter 4, both of these macrophage cell types respond to cryptococcal infection in a very comparable manner, showing similar relationships in uptake and control of fungal replication. I therefore wanted to know if human MDMs controlled cryptococcal replication in the same way as J774 macrophages. To test this, I infected human MDMs with opsonised KN99 GFP *C. neoformans*, and after allowing 2 hours for infection and washing away extracellular cryptococci, I followed the replication of the cryptococci over 24 hours using time lapse imaging to take an image every 2 minutes. I quantified doubling time by following individual cryptococci and noting when a budding event occurred, producing exponential growth curves for individual cells (Figure 5.6a). For comparison, I also followed individual cryptococci which were extracellular outside of MDMs (Figure 5.6b), and quantified growth of individual cryptococci in media alone.

Human MDMs potently inhibited the growth of intracellular cryptococci, with a mean doubling time of 23.89 hours for the 113 followed cryptococci (Figures 5.7a, 5.7c, and 5.7d). This was considerably longer than the doubling times for cryptococci which were extracellular (2.98 hours) and in media alone (3.15 hours) (Figures 5.7b, 5.7c, and 5.7d; one-way ANOVA $p < 0.0001$ comparing intracellular doubling times to the doubling times of extracellular cryptococci and *Cryptococcus* in media alone). This suggests that MDMs strongly reduced the rate of intracellular cryptococcal replication. Furthermore, because there was no significant difference in the doubling time of cryptococci which were extracellular compared to those that were in media alone, it was not likely that MDMs secreted extracellular antimicrobial effector molecules to inhibit cryptococcal growth in this system. These results showed that while comparable in many respects, the restriction of intracellular

growth of cryptococci was stronger by human MDMs than by J774 macrophages, and should therefore be appropriately modified in the computational simulation to reflect human infection.

a.

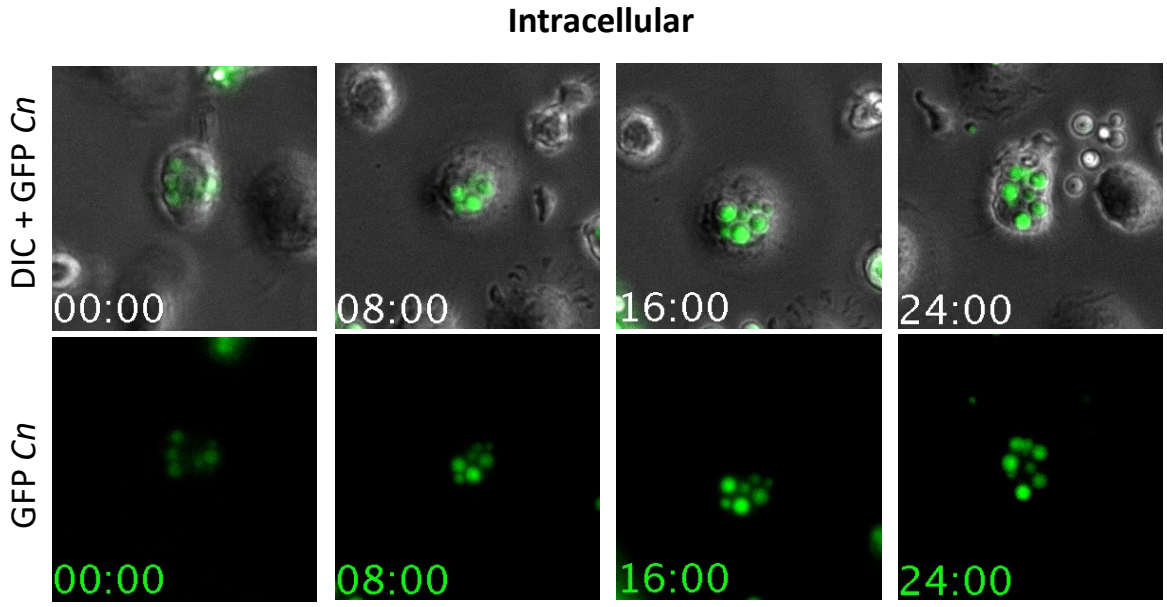

b.

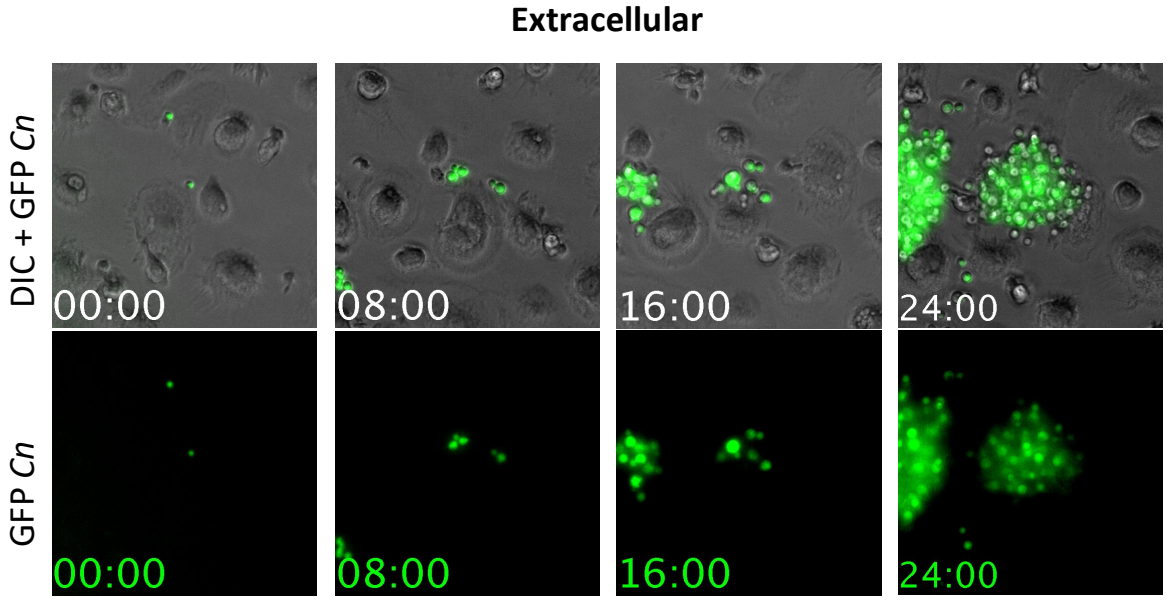

Figure 5.6. Intracellular *C. neoformans* replicated more slowly within human MDMs compared to extracellular cryptococci

To quantify the replication rates of cryptococci I infected human MDMs with KN99 GFP *C. neoformans* and performed time lapse imaging over 24 hours. I followed individual cryptococci and measured when they divided. Intracellular (a) and extracellular (b) cryptococci are shown. Cryptococci are in green and time is represented as hours : minutes.

(page intentionally left blank for figures + legends on following pages)

a.

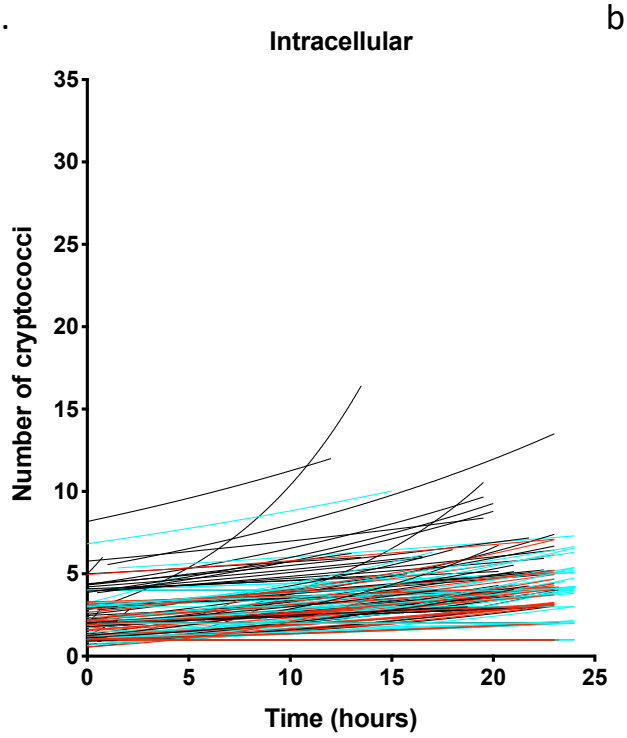

b.

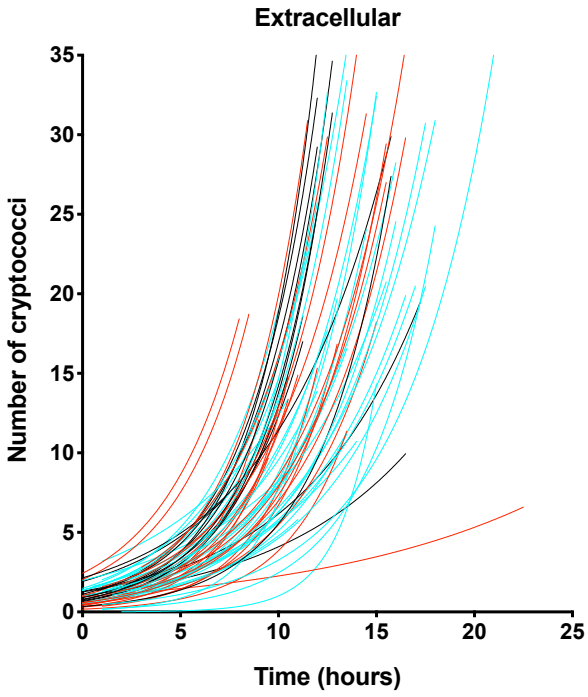

c.

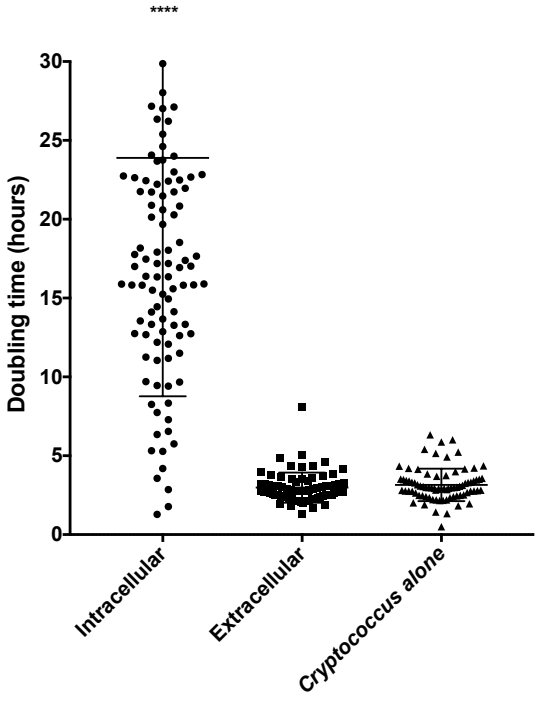

d.

Cryptococci	Doubling time		
	n	Mean	SD
Intracellular	113	23.89	15.12
Extracellular	75	2.978	0.954
Cryptococcus alone	79	3.15	1.032

Figure 5.7. Human monocyte derived macrophages controlled intracellular proliferation

Human MDMs were infected with KN99 GFP *C. neoformans* for 2 hours, extracellular cryptococci were washed away, and infection was followed for 24 hours using time lapse imaging with an image taken every 2 minutes. 10^5 macrophages were infected with 10^3-10^6 KN99 GFP *C. neoformans*. Replication of cryptococci was quantified by the formation of buds, and because there was no significant difference in doubling times within conditions between doses they are pooled together here (see previous chapter figures 4.4 and 4.6). 3 repeats are shown, with no fewer than 3 cells followed per dose in each repeat.

a. Growth of intracellular cryptococci within MDMs over 24 hours of infection. Each line is an individual fungal cell or small starting group of fungal cells, likely mother-daughter cells. Colours represent different donors.
b. Growth of cryptococci extracellularly in the presence of MDMs over 24 hours. Each line is an individual fungal cell or small starting group of fungal cells, likely mother-daughter cells. Colours represent different donors.
c. Doubling times of individual cryptococci which were intracellular, extracellular, or in media alone without macrophages. Each point represents one fungal cell. Mean and standard deviation shown. One-way ANOVA $p < 0.0001$ comparing the doubling time of intracellular cryptococci compared to those which were extracellular and in media alone.
d. Descriptive statistics comparing doubling times of cryptococci which were intracellular, extracellular, and in media alone. Three repeats are shown.

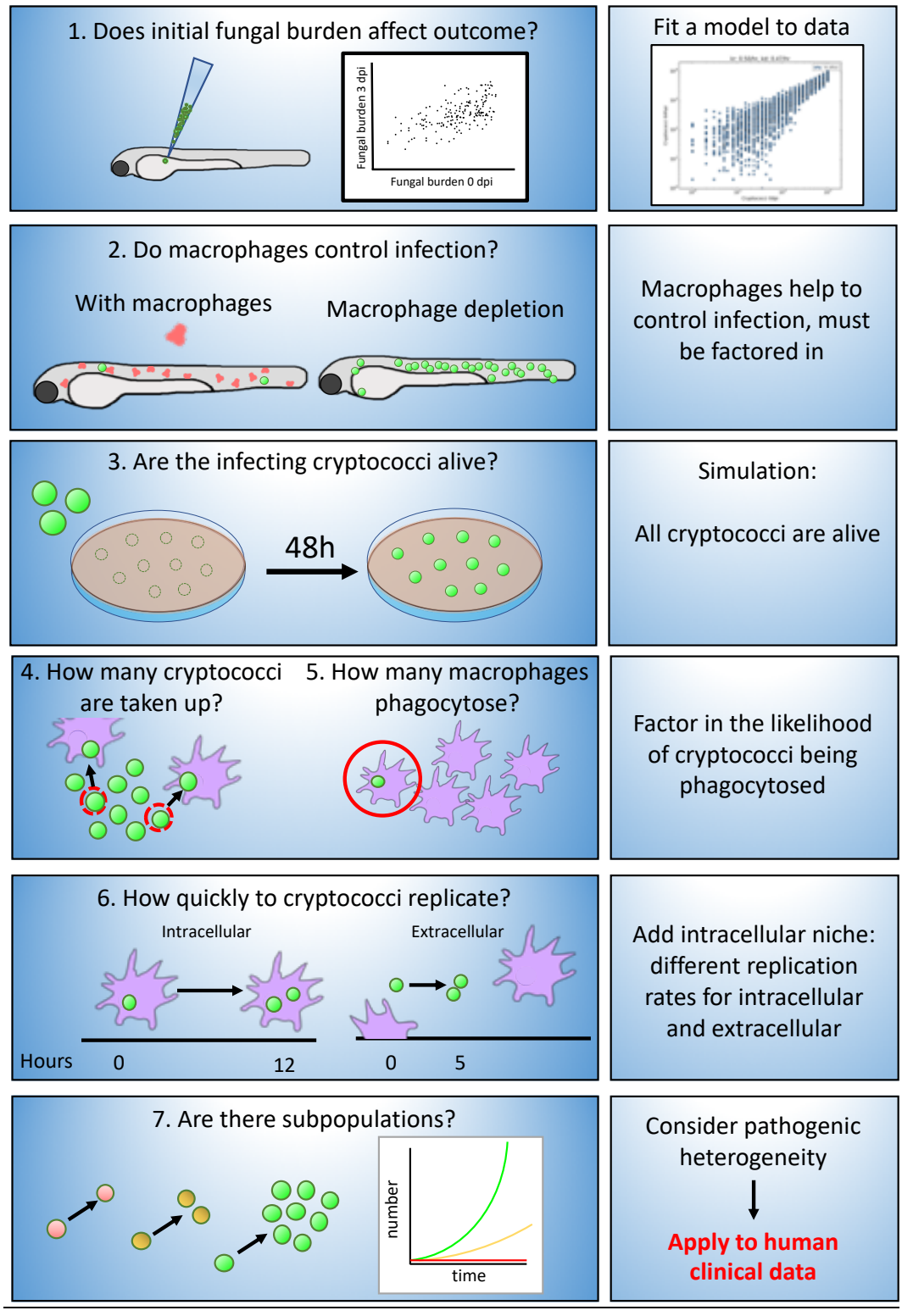

Figure 5.8. Building a computational simulation of *in vivo* cryptococcal infection

To build a computational simulation of cryptococcal infection, different *in vivo* and *in vitro* assays were performed to address questions about how macrophages and cryptococci interact to produce different infection outcomes. Data was added to the simulation in a step-wise manner.

5.9 Discussion

Host-pathogen interactions are complex because both the host and the pathogen mount strategies to prevail over the other. Host immune cells phagocytose and attempt to destroy pathogens, recruit additional effector cells, produce reactive species and destructive peptides, release granules, and even self-destruct to destroy invading pathogens within. Pathogens subvert immune responses, form barriers between themselves and host receptors, inject a milieu of effectors into target cells to produce a favourable environment, modulate host immune response, and even manipulate host cells to divide and spread. With moves and counter-moves producing a complex set of interactions, a vast spectrum of host-pathogen outcomes is possible. This is made even more complex by the heterogeneity that exists within host and pathogen populations and between cells, meaning that each host-pathogen interaction is an individual event that could have one of any number of consequences. As such, understanding the range of possible outcomes that may result from individual encounters is important in determining what drives complex, variable infection outcomes.

Pathogenic microbes can commonly occupy a number of different niches and may reside extracellularly, intracellularly within host cells, or may go through phases of both. This adds to the complexity of infection dynamics, and understanding variability in infection outcomes is made all the more challenging when considering the heterogeneity that exists both within the invading microbial population and in the host response to infection. Many studies focus on how heterogeneity in host immune activation state and response contributes to the array of infection outcomes observed. While this is certainly a contributing factor, a growing body of evidence shows that pathogenic heterogeneity in phenotype and virulence must be taken into account in order to fully understand the true nature of host-pathogen interactions, and how these interactions determine infection progression and outcome (Avraham and Hung, 2016). *Cryptococcus neoformans* is a facultative intracellular pathogen which can manipulate host macrophages to disseminate infection. Though interactions between macrophages and cryptococci are crucial in

determining infection dynamics, the variability in these fateful encounters remains largely unstudied, especially when considering cryptococcal growth rates. A 2014 study by Jarvis et al. demonstrated that CSF fungal burden correlated with mortality in human HIV-positive cryptococcal meningitis patients, but with a great degree of variability in infection outcomes based on initial burden (Jarvis et al., 2014). The aim of this chapter was to gain understanding into the role macrophages play in producing variable infection outcomes in cryptococcosis.

To discover if initial fungal burden was related to the outcome of infection, I used a well-described zebrafish model of cryptococcal infection (Bojarczuk et al., 2016; Tenor et al., 2015). Using zebrafish to model cryptococcal infection allowed me to follow of hundreds of individual infections and compare initial fungal burden to infection outcome three days later in separate fish. During the times tested in the *in vivo* assays, the zebrafish larvae possessed macrophages capable of phagocytosis in the absence of an adaptive immune response, allowing me to examine the specific role of macrophages during infection (Bojarczuk et al., 2016; Herbomel et al., 1999; Lam et al., 2004). In comparing fungal burdens at 0 and 3 days post infection, we used a computational simulation of *in vivo C. neoformans* infection with to examine host-pathogen interactions in cryptococcosis (Figure 5.8). Using macrophage depletion assays coupled with *in vitro* examination of cryptococcal growth in the presence of macrophages, I measured how interactions between cryptococci and macrophages contributed to variable infection outcomes, and used the data collected to inform the computational simulation to better understand the role of macrophages in contributing to the complex infection outcomes seen during cryptococcosis.

5.9.1 The relationship between infection burden and outcome *in vivo*

Evidence suggests that *Cryptococcus* infection occurs via the inhalation of few spores or desiccated yeast cells (Velagapudi et al., 2009). However, no studies have investigated if this low number of cryptococcal cells determines the course of infection, and thus how infection may potentially be caused by the germination of

a single cryptococcal cell. Indeed, most studies into the pathogenesis of *C. neoformans* report starting infections of 10^5 fungal cells (Giles et al., 2009), though it been reported that as few as 5 H99 *C. neoformans* cells are required to induce murine infection if injected intravenously (Ngamskulrungroj et al., 2012). In investigating cryptococcal infection dynamics with a starting fungal burden of less than 10 cryptococcal cells, I simulated the early stage of infection that is crucial in determining whether the host controls the infection, or ultimately whether the pathogen gains a foothold to instigate infection. At each initial infection 'dose', or starting number of cryptococcal cells, larvae showed a variety of infection outcomes; fungal burden at each dose increased, decreased, or remained the same after 3 days of infection. This suggests that at such low initial fungal burdens the outcome of infection is stochastic, with only a weak linear correlation between initial and final fungal burden. In general, there was an increase in fungal burden, consistent with previous reports comparing burdens at an earlier timepoint (Bojarczuk et al., 2016). While the mean infection burden generally increased with starting dose, the outcome of infection was largely stochastic and likely involved stochastic interactions between the host and the invading pathogen.

The onset of real-life infections are difficult to study because observation often does not start at the immediate introduction of a pathogen to a system, and thus determining the infective dose required to initiate infection cannot be reliably determined. In addition, most rodent models do not allow continuous monitoring of pathogen burden, preventing study of pathogen population dynamics over the course of infection. In the cryptococcal infections described, while the initial number of cryptococci and the final infection burden produced stochastic outcomes at such low doses of infection, this data illustrated what is likely to be true in actual infections; that infections can be instigated by one or a few pathogenic cells, and sometimes the body clears them while other times it fails to do so, producing a spectrum of infection possibilities that varies between patients or, in this case, zebrafish larvae. Studies into *S. aureus* infection have demonstrated that one or few bacteria survive a population bottleneck to clonally expand and produce lesions, and that the chance of a bacterium within the infecting population leading

to propagation of infection or clearance was apparently random (Grant et al., 2008; Prajsnar et al., 2012). Thus, pathogenicity of individual pathogenic cells may be important for the propagation of infection, though in my cryptococcal infections of zebrafish larvae the outcome was stochastic.

While there was no strong linear relationship between initial and final fungal burdens at minimal starting doses, a linear relationship emerged when zebrafish were infected with higher number of cryptococci. Because this high dose of fungal burden is unlikely to be the infecting dose at the onset of cryptococcal infection, but rather is more representative of fungal burden later in infection, the linear regression here suggested that the 'initial' fungal burden affected the outcome after 3 days – but at a later stage of infection. While this level of infection may not represent the onset of infection, patients are often diagnosed and treated after some phase of initial infection. The results here are relevant to such cases. A previous report by our lab showed that zebrafish infection with a similar dose of H99 *C. neoformans* produced a linear relationship between initial fungal burden and fungal burden at 24 hpi, with most cryptococci phagocytosed by this time (Bojarczuk et al., 2016). I achieved a similar outcome, though I followed the infection for an additional 2 days. However, while a linear relationship was produced between fungal burden at 0 and 3 dpi, the low R^2 value suggested that additional factors beyond initial fungal dose impact burden three days later. Factors which may contribute to this include intervention by host immune cells and exploitation by the pathogen, as discussed throughout. Nonetheless, the variability in infection outcome reflects that seen in human cryptococcal infection (Jarvis et al., 2014), verifying the use of the zebrafish host to model cryptococcal infection.

5.9.2 Macrophage control of replication

As discussed throughout the introduction, and reviewed widely in the field (Gibson and Johnston, 2015; Johnston and May, 2013; Mansour et al., 2014; McQuiston and Williamson, 2012; Voelz and May, 2010), *Cryptococcus neoformans* interacts with host macrophages in a variety of ways, either resisting phagocytosis, becoming

engulfed and killed, replicating within the macrophage intracellular niche, or escaping from the macrophage to propagate infection extracellularly. My aim was to quantify the phagocytosis of cryptococci and the rates of fungal replication to be able to understand not only how macrophages contributed to control of cryptococcal infection, but to use this quantification to illuminate the heterogeneity that exists both within the cryptococcal population and within the macrophage control of fungal replication. As shown previously, macrophages are essential for early control of cryptococcal infection in the zebrafish model of infection (Bojarczuk et al., 2016). In my experiments, using clodronate liposomes to deplete macrophages resulted in an increase in fungal burden after 3 days compared to zebrafish larvae treated with vehicle control liposomes; in fact, the depletion of macrophages resulted in a five-fold increase in fungal burden. Therefore, in the zebrafish model of *in vivo* infection, macrophages helped control cryptococcal infection, though they did not manage to completely halt fungal replication or clear infection over the time and fungal doses considered here.

After analysing the *in vivo* infection, we constructed a computational simulation of cryptococcal infection. *In silico* models are useful for the dissection of contributions of individual variables to infection dynamics. Our simulation was built in a stepwise manner and was initially fit to the zebrafish model by considering only cryptococcal death and replication rates. These rates are difficult to determine *in vivo*, with few studies having any success. As such, we provided a doubling time based on a known maximal cryptococcal replication rate and determined the theoretical death rate of cryptococci by fitting the simulation to the data points provided from the high range zebrafish infection assay described above. This provided a framework for the addition of further quantified variables. Infection of zebrafish in the absence of macrophages proved that macrophages did help to control cryptococcal infection, and therefore needed to be included in the simulation. However, quantifying replication of intracellular and extracellular cryptococci is difficult even in the zebrafish host because replication events are seen too rarely *in vivo* to obtain statistical significance, particularly with the imaging restraints that come with capturing *in vivo* infection. Therefore, I used a well-established J774 macrophage

model of *in vitro* cryptococcal infection to quantify cryptococcal growth and build upon the simulation (Ma et al., 2009).

To begin I quantified the proportion of the total cryptococci which were phagocytosed by macrophages. As the number of infecting cryptococci increased, the *percentage* of internalised cryptococci decreased, suggesting that increasing fungal burden somehow decreased uptake. However, because macrophages do not become overwhelmed in the conditions tested here (see previous chapter – percentage of infected macrophages increases linearly with dose), it is likely that some effect of the cryptococci hindered phagocytosis at higher doses. For example, when many cryptococci are used for infection often they may clump together due to the high concentration, making it more difficult for macrophages to engulf them. Furthermore, the *number* of phagocytosed cryptococci increased with infection burden. Here, the number of macrophages remained constant while the fungal infection increased, suggesting that the likelihood of a fungal cell being phagocytosed increased as the likelihood of meeting a macrophage increased. Thus, fungal uptake was again related to initial inoculum and macrophage density, though not all cryptococci were phagocytosed, and not all macrophages engulfed the pathogen.

While the macrophage intracellular niche may act as a safe haven for cryptococci to exist and replicate away from the harsh extracellular environment, during both J774 macrophage and human MDM infection intracellular cryptococci divided more slowly than those which were extracellular. This suggests that macrophages controlled the intracellular proliferation of cryptococci, or alternatively that the cryptococci slowed proliferation within the macrophage intracellular niche on purpose. This phenomenon has been seen during *Salmonella* infection, where a small subpopulation of *Salmonella* halted replication while intracellular in order to survive the initial immune response, enabling the reactivation of division later when the immune response to infection had subsided (Helaine et al., 2014).

A study by Feldmesser et al. compared the budding of yeast which were intracellular and extracellular in infected mouse lung slices, and found that the budding index of intracellular cryptococci was higher than that of extracellular cryptococci (Feldmesser et al., 2000). However, while useful, the budding index does not directly correlate with the doubling time of cryptococcal cells. In fact, if cryptococci divided more slowly you might expect the presence of budding cells to persist, thus increasing the likelihood of being included in the budding index, compared to budding yeasts which successfully detach more quickly in cells which replicate faster. Furthermore, reports have shown that while most cryptococci reside within macrophages after 2-8 hours of infection, after 24 hours more cryptococci exist outside of host cells than within them (Feldmesser et al., 2000; Voelz et al., 2009). This potentially suggests that cryptococci divided quickly outside of macrophages; however, Feldmesser showed that cryptococci can induce cytotoxic effects in host macrophages, causing them to rupture and expel intracellular cryptococcal cells (Feldmesser et al., 2000). Here, it was reasoned that because cellular debris was found in proximity to yeast cells that the fungi must have replicated and lysed the host cells, enabling the escape of the cryptococci to the extracellular environment. However, fungal replication was not quantified, and conclusions based on the presence of cellular debris do not prove the enhanced growth of intracellular cryptococci. Indeed, cryptococci may have exited the cell and continued expedient growth extracellularly.

Similarly, Voelz and colleagues (2009) suggested that more cryptococci were extracellular than intracellular at 24 h due to host cell lysis. However, macrophage levels in this study remained relatively constant despite fungal growth. Excessive extracellular proliferation coupled with vomocytosis of cryptococci to proliferate extracellularly would also produce the same result. While this study relied on haemocytometer counting of cryptococci, I followed individual cryptococci for 24 h using time lapse imaging and manually counted each division as it occurred. In both J774 macrophages and human MDMs extracellular proliferation was significantly faster than intracellular proliferation, showing for the first time the actual growth rates of cryptococci in the presence of macrophages *in vitro*.

5.9.3 Heterogeneity in pathogen phenotype and immune response

Variation within the pathogenic population is a driver of infection variability. While some microbial cells respond to population cues which drive alternative cellular activity states (Snijder et al., 2009), some alter the expression of intracellular virulence factors which alter host immune cell activation and drive heterogeneous macrophage responses (Avraham et al., 2015). *Salmonella* divides at different rates depending on the type of host cell it occupies and the location of the bacteria within these cells (Knodler et al., 2017). The mere existence of different host niches provides different infection environments, and the ability of pathogens to exploit these different environments may enhance survival of the population as a whole when compared to pathogens with limited adaptations and abilities to thrive in varied environments. This inherently instils the potential for variable host-pathogen interactions and infection outcomes.

For instance, because *Cryptococcus neoformans* is a facultative intracellular pathogen the different growth rates of cryptococci which are intracellular and extracellular must be considered, as these varied environments induce different behaviours which could differentially affect the course and outcome of infection. From the time lapse proliferation assays, I quantified the doubling times of the intracellular and extracellular cryptococci during exponential growth. Following the growth of individual cells illustrated the range of potential growth rates exhibited by the intracellular and extracellular cryptococci, providing a measure of growth heterogeneity within the cryptococcal population. This, combined with the quantification of the proportion of cryptococci which were intracellular and extracellular, provided evidence for the existence of discrete populations of cryptococci with distinct growth rates *in vitro*. These data were incorporated into the computational simulation by including two subpopulations of cryptococci – those intracellular and those extracellular, each with their own growth rates (Figure 5.8). After altering replication times for the different subpopulations of cryptococci the death rate of the fungal cells was held constant, as killing of cryptococci was not

witnessed in any of the repeats and assays performed. This is in line with previous *in vitro Cryptococcus* infections where killing by macrophages was not observed, though killing may have been obscured by fungal growth (Levitz and Farrell, 1990). This also enabled us to consider the effect of individual variables on the distribution of disease outcomes, such as the effect of transitioning between states and niches.

Additionally, quantifying the proportion of intracellular and extracellular cryptococci which failed to grow produced a further measure of pathogenic heterogeneity, illustrating that not all cryptococci are in an actively dividing state. While this population of non-dividing cryptococci was very small and showed that most cryptococci were viable at the time of infection, it still provided some evidence of a subpopulation of cryptococci which existed within the whole population of actively replicating fungal cells. Of course, the failure of these cryptococci to proliferate intracellularly may not have meant that they were dead; rather, they may have adopted a dormant state of survival. In a similar fashion, *Salmonella* displays pathogenic heterogeneity, with a small proportion of the bacteria entering a non-replicating state within murine BMMs, maintaining a metabolically active state while resisting antibiotic treatment (Helaine et al., 2014). This was a proposed adaptation to host defences, enabling the persistent bacteria to survive without replicating within the harsh environment of the acidic phagosome while the pro-inflammatory phase of infection continued and eventually subsided outside (Helaine et al., 2014). Here, pathogenic heterogeneity enabled the survival of a subpopulation of bacteria, illustrating the importance of individualistic phenotypes in long-term infection. *Cryptococcus* can cause latent infection with the reactivation of dormant cryptococci after extended periods of sub-clinical infection (Garcia-Hermoso et al., 1999; Goldman et al., 2000). Therefore, it is important to consider the existence of different living states of cryptococci. In considering these different phenotypes, we were able to include these further subpopulations into the computational simulation, with the goal of using the simulation to understand more about how diverse cryptococci interact with host macrophages during infection.

The distribution of heterogeneous subpopulations and the growth of various phenotypes within the host in time are factors which also must be considered. A study by Grant and colleagues used a murine model of acute *Salmonella enterica* Typhimurium infection to investigate the spatio-temporal distribution of bacteria throughout the host during infection. Using 'wildtype isogenic tagged strains' (WITS) of genetically identical bacteria, this study quantified death and replication rates of subpopulations at different phases of infection, and showed that some WITS randomly survived to replicate while others were killed soon after infection. The probability of a WITS-derived population surviving or diminishing was apparently random. The first 24 hours of infection were characterised by local colonisation and limited mixing of populations, representing independent infections, while later infection included mixing of populations and systemic dissemination (Grant et al., 2008). In our computational simulation of cryptococcal *in vivo* infection, a stochastic component representing the probability of different phenotypes thriving over others must be included. A previous study from our lab used cryptococci expressing different fluorescence proteins to illustrate the clonal expansion of cryptococcal subpopulations in the zebrafish larva model of infection (Gibson et al., 2017). Adaptation of this technique to observe the colonisation and dissemination of different subpopulations may provide some explanation into the stochastic outcome of cryptococcal infection at low initial infection doses, representative of early cryptococcal infection.

As in other infections, there is considerable variability in host response to cryptococcal infection. For example, a study by Jarvis et al. showed that host immune cytokine profile affected the outcome of HIV-associated cryptococcal meningitis (Jarvis et al., 2015). Using principal component analysis, high levels of CSF pro-inflammatory cytokines correlated with increased clearance of fungi from the CSF. Because patients had variable cytokine profiles, responses to cryptococcal infection were heterogeneous along a spectrum of potential burdens and outcomes, illustrating that host variability produced complex responses to infection. Interestingly, Garelnabi et al. showed that donor-to-donor variation in MDM control of cryptococcal infection did not produce differences in intracellular proliferation

rate of cryptococci *in vitro*; however, repeated measurements of individual donor MDMs produced variable responses based on seasonality, suggesting that yet unknown environmental variables contribute to complex responses to cryptococci in individual donors (Garelnabi et al., 2018). Variable outcomes of C57BL/6J mice infected with *H. pylori* and influenza A virus have been attributed to subtle genetic and biological difference among inbred mice thought to be genetically identical, suggesting host individuality rather than infection stochasticity can drive disparate infection outcomes (Martin et al., 2012). Such heterogeneity is also observed in the development of murine subpopulations which display different abilities to resist colitis and transmit bacteria in faeces from *Salmonella enterica* serovar Typhimurium infections, based on intestinal microbiota composition (Lawley et al., 2008). There is variation within host immune cell populations which may contribute to the variability in immune response. Analysis of many individual murine bone marrow-derived dendritic cells showed differences in inflammatory cytokine expression profiles amongst cells, and that expression changed temporally and was dependent on the initial paracrine signalling by few precocious cells – though what activated these early responders was not clarified (Shalek et al., 2014). While a single cell may not necessarily drive the direction of the infection enough to influence the entirety of the outcome, if enough heterogeneity exists in the host immune response it can lead to disparate outcomes of varying magnitudes. Thus, host heterogeneity is important in a variety of infections.

With the ultimate goal of determining how macrophages contribute to complex, variable outcomes of *Cryptococcus neoformans* infection, I quantified some sources of variability in macrophage-*Cryptococcus* interactions *in vitro*. In counting macrophages which phagocytosed cryptococci I identified the proportion of macrophages which were capable phagocytosis, and also quantified the variation in this measurement. While there is variation in how the macrophages may respond, analysing the proportion which are capable of responding to infection via phagocytosis provides insight into the heterogeneity in this initial host-pathogen interaction which can lead to control or propagation of fungal infection. In the computational simulation we produced, the variability in the macrophage response

was addressed by providing a range of phagocytosis capabilities. Variation in host response can also be represented through varying the intracellular replication rate of the cryptococci, since this can be seen as the variation in the macrophage permissiveness to intracellular replication.

5.9.4 Conclusions and Future work

While the experiments performed throughout this chapter have shown that macrophages help to control cryptococcal infection, and part of how they do this may be through limiting the intracellular replication of phagocytosed cryptococci, the cryptococci were only followed for 24 hours. While this provides a good measure of the replication during the exponential phase of growth, it does not consider the stationary growth phase where the pathogen reaches capacity and the number of cryptococci plateaus (Almeida et al., 2017), or when the level of intracellular cryptococcal infection meets the spatial and nutritional limitations imposed by the macrophage intracellular niche. It is difficult to quantify cryptococcal growth for longer than 24 hours *in vitro* by manually counting because after this time the number of extracellular cryptococci becomes overwhelming, making it difficult to reliably quantify growth of individual cells. While quantifying the growth of the population as a whole is one potential solution to this, grouping all microbes together to quantify replication obscures the heterogeneity within the fungal population and between phagocytes. Also, during the *in vivo* zebrafish infection the maximum number of detectable GFP+ pixels was around $10^{4.}$ This suggests that after this level of infection the larvae may die, or alternatively that fungal replication increases to this level then slows. This may be due to factors such as spatial restrictions and maximum carrying capacity in the small living host, and may illustrate that the maximum level of infection has been reached and that all possible infection locations have been infected to capacity. This threshold may also represent nutrient availability, and may fail to omit the temporary retention of GFP signal of cryptococci which had recently died. Regardless, exponential growth does not continue indefinitely in infection systems, and as such the computational simulation must account for the changes in replication rate throughout the

infection. Similarly, the re-activation of cryptococcal growth after potential dormancy in the environment or after introduction into the host should be studied and included in the simulation. While cryptococcal replication is seen as soon as 2 hours *in vitro*, daughter cells are not observed in the mouse lung until 15 hours of infection (Alanio et al., 2015).

Another consideration which the experiments I performed failed to address is the acquisition of diverse phenotypes after the initial onset of infection. Microbial phenotypic diversity can be observed during human infection, especially when infections are chronic and have been treated therapeutically (Darch et al., 2014; Lee et al., 2017). Phenotypic switching by pathogens enables microbes to adapt to assorted, hostile environments and to produce varied phenotypes to enhance the probability of survival should conditions suddenly change (Tadrowski et al., 2018). Cryptococci exist in metabolically diverse states within the host, and these different phenotypes must also be included in the computational simulation, with special implications for cryptococcal dormancy, granuloma formation, and reactivation after latent infection (Alanio et al., 2015). Fries et al. showed that cryptococci switched phenotype *in vivo* from smooth to mucoid, and the possibility of generating this phenotype during *in vitro* culture should be explored (Fries et al., 2001). A more recent study showed that serial cryptococcal passage within the same host produced the accumulation of genetic mutations which conferred virulence and enhanced resistance to antifungal drugs, therefore showing that phenotypic variation via genotypic mutation is possible in *C. neoformans* infection of human patients (Chen et al., 2017). Further investigation into pathogenic micro-evolution during sustained infection is prompted.

Additional factors such as the effect of heterogeneity in host response may provide further insight into the varied outcome of human cryptococcal infection. For example, genotyping of zebrafish larvae which more effectively controlled cryptococcal infection may enable us to elucidate what makes some hosts more capable of controlling infection compared to others. With the aim of understanding how macrophages contribute to complex outcomes in human cryptococcal

infection, special attention to macrophage phenotype and genetic manipulation is crucial. Similar assays should be adapted for *in vitro* investigation, potentially performing RNA-seq and cytokine profiling experiments to understand the variability in macrophage response.

In this chapter I have shown that cryptococci may inhabit the macrophage intracellular niche to replicate, but that doing so reduces the rate of replication compared to those which exist outside of host cells. The growth of cryptococci is not uniform, nor is phagocytosis by macrophages. These sources of variability may contribute to stochastic infection outcomes *in vivo*, and the continued quantification of macrophage-*Cryptococcus* interactions is enabling us to build a computational simulation of *in vivo* cryptococcal infection. In doing so, we are working toward understanding how the relationship between macrophages and cryptococci produces variable infection outcomes.

Chapter 6. Human PBMC response to cryptococcal infection

6.1 Introduction

I have described how macrophages contribute to the control of cryptococcal infection and how cryptococci manipulate this host phagocyte for the exploitation of an intracellular niche, which grants them the opportunity to replicate within a relatively protected environment. There is substantial evidence that macrophages are the key immune cell associated with *Cryptococcus neoformans* control, especially as alveolar macrophages are the primary immune cell to encounter and respond to infection, thus warranting the continued interest in the role of macrophages in cryptococcosis (Feldmesser et al., 2000; Gibson and Johnston, 2015; Giles et al., 2009; McQuiston and Williamson, 2012; Rudman et al., 2019). However, the immune system is a vast network of interacting components, each contributing to the maintenance of the system as a whole in order to protect the host from invading threats. As such, it is impossible to know the absolute effects of individual immune cells in isolation from the rest of the immune system, and we must attempt to gain a better understanding of the immune response as a whole to ascertain the effects of individual components within.

6.1.1 The innate response to cryptococcal infection

The innate immune response is the first line of defence in many infections, with effector cells widespread in the tissues and periphery able to induce immediate action to protect against invading threats. Macrophages not only engulf the invading yeast cells, but also secrete cytokines and chemokines to recruit innate immune cells. These cells induce cellular cytotoxic responses and also present antigens to T cells and B cells to traffic to the sight of infection and mount an adaptive immune response. As *Cryptococcus* is inhaled into the lung, the pulmonary innate immune defences must attempt to clear the infection and largely rely on macrophages with potential aid from neutrophils, natural killer (NK) cells, and dendritic cells (DC) (Gibson and Johnston, 2015).

Neutrophils

Neutrophils are not largely considered a key innate immune cell in cryptococcal disease. Indeed, no neutropenic conditions are associated with susceptibility to *Cryptococcus neoformans* and depletion of neutrophils does not result in higher fungal burden in neutrophil-depleted BALB/c mice (Mednick et al., 2003; Wozniak et al., 2012), suggesting that they do not substantially control cryptococcal growth *in vivo*. While neutrophils can phagocytose cryptococci at a low level in mice, they are mostly associated with dying macrophages in the infected tissues (Feldmesser et al., 2000). However, several studies have demonstrated the potential for neutrophils to exert anti-cryptococcal activity. Early studies into the fungicidal activity of neutrophils illustrated that oxidative mechanisms kill phagocytosed cryptococci (Diamond et al., 1972), and distal hydroxyl radicals are important for cryptococcal killing *in vitro* (Chaturvedi et al., 1996). While the oxidative burst of neutrophils is short-lived and lasts only about 2 hours *in vitro*, calprotectin, defensin, and primary granules of neutrophils exert anti-cryptococcal activity to support killing of cryptococci (Mambula et al., 2000). Furthermore, conditioned media from neutrophils has been shown to reduce the number of viable cryptococci in culture, implicating a neutrophil-secreted factor in cryptococcal killing; however co-incubation of cryptococci with neutrophils suppressed killing, hinting that *Cryptococcus* may neutralise or degrade the secreted factor (Qureshi et al., 2010, 2011). In a zebrafish model of infection neutrophils were seen with intracellular cryptococci and reduced the fungal burden in the absence of macrophages, suggesting that they may contribute to cryptococcal control in this model; however, when both macrophages and neutrophils were present, the number of macrophages which engulfed cryptococci far outnumbered neutrophils (Davis et al., 2016).

Though neutrophils may exert fungicidal and fungistatic control over *C. neoformans*, they are not widely associated with cryptococci *in vivo* (Feldmesser et al., 2000; Mednick et al., 2003). They may, however, affect the course of cryptococcal infection through immune modulation of Th1/Th2 polarisation. For example, one study showed that cryptococcal capsule induced the secretion of pro-inflammatory

IL-1β, IL-8, IL-6, and TNF-α by polymorphonuclear cells *in vitro* (Retini et al., 1996), suggesting that neutrophils may contribute to the Th1 polarisation of macrophages. However, while neutrophils may secrete pro-inflammatory cytokines in response to cryptococcal capsule, cryptococcal melanin and mannitol afford protection from neutrophilic oxidative killing (Chaturvedi et al., 1996; Doering et al., 1999; Qureshi et al., 2011), meaning that neutrophils may contribute to a pro-inflammatory environment while failing to kill the fungal cells.

In fact, another study showed that neutrophil depletion resulted in higher levels of IL-4, IL-10, IL-12, and TNF-α in BALB/c mice, suggesting a suppressive role for neutrophils on the production of these anti-inflammatory cytokines (Mednick et al., 2003). In this study neutropenia enhanced the survival of infected mice, suggesting that the increase in these cytokines contributed to the effective control of cryptococcal growth, and that neutrophil suppression of these cytokines may have actually been detrimental to health *in vivo*. Furthermore, in a murine model of cryptococcal infection, loss of functional cell death regulators produced an aberrant neutrophilic response; an exaggerated Th1 cytokine profile was associated with increased neutrophilic infiltration to the lungs and the induction of 'cytokine storm', which produced extensive tissue damage and resulted in increased mortality (Fa et al., 2017). Thus, control over neutrophilic influx and cytokine production must be maintained throughout infection as the pro-inflammatory actions of neutrophils are detrimental to host health and survival if left unchecked, despite the support neutrophils induce by providing Th1 polarisation cues to macrophages to suppress cryptococcal growth and dissemination.

Eosinophils

Eosinophils are granulocytes that are most often associated with immunity against parasites. Studies into the roles of eosinophilic response to *C. neoformans* infection have shown somewhat contrasting roles for this immune cell based on the model organism used for infection. Early studies by Feldmesser et al. showed that during C57BL/6 murine infection, eosinophilic infiltrates in the lung contacted cryptococci, though phagocytosis of cryptococci by eosinophils was not common (Feldmesser et

al., 1997). Chronic eosinophilia was associated with 5000-fold higher lung fungal burden in susceptible C57BL/6 mice compared to resistant CBA/J and BALB/c mice (Huffnagle et al., 1998), suggesting that eosinophils may be detrimental to susceptible hosts during cryptococcal infection. Interestingly, excessive eosinophil infiltration was associated with eosinophilic crystal deposition in macrophages and in the extracellular space, which was associated with extensive tissue damage in susceptible mice (Huffnagle et al., 1998). While *in vitro* eosinophils phagocytosed cryptococci after opsonisation and showed signs of degranulation (Feldmesser et al., 1997), limitation of eosinophils in the lungs of mice via treatment with anti-IL-5 mAbs showed that reducing eosinophils did not result in increased fungal burden (Huffnagle et al., 1998), suggesting that they are not important effector cells during cryptococcosis in mice. Furthermore, studies on eosinophil-deficient mice showed that these mice had increased Th1 polarisation, reduced Th2 polarisation and leukocyte infiltration, and reduced pulmonary fungal burden (Piehler et al., 2011). Thus, in susceptible mice, eosinophils are detrimental for the response against cryptococcal infection.

Studies examining the interaction between *C. neoformans* and rat eosinophils *in vitro* showed opposing results. Here, ingestion of opsonised yeasts resulted in activation of eosinophils and the upregulation of MHC-II, MHC-I, CD80, and CD86 molecules by eosinophils (Garro et al., 2010). Activated eosinophils induced the expansion of primed T cells, as well as the expression of Th1 cytokines by both eosinophils and T cells after cryptococcal challenge (Garro et al., 2010). *In vivo*, *Cryptococcus*-primed eosinophils migrated to the mesenteric lymph nodes of rats and induced the proliferation of leukocytes and subsequent Th1 cytokine polarisation, as well as NO production in the spleen (Garro et al., 2011). These rats also showed decreased production of Th2 cytokines which promote cryptococcal growth and dissemination. Thus, in rats, eosinophils contribute to the pro-inflammatory response to cryptococcal infection. However, pro-inflammatory cascades must be tightly regulated as excessive inflammation can be damaging to host tissues, as was shown in the mice experiments above. Thus, the different models of cryptococcal infection suggest opposing roles for eosinophils during

cryptococcal infection, and warrant investigation into the different immune responses elicited by these common infection models.

Dendritic cells

Dendritic cells (DCs) are professional phagocytes and antigen presenting cells (APC) with the ability to destroy invading pathogens and induce the activation of innate immune cells, and are important for the control of cryptococcal infection (Wozniak, 2018). These cells kill cryptococci by oxidative and non-oxidative methods, and inhibiting the production of ROS decreases antifungal activity of DC (Kelly et al., 2005). Loss of DC recruitment allows enhanced fungal growth in the lungs of infected mice (Osterholzer et al., 2008); CCR2 is required for DC recruitment to the lungs, the site most associated with initial cryptococcal infection, and relies on the expression of CCR2 ligands CCL2 and CCL7 (Osterholzer et al., 2008). After recruitment to the site of infection DC may then phagocytose the cryptococcal cells, though cryptococci must be opsonised in order to be effectively phagocytosed and subsequently killed by human monocyte-derived DC (Kelly et al., 2005). After phagocytosis *C. neoformans* traffics to the lysosomal compartment of DCs within 20 minutes, where lysosomal contents have potent anti-cryptococcal activity (Wozniak and Levitz, 2008). Lysosomal cathepsin B induces cell wall damage and kills cryptococci by osmotic lysis in a manner similar to antimicrobial peptides (Hole et al., 2012).

While direct cryptococcal killing is beneficial for limiting infection, the activation of a wider immune response by DCs is important for control and clearance of cryptococci. As antigen-presenting cells, DC are particularly important for T cell stimulation. For example, cryptococcal DNA activates TLR9 on DCs which induces the expression of the costimulatory molecule CD40 and the production of pro-inflammatory IL-12p40 by murine bone marrow-derived DCs (Nakamura et al., 2008; Tanaka et al., 2012; Wozniak et al., 2006). These stimulate T cells and support Th1 polarisation. Furthermore, mannose receptors on dendritic cells capture cryptococcal mannoprotein for presentation to T cells, which induces them to proliferate and produce IL-2 (Mansour et al., 2006; Pietrella et al., 2005). Loss of DC

accumulation and activation and is associated with poor CD4+ and CD8+ T cell recruitment, which results in increased fungal burden in mice at 3 weeks post infection (Qiu et al., 2012b). DC are therefore important in the activation of the adaptive immune response via the stimulation and recruitment of T cells.

In addition to T cell activation and recruitment, cytokines produced by DC polarise the immune response toward pro-inflammatory action which is beneficial for the control of cryptococcal infection. In the infected lungs of mice, DC and T cells express IL-12 and IFN-γ, producing a Th1 cytokine profile that is dependent on CCR2 expression (Osterholzer et al., 2008). Furthermore, when DC recognition of cryptococcal mannoproteins is combined CpG oligodeoxynucleotide stimulation, DCs produce pro-inflammatory cytokines IL-6, IL-12p40/p70, IL-1α, as well as chemokines MIP-1α and MCP-1 (Dan et al., 2008). These cytokines and chemokines are involved in Th1 polarisation, which is beneficial for the control of cryptococcal infection.

While dendritic cells play important immunomodulatory roles in *Cryptococcus* infection, cryptococci employ defensive strategies to inhibit DC activation. For example, in a study comparing the ability of capsular mutants to activate DCs, Grijpstra et al. found that the *Δcap59* cryptococci potently activated DC to express costimulatory molecules CD80 and CD86, which are important for the effective activation of T cells; however, wild type *C. neoformans* failed to produce the same result (Grijpstra et al., 2009). The *Δcap59* mutant has reduced capsular GXM, and cryptococcal cell wall constituents are more likely to be revealed in the absence of GXM. Here, exposure of such motifs enabled the activation of DC to express activation markers (Grijpstra et al., 2009). The capsule present on wild type *C. neoformans* therefore acts to conceal important motifs required for DC activation and maturation, and thus prevented these APC from instigating downstream cellular anti-cryptococcal actions. Conversely, a study by Yauch et al. found that GXM inhibited the proliferation of T cells directly and did not interfere with DC maturation, as GXM did not inhibit LPS-induced upregulation of DC maturation markers (Yauch et al., 2006). However, this study examined the effect of capsular

GXM and mannoprotein in the absence of cryptococcal cells, and it is possible that additional motifs on the cryptococcal surface are required for the effective inhibition of DC maturation. This is supported by Vecchiarelli et al., who showed that soluble GXM was unable to block DC stimulation on its own (Vecchiarelli et al., 2003).

Cryptococcus gattii also dampens the DC response, and though it is killed by dendritic cells in immunocompetent patients, DCs fail to express maturation markers or produce TNF-α during *C. gattii* infection and thus fail to effectively induce an adaptive T cell response (Huston et al., 2013). Furthermore, DCs in *C. gattii* infection fail to express appreciable levels of MHC-II and costimulatory molecules needed for antigen presentation and activation of T cells, and mice infected with *C. gattii* produce attenuated levels of T cell chemokines and Th1/Th17 cytokines, resulting in poor induction of a Th1/Th17 response (Angkasekwinai et al., 2014). Thus, while DCs are important for control of cryptococcal infection, *C. neoformans* and *C. gattii* are able to modulate the DC-driven immune response.

NK cells

Natural killer (NK) cells are members of the innate immune system that are best known for their ability to kill tumour cells, but they may also play a role in anti-cryptococcal immunity. A study of mice infected intravenously with *C. neoformans* showed increased fungal burden in the lungs when NK cells were depleted, though no effect on survival or organ burden was noted after intratracheal inoculation (Lipscomb et al., 1987). *In vitro* studies have shown that NK cells kill cryptococci (Hidore et al., 1991), though NK cells also produce modulating effects on the immune system for combatting cryptococcal infection. During HIV and *C. neoformans* co-infection there are more immunomodulatory, cytokine-secreting NK cells in the CSF and more cytotoxic NK cells in the blood of patients, suggesting distinct roles for NK cells in different niches in the human host during infection (Naranbhai et al., 2014).

Cryptococcus binds to the NK receptor NKp30, which is involved signalling required for fungicidal activity and the cytotoxic, pore-forming activity of perforin (Li et al., 2013; Ma et al., 2004). Cryptococcal contact not only stimulates perforin degranulation, resulting in cryptococcal destruction, but *C. neoformans* induces subsequent perforin mRNA transcription by NK cells, allowing the cytotoxic cells to re-arm against continued cryptococcal threat (Marr et al., 2009). NK cells from patients with HIV show reduced NKp30 expression which correlates with reduced perforin levels, aberrant granule polarisation, and markedly decreased cryptococcal killing; however this deficit is restored with the addition of IL-12, which upregulates the expression of the NK cell receptor (Kyei et al., 2016; Li et al., 2013). This is critical, as HIV patients are severely immunocompromised and as such are highly susceptible to cryptococcal infection. IL-12 therefore represents a potential source of therapeutic intervention that may increase anti-cryptococcal cellular defences in HIV patients.

While direct killing of cryptococci by NK cells helps to control infection, NK cells also exert some immunomodulatory effects as well. NK cells and macrophages stimulated with IL-12 and IL-8 reduced the number of cryptococci in culture in an IFN-γ-dependent manner (Kawakami et al., 2000). The reduction in cryptococci that was induced by the combination of stimulated NK cells and macrophages was greater than that of either of the stimulated cells in isolation, suggesting that there is enhanced fungicidal activity when NK cells and macrophages cooperate to control the fungal growth (Kawakami et al., 2000). Furthermore, anti-NK cell antibodies reduced IL-12- and IL-18-induced production of IFN-γ and NO in solution, abrogating anti-cryptococcal activity and demonstrating the role of NK cells in the production of important secreted factors which lead to the killing of cryptococci *in vitro* (Zhang et al., 1997). Thus, NK cells may aid in the production of immune stimulating cytokines, especially IFN-γ which activates macrophages and other immune cells to exert anti-cryptococcal activity.

While NK cells possess the ability to kill cryptococci and to induce immune signalling cascades which recruit enforcements, *C. neoformans* is able to abrogate the effects

of NK cells during infection. For example, cryptococci moderate the immune response to infection by limiting GM-CSF and TNF-α transcription by NK cells (Murphy et al., 1997), thus altering recruitment of granulocytes and monocytes, as well as removing Th1 stimuli for classical macrophage activation which is necessary for cryptococcal clearance and control (Lacey et al., 2012). Furthermore, cryptococcal capsular mutant *Δcap59* induces more perforin transcription than wildtype *C. neoformans*, suggesting a role for cryptococcal capsule in protection against granulocytic host defences, and potentially the 're-arming' of NK cells for subsequent cryptococcal killing (Marr et al., 2009). Thus, while NK cells kill cryptococci and have the potential to modulate the immune response, cryptococci again maintain strategies to avoid killing and immune activation.

Monocytes

Monocytes differentiate into macrophages and dendritic cells, and are therefore important in the fight against *Cryptococcus*. During human peripheral blood mononuclear cell (PBMC) infection, cryptococci are often found within aggregates of monocytes (Siddiqui et al., 2006). Human monocytes are capable of engulfing *C. neoformans in vitro* (Diamond et al., 1972), and the CSF of HIV patients infected with *C. neoformans* is enriched with monocytes with markers which show they are capable of cytokine secretion (Naranbhai et al., 2014). Human monocytes produce TNF-α and are stimulated to produce IL-6 except when there is excessive capsule (Delfino et al., 1997; Levitz et al., 1994), demonstrating that they are capable of mounting anti-cryptococcal defences. Therefore, monocytes are capable of secreting cytokines which may polarise the immune response toward a pro-inflammatory profile that is required for control of cryptococcal infection.

During infection and injury, monocytes leave the bloodstream to enter the tissues where they can differentiate into macrophages or DCs. As discussed throughout, macrophage interactions with cryptococci are complex, as macrophages can engulf cryptococci and destroy them, or cryptococci can replicate within the macrophage intracellular niche and escape to disseminate infection (Johnston and May, 2013; Mansour et al., 2014; Rudman et al., 2019). T cell activation of macrophages is

crucially important in *C. neoformans* infection, as stimulation by Th1 T cell cytokines induces classically activated pro-inflammatory macrophages (M1), whereas Th2 cytokines produce alternatively activated anti-inflammatory macrophages (M2). Pro-inflammatory M1 macrophages are associated with the control of cryptococcal infection, where anti-inflammatory M2 macrophages result in uncontrolled cryptococcal growth (Arora et al., 2011; Stenzel et al., 2009). While the macrophage activation state is plastic and can be intermediate during cryptococcal infection (Arora et al., 2011; Davis et al., 2013), the activation of macrophages by CD4+ T cells is one of the most important factors that decides the outcome of cryptococcal infection.

6.1.2 The adaptive immune response to cryptococcal infection

T cells are important in mounting an effective humoral and immunostimulatory response against cryptococcal infection. As I have discussed their roles in detail in the introduction, I will give only a brief overview of their role here. T cells receive stimulus for activation by recognising processed antigen presented to them by APC through the T cell receptor. CD4+ T cells provide help through cell contact via costimulatory molecules, through promoting B cell maturation, and by transcriptionally upregulating the production and secretion of cytokines and chemokines which recruit and activate a robust set of immune cells. CD4+ Th1 T cells produce pro-inflammatory cytokines such as IFN-γ, TNF-α, IL-2, IL-12, and GM-CSF, whereas Th2 T cells produce the anti-inflammatory cytokines IL-4, IL-10, IL-13. iNOS activity and nitric oxide production are markers for Th1 polarisation, with NO being important for the destruction of invading pathogens. Arg-1 activity marks Th2 activity and is associated with tissue repair.

T cells are required for the control of cryptococcal infection. An early study by Huffnagle et al. showed that in the absence of CD4+ and CD8+ T cells, mice failed to suppress pulmonary growth of *C. neoformans* (Huffnagle et al., 1991). Here, both subsets of T cells were required for the prevention of cryptococcal dissemination throughout the host, though CD4+ T cells were especially important for limiting

early brain dissemination (Huffnagle et al., 1991). T cells are also required for the efficient recruitment of leukocytes to the lungs, which is largely dependent on the presence of IFN-γ; indeed, in the absence of IFN-γ more alternatively activated macrophages were recruited to the lungs of infected mice, and a higher pulmonary infection burden was produced (Arora et al., 2005). Studies have also shown that T cells helped human PBMCs control cryptococcal infection *in vitro* (Siddiqui et al., 2006), and that ablation of T cells and Th1 cytokines in mice infected with IFN-γ-producing *C. neoformans* resulted in early mortality, demonstrating the requirement for T cells, specifically Th1 cytokines, in protective immunity against cryptococcal infection (Wozniak et al., 2009). The requirement for T cells in protection against *C. neoformans* infection in humans is underpinned by the fact that most people who suffer from cryptococcal infection are severely immunocompromised, and especially include HIV patients who lack sufficient numbers of T cells (Park et al., 2009; Rajasingham et al., 2017). However, it is also worth noting that depletion of T cells in a murine model of infection resulted in failure to control cryptococcal infection, yet prolonged mouse survival, demonstrating that T cells also contribute to disease pathology and that strict control over T cell action is required (Neal et al., 2017).

The host cytokine profile is important in balancing the pro- and anti-inflammatory forces in infection, and as such cytokines are key factors which determine the course and outcome of infection. For example, in resistant C.B-17 mice, Th1 cytokines IFN-γ and IL-12 were shown to be necessary for pulmonary clearance, and antibody treatment against these cytokines resulted in loss of control, influx of eosinophils, and an increase in the Th2 cytokine IL-4, which produced a higher fungal burden (Hoag et al., 1995, 1997). However, short- and long-term treatment of mice with IL-12 was shown to prolong survival and limit fungal burdens to levels lower than those of untreated mice (Decken et al., 1998). In the absence of IL-12 from T cells, mice produced increased levels of the Th2 cytokine IL-4, and had higher fungal burdens and increased mortality (Decken et al., 1998), showing that in the absence of Th1 stimulus, a Th2 polarisation state develops which is detrimental for the host (Zhang et al., 2009). A similar result was achieved by TNF-α neutralisation early in murine

infection (Herring et al., 2002), again highlighting the need for Th1 polarisation in control of cryptococcal infection. IL-17 is also produced by CD4+ T cells and is associated with IFN-γ production and fungal clearance in mice. Indeed, IL-17-deficient mice failed to appropriately activate macrophages and DC, which resulted in the aberrant activation of the immune system and higher lung burdens, highlighting the role of IL-17 in control of cryptococcal infection (Murdock et al., 2014).

Th2 cytokines produce poor cryptococcal infection outcomes. Indeed, in BALB/c mice IL-13 was shown to induce the expression of Th2 cytokines IL-4 and IL-5, associated with pronounced fungal burdens and poor survival rates (Müller et al., 2007). However, limitation of Th2 stimulation is protective for hosts, as loss of IL-4 in mice produced a protective outcome with lower fungal burdens that wildtype mice (Decken et al., 1998). Thus, the Th1/Th2 cytokine balance largely determines fungal growth and disease outcome, and the polarisation away from the Th2 response toward a pro-inflammatory, pro-clearance Th1 response results in better infection outcomes. Differential cytokine profiles in human cryptococcosis patients even correlate with patient fungal burden and infection outcome. Patients with high CSF levels of Th1 cytokines IFN-γ, TNF-α, IL-6, IL-8 and IL-17a typically had better clinical outcomes compared to patients with high CSF levels of Th2 cytokines IL-4 and IL-10 (Jarvis et al., 2015, 2013, 2014; Mora et al., 2015). Thus, T cells and their resultant cytokines are important for the control of human cryptococcal infection and in determining disease outcome.

The CD4+ T cell cytokine polarisation state acts upon immune cells to elicit specific responses. During cryptococcal infection, the activation of macrophages by T cell cytokines drives clearance by classically activated macrophages or dissemination by alternatively activated macrophages. In mice infected with heat-killed *C. neoformans*, treatment with anti-CD4+ and -CD8+ mAbs reduced activation markers on the surface on macrophages as well as macrophage phagocytosis of cryptococci, demonstrating the requirement for T cells to activate macrophages for phagocytosis (Kawakami et al., 1995). Murine macrophages require IFN-γ for phagocytosis of

cryptococcal cells (Kawakami et al., 1995), and a C57BL/6 model of *C. neoformans* infection showed that CD4+ T cells were the main source of IFN-γ in the CNS during infection (Neal et al., 2017). Thus, T cell stimulation of effector cells can drive immune cell activation and cryptococcal clearance.

CD8+ T cells also contribute to control of cryptococcal infection. Studies on mice lacking CD8+ T cells showed that these mice were unable to recruit immune cells to the sites of infection, and that they failed to clear pulmonary infection and stop dissemination to the brain and spleen (Hill and Harmsen, 1991; Huffnagle et al., 1991). Furthermore, in a CBA/J murine intratracheal model of cryptococcal infection, reduced numbers of CD4+ and CD8+ T cells were associated with the influx of more macrophages to the lung which were permissible to intracellular cryptococcal growth (Huffnagle et al., 1991), and both subsets of T cells were required for limiting cryptococcal growth during human PBMC infection (Siddiqui et al., 2006). Thus, CD8+ T cells aid in limiting cryptococcal infection. Finally, it has been suggested that while CD4+ T cells recruit and activate immune effector cells to destroy cryptococci, CD8+ T cells lyse infected, unactivated macrophages to release intracellular cryptococci exploiting the niche (Huffnagle et al., 1991). Therefore, the combined actions of different T cell subsets may play different roles in the control of cryptococcal infection.

6.1.3 Understanding a robust immune response to *C. neoformans* infection

The immune system represents an interconnected network of individual components that work together to combat infection. So far, I have discussed my work using macrophages to understand how these host cells control cryptococcal growth. While macrophages are important in controlling fungal infection, studying them in isolation from other immune cells represents an immunocompromised system which lacks additional phagocytes and adaptive immune cells. To understand more about how *Cryptococcus neoformans* interacts with a more

complete immune system, I infected human peripheral blood mononuclear cells (PBMCs) with *C. neoformans*.

Previous studies have investigated how PBMCs respond to cryptococcal infection. Levitz et al. showed that PBMCs phagocytosed cryptococci in the presence of opsonins, and that *C. neoformans* stimulated PBMCs, particularly monocytes, to produce TNF-α (Levitz et al., 1994). Interestingly, PBMCs phagocytosed nearly threefold more cryptococci 6 days after plating compared to freshly isolated PBMCS; because PBMCs differentiate into macrophages in culture, macrophages here showed greater phagocytic activity than freshly isolated, un-differentiated PBMCs (Levitz et al., 1994). Harrison and Levitz also showed that PBMCs stimulated with *C. neoformans* expressed IL-12p40 mRNA, though expression occurred later compared to PBMCs stimulated with *C. albicans* and *S. aureus*, reflecting the lower activation of PBMCs by cryptococci (Harrison and Levitz, 1996).

Work by Siddiqui et al. characterised the behaviour of cryptococci in the presence of human PBMCs. Pre-stimulation of PBMCs with heat-killed *C. neoformans* resulted in better control of cryptococcal growth and enhanced killing of cryptococci by the human cells upon secondary live infection, especially when acapsular cryptococci were used (Siddiqui et al., 2006). This was associated with the increased expression of IL-6 by PBMCs afforded by the lack of cryptococcal capsule. Interestingly, PBMC aggregates formed in response to cryptococcal infection, and cryptococci replicated within the aggregates and produced excessive capsule (Siddiqui et al., 2006). Further work by Alvarez et al. showed that cryptococci replicated within human peripheral blood monocytes, shed capsule, vomocytosed, and transferred between the human cells, though here the human cells were not freshly isolated and therefore were likely partially differentiated into macrophages (Alvarez et al., 2009). Nonetheless, these studies show that cryptococci are able to exploit the PBMC niche for survival and replication in the absence of PBMC control.

While behaviours of cryptococci in human leukocyte subsets have been shown, the influence of PBMC interaction on cryptococcal uptake and replication rates is not

known. Though it is understood that cryptococci are typically inhaled into the lungs, little is known about the progression of initial infection to the development of widespread fungemia which may ultimately lead to CNS infection and cryptococcal meningitis. Because PBMCs represent the circulating immune cells patrolling for invading threats throughout the body, it is important to understand how they respond to *C. neoformans* infection as this intermediate step in cryptococcosis infection may depend on peripheral control. Therefore, the aim of this chapter was to address how peripheral immune cells phagocytose and control cryptococcal infection, and to quantify how cryptococci manipulate this host cell niche for replication. Here I show that human PBMCs phagocytose cryptococci, that human PBMCs limit intracellular cryptococcal growth, and that this model may be used to simulate cryptococcal granuloma formation in response to cryptococcal infection.

6.2 Freshly cultured human PBMCs were composed primarily of monocytes and T cells

In order to discern which cell types composed the donor PBMCs, I labelled the donor cells with CD3 FITC and CD14 APC anti-human antibodies to identify T cells and monocytes, respectively. I decided to examine these subsets specifically because peripheral monocytes eventually differentiate into macrophages after sufficient activation, and T cells frequently aid in providing stimulus. Because both of these cell types are crucial to control of cryptococcal infection, studying their behaviour toward cryptococci early after dissemination to the periphery, which is modelled here, could illuminate the role and behaviour of these immune cells in response to cryptococci within the bloodstream and peripheral tissues of the body.

While there was some localisation of CD3 antibody on CD14-labelled cells, the APC signal differentiated monocytes from T cells (Figure 6.1a). CD3+ T cells also exhibited a more uniformly circular appearance, while CD14+ monocytes were larger and more heterogeneous. There were also smaller cells present, likely platelets based on size, and other subsets not labelled by the CD3 and CD14 antibodies. CD14 also weakly labels neutrophils, and it is possible that any neutrophils which remained in the PBMCs were labelled by this antibody. However, since CD14 is more strongly expressed on monocytes such as macrophages, and because neutrophils are generally excluded by PBMC isolation techniques, I will refer to CD14+ cells as monocytes. Imaging from this assay showed that both T cells and monocytes composed the majority of isolated PBMCs. Monocytes within the PBMC population differentiate into macrophages, but at the times considered here the monocytes did not evolve a distinctly macrophage appearance and as such were not considered to be differentiated macrophages.

At 0h both T cells and monocytes were largely adherent to the plate; however, at 24h T cells typically floated freely in media (Bennett and Breit, 1994). If aggregates of PBMCs existed they appeared to be composed mainly of CD14+ monocytes, though the absence of antibody labelling indicated that either antibody staining was

not uniform, or that other immune cells such as NK cells or B cells may have contributed to PBMC aggregates. T cells did contribute to aggregates at 0h, and to a lesser extent at 24 hours (Figure 6.1a). In the presence of KN99 GFP *C. neoformans*, the bright fluorescence of the cryptococcal cells tended to saturate the fluorescence in the image, obscuring the fainter CD3+ FITC signal.

I also performed antibody staining before the onset of 24 hour time lapse imaging, again using CD3 FITC and CD14 APC to label T cells and monocytes, respectively. I applied the antibodies to the human PBMCs one hour before infecting the cells with KN99 GFP *C. neoformans*, and began imaging immediately after infecting the human cells (Figure 6.1b). Unfortunately, the CD3 labelling was faint at 20x magnification and was difficult to detect in the presence of the bright GFP signal of the cryptococci. Furthermore, the CD14 signal illuminated the presence of monocytes at the start of the time lapse (Figure 6.1b), but signal was significantly faded at 8 hours and was almost completely imperceptible at 24 hours. However, this was not due to cytotoxicity of the PBMCs, as the same density of PBMCs was observed at 0 and 24 hours. Despite this, early imaging did show that PBMC swarms were composed mainly of CD14-labelled monocytes, as demonstrated in the x60 imaging (Figure 6.1a).

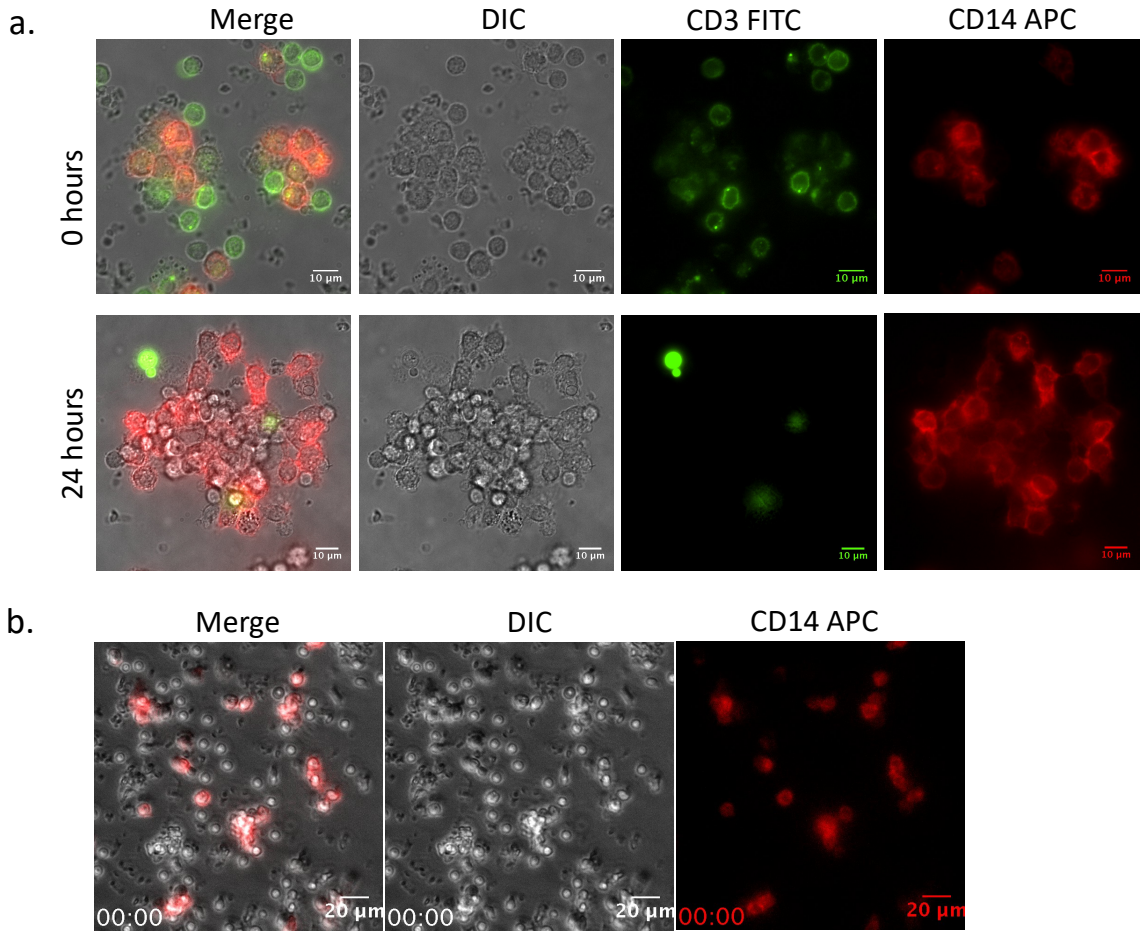

Figure 6.1. Freshly isolated human PBMCs are composed of T cells and monocytes

To determine the immune cell subsets within the donor PBMCs, PBMCs were labelled with CD3 FITC and CD14 APC anti-human antibodies. After allowing one hour for the antibodies to bind, the wells were imaged at x60 (a) or x20 magnification (b). Green cells are labelled with CD3 FITC which labels T cells, red cells are labelled with CD14 APC which labels monocytes.

a. Cells from donors were imaged at 0 and 24 hours. Donor PBMCs were composed of CD3+ T cells and CD14+ monocytes. Fewer CD3-labelled cells were adherent at 24 hours. 3 separate donors confirmed the presence of T cells and monocytes in PBMCs.

b. To determine how PBMCs swarm around cryptococci over the course of the time lapse experiments human PBMCs were labelled with CD3 and CD14 anti-human antibodies. CD3 labelling was so faint that the images were saturated at x20 magnification and were blurred by the strong GFP signal of the KN99 *C. neoformans*, and as such are excluded here. CD14 APC reliably

labelled monocytes up to 4 hours, though signal faded after 8 hours and was mostly absent by 24 hours. This was not due to toxicity to the PBMCs, as the number of cells did not decrease.

6.3 Phagocytosis of *Cryptococcus neoformans* by human PBMCs

To understand how cryptococci interact with PBMCs, I performed time lapse imaging which allowed me to follow individual cryptococci and observe their interactions with human peripheral immune cells. At approximately 24 hours after donor cell collection I infected human PBMCs with KN99 GFP *C. neoformans* opsonised with 18B7. I used GFP cryptococci in part to retain relevance to my previous experiments, but also to enable me to follow the cryptococci throughout the course of the experiment. This was necessary as the cryptococci were of similar size and shape as the human cells. Cryptococci were phagocytosed by individual monocytes (Figure 6.2a) and by PBMC aggregates (Figure 6.2b), though not all cryptococci were phagocytosed. Additionally, cryptococci were phagocytosed as individual cells, or as small groups of up to four cryptococci, which likely arose due to budding and replication (Figure 6.2a). Most phagocytosis events occurred within two hours of infection (Figure 6.2c), though additional phagocytosis of cryptococci by swarms of PBMCs was occasionally observed throughout the duration of the assays.

(page intentionally left blank for figures + legends on following pages)

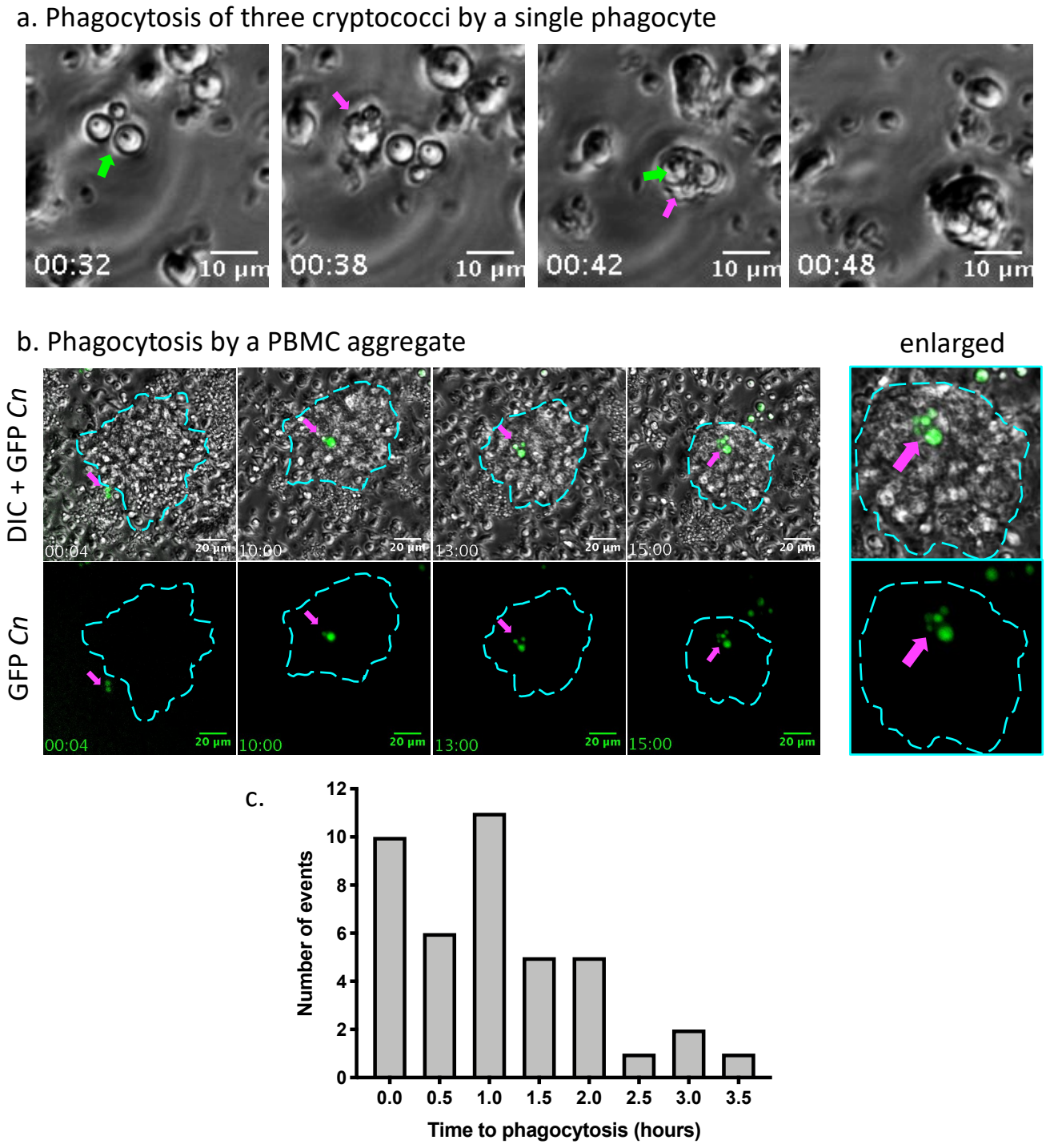

Figure 6.2. Human PBMCs phagocytosed *C. neoformans*

To determine the rate of phagocytosis of cryptococci by human PBMCs, I infected one day old human PBMCs with KN99 GFP *C. neoformans* and performed time lapse imaging immediately after infection. Images were captured at x20 magnification every 2 minutes for 24 hours.

a. Phagocytosis of *C. neoformans* by human PBMCs. Individual cryptococci were phagocytosed by PBMCs or were phagocytosed as small clusters of cryptococci likely resulting from budding and replication. Here the green arrow points to the *Cryptococcus*, as determined by GFP fluorescence (not shown), and the magenta arrow points to the phagocyte. Scale bars are 10 μm, and times are shown as hours : minutes.
b. Phagocytosis of *C. neoformans* by an aggregation of human PBMCs. Two cryptococci were phagocytosed by a pre-existing swarm of human PBMCs. *C. neoformans* is GFP and marked by a magenta arrow, while the approximate boundary of the phagocytic mass is shown in cyan dashed lines. As the experiment progressed the cryptococcal cell divided from 2 to 5 cryptococcal cells. Scale bars are 20 μm, and times are shown as hours : minutes. Final panel is an enlarged image of cryptococci within the swarm.
c. The time each *Cryptococcus* was phagocytosed was determined and plotted as a histogram. Bars represent the number of cryptococci phagocytosed at each time point. 3 repeats were performed, with each repeat representing a different PBMC donor. 41 starting cryptococci were followed.

6.4 Formation of PBMC aggregates

Frequently after phagocytosis additional PBMCs swarmed to contact the phagocyte with intracellular cryptococci. Aggregates of PBMCs were variable; many were only small and transient, while others were lasting swarms or larger masses (Figure 6.3a). PBMCs were seen to form a mass of cells around the infected phagocyte, though cryptococci were also occasionally phagocytosed by pre-existing masses (Figure 6.3a – right panel, figure iv). Swarms of infected phagocytes could fuse with additional aggregates which did not contain intracellular cryptococci (Figure 6.3b). Separate swarms which each contained intracellular cryptococci did occasionally meet; however, larger swarms which met did so only transiently before splitting apart, each retaining their 'original' intracellular cryptococci with any resultant daughter cells. Swarms and masses appeared amorphous with indistinct edges as cells within moved, and clear imaging was difficult due to the three-dimensional structure of the granulomatous formations.

Most aggregates formed within 4 hours of phagocytosis (Figure 6.4a), though not all remained throughout the course of the experiment, and individual phagocytes were seen to split away from masses at apparently random times throughout. While the formation of PBMC aggregates has been described before (Siddiqui et al., 2006), I also quantified the size of the swarms in relation to the number of cryptococci within. I wondered if the area of the swarm was related to the number of intracellular cryptococci, and hypothesised that if there was immune activation in response to the cryptococcal phagocytosis that more intracellular cryptococci would result in a larger swarm area. A relationship between swarm size and the number of cryptococci could also suggest that cryptococci recruited more PBMCs to utilise the swarm as a niche. To test this, I measured the area of the swarm each time a cryptococcal cell replicated and plotted the size of the mass against the number of intracellular cryptococci. It should be noted that I only measured the area of the aggregates in a two-dimensional manner corresponding to the surface area of the plate they occupied; however, swarms were three-dimensional with cells tumbling on top of one another, which not only made antibody staining difficult, but volume

measurement was not possible using the microscope employed for time lapse imaging. After measuring the plate surface area occupied by the PBMC aggregates, there was no clear relationship between swarm size and the number of cryptococcal cells within (Figure 6.4b). Indeed, while many swarm sizes increased in area, some did so only slightly, while others decreased in size. This suggests that there was not strong immune activation in response to PBMC phagocytosis of cryptococci, and that cryptococci did not strongly induce PBMC recruitment. Similarly, cryptococci did not consistently downregulate the immune response by inducing a decrease in mass size.

There was, however, a positive linear relationship between the relative fold change of intracellular cryptococci and the maximum size of the swarm (Figure 6.4c; linear regression $p = 0.0014$, $R^2 = 0.283$). Here, the maximum size of the swarm increased with the cryptococcal fold change, suggesting that larger swarms were more permissive to cryptococcal replication. This was potentially due to better dividing cryptococci purposely recruiting more PBMCs for use as an immune cell niche for replication, or was due to immune recruitment of PBMCs to cryptococci which replicated more readily in order to combat the infection. However, while there was a relationship between cryptococcal fold change and the maximum size of the mass which contained the fungal cells, the mass sizes were variable within each level of cryptococcal fold change, and the size of each PBMC aggregate could either increase or decrease as the number of cryptococci within grew (Figure 6.4b). The size of aggregates lacking intracellular cryptococci was also measured at the start and end of time lapse videos, and revealed no general trend for overall increase or decrease in size in time, with some increasing and some decreasing in area (Figure 6.4d). This suggests that the size of the swarm may increase or decrease irrespective of cryptococci, and in general do not necessarily increase in time. However, only few of these swarms were noted, and quantification of additional donors may illuminate more trends or lack thereof. Nonetheless, the inability of all ‘empty’ swarms to increase in time supports the idea that the increase in PBMC mass size with increasing fungal fold change may be related to the replication of cryptococci contained within, and may not be due merely to chance.

Once within a swarm or larger mass, cryptococci exhibited a number of behaviours; they replicated (Figure 6.2b), died or disappeared (albeit rarely), vomocytosed as fungal cells (Figure 6.5a), or left the swarm inside a phagocyte. Some cryptococci within grew large capsules, though the notable existence of large capsule was not prevalent (Figure 6.5b). Cryptococci ranged in size from 3 μm to roughly 8 μm in diameter, and no titan cells were observed (not shown).

(page intentionally left blank for figures + legends on following pages)

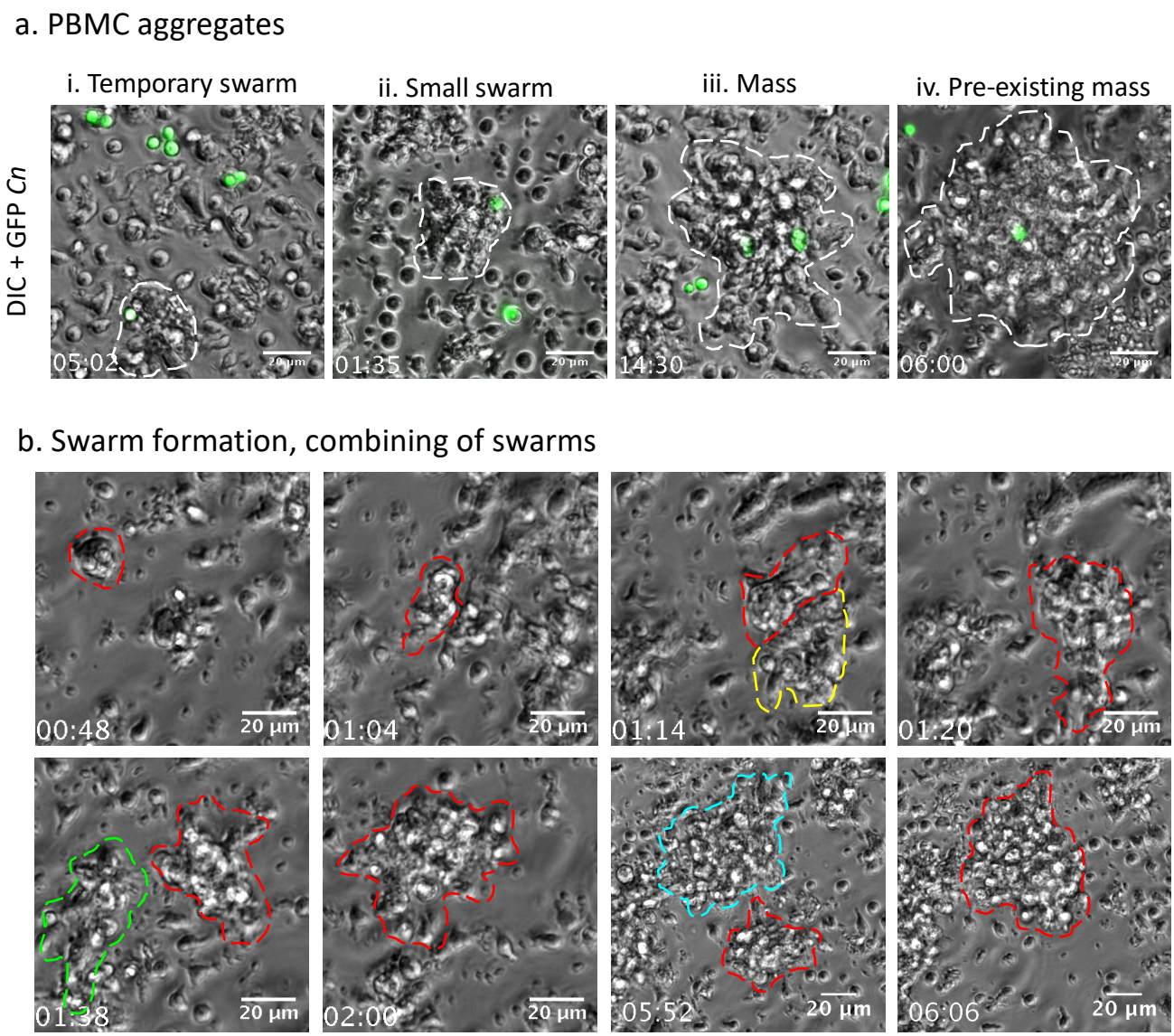

Figure 6.3. PBMCs can form different types of aggregates

Human PBMCs were infected with KN99 GFP *C. neoformans* one day after isolation. Time lapse imaging was performed at x20 magnification, and cryptococci were followed for 24 hours with images captured every 2 minutes. Different types of PBMC aggregates were seen with intracellular cryptococci.

a. Examples of different types of PBMC aggregates seen over 24 hours of infection. Scale bars are 20 µm and times are shown as hours : minutes. Cryptococci are shown in green, and aggregate boundaries are marked with white dashes.

i. Small temporary swarm of PBMC cells around a phagocyte with intracellular cryptococci. Swarm formed briefly then dissolved to leave a single monocyte containing a cryptococcal cell.
ii. Swarm which persisted around an infected phagocyte.
iii. Formation of a larger mass with intracellular cryptococci.
iv. Phagocytosis of a cryptococcal cell by a pre-existing mass similar to a granuloma. Cryptococcal cell was phagocytosed by the swarm or by a phagocyte in the margin of the swarm, as opposed to first being phagocytosed by a monocyte before the formation of a swarm.

b. The formation of a swarm around an infected phagocyte in time. Swarm boundaries are marked with coloured dashed lines, and red represents the evolution of the original phagocyte. The phagocyte was met with a small number of PBMCs to from a small swarm (second frame) which then combined with subsequent swarms (yellow, green, cyan lines) to produce a larger swarm. While there are cryptococci within they are not represented here.

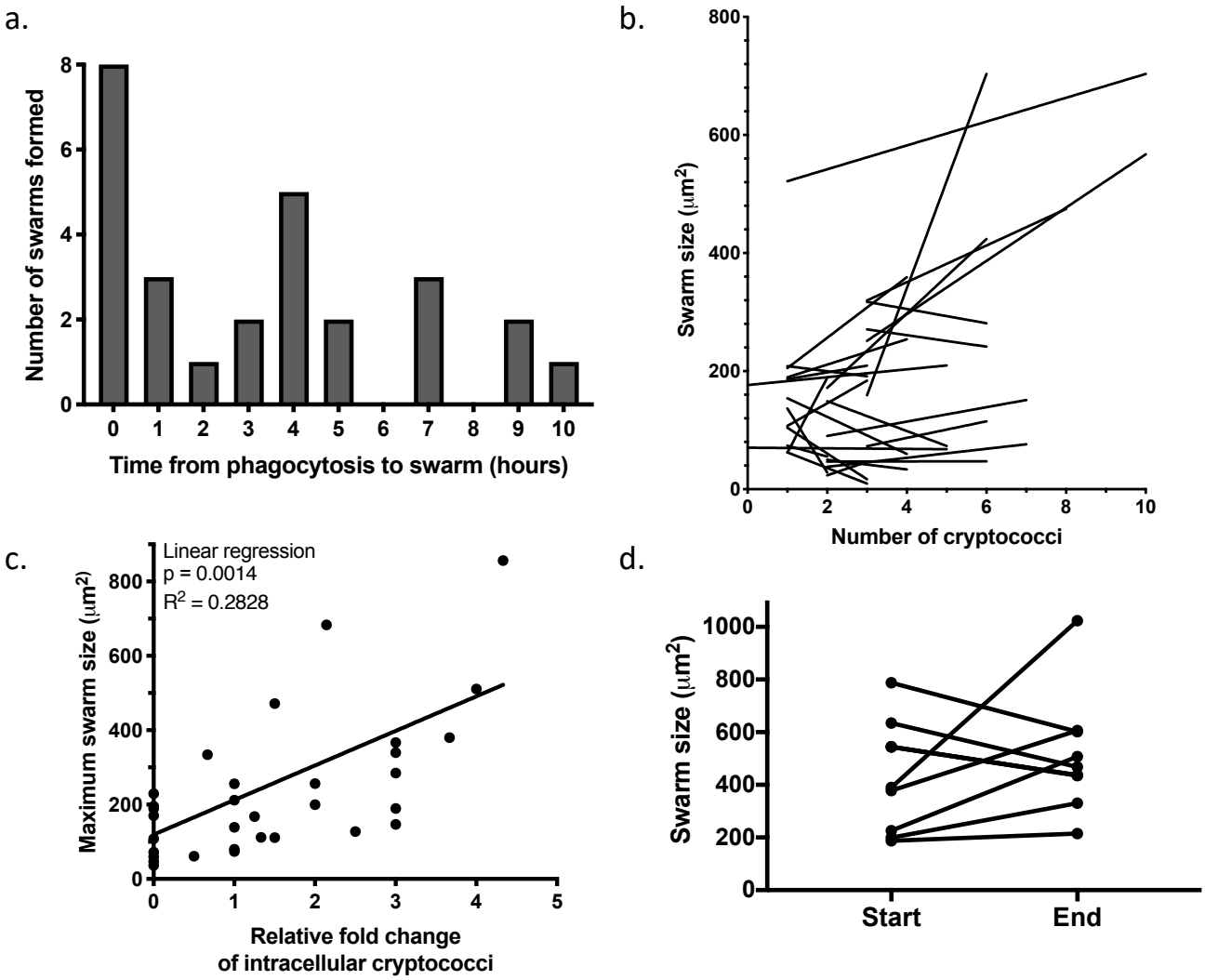

Figure 6.4. The size of the PBMC aggregates was variable, but increased

Human PBMCs were infected with KN99 GFP and followed for 24 hours. The formation of PBMC swarms was quantified. 3 experiments were performed with 39 starting cryptococci followed total, and each repeat was performed on cells from a different donor.

a. The time between phagocytosis of cryptococci by phagocytes and the formation of PBMC aggregates was measured. Bars represent numbers of swarms formed at each time after phagocytosis. Swarms usually formed almost immediately in less than an hour. However, swarms could form throughout the experiment, though the majority aggregated within 4 hours of phagocytosis.

b. The size of the swarm was determined by drawing around the swarm and measuring the area in square μm. Measurements were made each time a division occurred. Each line is representative of one phagocytosis event leading to the formation of a swarm.
c. The relative fold change for each intracellular cryptococcal cell was measured and compared to the maximum size the swarm reached throughout the experiment. There was a positive linear relationship between the fungal relative fold change and the size of the mass (linear regression $p = 0.0014$, $R^2 = 0.2828$).
d. The size of swarms for aggregates which did not contain cryptococci but were within the same well was measured at the start and end of time lapse videos. Few of these types of aggregates existed and remained within the field of view. Those that did showed variable changes in size. 3 repeats were considered.

a. Vomocytosis of cryptococci from PBMC swarm

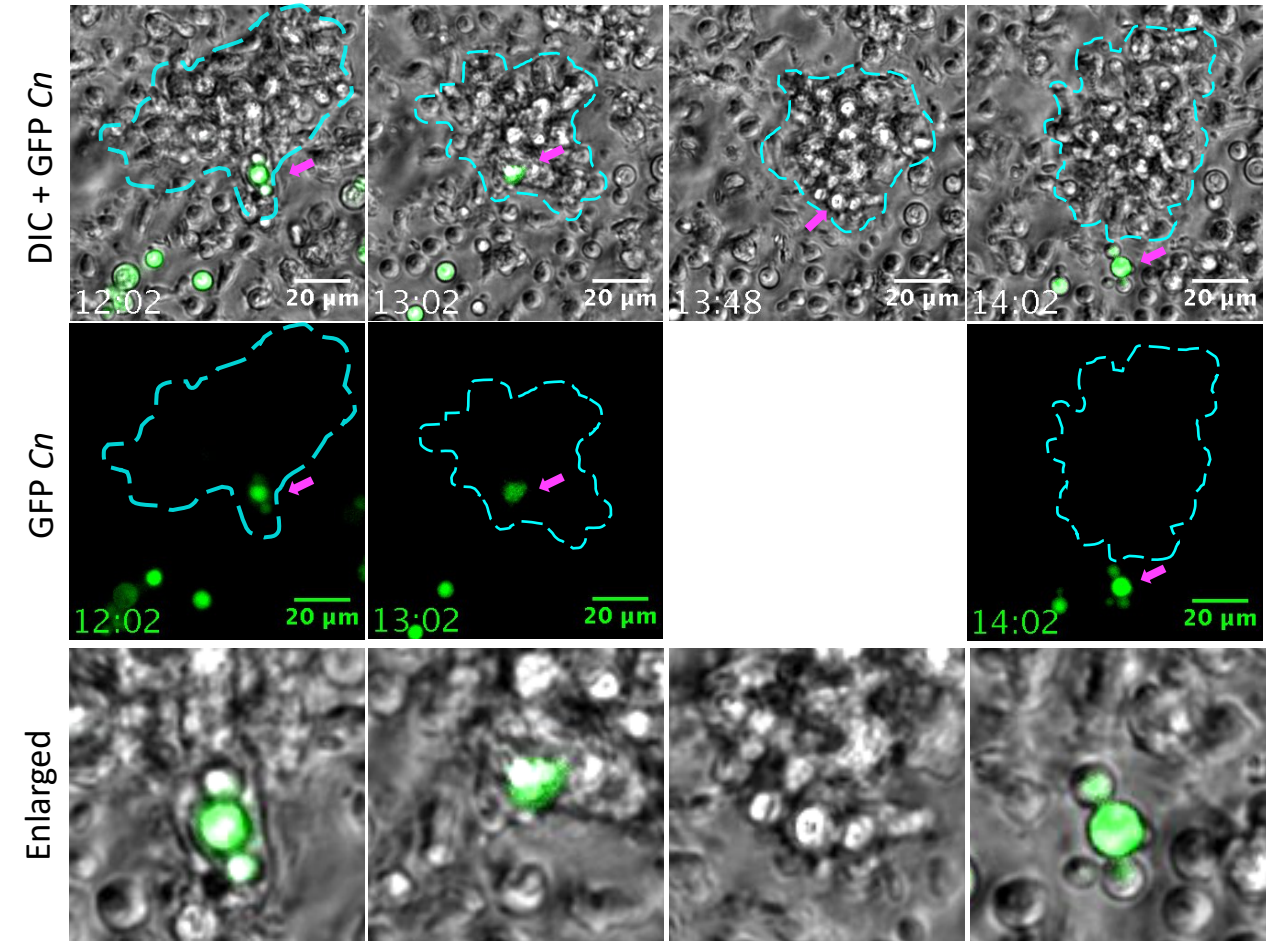

b. *Cryptococcus* with large capsule

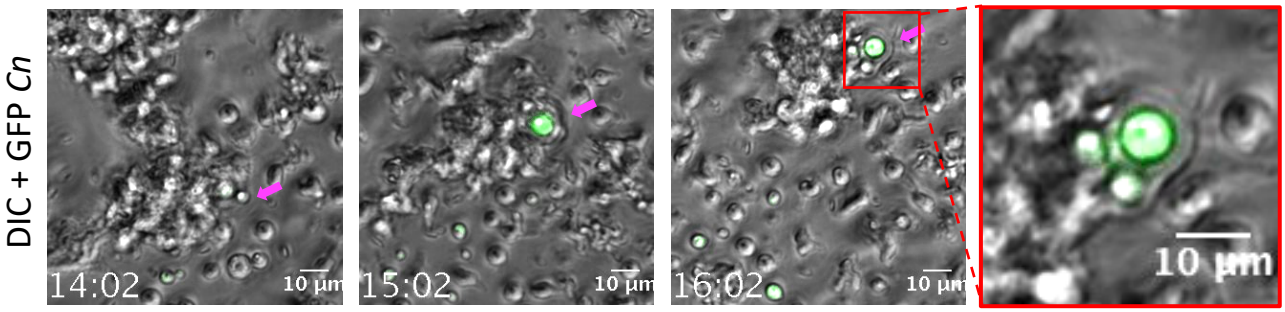

Figure 6.5. Cryptococci escaped from PBMC masses, produced large capsules

Human PBMCs were infected with KN99 GFP *C. neoformans* and followed for 24 hours via time lapse imaging, with an image taken every 2 minutes. Behaviour of cryptococci within PBMCs was noted.

a. Cryptococci were able to escape both from individual phagocytes and from PBMC masses. They were vomocytosed as cryptococcal cells, or escaped the

swarm in phagocytes. The vomocytosis of three joined cryptococcal cells is pictured, with cryptococci in green marked by the magenta arrow. The PBMC mass boundary is marked by cyan dashed lines. One panel is missing because GFP images were taken only once per hour. Scale bars represent 20 μm and the time is shown as hours : minutes. Enlarged images are given below to illustrate intracellular and extracellular states (bottom panel).

b. The formation of an extended capsule formed around a GFP cryptococcal cell during its inhabitation of a PBMC swarm. The magenta arrow marks the location of the GFP cryptococcal cell. Throughout the time lapse this fungal cell with its hazy ring of a capsule was seen to struggle at the edge of the swarm, yet failed to escape. Scale bars represent 10 μm and the time is shown as hours : minutes.

6.5 Cryptococcal proliferation in the presence of PBMCs

As with J774 murine macrophages and human MDMs, I quantified the growth of cryptococci in the presence of PBMCs. I performed 24 hour time lapses of human PBMCs infected with KN99 GFP *C. neoformans*, with an image taken every 2 minutes. By following individual cryptococci I was able to count when each cryptococcal cell replicated. While I followed the intracellular cryptococci for the duration of the time lapse videos, for comparison here I did not include further replications of intracellular cryptococci after a daughter cell vomocytosed from the PBMCs. This is because continuing to count only the intracellular cryptococci would exclude the further replications of cryptococci which had been intracellular yet had vomocytosed and could have potentially contributed to the intracellular numbers of cryptococci; this would underrepresent the proliferative ability of those cryptococci which remained intracellular. While most cryptococci within phagocytes did replicate (Figure 6.6a), those which were extracellular showed faster exponential growth (Figure 6.6b). Again, the doubling time of cryptococci was shorter when in the extracellular environment compared to cryptococci which were intracellular within phagocytes or swarms (Figures 6.6d and 6.6e; one-way ANOVA $p < 0.0001$ when comparing intracellular doubling time to all other conditions). In fact, cryptococci which were intracellular took more than twice as long to replicate compared to those which were extracellular (mean doubling times = 9.34 ± 3.9 hours for intracellular cryptococci, 4.39 ± 1.6 hours for extracellular cryptococci). Cryptococci which had been intracellular but vomocytosed from phagocytes or masses grew more quickly after vomocytosis compared to intracellular cryptococci (Figures 6.6c and 6.6d; mean doubling time = 5.0 ± 3.5 hours).

The fold change was difficult to compare across conditions as the PBMCs and cryptococci proved to be very mobile and frequently left the field of view. As such, I measured the fold change of intracellular and extracellular cryptococci and normalised this by dividing the relative fold change for each fungal cell by the number of hours I managed to follow it (Figure 6.6e – compares fold change over the time followed, and the adjusted fold change mentioned here). While not ideal,

this allowed me to compare the fold change of cryptococci in a way that did not underestimate the replication of those which left the field of view. Again, extracellular cryptococci proliferated better than intracellular cryptococci with a higher fold change, whether normalised or not. Vomocytosed cryptococci did not replicate as much as extracellular cryptococci, though this was likely due to the late timepoints at which they were vomocytosed, limiting the time remaining to observe many replications. While it is possible that there was some negative effect of vomocytosis on replication, and that transferring from an intracellular to an extracellular state may require time to adjust to the change in environment which hindered replication, because doubling times of vomocytosed and extracellular cryptococci were so closely comparable, this is not likely the case. Finally, there was no significant difference between the doubling times of extracellular cryptococci and those in media alone without the presence of PBMCs (Figures 6.6d and 6.6e; one-way ANOVA $p = 0.0567$). While this suggests that over the time considered here there was no extracellular killing or cytotoxic functions of PBMCs against cryptococci, the slightly higher doubling time of extracellular cryptococci in the presence of PBMCs suggests there may have been some slight inhibitory effect on growth. Taken together, these results suggest that human PBMCs limit intracellular growth of cryptococcal cells compared to cryptococci which exist outside of PBMCs.

a.

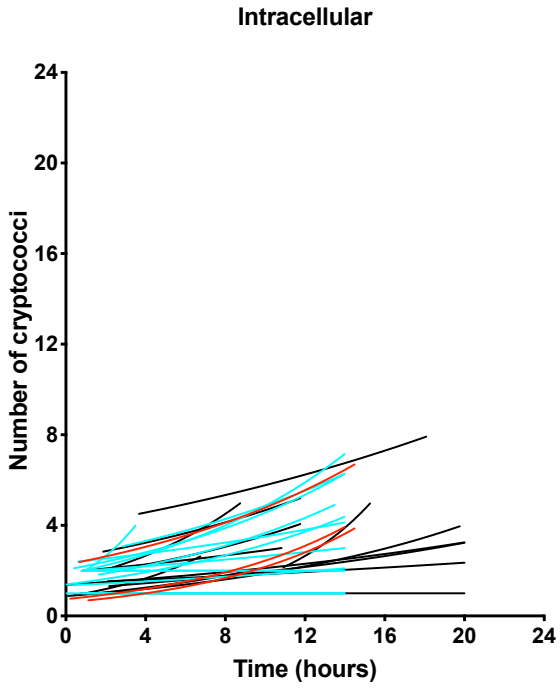

b.

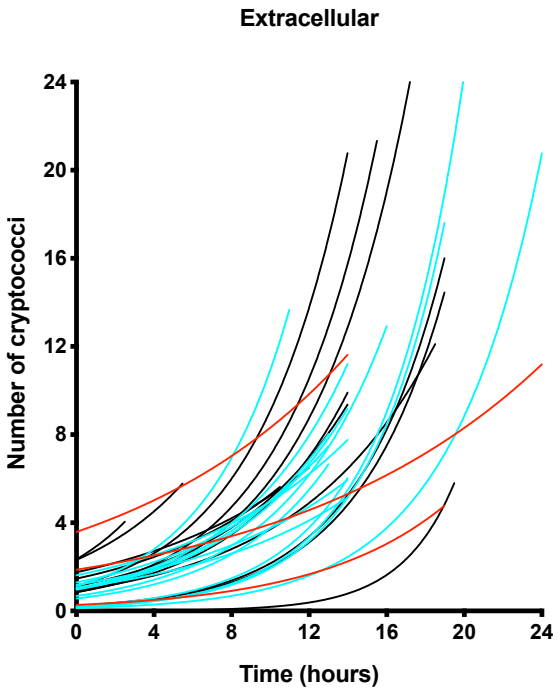

c.

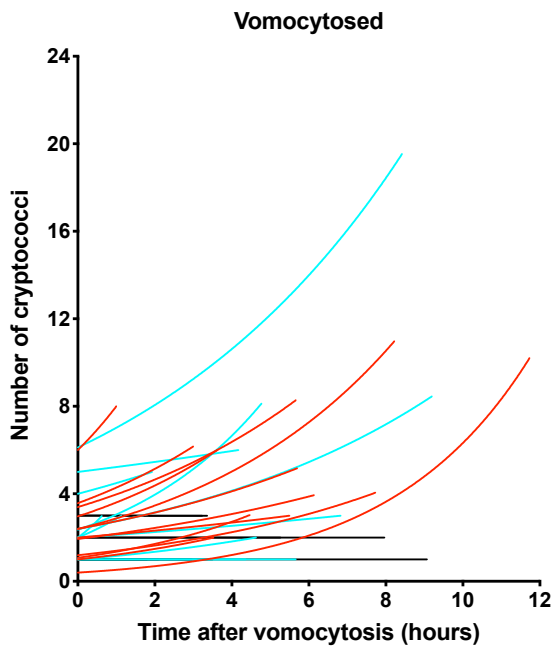

d.

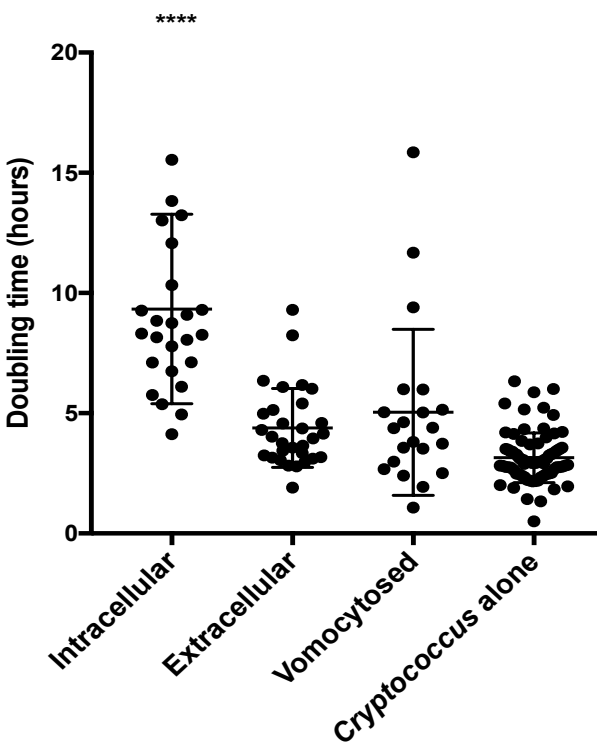

e.

Cryptococci	n	Doubling time (hours) Mean	SD	Fold change Mean	SD	Fold change per hour Mean	SD
Intracellular	39	9.34	3.94	2.62	1.77	0.16	0.11
Extracellular	30	4.39	1.65	11.58	8.39	0.74	0.42
Vomocytosed	33	5.04	3.46	1.75	2.04	0.35	0.47
Cryptococcus alone	79	3.15	1.03	-	-	-	-

Figure 6.6. Cryptococcal replication in the presence of human PBMCs

Human PBMCs were infected with KN99 GFP *C. neoformans* one day after isolation. Time lapse imaging was used to follow the infection for 24 hours, and the replication of individual cryptococci was measured. 3 repeats were performed, with different repeats representing different donors. Each line (a-c) or point (d) represents the growth of one cryptococcal cell, or groupings of mother-daughter cells if the initial cryptococci were buds.

a. The growth of individual cryptococci which were intracellular within phagocytes and PBMC swarms.
b. Quantification of the growth of individual extracellular cryptococci in the presence of human PBMCs.
c. The growth of individual cryptococci which had vomocytosed from phagocytes and PBMC masses.
d. The doubling times of cryptococci which were intracellular, extracellular, vomocytosed, or in SF RPMI media alone. Means and standard deviations are represented. The doubling time was calculated by fitting an exponential curve. Doubling time of intracellular cryptococci was significantly longer than other conditions (one-way ANOVA $p < 0.0001$ when comparing the mean doubling time of each condition to the doubling time of intracellular cryptococci). Cryptococci which were vomocytosed also had a longer doubling time than cryptococci which were alone in media in the absence of PBMCs, though the significance is left off the graph for the sake of clarity (one-way ANOVA $p = 0.0048$).
e. Descriptive statistics comparing the doubling times between cryptococci in different niches. N represents the number of cryptococci followed, with mother-daughter buds counted as one. Fold change of cryptococci is also shown, though for comparison the fold change normalised to the time followed is also given. This is because some cells left the field of view or became difficult to count, and failing to normalise to time may underestimate the growth of some cells in the shortened available timeframe. SD is standard deviation.

6.6 Discussion

The development of fungemia via dissemination from the lung environment to the periphery of the body is an important step that may lead to the development of cryptococcal infiltration of the CNS, yet the interactions between cryptococci and the peripheral immune system remain largely unstudied (Denham and Brown, 2018). Much is known about cryptococcal interactions with macrophages, but to fully understand the immune response to *Cryptococcus neoformans* the involvement of a more robust immune response must be considered. In this chapter I have shown that T cells and monocytes responded to cryptococcal infection by forming aggregates of immune cells after phagocytosis of cryptococci by monocytes, and that the intracellular environment was prohibitive to cryptococcal growth in the presence of human PBMCs *in vitro*. However, these interactions failed to halt cryptococcal division, and cryptococci were able to escape from immune capture even in a theoretically immunocompetent experimental system. Studying how cryptococci interact with a robust immune subset provides insight into immune control of peripheral fungemia.

6.6.1 Phagocytosis of cryptococci by peripheral immune cells

In the course of infection, phagocyte responses to invading pathogens may determine whether the pathogen is destroyed, or whether it survives to propagate infection. During infection, cryptococci may be phagocytosed or may evade capture to proliferate extracellularly. Because interactions between phagocytes and cryptococci are important for controlling cryptococcal infection, studying phagocyte responses during infection illustrates host defensive behaviours and helps us to understand how control is achieved or lost. Investigating the interaction between cryptococci and phagocytic cells in the setting of a robust immune cell cohort gives us an idea as to what happens to between host immune cells and this fungal pathogen during peripheral cryptococcal infection.

While bloodstream colonisation is a hallmark of many infections, infection assays typically look at differentiated immune cells. However, PBMCs are important in

infection, as they encounter pathogens in the periphery and as such must mediate infection control prior to specific differentiation. For example, the measles virus is detected in the blood of patients after the onset of rash, and PBMC monocytes phagocytose the virus to prevent uncontrolled growth throughout the body (Esolen et al., 1993). Similar to the immune response in cryptococcosis, the inflammatory state of monocytes determines the anti-microbial response in visceral leishmaniasis (VL) (Singh et al., 2018). Patients suffering from VL have increased CD14+ monocyte frequency at presentation, and monocytes which have anti-inflammatory phenotypes show decreased phagocytic ability and reduced production of reactive oxygen species, which ultimately result in poor infection outcome (Singh et al., 2018). In VL infection peripheral blood monocytes combat infection, though appropriate activation is required for effective control. PBMCs are able to phagocytose *Lacazia loboi,* the causative agent of lobomycosis, while a soluble factor secreted by human PBMCs stimulates *Candida albicans* to produce thick biofilms which inhibit PBMC phagocytosis of *Candida* (Chandra et al., 2007; Vilani-Moreno et al., 2004). Thus, PBMCs and peripheral monocytes interact with invading pathogens in different ways, and understanding the relationships between this circulating immune population and pathogenic threats is vital in understanding the effect of immune intervention on infection progression.

After infection with KN99 *C. neoformans*, PBMC-derived monocytes phagocytosed cryptococci rapidly, most commonly within two hours of infection. The rapid phagocytosis rate here confirms that monocytes were capable of rapid response to invading cryptococci before they differentiated into macrophages. This is important, because the progression of cryptococcal infection from the initial site of infection in the lung (Velagapudi et al., 2009) to sites throughout the body likely involves the interaction of cryptococci with cells beyond differentiated alveolar macrophages. As such, cryptococcal interactions with peripheral blood mononuclear cells is likely an important step in the propagation of peripheral fungemia. Here, I have shown that peripheral monocytes were capable of responding to cryptococcal threat.

6.6.2 Immune cell recruitment and aggregate composition

While phagocytosis of invading pathogens is often imperative for control of infection, the behaviour of phagocytes after engulfing invading pathogens further determines the progression of infection. For example, recruitment of additional immune cells to contain the microbe is often necessary for control by the immune system. In this chapter I described how human PBMCs responded to cryptococcal infection after phagocytosis, especially via the formation of PBMC aggregates. After phagocytosis of cryptococci by CD14-labelled monocytes, additional PBMCs frequently swarmed to join the infected monocyte. Events like this have been described previously by Siddiqui et al. who noted that after pre-stimulation of human PBMCs with heat-killed *C. neoformans*, aggregates of PBMCs formed around the engulfed cryptococci (Siddiqui et al., 2006). This study looked at host cell aggregates after 12 days of pre-stimulation with heat-killed cryptococci followed by 6 days of live infection, and represents the host response after immune activation to cryptococcal infection has been mounted. The time points I used for my assays were representative of initial introduction of cryptococci without any immune pre-stimulation, which may occur after cryptococci evade alveolar macrophages and escape from the initial site of infection to disseminate throughout the body. Here, the formation of PBMC aggregates after the phagocytosis of cryptococci demonstrated an interesting reaction by a robust immune model of infection, which resulted in the slowed growth of intracellular cryptococci.

In the study by Siddiqui et al., cells were labelled with CD68 and CD3 to mark phagocytes and lymphocytes, respectively; while the imaging was not shown in the paper, the presence of phagocytic and lymphocytic populations within the human PBMCs is consistent with the antibody labelling I observed in my experiments (Siddiqui et al., 2006). Indeed, at both 0 and 24 hours, CD3+ lymphocytes and CD14+ phagocytes cells were labelled in the donor PBMCs and composed the majority of the PBMC aggregates, particularly at 0h before the adherence of T cells began to diminish. These cell types are important in the fight against cryptococcosis as monocytes eventually differentiate into macrophages after activation, with input

from T cells. Monocytes may also differentiate into DCs which traffic to lymph nodes to activate antigen-specific T cells to respond to infection. As discussed in the introduction, the actions of these differentiated T cells are important for limitation of cryptococcal infection. It is worth noting that additional cell subsets were present within the isolated PBMCs, though labelling of CD3+ and CD14+ cells showed that they made up the majority of the cells included, besides platelets.

6.6.3 Cryptococcal granulomas

The formation of PBMC aggregates during cryptococcal infection calls into question the purpose of such assembly. Many infections result in the production of granulomas, including the bacteria *Mycobacterium tuberculosis*, *Brucella,* and *Listeria monocytogenes*, as well as fungal infections such as *Histoplasma capsulatum*, *Coccidioides immitis*, *Blastomyces dermatitidis*, and *Candida albicans* (Bingöl et al., 1999; DiCaudo and Connolly, 2001; Goel et al., 1996; Heninger et al., 2006; Mielke et al., 1989; Thron and Wiethtilter, 1982). Granulomas have also been described during cryptococcal infection. Typically, *C. gattii* infections are associated with granulomatous formations in the lung while *C. neoformans* infection is associated with pulmonary lesions, though granuloma formation is possible during *C. neoformans* infection (Chen et al., 2000b; Galanis and MacDougall, 2010; Mitchell et al., 1995).

Different types of cryptococcal granulomas are classified by the involvement of monocytic precursors and giant-cells, the density of the aggregates, and the disruption caused to local tissues (Shibuya et al., 2005). In a post-humous study of patients who succumbed to cryptococcal infection, cryptococcal granulomas were characterised by densely packed monocytes and macrophages with multinucleated giant cells containing intracellular cryptococci. While there was evidence for the involvement of T cells, CD4+ lymphocytes in cryptococcal granulomatous lesions were absent in HIV patients unless they had received highly active antiretroviral therapy (Shibuya et al., 2002, 2005). Thus, while CD4+ T cells are characteristic of cryptococcal granulomas, the presence of T cells depends on the host immune state

and may explain why AIDS patients fail to induce T cell granulomatous infiltration. A murine model of cryptococcal infection in which mice were immunised with IFN-γ-producing *C. neoformans* to induce protection before a second challenge with the fungus, showed that the protective phenotype was associated with the recruitment of macrophages and lymphocytes, with CD4+ cells contributing to the granulomatous formation (Wozniak et al., 2009). Several additional murine studies have shown that granulomas in the lungs were densely packed with mononuclear cells and macrophages with the addition of leukocytes, resulting in dense aggregates of organised immune cells (Osterholzer et al., 2009; Zhang et al., 2010). A rat model of cryptococcal infection showed that granulomas were surrounded by CD3+ T cells and CD45R+ B cells, though this varied between cryptococcal strains (Kobayashi et al., 2001). Thus, while populations of immune cells contribute to the formation of granulomas around cryptococcal cells, the composition of these aggregates can vary based on the immune state of the host and the infection model.

It is interesting to consider the role of granulomas during infection because though the immune system may hinder the propagation of many types of infection, pathogens are cunning and can exploit host responses for their own benefit. *Mycobacterium tuberculosis* is the pathogen perhaps most famous for the formation of granulomas, which until recently were believed to be purely protective for the host. Studies investigating *Mtb* infection in zebrafish using *Mycobacterium marinum* (*Mm*), a close relative of *M. tuberculosis* that is a natural pathogen of fish, have enabled the *in vivo* imaging of *Mycobacterium* infection and granuloma formation. A study by Volkman and colleagues showed that increase in bacterial load was not initiated until after the formation of macrophage aggregates, suggesting that granuloma formation was induced by the bacteria for the purpose of intracellular replication (Volkman et al., 2004). Furthermore, mutation of the bacterial gene encoding the virulence factor RD1 resulted in failure to initiate aggregate formation and subsequent macrophage recruitment. This indicated a role for this bacterial virulence factor in the initiation of aggregate formation which was ultimately beneficial for bacterial growth (Volkman et al., 2004). Another study showed that formation of *Mm*-infected granulomas resulted from the recruitment

of *uninfected* macrophages to the granuloma by the bacteria; subsequent apoptosis of infected macrophages released intracellular bacteria which infected a higher multiplicity of the newly recruited macrophages, thus propagating intracellular infection and enabling granuloma expansion (Davis and Ramakrishnan, 2009). While granuloma formation during *Mycobacterium* infection may be protective for the host, the bacteria may manipulate phagocytes to expand amongst the immune cell population within the granuloma.

The function of cryptococcal granulomas is to limit proliferation and dissemination, and to contain the pathogen if killing is hindered (Pagán and Ramakrishnan, 2018). However, as is the case with *Mycobacterium* infection, it is possible that granulomas may be manipulated for exploitation by the pathogen. Throughout the course of my PBMC infections, congregations of PBMCs composed of CD3+ and CD14+ cells formed around cryptococci to produce structures similar to those described in the lung. The common presence of mononuclear cells in cryptococcal granulomas suggests that the aggregates I saw throughout the time lapse videos may represent the generation of immune masses which are analogous to early granulomas. During infection, immune cells were attracted to infected phagocytes and produced masses, many of which showed an increase in recruitment and size throughout the course of the experiment. This may have been recruitment for the sake of immune control by PBMCs, or may have been recruitment by cryptococci for the potential exploitation of the intracellular niche. If the recruitment was for the benefit of cryptococci, you would expect an increase in cryptococcal fold change or an enhanced rate of proliferation. However, intracellular cryptococcal proliferation was considerably slowed compared to cryptococci which remained extracellular, suggesting an inhibitory role for the PBMC aggregates on cryptococcal growth. Thus, in early PBMC swarm formation, here induced by the phagocytosis of cryptococcal cells, the formation of monocyte- and lymphocyte-derived PBMC swarms was not beneficial for cryptococcal growth, and instead was likely enforced as a measure of immune control.

6.6.4 Inhibition of cryptococcal growth by human PBMCs

The effect of PBMC interaction with cryptococci must be considered as these interactions may alter the activity and infection success of cryptococci. Therefore, the impact of immune intervention on cryptococcal replication must be considered carefully. Despite being significantly slowed, cryptococcal intracellular replication was not altogether halted by PBMCs. It is possible that the time given for cryptococcal expansion was not sufficient, though this seems unlikely given that extracellular growth was exponential from the start. The slowed intracellular growth of cryptococci within phagocytes and PBMC aggregates may have been a strategy employed by the cryptococci to remain in a stable intracellular environment in order to enable to long-term survival. Rat models of cryptococcal infection show that cryptococci persist within the lung, and are contained within macrophages and granulomas (Goldman et al., 2000). Thus, cryptococci may have slowed replication to remain within the intracellular niche and enable persistence in an environment in which they may survive and replicate.

The adoption of a quiescent state may be employed to reactivate latent infection during a later period of immune susceptibility. Serological evidence shows that children without symptomatic cryptococcosis have antibodies which are reactive with cryptococcal proteins, suggesting potential quiescent infection or, more likely, prior defeat of this pathogen by the host immune system (Goldman et al., 2001). Identification of cryptococcal isolate subgroups has shown that cryptococcosis patients in Europe encountered the offending cryptococci whilst in Africa, sometimes after a great deal of time had passed before the onset of symptomatic infection, supporting the idea that latent cryptococcal infection may lie dormant before manifestation of clinical symptoms (Garcia-Hermoso et al., 1999). Latent infection and subsequent reactivation is also defined for tuberculosis, human cytomegalovirus, herpes simplex virus, histoplasmosis, and many other infections including various mycoses (Brunet et al., 2018; Gideon and Flynn, 2011; Mence Richaud et al., 2014; Numazaki et al., 1995; Yao et al., 2014). Furthermore, within the host diverse subsets of cryptococci develop over time; these subsets show

varied growth rates and stress responses. This supports the idea that some cryptococcal subpopulations may adopt characteristics that enable dormant infection (Alanio et al., 2015). While the literature supports the possibility of cryptococcal quiescence and long-term dormancy, the likelihood of cryptococci adopting a dormant phenotype during the timeframe considered here is unlikely. Furthermore, because dormancy often results from response to environmental stress or population cues, it is improbable that sufficient cellular stress was provided in the infection assays here to induce such a state.

While granulomas are associated with infection dormancy in some diseases, the more plausible explanation for the slowed fungal growth was control by the immune cells, as I have demonstrated previously in the case of human MDM and murine J774 macrophage infection. Interestingly, the doubling time for intracellular cryptococci was considerably longer in the human MDM model of infection compared to the human PBMC assay (mean doubling times with SD = 23.89 ± 15.12 and 9.34 ± 3.94 hours for cryptococci in MDMs and PBMCs, respectively). This shows that control over intracellular cryptococcal growth was vastly more restrictive in the MDM model of infection compared to PBMC infection, suggesting that differentiated human MDMs more effectively control intracellular cryptococcal growth *in vitro*.

6.6.5 Cryptococcal behaviour during PBMC infection

In this chapter I also described behaviours exhibited by cryptococci within PBMC aggregates which demonstrate various reactions of cryptococci to phagocytosis by peripheral cells, and thus events that may occur during fungemia. A study by Alvarez et al. showed that *C. neoformans* could extrude from human peripheral monocytes into the extracellular environment (Alvarez et al., 2009). Cryptococci have also been shown to escape from macrophages non-lytically through vomocytosis (Johnston and May, 2010; Ma et al., 2006). In the assays described here, cryptococci vomocytosed non-lytically from immune cells, and also escaped from PBMC aggregates within a monocyte or as free cryptococci. This is interesting, as a similar behaviour is observed during *Mycobacterium* infection in zebrafish. During

Mycobacterium infection, infected macrophages which had been recruited to sites of granulomatous infection for bacterial expansion split away from the main granuloma and travelled to throughout the body to seed secondary granulomas, thus propagating the infection (Davis and Ramakrishnan, 2009). This is one possible explanation for the division of PBMC masses into the original aggregates that existed before joining together, and the detachment of individual infected monocytes from PBMC masses. However, just as swarm formation was seen without intracellular cryptococci, the formation and subsequent split of these masses may have been due to PBMC motility in culture. Nonetheless, vomocytosis is one method by which cryptococci escape phagocytes to exist extracellularly, enabling them to freely divide and disseminate infection, and was observed during cryptococcal infection of peripheral immune cells.

Throughout the course of the experiments, few cryptococci were observed which appeared to be bordered by thick halos. Though the isolation of cryptococci from PBMCs after the conclusion of time lapse assays did not produce sufficient pellet to effectively stain and image for capsule, the halo around these cryptococci strongly suggested that it was enlarged capsule. This is one method by which cryptococci protect themselves from harmful reactive species within host cells (Zaragoza et al., 2008). Furthermore, throughout the time lapse assay little, if any, death of cryptococci was noted. Occasionally the fading of cryptococcal GFP signal was seen, though this occurred only in 6% of followed cryptococci and could have been the result of cryptococcal destruction, failure to follow the cryptococcal cell between images (taken 2 minutes apart), or obscuring of the signal due to the 3D structure of the aggregates. While rat models of infection showed that cryptococci remained within macrophages and aggregates for extended periods of time, despite granuloma formation and reduction in fungal burden due to iNOS activity (Goldman et al., 1996, 2000), in the assays I performed here the lack of cryptococcal death was more likely due to inadequate immune activation *in vitro* and the relatively short timeframe considered.

6.6.6 Future work and conclusions

While CD3 and CD14 antibody labelling revealed that T cells and monocytes were the primary cell subsets in donor PBMCs and granulomatous aggregates, additional immune cell populations may have been present and active in the experiments described. As discussed in the chapter introduction, a multitude of immune cells help to control cryptococcal growth during infection. Because the immune system is a network of many cooperating cell types, the participation of interacting components is important. Here, monocytes and T cells were the focus because the interaction between these cells types is of particular importance in cryptococcosis, especially in terms of macrophage action. Future studies should examine the function of additional immune cell subsets in early granuloma formation and the effect they have on intracellular cryptococcal replication. The incorporation of flow cytometry assays may provide additional insight into the composition of PBMC aggregates, and illuminate how aggregate composition affects cryptococcal growth.

Initially, the relative contribution of T cells was to be determined by comparing phagocytosis and inhibition of cryptococcal replication in the presence and absence of different T cell subsets, possible through the repeated PBMC donation from individual donors and isolation of various T cell subsets. However, time did not permit the performance of these assays. Additional studies should compare the effect of T cell-generated cytokines on PBMC inhibition of cryptococcal growth, and should determine the contribution of different T cell subsets to PBMC mass formation and control of cryptococcal growth. This is important as different T cell subsets produce different cryptococcal infection outcomes. Media that more closely resembles the human peripheral immune system may also provide insight into host-pathogen interactions during cryptococcosis.

Finally, future work should investigate the effect of PBMC aggregates on intracellular cryptococcal replication at longer timepoints representative of more advanced infection. This may prove difficult as cryptococcal growth rate was determined by following individual cryptococci in time, which would be implausible

to do for time periods much longer than the 24 hours considered here. However, IPR assays and flow cytometry techniques may prove helpful (Evans et al., 2017; Ma et al., 2009; Voelz et al., 2009).

In this chapter I have demonstrated that human PBMCs effectively phagocytose cryptococci soon after infection (Figure 6.7). PBMCs may form aggregates which slow the intracellular proliferation of cryptococci compared to those which remain extracellular. Cryptococci exhibit behaviours consistent with immune escape which may facilitate extracellular dissemination. The results presented here demonstrate how immune cells may react with cryptococci in the periphery, which is important for the control of widespread fungemia. The actions of peripheral blood mononuclear cells in cryptococcosis, though largely ignored by current literature, may be important in containing cryptococcal disease after escape from the primary infection site in the lung before the infiltration of cryptococci into the CNS. The work I have presented here represents a more immunocompetent model of immune cell interactions with *Cryptococcus neoformans* than presented throughout this body of work, and may serve as a baseline for specific investigations into human peripheral immune cell response to cryptococcal infection in the future.

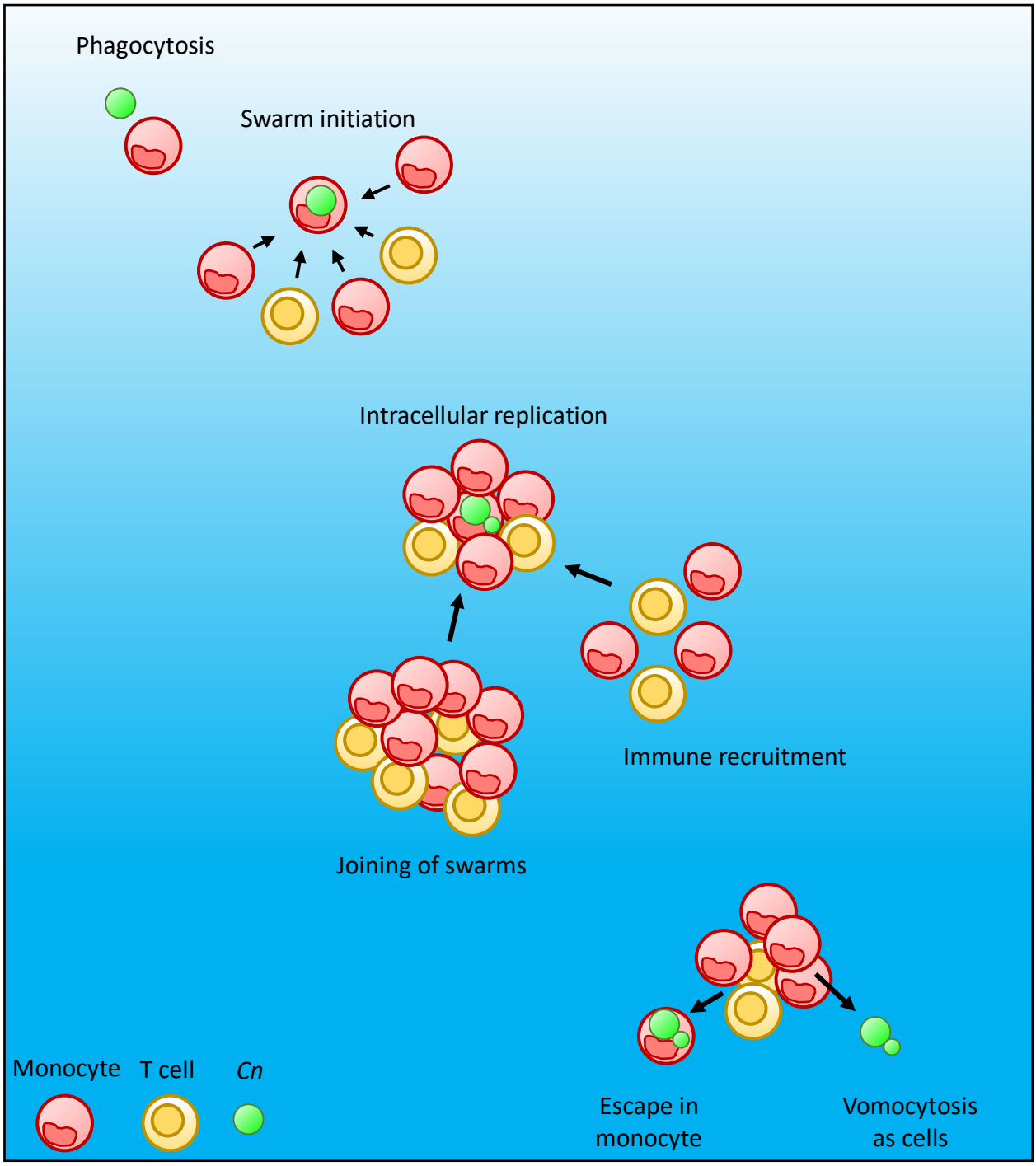

Figure 6.7. Human PBMC response to cryptococcal infection

When PBMCs are infected with *C. neoformans,* monocytes (red) phagocytose the invading fungal cells. Swarms of monocytes and T cells (yellow) often form in response. Inside of swarms the cryptococci may replicate. Immune cells are recruited, and swarms may join and separate. Swarms may persist or dissolve, and cryptococci may escape either inside of a monocyte which splits off, or via vomocytosis into the extracellular environment.

Chapter 7. Final discussion

Interactions between host and pathogen drive the progression of infection and largely determine the outcome of disease. Cryptococcal meningitis kills over 180,000 people per year (Rajasingham et al., 2017), affecting mainly immunocompromised people whose immune response fails to effectively clear infection, especially people who suffer from HIV/AIDS infection. Macrophages are especially important in the control of this infection, though *Cryptococcus* may exploit this host niche for replication and dissemination. As such, how this facultative intracellular pathogen interacts with the macrophage intracellular niche must be understood to discern what decides the outcome in the fight between immune control and pathogenic success. As human cryptococcal infection outcome is incredibly variable, both in HIV-negative (Pappas et al., 2001), and HIV-positive patients (Jarvis et al., 2014; Lee et al., 2011), understanding the complex and variable relationship between fungal cells and host phagocytes provides insight into the complex infection outcomes seen in real-life cryptococcal infection. How macrophages respond to cryptococcal infection, and how cryptococci in turn respond to immune control, are therefore important factors which must be studied to understand how host-pathogen interactions affect cryptococcal infection outcome.

7.1 Evidence for the individuality of *Cryptococcus*-macrophage interactions

The ability of pathogens within a population to coordinate gene expression, growth, and virulence is reported for many infections. A study by Albuquerque et al. showed that when conditioned media (CM) from high-density cryptococcal culture was added to low-density culture, the cryptococci grew at a faster rate; furthermore, dilution of CM produced a dose-dependent effect on the enhanced growth rate, suggesting that a factor secreted by cryptococci at high density in CM induced fungal proliferation (Albuquerque et al., 2014). Albuquerque also suggested that the secreted factor may affect cryptococcal melanisation and biofilm growth, factors

which could affect cryptococcal virulence and interactions with host phagocytes. Cooperation amongst cryptococci to promote growth and virulence is therefore important, and must be considered to discern if the pathogen population cooperates to prevent phagocytosis and to manipulate the macrophage intracellular niche.

While Albuquerque et al. showed that cryptococci may utilise quorum sensing to promote growth in culture, to discern if these effects alter phagocyte-pathogen interactions, the effect of fungal dose on *Cryptococcus*-macrophage interactions must be investigated. Quorum sensing amongst *Histoplasma capsulatum* induces the yeast cells to produce cell wall glucans at high density; this effectively inhibits recognition by host macrophages, and may protect the yeast from the harsh intracellular environment should phagocytosis occur (Kügler et al., 2000; Rappleye et al., 2007). To determine if the multiplicity of *Cryptococcus neoformans* affects uptake by macrophages, I compared the percentage of macrophages which phagocytosed cryptococci, and the number of cryptococci which were phagocytosed, over increasing levels of fungal burden. I showed that as the multiplicity of cryptococcal infection increased, percentage of infected macrophages and the number of engulfed cryptococci also increased. Here, there was no cooperation amongst cryptococci to avoid phagocytosis as higher initial burden did not result in lower uptake; there was also no cooperation amongst macrophages to enhance uptake based on the level of cryptococci present, as the proportion of infected macrophages increased linearly with dose. Thus, in both J774 macrophage and human MDM models of cryptococcal infection, fungal burden did not confer resistance to cryptococci or induce enhanced uptake activation of macrophages. In fact, because phagocytosis increased linearly with cryptococcal infection, the likelihood of a macrophage phagocytosing a cryptococcal cell, or the likelihood of a cryptococcal cell becoming phagocytosed, was due to a single rate determining uptake. Here, each phagocyte-pathogen interaction was determined by encounter, irrespective of cooperation amongst cryptococci or amongst macrophages, and supports the idea that each *Cryptococcus*-macrophage interaction was an individual infection (Figure 7.1).

I also determined the effect of fungal dose on macrophage control of intracellular replication. Because pathogens can upregulate factors which enhance virulence and exploitation of host cells, the effects of infection dose on proliferation must be determined. During J774 infection the fungal dose did not affect the intracellular replication rate of cryptococci, suggesting that cryptococci did not cooperate to upregulate replication, and that macrophages did not become overwhelmed to permit excessive intracellular replication at high fungal doses. This is supported by work in zebrafish showing that phagocytosis failed to plateau at high infection doses (Bojarczuk et al., 2016). Replication rates of intracellular cryptococci did grow longer as the number of cryptococci within MDM phagosomes increased, suggesting that cryptococci downregulated replication or that macrophages enhanced control over intracellular replication when more cryptococci occupied the intracellular niche. However, if considering total infection dose (extracellular cryptococci added to macrophage wells), macrophages did not relinquish control over cryptococcal replication as infection dose increased. Again, fungal dose did not enhance or inhibit either cryptococcal intracellular parasitism or macrophage control, further supporting that fungal density does not induce concerted action and that macrophage-*Cryptococcus* interactions must be considered individual infections.

Considering individual interactions is important as these interactions can result in invading pathogens parasitising the macrophage niche and clonally expanding to propagate infection, *or* can result in the destruction of the pathogen and clearance by the host (Grant et al., 2008). The combination of these host-pathogen interactions within the host produces a multitude of different infection outcomes, and thus the heterogeneity in these interactions drives disparate infection outcomes. In fact, I showed that during zebrafish larva infection outcome was variable based on initial fungal burden, especially at low initial fungal burdens, supporting the idea that initial infecting burden does not determine infection outcome, and that encounters between cryptococci and macrophages must be considered individually.

While these results show that each *Cryptococcus*-macrophage interaction should be considered an independent interaction, future work should explore the effect of conditioned media on the macrophage response to cryptococcal infection. It would be interesting to see if some factor in the media induced cryptococci to avoid phagocytosis, or if the addition of this media encouraged cryptococci to alter replication rates inside of macrophages. The macrophage response to coordinated cryptococcal growth may illustrate enhanced phagocytosis in response to a higher number of encounters resulting from enhanced growth, or may show that uncontrolled fungal growth is detrimental for macrophage control of infection.

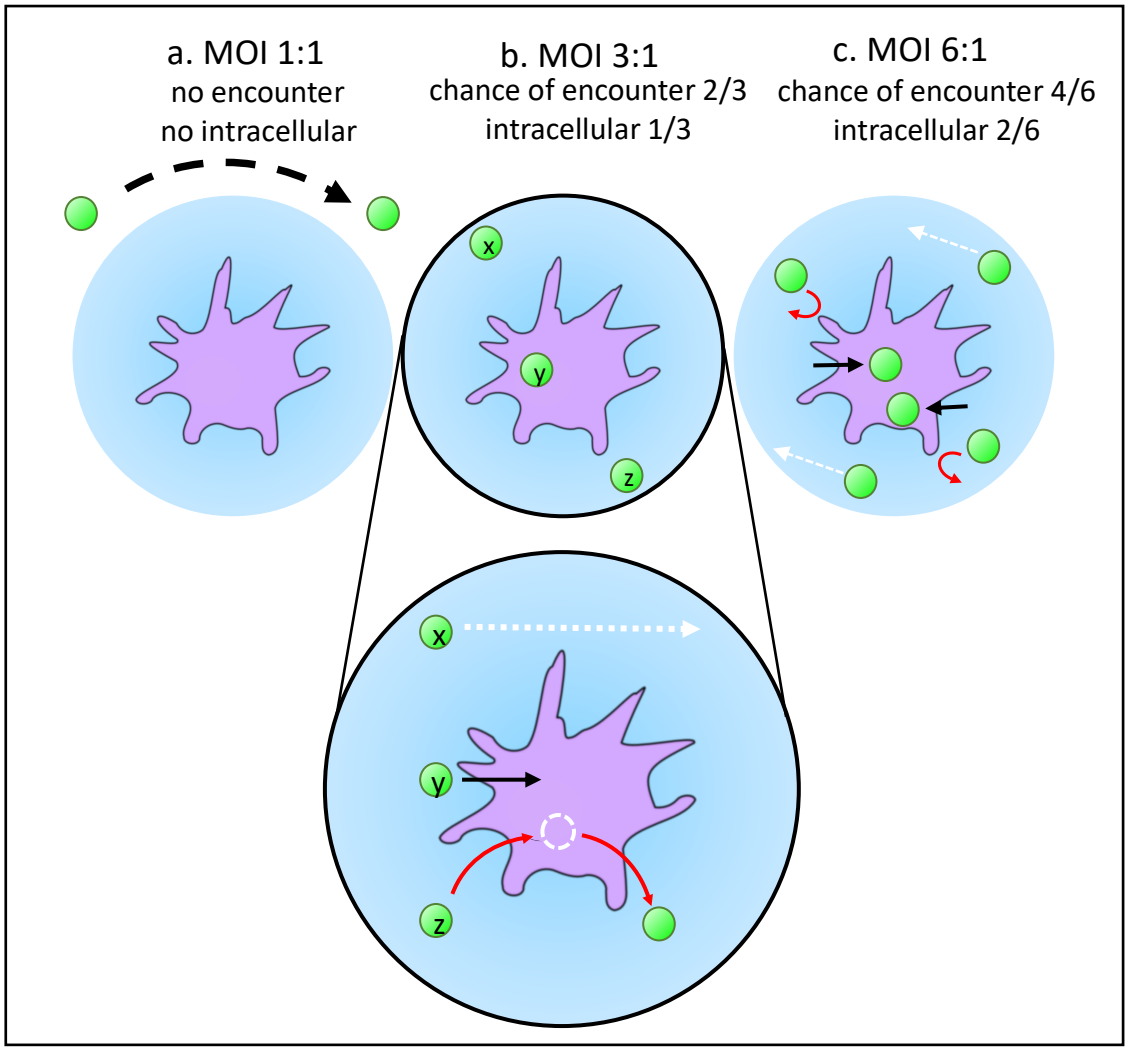

Figure 7.1. *Cryptococcus* interactions with macrophages are independent of one another and rely on chance of encounter

a. At low MOI the chance of a macrophage meeting a cryptococcal cell is low and may not occur.
b. As the MOI increases the chance of encounter increases and results in a higher rate of phagocytosis. The outcome of individual *Cryptococcus*-macrophage encounters may include:
    x. white arrow - failure to encounter
    y. black arrow - successful phagocytosis
    z. red arrow - phagocytosis and subsequent vomocytosis.

    These interactions occur in different macrophages or in subsequent encounters with one macrophage. One macrophage is shown for clarity.
c. As the MOI increases the chance of macrophage-*Cryptococcus* encounters increases with dose. Independent interactions occur between macrophages and cryptococci for each individual encounter.

7.2 Cryptococci replicate more slowly within the macrophage intracellular niche

Because *Cryptococcus neoformans* is a facultative intracellular pathogen, intracellular and extracellular behaviours must be considered. This is especially important as different behaviours during intracellular and extracellular phases may be required for different stages of pathogenesis, with special emphasis on cryptococcal replication. For example, several studies have shown that *Cryptococcus* may use host macrophages as a vehicle to escape the lung environment to facilitate dissemination to the central nervous system via a 'Trojan horse' method (Charlier et al., 2009; Chretien et al., 2002; Santiago-Tirado et al., 2017; Walsh et al., 2019). If CNS dissemination was the goal, excessive intracellular proliferation of cryptococci resulting in macrophage lysis would be detrimental (Feldmesser et al., 2000), preventing cryptococci from using the macrophage as a vehicle to mediate transgression of the blood-brain barrier (Figure 7.2a). Thus, for manipulation of the macrophage intracellular niche as a method of dissemination, limited intracellular replication may be advantageous.

For extracellular growth, a faster rate of replication is likely to be beneficial to cryptococci. *In vivo*, the yeast must adapt to the host environment before replication may commence, resulting in a delay in extracellular growth (Alanio et al., 2015; Bojarczuk et al., 2016). A fast rate of extracellular replication may be important for infection after the initial delay in growth, enhancing fungal burden after infection has been established. For example, a high rate of extracellular growth may enable the cryptococci to propagate infection quickly after escaping from macrophages in target tissues such as the central nervous system. Furthermore, because extracellular cryptococci are vulnerable to attack by host immune cells and antimicrobial effector molecules, fast extracellular growth may be required by the cryptococci to produce enough cells to increase the likelihood of some cells avoiding destruction, enabling propagation of infection by the survivors. Bojarczuk et al. showed that during zebrafish infection, cryptococci which were not phagocytosed quickly enough replicated extracellularly and produced excessive capsule which

interfered with phagocytic uptake by macrophages (Bojarczuk et al., 2016). Here, expedient extracellular growth enabled cryptococci to replicate to a high level extracellularly, avoid phagocytosis due to excessive capsule, and subsequently divide more. Thus, fast extracellular proliferation may enable cryptococci to avoid phagocytosis, colonise host tissues, and contribute to fungal burden after the onset of infection (Figure 7.2b).

To discern if the intracellular and extracellular location of cryptococci affected fungal replication, I quantified the proliferation of individual cryptococci which were intracellular and extracellular. I found that cryptococci which were not contained within macrophages grew to a higher number, and did so at a faster rate. Because extracellular growth was faster than intracellular growth, macrophages controlled the rate and level of intracellular cryptococcal replication, illustrating that during cryptococcal infection macrophages inhibit intracellular cryptococcal growth. Macrophage control of cryptococcal infection was confirmed in zebrafish where macrophage depletion resulted in higher fungal load.

While macrophages controlled intracellular replication they did not manage to fully inhibit cryptococcal proliferation, allowing cryptococci to utilise the macrophage intracellular niche for replication. Studies have shown that cryptococci prevent phagosome acidification and proliferate within these mildly acidic phagosomes, though the harsh environment reduces budding compared to growth of cryptococci in media (Smith et al., 2015). In my experiments, cryptococci divided more slowly within macrophages, supporting this, and while lower intracellular fungal replication rate may be viewed as inhibition by macrophages, it may also represent slower replication in attempt to avoid depleting the niche. Cryptococci may also replicate more slowly intracellularly to avoid exiting from the Trojan horse prematurely before the final (theoretical) destination is reached. In fact, cryptococci which had been intracellular but had escaped from macrophages showed resumption of fast extracellular growth after vomocytosis, supporting the hypothesis that cryptococcal growth rate depends on context, though further work is prompted to determine if the stage of pathogenesis affects this or if replication is

determined by environmental niche. Because the switch from slow intracellular growth to fast extracellular growth occurred so quickly after vomocytosis, the slower intracellular growth rate in these assays was likely due to constraints imposed by the intracellular environment rather than by the expression of genes, freeing cryptococci to replicate faster almost immediately once free from the restrictive intracellular niche. Nonetheless, replication of cryptococci was limited inside of macrophages, illustrating that one way by which macrophages control cryptococcal infection is through reducing replication compared to extracellular cryptococci, though whether this is due to the actions of macrophage or cryptococci remains unclear.

Future work should attempt to discover if macrophages similarly control intracellular cryptococcal replication in a media that is more representative of *in vivo* conditions, mimicking nutrient and cytokine conditions. This may illustrate how the real-life infection conditions affect cryptococcal growth and how immune factors affect macrophage control of infection. This may also illustrate an extracellular growth rate more representative of the host environment compared to that of provided media. Future work should also perform these assays using mutant cryptococci which show different abilities to parasitise the macrophage intracellular niche, and different types of macrophages which show varied abilities to control intracellular growth. In doing so, the differences between macrophage control and cryptococcal parasitism may be better understood.

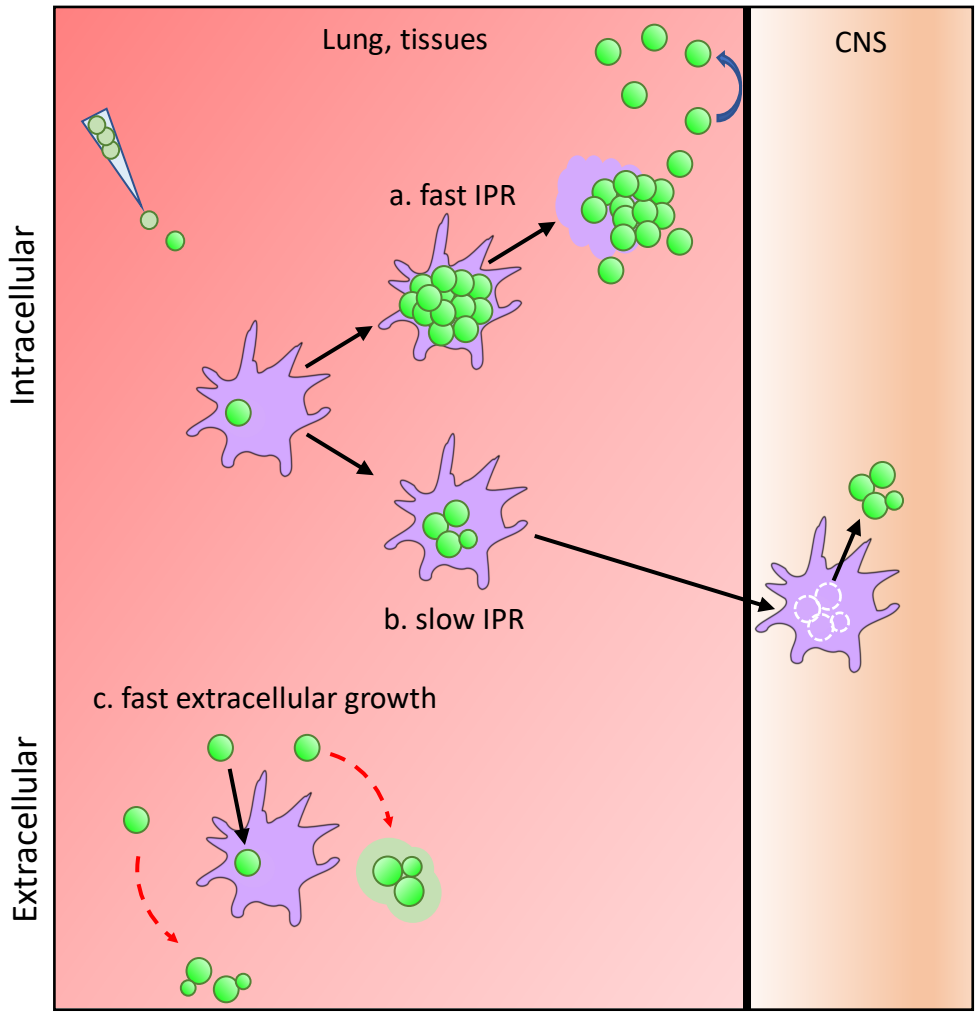

Figure 7.2. Intracellular and extracellular growth of cryptococci

a. For the effective delivery of cryptococci to target tissues (e.g. the central nervous system) it is beneficial for the cryptococci to remain within host macrophages. Excessive intracellular proliferation may lyse the host cell, preventing many of the cryptococci from reaching the target tissues.
b. Slower intracellular growth enables cryptococci to remain within the macrophage niche until the target tissue is reached.
c. The accelerated growth of extracellular cryptococci produces enough fungal cells to enable some cryptococci to remain extracellular (red arrows) after others are captured by host phagocytes. Cryptococci which avoid early phagocytosis grow thick capsules to evade capture and replicate extracellularly. Cryptococci also grow quickly after escaping from macrophages, enabling the effective propagation of infection in target tissues.

7.3 Fungal prostaglandins enable intracellular parasitism and interfere with host immune signalling

Prostaglandins are produced by hosts in response to infection, yet pathogens may also produce prostaglandins to modulate the host immune response and to confer enhanced pathogenicity. *Cryptococcus neoformans* produces prostaglandins which are very similar to those produced by humans (Noverr et al., 2001, 2002), and which confer enhanced intracellular parasitism in macrophages (Evans et al., 2015) (Figure 7.3a). Because prostaglandins produced by cryptococci may interfere with host prostaglandin signalling to enhance virulence, I investigated the role of host- and fungal-derived prostaglandins on cryptococcal intracellular virulence. While the absence of host prostaglandins did not affect fungal growth or uptake either *in vitro* or *in vivo*, fungal prostaglandins enabled macrophage infiltration and intracellular proliferation *in vitro*, resulting in higher fungal burden *in vivo*. I also showed that cryptococci induced macrophage PPAR-γ nuclear translocation, and that fungal prostaglandins were required to induce this activation (Figure 7.3b).

PPAR-γ is involved in many immune signalling cascades, and one possible method by which *C. neoformans* supports intracellular parasitism is by modulating host PPAR-γ signalling and subsequent immune response. Because phospholipase-deficient cryptococci were unable to modulate host PPAR-γ activation and showed reduced intracellular proliferation, it is possible that fungal prostaglandins temper the host intracellular environment via host PPAR-γ signalling, and that inability to do so produced a less permissive intracellular environment for *Δplb1* cryptococci. Interestingly, during co-infection of macrophages with phospholipase-deficient and wild type *C. neoformans*, the presence of prostaglandins produced by the wild type strain enhanced the intracellular proliferation of the mutant strain, suggesting that PPAR-γ activation by the wild type enabled growth of the mutant strain. While the exact manner by which PPAR-γ activation enhances fungal intracellular parasitism is still unknown, these experiments showed a novel mechanism by which fungal factors affect host immune signalling, which in turn affects macrophage-*Cryptococcus* interactions. Future experiments should explore the mechanisms by

which fungal prostaglandins enhance intracellular parasitism and how manipulation of host PPAR-γ signalling enables this phenomenon. Downstream effects of PPAR-γ signalling should be explored in depth, and may illuminate potential sources of intervention to prevent macrophage parasitism by invading cryptococci.

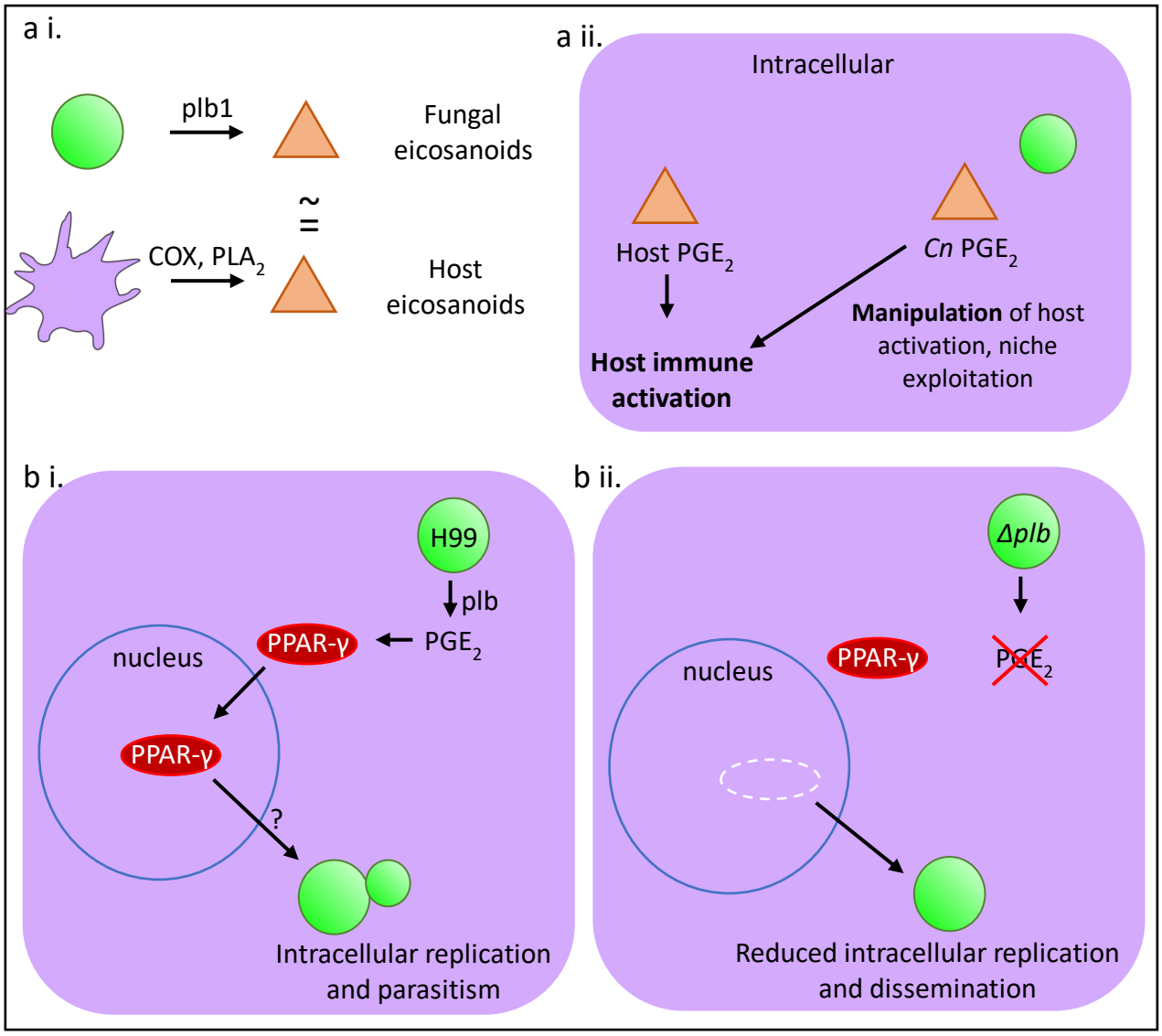

Figure 7.3. Fungal prostaglandins enable exploitation of the macrophage niche

a. *C. neoformans* produces eicosanoids through phospholipase B1 which are indistinguishable from host eicosanoids (i). During infection fungal PGE_2 has the potential to interfere with host signalling (ii). Fungal PGE_2 enables intracellular parasitism of host macrophages.

b. During intracellular macrophage infection, H99 *C. neoformans* activates the translocation of host PPAR-γ to the nucleus (i). This is prostaglandin-dependent as *Δplb1 C. neoformans* is unable to activate host PPAR-γ, which remains in the cytosol rather than translocating to the macrophage nucleus (ii). How the activation of host PPAR-γ by fungal prostaglandins enables the intracellular replication and parasitism of the macrophage niche remains unclear.

7.4 Modelling the heterogeneity in host-pathogen interactions during cryptococcosis

Cryptococcal infection in humans is variable; human patients show different immune responses to cryptococcal infection (Jarvis et al., 2015; Mora et al., 2015) and respond differently antifungal medications (Jarvis et al., 2014). Because that there are many ways in which cryptococci interact with host macrophages (Johnston and May, 2013), I performed assays to determine how the macrophage intracellular niche produces complex infection outcomes. From my zebrafish infection data, James Bradford (Department of Physics and Astronomy, University of Sheffield) produced a computational simulation of *in vivo* cryptococcal infection, considering only cryptococcal growth and death. Using J774 murine macrophages, and later human MDMs, I quantified macrophage-*Cryptococcus* interactions and provided the simulation with measures of cryptococcal uptake, division, and assumed quiescence. In building this model in a step-wise fashion, the effect of individual host-pathogen interactions on infection outcome can be visualised. Through following individual cryptococci and watching how they interacted with macrophages, I was able to show a variety of interaction rates for the variables considered. These variable interactions provided the simulation with sources of stochasticity, showing how different interactions between macrophages and cryptococci produce a variety of infection outcomes, and illuminating how permutations of individual *Cryptococcus* interactions with host macrophages produce the variable infection outcomes we see *in vivo* (Figure 7.4).

In incorporating measurements from individual phagocyte-pathogen interactions, the model showed that while extracellular growth was exponential, intracellular growth of cryptococci was linear; this linear growth may be due to space and nutrient limitations imposed by the macrophage intracellular niche. Through combining computational simulations with measured *in vitro* variables, novel factors governing host-pathogen interactions have been illuminated and represent new avenues of exploration. Further variables being considered for incorporation into the simulation include *in vivo* growth and vomocytosis rates, and while the

death rate of cryptococci *in vivo* remains unknown, this simulation may eventually enable the rate at which cryptococci are killed to be calculated. The ultimate goal of this simulation is to be able to apply it to human cryptococcal infection to determine how different host macrophage factors and antifungal treatments may affect the relationship between *Cryptococcus* and the macrophage intracellular niche, and how these interactions affect the outcome of infection.

Future work should explore how host factors, such as cytokine profile and resulting macrophage polarisation state, affect the interactions between macrophages and cryptococci. The presence of cryptococcal subpopulations should be explored in finer detail, focusing on different cryptococcal phenotypes *in vivo* and how the *combined* host and pathogen heterogeneity produces complex interactions which result in heterogenous outcomes. Furthermore, *in vitro* assays should involve media representative of *in vivo* infection, including nutrients, cytokines, and effector molecules representative of different host environments.

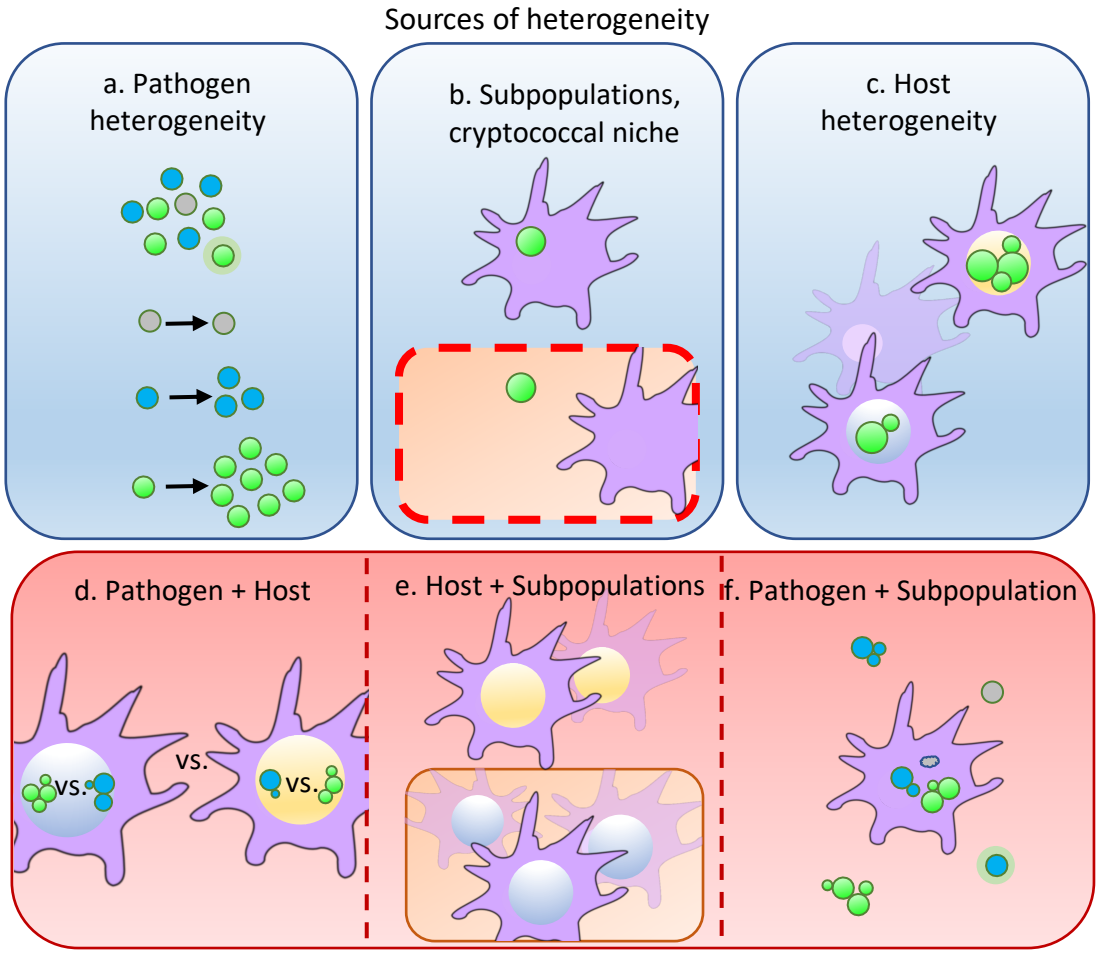

Figure 7.4. Heterogeneity in host-pathogen interactions

Differences between hosts, between pathogens, and between host-pathogen interactions may produce complex infection outcomes

a. Within a microbial population, different pathogens may show different levels of fitness and different replication rates.
b. Pathogens may show different behaviours based on the environment they are in, for example intracellular versus extracellular environments.
c. Host cells may show different levels of phagocytosis and different levels of control over intracellular proliferation and cytotoxic activity.
d. Combined heterogeneity between the host and the phagocytosed pathogens produces different outcomes between these individual infections.
e. Host cells may display different behaviours and different levels of permissiveness between environments and differentially activated cells.
f. Pathogens which are intracellular may show different growth rates from sister cells which are extracellular, and disparate fungal populations may produce further heterogeneity between host environments.

7.5 The formation of the cryptococcal granuloma can be modelled by human PBMCs *in vitro*

Humans produce granulomas in attempt to contain cryptococcal infection, preventing the fungal cells from disseminating throughout the host (Shibuya et al., 2002, 2005). Siddiqui et al. previously showed the composition of these immune aggregates, modelled by human PBMC infection (Siddiqui et al., 2006). In performing time lapse analysis of the interactions between human PBMCs and *C. neoformans*, I further characterised the formation of these aggregates (Figure 7.5). I showed that cryptococci were phagocytosed by both monocytes and pre-existing PBMC swarms quickly after infection, that aggregates formed around most phagocytosed cryptococci, and that replication of cryptococci occurred within, though at a slower rate than cryptococci which were extracellular. I also showed that swarms met and dispersed, and that cryptococci were able to escape from monocytes and swarms to replicate extracellularly at a higher rate. The experiments I performed showed that early human PBMC granuloma formation can be followed in real time and provide a baseline for the continued investigation into the interaction between human granuloma formations and cryptococcal infection. Future work should investigate the role of different T cell phenotypes and cytokines to the formation of cryptococcal granulomas, and should consider the effects of these profiles on cryptococcal replication and PBMC control of growth. Altering the cytokine profile will illuminate the effect on monocyte differentiation and show how activation state affects the progression of the immune response. Following these swarms over a longer time frame may also illuminate how the response to cryptococcal infection changes as monocytes differentiate into macrophages, and how the resulting macrophage intracellular niche contributes to the control, or progression, of *C. neoformans* infection.

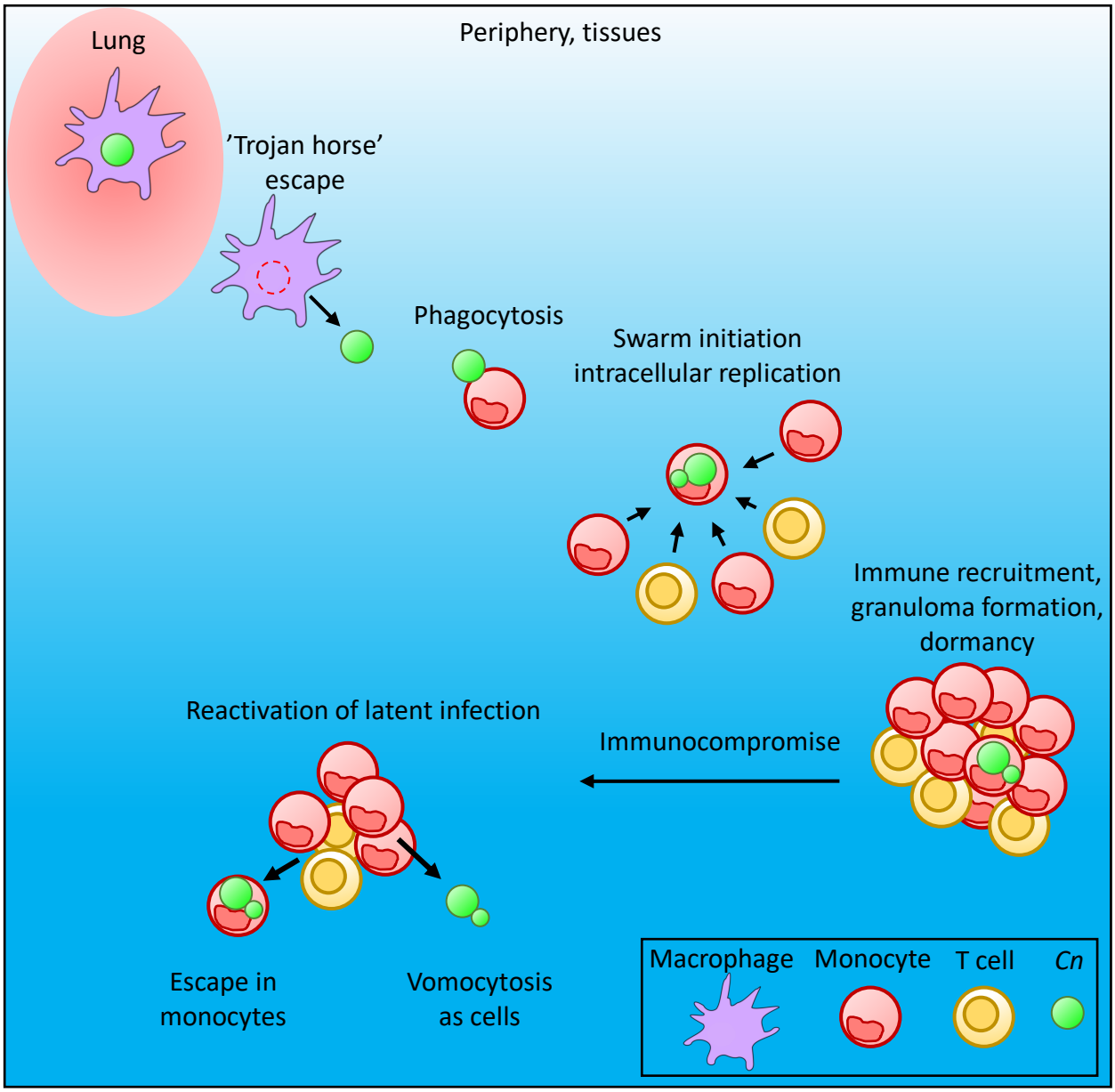

Figure 7.5. Cryptococcal interactions with PBMCs and the formation of granulomas

During cryptococcal infection, evidence suggests that macrophages aid in helping cryptococci to escape from the lung environment via a trojan horse mechanism. Once in the periphery cryptococci are likely to interact with PBMCs such as monocytes and T cells. Monocytes phagocytose cryptococci, though cryptococci may replicate intracellularly. During *in vivo* infection, granulomas contain cryptococci which are composed of macrophages and T cells. Cryptococci may enter a quiescent, dormant state. After the host enters an immunocompromised state, cryptococci may reactivate latent infection to resume growth and cause symptomatic infection. Cryptococci may escape PBMC swarms inside of monocytes or may vomocytose as individual cells.

7.6 Concluding remarks

Cryptococcus neoformans interactions with macrophages represent the complexity of possible infection outcomes. Because macrophages may control cryptococcal infection, and because cryptococci may exploit the macrophage intracellular niche for replication and dissemination of infection, understanding these interactions and how they impact infection progression is critical. Throughout this thesis, I have presented evidence examining different aspects of this relationship, focusing on fungal cooperation, exploitation, and modulation of host-pathogen interactions during cryptococcosis. I showed that cryptococci do not cooperate to enhance invasion and replication based on density, and that macrophages do not show enhanced or inhibited control based on infection burden. I also showed macrophages control intracellular proliferation of cryptococci, but that cryptococci still manipulate this host niche for replication. I also showed a pathway by which cryptococci affect macrophage immune signalling, potentially modifying the host immune response to enhance fungal pathogenicity. Through following macrophage infection with individual cryptococci I quantified heterogeneous pathogenic behaviours, helping to produce a computational simulation of *in vivo* cryptococcal infection which shows how different infection variables affect infection outcome. Finally, I described human granuloma formation during cryptococcal infection *in vitro*. In examining *Cryptococcus*-macrophage interactions from the level of intracellular signalling to *in vivo* infection and *in silico* modelling, I have illustrated how macrophage control and cryptococcal parasitism are affected by interactions between *Cryptococcus neoformans* and the macrophage intracellular niche.

Appendix – Solution Protocols

A. E3 medium

Dilute E3 to 1X in distilled H_2O

2 drops methylene blue, to prevent fungal growth

store in 38°C incubator

B. YPD agar plates

5% (25 g) YPD broth (yeast extract peptone dextrose, Fisher Scientific)

2% (10 g) agar (Sigma-Aldrich)

fill to 500ml with distilled H_20

store at 5°C

C. E3 agar plates

2% (10 g) agar (Sigma-Aldrich)

500 ml with 1X E3

boil, pour into plates

store at 5°C

D. Agar for 0 dpi imaging plates

2% (2 g) agar (Sigma-Aldrich)

100 ml water or 1X E3

boil, pipette into 96 well plate

E. Low gelling agarose

1% (0.1 g) low gelling agarose (Sigma-Aldrich)

OR 0.5* (0.05 g) low gelling agarose (Sigma-Aldrich)

9.6ml clear E3 (1X E3, no methylene blue)

420 µl tricaine

boil, place eppendorfs in heat block at 38°C

Ensure cool before adding to wells

F. Serum Free DMEM

500 ml Dulbecco's Modified Eagle's Medium – low glucose (Sigma-Aldrich)

1% (5 g) L-glutamine (Sigma-Aldrich)

1% (5 g) penicillin/streptomycin antibiotics (Sigma-Aldrich)

store at 6°C

G. Complete DMEM

500 ml Dulbecco's Modified Eagle's Medium – low glucose (Sigma-Aldrich)

1% (5 ml) L-glutamine (Sigma-Aldrich)

1% (5 ml) penicillin/streptomycin antibiotics (Sigma-Aldrich)

10% (50 ml) foetal bovine serum (Sigma-Aldrich)

Store at 6°C

H. Serum free RPMI

500 ml Rosewell Park Memorial Institute (RPMI) – L-glutamine added (BioWhittaker)

1% (5 g) penicillin/streptomycin antibiotics (Sigma-Aldrich)

store at 6°C

I. Complete RPMI

500ml Rosewell Park Memorial Institute (RPMI) – L-glutamine added (BioWhittaker)

1% (5 g) penicillin/streptomycin antibiotics (Sigma-Aldrich)

10% (50 ml) foetal bovine serum (Sigma-Aldrich)

store at 6°C

J. J. 2.5% gel for electrophoresis

(gloves must be worn at all times)

250 ml 1x TAE

6.25 g agarose (Bioline)

Boil

4 μl ethidium bromide per 50 ml gel

100 ml per gel

K. Freeze down media

500 ml Dulbecco's Modified Eagle's Medium – low glucose (Sigma-Aldrich)

1% (5 ml) penicillin/streptomycin antibiotics (Sigma-Aldrich)

20% (100 ml) foetal bovine serum (Sigma-Aldrich)

10% (50 ml) DMSO

References

Abu Kwaik, Y., and Bumann, D. (2013). Microbial quest for food *in vivo* : 'Nutritional virulence' as an emerging paradigm. Cell. Microbiol. *15*, 882–890.

Aguirre, K., Havell, E., and Gibson, G. (1995). Role of tumor necrosis factor and gamma interferon in acquired resistance to Cryptococcus neoformans in the central nervous system of mice. Infect. Immun.*63*, 1725-1731.

Ahmed, S.A.K.S., Rudden, M., Smyth, T.J., Dooley, J.S.G., Marchant, R., and Banat, I.M. (2019). Natural quorum sensing inhibitors effectively downregulate gene expression of Pseudomonas aeruginosa virulence factors. Appl. Microbiol. Biotechnol. *103*, 3521–3535.

Aimanianda, V., Bayry, J., Bozza, S., Kniemeyer, O., Perruccio, K., Elluru, S.R., Clavaud, C., Paris, S., Brakhage, A.A., Kaveri, S. V., et al. (2009). Surface hydrophobin prevents immune recognition of airborne fungal spores. Nature *460*, 1117–1121.

Alanio, A., Vernel-Pauillac, F., Sturny-Leclère, A., and Dromer, F. (2015). Cryptococcus neoformans Host Adaptation: Toward Biological Evidence of Dormancy. MBio *6*, e02580-14.

Albuquerque, P., Nicola, A.M., Nieves, E., Paes, H.C., Williamson, P.R., Silva-Pereira, I., and Casadevall, A. (2014). Quorum sensing-mediated, cell density-dependent regulation of growth and virulence in Cryptococcus neoformans. MBio *5*, e00986-13.

Alem, M.A.S., Oteef, M.D.Y., Flowers, T.H., and Douglas, L.J. (2006). Production of tyrosol by Candida albicans biofilms and its role in quorum sensing and biofilm development. Eukaryot. Cell *5*, 1770–1779.

Allesen-Holm, M., Barken, K.B., Yang, L., Klausen, M., Webb, J.S., Kjelleberg, S., Molin, S., Givskov, M., and Tolker-Nielsen, T. (2006). A characterization of DNA release in Pseudomonas aeruginosa cultures and biofilms. Mol. Microbiol. *59*, 1114–1128.

Alleva, D., Johnson, E., Lio, F., Boehme, S., Conlon, P., and Crowe, P. (2002). Regulation of murine macrophage proinflammatory and anti-inflammatory cytokines by ligands for peroxisome proliferator-activated receptor-γ: counter regulatory activity by IFN-γ. J. Leukoc. Biol. *71*, 677–685.

Almeida, F., Wolf, J.M., Da Silva, T.A., Deleon-Rodriguez, C.M., Rezende, C.P., Pessoni, A.M., Fernandes, F.F., Silva-Rocha, R., Martinez, R., Rodrigues, M.L., et al. (2017). Galectin-3 impacts Cryptococcus neoformans infection through direct antifungal effects. Nat. Commun. *8*, 1–13.

Alonzo, F., and Torres, V.J. (2014). The bicomponent pore-forming leucocidins of Staphylococcus aureus. Microbiol. Mol. Biol. Rev. *78*, 199–230.

Altan-Bonnet, G., and Mukherjee, R. (2019). Cytokine-mediated communication: a quantitative appraisal of immune complexity. Nat. Rev. Immunol. *19*, 205–217.

Altfeld, M., Addo, M.M., Kreuzer, K.A., Rockstroh, J.K., Dumoulin, F.L., Schliefer, K., Leifeld, L., Sauerbruch, T., and Spengler, U. (2000). T(H)1 to T(H)2 shift of cytokines in peripheral blood of HIV-infected patients is detectable by reverse transcriptase polymerase chain reaction but not by enzyme-linked immunosorbent assay under nonstimulated conditions. J. Acquir. Immune Defic. Syndr. *23*, 287–294.

Alvarez, M., and Casadevall, A. (2006). Phagosome Extrusion and Host-Cell Survival after Cryptococcus neoformans Phagocytosis by Macrophages. Curr. Biol. *16*, 2161–2165.

Alvarez, M., and Casadevall, A. (2007). Cell-to-cell spread and massive vacuole formation after Cryptococcus neoformans infection of murine macrophages. BMC Immunol. *8*.

Alvarez, M., Burns, T., Luo, Y., Pirofski, L., and Casadevall, A. (2009). The outcome of Cryptococcus neoformans intracellular pathogenesis in human monocytes. BMC Microbiol. *9*, 51.

Amin, A., Attur, M., Patel, R., Thakker, G., Marshall, P., Rediske, J., Stuchin, S., Patel, I., and Abramson, S. (1997). Superinduction of cyclooxygenase-2 activity in human osteoarthritis-affected cartilage: Influence of nitric oxide. J. Clin. Invest. *99*, 1231–1237.

Anderson, G., Hauser, S., McGarity, K., Bremer, M., Isakson, P., and Gregory, S. (1996). Selective inhibition of cyclooxygenase (COX)-2 reverses inflammation and expression of COX-2 and interleukin 6 in rat adjuvant arthritis. J. Clin. Invest. *87*, 2672–2679.

Angkasekwinai, P., Sringkarin, N., Supasorn, O., Fungkrajai, M., Wang, Y.-H., Chayakulkeeree, M., Ngamskulrungroj, P., Angkasekwinai, N., and Pattanapanyasat, K. (2014). Cryptococcus gattii Infection Dampens Th1 and Th17 Responses by Attenuating Dendritic Cell Function and Pulmonary Chemokine Expression in the Immunocompetent Hosts. Infect. Immun. *82*, 3880-3890.

Antunes, L.C.M., and Ferreira, R.B. (2009). Intercellular communication in bacteria. Crit. Rev. Microbiol. *35*, 66–80.

Aparecida, P., Pereira, T., Trindade, B.C., Secatto, A., Nicolete, R., Peres-Buzalaf, C., Ramos, S.G., Sadikot, R., Da, C., Bitencourt, S., et al. (2013). Celecoxib Improves Host Defense through Prostaglandin Inhibition during Histoplasma capsulatum Infection. Mediators Inflamm. *2013*

Armstrong, J.A., and Hart, A. (1971). Response of cultured macrophages to

Mycobacterium tuberculosis, with observations on fusion of lysosomes with phagosomes. J. Exp. Med. *134*, 713–740.

Arora, S., Hernandez, Y., Erb-Downward, J., McDonald, R.A., Toews, G.B., and Huffnagle, G.B. (2005). Role of IFN-gamma in regulating T2 immunity and the development of alternatively activated macrophages during allergic bronchopulmonary mycosis. J. Immunol. *174*, 6346–6356.

Arora, S., Olszewski, M.A., Tsang, T.M., McDonald, R.A., Toews, G.B., and Huffnagle, G.B. (2011). Effect of cytokine interplay on macrophage polarization during chronic pulmonary infection with Cryptococcus neoformans. Infect. Immun. *79*, 1915–1926.

Aussel, L., Zhao, W., Hébrard, M., Guilhon, A.A., Viala, J.P.M., Henri, S., Chasson, L., Gorvel, J.P., Barras, F., and Méresse, S. (2011). Salmonella detoxifying enzymes are sufficient to cope with the host oxidative burst. Mol. Microbiol. *80*, 628–640.

Avraham, R., and Hung, D.T. (2016). A perspective on single cell behavior during infection. Gut Microbes *7*, 518–525.

Avraham, R., Haseley, N., Brown, D., Penaranda, C., Jijon, H.B., Trombetta, J.J., Satija, R., Shalek, A.K., Xavier, R.J., Regev, A., et al. (2015). Pathogen Cell-to-Cell Variability Drives Heterogeneity in Host Immune Responses. Cell *162*, 1309–1321.

Bain, J.M., Louw, J., Lewis, L.E., Okai, B., Walls, C.A., Ballou, E.R., Walker, L.A., Reid, D., Munro, C.A., Brown, A.J.P., et al. (2014). Candida albicans Hypha Formation and Mannan Masking of β-Glucan Inhibit Macrophage Phagosome Maturation. MBio *5*, e01874-14.

Bassani, B., Baci, D., Gallazzi, M., Poggi, A., Bruno, A., and Mortara, L. (2019). Natural Killer Cells as Key Players of Tumor Progression and Angiogenesis: Old and Novel Tools to Divert Their Pro-Tumor Activities into Potent Anti-Tumor Effects. Cancers (Basel). *11*, 461.

Bassler, B.L., and Losick, R. (2006). Bacterially Speaking. Cell *125*, 237–246.

Bazzi, S., El-Darzi, E., McDowell, T., Modjtahedi, H., Mudan, S., Achkar, M., Akle, C., Kadara, H., and Bahr, G. (2017). Defining Genome-Wide Expression and Phenotypic Contextual Cues in Macrophages Generated by Granulocyte/Macrophage Colony-Stimulating Factor, Macrophage Colony-Stimulating Factor, and Heat-Killed Mycobacteria. Front. Immunol. *8*, 1253.

Belley, A., and Chadee, K. (1995). Eicosanoid production by parasites: From pathogenesis to immunomodulation? Parasitol. Today *11*, 327–334.

Bennett, S., and Breit, S.N. (1994). Variables in the isolation and culture of human monocytes that are of particular relevance to studies of HIV. J. Leukoc. Biol. *56*, 236–240.

Bermudez, L.E., Shelton, K., and Young, L.S. (1995). Comparison of the ability of Mycobacterium avium, M. smegmatis and M. tuberculosis to invade and replicate within HEp-2 epithelial cells. Tuber. Lung Dis. *76*, 240–247.

Bernut, A., Herrmann, J.-L., Kissa, K., Dubremetz, J.-F., Gaillard, J.-L., Lutfalla, G., and Kremer, L. (2014). Mycobacterium abscessus cording prevents phagocytosis and promotes abscess formation. Proc. Natl. Acad. Sci. *111*, E943-52.

Betz, M., and Fox, B.S. (1991). Prostaglandin E2 inhibits production of Th1 lymphokines but not of Th2 lymphokines. J. Immunol. *146*, 108–113.

Bhakdi, S., Kuller, G., Muhly, M., Fromm, S., Seibert, G., and Parrisius, J. (1987). Formation of transmural complement pores in serum-sensitive Escherichia coli. Infect. Immun. *55*, 206–210.

Bhattacharjee, A.K., Bennett, J., and Glaudemans, C.P.J. (1984). Capsular Polysaccharides of Cryptococcus neoformans. Clin. Infect. Dis. *6*, 619–624.

Bielska, E., Sisquella, M.A., Aldeieg, M., Birch, C., O'Donoghue, E.J., and May, R.C. (2018). Pathogen-derived extracellular vesicles mediate virulence in the fatal human pathogen Cryptococcus gattii. Nat. Commun. *9*, 1556.

Bingöl, A., Yücemen, N., and Meço, O. (1999). Medically treated intraspinal "brucella" granuloma. Surg. Neurol. *52*, 570–576.

Biondo, G.A., Dias-Melicio, L.A., Bordon-Graciani, A.P., Acorci-Valério, M.J., and Soares, A.M.V.C. (2010). Paracoccidioides brasiliensis Uses Endogenous and Exogenous Arachidonic Acid for PGE x Production. Mycopathologia *170*, 123–130.

Birnbaum, M.E., Mendoza, J.L., Sethi, D.K., Dong, S., Glanville, J., Dobbins, J., Özkan, E., Davis, M.M., Wucherpfennig, K.W., and Garcia, K.C. (2014). Deconstructing the Peptide-MHC Specificity of T Cell Recognition. Cell *157*, 1073–1087.

Bojarczuk, A., Miller, K.A., Hotham, R., Lewis, A., Ogryzko, N. V, Kamuyango, A.A., Frost, H., Gibson, R.H., Stillman, E., May, R., et al. (2016). Cryptococcus neoformans Intracellular Proliferation and Capsule Size Determines Early Macrophage Control of Infection. Sci. Rep. *6*, 21489.

Bordon, A.P., Alarcaõ Dias-Melicio, L., Janegitz Acorci, M., Augusto Biondo, G., Fecchio, D., Terezinha Serraõ Peracoli, M., and Maria Victoriano Campos de Soares, A. (2007). Prostaglandin E2 production by high and low virulent strains of Paracoccidioides brasiliensis. Mycopathologia *163*, 129–135.

Bose, I., Reese, A.J., Ory, J.J., Janbon, G., and Doering, T.L. (2003). A yeast under cover: the capsule of Cryptococcus neoformans. Eukaryot. Cell *2*, 655–663.

Botts, M.R., and Hull, C.M. (2010). Dueling in the lung: how Cryptococcus spores

race the host for survival. Curr. Opin. Microbiol. *13*, 437–442.

Brizendine, K., Baddley, J., and Pappas, P. (2013). Predictors of Mortality and Differences in Clinical Features among Patients with Cryptococcosis According to Immune Status. PLoS One *8*, e60431.

Brubaker, S.W., Bonham, K.S., Zanoni, I., and Kagan, J.C. (2015). Innate Immune Pattern Recognition: A Cell Biological Perspective. Annu. Rev. Immunol. *33*, 257–290.

Brunet, K., Alanio, A., Lortholary, O., and Rammaert, B. (2018). Reactivation of dormant/latent fungal infection. J. Infect. *77*, 463–468.

Buchanan, K., and Doyle, H. (2000). Requirement for CD4+ T lymphocytes in host resistance against Cryptococcus neoformans in the central nervous system of immunized mice. Infect. Immun. *68*, 456–462.

Caetano, L., Antunes, M., Ferreira, R.B.R., Buckner, M.M.C., and Finlay, B.B. (2010). Quorum sensing in bacterial virulence. Microbiology *156*, 2271–2282.

Callejas, A., Ordonez, N., Rodriguez, M., and Castaneda, E. (1998). First isolation of Cryptococcus neoformans var. gattii, serotype C, from the environment in Colombia. Med. Mycol. *36*, 341–344.

Carbo, A., Bassaganya-Riera, J., Pedragosa, M., Viladomiu, M., Marathe, M., Eubank, S., Wendelsdorf, K., Bisset, K., Hoops, S., Deng, X., et al. (2013). Predictive Computational Modeling of the Mucosal Immune Responses during Helicobacter pylori Infection. PLoS One *8*, e73365.

Casadevall, A. (2012). Amoeba Provide Insight into the Origin of Virulence in Pathogenic Fungi. (Springer, New York, NY), pp. 1–10.

Castillo-Juárez, I., Maeda, T., Mandujano-Tinoco, E.A., Tomás, M., Pérez-Eretza, B., García-Contreras, S.J., Wood, T.K., and García-Contreras, R. (2015). Role of quorum sensing in bacterial infections. World J. Clin. Cases *3*, 575–598.

Chakrabarti, A., Jatana, M., Kumar, P., Chatha, L., Kaushal, A., and Padhye, A.A. (1997). Isolation of Cryptococcus neoformans var. gattii from Eucalyptus camaldulensis in India. J. Clin. *355*, 3340–3342.

Chakravortty, D., Rohde, M., Jä Ger, L., Deiwick, J., and Hensel, M. (2005). Formation of a novel surface structure encoded by Salmonella Pathogenicity Island 2. EMBO J. *24*, 2043–2052.

Chandra, J., Mccormick, T.S., Imamura, Y., Mukherjee, P.K., and Ghannoum, M.A. (2007). Interaction of Candida albicans with Adherent Human Peripheral Blood Mononuclear Cells Increases C. albicans Biofilm Formation and Results in

Differential Expression of Pro-and Anti-Inflammatory Cytokines. Infect. Immun. *75*, 2612–2620.

Chang, K.P. (1980). Human cutaneous Leishmania in a mouse macrophage line: Propagation and isolation of intracellular parasites. Science (80-.). *209*, 1240–1242.

Chang, Y.C., and Kwon-Chung, K.J. (1994). Complementation of a capsule-deficient mutation of Cryptococcus neoformans restores its virulence. Mol. Cell. Biol. *14*, 4912–4919.

Chang, Y.C., Stins, M.F., McCaffery, M.J., Miller, G.F., Pare, D.R., Dam, T., Paul-Satyaseela, M., Kim, K.S., Kwon-Chung, K.J., and Paul-Satyasee, M. (2004). Cryptococcal yeast cells invade the central nervous system via transcellular penetration of the blood-brain barrier. Infect. Immun. *72*, 4985–4995.

Charlier, C., Nielsen, K., Daou, S., Brigitte, M., Chretien, F., and Dromer, F. (2009). Evidence of a role for monocytes in dissemination and brain invasion by Cryptococcus neoformans. Infect. Immun. *77*, 120–127.

Chaturvedi, V., Wong, B., and Newman, S.L. (1996). Oxidative killing of Cryptococcus neoformans. Evidence that fungal mannitol protects by scavenging reactive oxygen intermediates. J. Immunol. *156*, 3836–3840.

Chayakulkeeree, M., Johnston, S.A., Oei, J.B., Lev, S., Williamson, P.R., Wilson, C.F., Zuo, X., Leal, A.L., Vainstein, M.H., Meyer, W., et al. (2011). SEC14 is a specific requirement for secretion of phospholipase B1 and pathogenicity of Cryptococcus neoformans2. Mol. Microbiol. *80*, 1088–1101.

Chen, H., Fujita, M., Feng, Q., Clardy, J., and Fink, G.R. (2004). Tyrosol is a quorum-sensing molecule in Candida albicans. Proc. Natl. Acad. Sci. U. S. A. *101*, 5048–5052.

Chen, J., Varma, A., Diaz, M.R., Litvintseva, A.P., Wollenberg, K.K., and Kwon-Chung, K.J. (2008). Cryptococcus neoformans strains and infection in apparently immunocompetent patients, China. Emerg. Infect. Dis. *14*, 755–762.

Chen, Q., Muramoto, K., Masaaki, N., Ding, Y., Yang, H., Mackey, M., Li, W., Inoue, Y., Ackermann, K., Shirota, H., et al. (2010). A novel antagonist of the prostaglandin E 2 EP 4 receptor inhibits Th1 differentiation and Th17 expansion and is orally active in arthritis models. Br. J. Pharmacol. *160*, 292–310.

Chen, S., Muller, M., Zhou, J., Wright, L., and Sorrell, T. (1997a). Phospholipase Activity in Cryptococcus neoformans: A New Virulence Factor? J. Infect. Dis. *175*, 414–420.

Chen, S., Wright, L., Santangelo, R., Muller, M., Moran, V., Kuchel, P., and Sorrell, T. (1997b). Identification of extracellular phospholipase B, lysophospholipase, and acyltransferase produced by Cryptococcus neoformans. Infect. Immun. *65*, 405–

411.

Chen, S., Wright, L., Golding, J., and Sorrell, T. (2000a). Purification and characterization of secretory phospholipase B, lysophospholipase and lysophospholipase/transacylase from a virulent strain of the pathogenic fungus Cryptococcus neoformans.

Chen, S., Sorrell, T., Nimmo, G., Speed, B., Currie, B., Ellis, D., Marriott, D., Pfeiffer, T., Parr, D., and Byth, K. (2000b). Epidemiology and Host- and Variety-Dependent Characteristics of Infection Due to Cryptococcus neoformans in Australia and New Zealand. Clin. Infect. Dis. *31*, 499–508.

Chen, Y., Farrer, R.A., Giamberardino, C., Sakthikumar, S., Jones, A., Yang, T., Tenor, J.L., Wagih, O., Van Wyk, M., Govender, N.P., et al. (2017). Microevolution of Serial Clinical Isolates of Cryptococcus neoformans var. grubii and C. gattii. MBio *8*, e00166-17.

Choi, J., Shin, D., Kim, M., Park, J., Lim, S., and Ryu, S. (2012). LsrR-Mediated Quorum Sensing Controls Invasiveness of Salmonella typhimurium by Regulating SPI-1 and Flagella Genes. PLoS One *7*, e37059.

Chou, W., Chuang, L., Chou, C., Wang, A., Lawson, J., FitzGerald, G., and Chang, Z. (2007). Identification of a novel prostaglandin reductase reveals the involvement of prostaglandin E2 catabolism in regulation of peroxisome proliferator-activated receptor γ. J. Biol. Chem. *282*, 18162–18172.

Chrétien, F., Lortholary, O., Kansau, I., Neuville, S., Gray, F., and Dromer, F. (2002). Pathogenesis of cerebral Cryptococcus neoformans infection after fungemia. J. Infect. Dis. *186*, 522–530.

Cossart, P., Vicente, M.F., Mengaud, J., Baquero, F., Claudio Perez-Diaz, J., and Berche, P. (1989). Listeriolysin O Is Essential for Virulence of Listeria Monocytogenes: Direct Evidence Obtained by Gene Complementation.
Infect. Immun. *57*, 3629-3636.

Coulombe, F., Jaworska, J., Verway, M., Tzelepis, F., Massoud, A., Gillard, J., Wong, G., Kobinger, G., Xing, Z., Couture, C., et al. (2014). Targeted Prostaglandin E2 Inhibition Enhances Antiviral Immunity through Induction of Type I Interferon and Apoptosis in Macrophages. Immunity *40*, 554–568.

Couper, K.N., Blount, D.G., and Riley, E.M. (2008). IL-10: the master regulator of immunity to infection. J. Immunol. *180*, 5771–5777.

Cox, G.M., McDade, H.C., Chen, S.C.A., Tucker, S.C., Gottfredsson, M., Wright, L.C., Sorrell, T.C., Leidich, S.D., Casadevall, A., Ghannoum, M.A., et al. (2001). Extracellular phospholipase activity is a virulence factor for Cryptococcus neoformans. Mol. Microbiol. *39*, 166–175.

Crabtree, J.N., Okagaki, L.H., Wiesner, D.L., Strain, A.K., Nielsen, J.N., and Nielsen, K. (2012). Titan Cell Production Enhances the Virulence of Cryptococcus neoformans. Infect. Immun. *80*, 3776–3785.

Crofford, L.J. (1997). COX-1 and COX-2 tissue expression: implications and predictions. J. Rheumatol. Suppl. *49*, 15–19.

Cross, C.E., and Bancroft, G.J. (1995). Ingestion of Acapsular Cryptococcus neoformans Occurs via Mannose and beta-Glucan Receptors, Resulting in Cytokine Production and Increased Phagocytosis of the Encapsulated Form. Infect. Immun. *63*, 2604–2611.

Curtsinger, J.M., Johnson, C.M., and Mescher, M.F. (2003). CD8 T Cell Clonal Expansion and Development of Effector Function Require Prolonged Exposure to Antigen, Costimulation, and Signal 3 Cytokine. J. Immunol. *171*, 5165–5171.

Dambuza, I.M., Drake, T., Chapuis, A., Zhou, X., Correia, J., Taylor-Smith, L., LeGrave, N., Rasmussen, T., Fisher, M.C., Bicanic, T., et al. (2018). The Cryptococcus neoformans Titan cell is an inducible and regulated morphotype underlying pathogenesis. PLOS Pathog. *14*, e1006978.

Dan, J.M., Wang, J.P., Lee, C.K., and Levitz, S.M. (2008). Cooperative Stimulation of Dendritic Cells by Cryptococcus neoformans Mannoproteins and CpG Oligodeoxynucleotides. PLoS One *3*, e 2046.

Darch, S.E., Mcnally, A., Harrison, F., Corander, J., Barr, H.L., Paszkiewicz, K., Holden, S., Fogarty, A., Crusz, S.A., and Diggle, S.P. (2014). Recombination is a key driver of genomic and phenotypic diversity in a Pseudomonas aeruginosa population during cystic fibrosis infection. Sci. Rep. *5*, 1063-1073.

Das, P., Lahiri, A., Lahiri, A., Chakravortty, D., Kossel, A., Dakin, H., Mori, M., Wu, G., Jr, S.M., Cederbaum, S., et al. (2010). Modulation of the Arginase Pathway in the Context of Microbial Pathogenesis: A Metabolic Enzyme Moonlighting as an Immune Modulator. PLoS Pathog. *6*, e1000899.

Davis, J.M., and Ramakrishnan, L. (2009). The Role of the Granuloma in Expansion and Dissemination of Early Tuberculous Infection. Cell *136*, 37–49.

Davis, J.M., Huang, M., Botts, M.R., Hull, C.M., and Huttenlocher, A. (2016). A Zebrafish Model of Cryptococcal Infection Reveals Roles for Macrophages, Endothelial Cells, and Neutrophils in the Establishment and Control of Sustained Fungemia. Infect. Immun. *84*, 3047–3062.

Davis, M.J., Tsang, T.M., Qiu, Y., Dayrit, J.K., Freij, J.B., Huffnagle, G.B., and Olszewski, M.A. (2013). Macrophage M1/M2 polarization dynamically adapts to changes in cytokine microenvironments in Cryptococcus neoformans infection.

MBio *4*, e00264-13.

Decken, K., Köhler, G., Palmer-Lehmann, K., Wunderlin, A., Mattner, F., Magram, J., Gately, M.K., and Alber, G. (1998). Interleukin-12 is essential for a protective Th1 response in mice infected with Cryptococcus neoformans. Infect. Immun. *66*, 4994–5000.

DeLeon-Rodriguez, C.M., and Casadevall, A. (2016). Cryptococcus neoformans: Tripping on Acid in the Phagolysosome. Front. Microbiol. *7*, 164.

Delfino, D., Cianci, L., Lupis, E., Celeste, A., Petrelli, M.L., Curró, F., Cusumano, V., and Teti, G. (1997). Interleukin-6 production by human monocytes stimulated with Cryptococcus neoformans components. Infect. Immun. *65*, 2454–2456.

Denham, S., and Brown, J. (2018). Mechanisms of Pulmonary Escape and Dissemination by Cryptococcus neoformans. J. Fungi *4*.

Deveau, A., Piispanen, A.E., Jackson, A.A., and Hogan, D.A. (2010). Farnesol Induces Hydrogen Peroxide Resistance in Candida albicans Yeast by Inhibiting the Ras-Cyclic AMP Signaling Pathway. Eukaryot. Cell *9*, 569–577.

Diamond, R., and Bennett, J. (1973). Growth of Cryptococcus neoformans within human macrophages in vitro. Infect. Immun. *7*, 231–236.

Diamond, R.D., Root, R.K., and Bennett, J.E. (1972). Factors Influencing Killing of Cryptococcus neoformans by Human Leukocytes In Vitro. J. Infect. Dis. *125*, 367–376.

DiCaudo, D.J., and Connolly, S.M. (2001). Interstitial granulomatous dermatitis associated with pulmonary coccidioidomycosis. J. Am. Acad. Dermatol. *45*, 840–845.

Dinarello, C.A. (2007). Historical insights into cytokines. Eur. J. Immunol. *37*, S34-45.
Ding, A.H., Nathan, C.F., and Stuehr, D.J. (1988). Release of reactive nitrogen intermediates and reactive oxygen intermediates from mouse peritoneal macrophages. Comparison of activating cytokines and evidence for independent production. J. Immunol. *141*, 2407–2412.

Djordjevic, J.T., Del Poeta, M., Sorrell, T.C., Turner, K.M., and Wright, L.C. (2005). Secretion of cryptococcal phospholipase B1 (PLB1) is regulated by a glycosylphosphatidylinositol (GPI) anchor. Biochem. J. *389*, 803–812.

Dockerell, D., Marriott, H., Prince, L., Ridger, V., Ince, P., Hellewell, P., and Whyte, M. (2003). Alveolar macrophage apoptosis contributes to pneumococcal clearance in a resolving model of pulmonary infection. J. Immunol. *1711*, 5380–5388.

Doering, T. (2009). How sweet it is! Cell wall biogenesis and polysaccharide capsule formation in Cryptococcus neoformans. Annu. Rev. Microbiol. *63*, 223–247.

Doering, T.L., Nosanchuk, J.D., Roberts, W.K., and Casadevall, A. (1999). Melanin as a potential cryptococcal defence against microbicidal proteins. Med. Mycol. *37*, 175–181.

Dolan, J.M., Weinberg, J.B., O'Brien, E., Abashian, A., Procario, M.C., Aronoff, D.M., Crofford, L.J., Peters-Golden, M., Ward, L., and Mancuso, P. (2016). Increased lethality and defective pulmonary clearance of *Streptococcus pneumoniae* in microsomal prostaglandin E synthase-1-knockout mice. Am. J. Physiol. Cell. Mol. Physiol. *310*, L1111–L1120.

Dubois, R.N., Abramson, S.B., Crofford, L., Gupta, R.A., Simon, L.S., Van De Putte, L.B.A., and Lipsky, P.E. (1998). Cyclooxygenase in biology and disease. *12*, 1063-1073.

Dunman, P.M., Murphy, E., Haney, S., Palacios, D., Tucker-Kellogg, G., Wu, S., Brown, E.L., Zagursky, R.J., Shlaes, D., and Projan, S.J. (2001). Transcription profiling-based identification of Staphylococcus aureus genes regulated by the agr and/or sarA loci. J. Bacteriol. *183*, 7341–7353.

Duque, G.A., and Descoteaux, A. (2014). Macrophage cytokines: involvement in immunity and infectious diseases. Front. Immunol. *5*, 491.

Eberl, G., Colonna, M., Di Santo, J.P., and McKenzie, A.N.J. (2015). Innate lymphoid cells: A new paradigm in immunology. Science (80-.). *348*, aaa6566–aaa6566.

Egbe, N.E., Dornelles, T.O., Paget, C.M., Castelli, L.M., and Ashe, M.P. (2017). Farnesol inhibits translation to limit growth and filamentation in C. albicans and S. cerevisiae. Microb. Cell *4*, 294–304.

Eisenman, H.C., Mues, M., Weber, S.E., Frases, S., Chaskes, S., Gerfen, G., and Casadevall, A. (2007). Cryptococcus neoformans laccase catalyses melanin synthesis from both D- and L-DOPA. Microbiology *153*, 3954–3962.

Erb-Downward, J., and Huffnagle, G. (2007). Cryptococcus neoformans produces authentic prostaglandin E2 without a cyclooxygenase. Eukaryot. Cell *6*, 346–350.

Erb-Downward, J., Noggle, R., Williamson, P., and Huffnagle, G. (2008). The role of laccase in prostaglandin production by Cryptococcus neoformans. Mol. Microbiol. *68*, 1428–1437.

Erwig, L., Kluth, D., and Walsh, G. (1998). Initial cytokine exposure determines function of macrophages and renders them unresponsive to other cytokines. J. Immunol. *161*, 1983–1988.

Esolen, L.M., Ward, B.J., Moench, T.R., and Griffin, D.E. (1993). Infection of Monocytes during Measles. J. Infect. Dis. *168*, 47–52.

Evans, R.J., Li, Z., Hughes, W.S., Djordjevic, J.T., Nielsen, K., and May, R.C. (2015). Cryptococcal Phospholipase B1 Is Required for Intracellular Proliferation and Control of Titan Cell Morphology during Macrophage Infection. Infect. Immun. *83*, 1296–1304.

Evans, R.J., Voelz, K., Johnston, S.A., and May, R.C. (2017). Using Flow Cytometry to Analyze Cryptococcus Infection of Macrophages. (Humana Press, New York, NY), pp. 349–357.

Evans, R.J., Pline, K., Loynes, C.A., Needs, S., Aldrovandi, M., Tiefenbach, J., Bielska, E., Rubino, R.E., Nicol, C.J., May, R.C., et al. (2019). 15-keto-prostaglandin E2 activates host peroxisome proliferator-activated receptor gamma (PPAR-γ) to promote Cryptococcus neoformans growth during infection. PLOS Pathog. *15*, e1007597.

Fa, Z., Xie, Q., Fang, W., Zhang, H., Zhang, H., Xu, J., Pan, W., Xu, J., Olszewski, M.A., Deng, X., et al. (2017). RIPK3/Fas-Associated Death Domain Axis Regulates Pulmonary Immunopathology to Cryptococcal Infection Independent of Necroptosis. Front. Immunol. *8*, 1055.

Fan, W., Kraus, P., Boily, M., and Heitman, J. (2005). Cryptococcus neoformans gene expression during murine macrophage infection. Eukaryot. Cell *4*, 1420–1433.

Feldmesser, M., Casadevall, A., Kress, Y., Spira, G., and Orlofsky, A. (1997). Eosinophil-Cryptococcus neoformans interactions in vivo and in vitro. Infect. Immun. *65*, 1899–1907.

Feldmesser, M., Kress, Y., Novikoff, P., and Casadavell, A. (2000). Cryptococcus neoformans is a facultative intracellular pathogen in murine pulmonary infection. Infect. Immun. *68*, 4225–4237.

Fernández-Arenas, E., Bleck, C.K.E., Nombela, C., Gil, C., Griffiths, G., and Diez-Orejas, R. (2009). *Candida albicans* actively modulates intracellular membrane trafficking in mouse macrophage phagosomes. Cell. Microbiol. *11*, 560–589.

Figueira, R., and Holden, D.W. (2012). Functions of the Salmonella pathogenicity island 2 (SPI-2) type III secretion system effectors. Microbiology *158*, 1147–1161.

Fiorentino, D.F., Zlotnik, A., Vieira, P., Mosmann, T.R., Howard, M., Moore, K.W., and O'Garra, A. (1991). IL-10 acts on the antigen-presenting cell to inhibit cytokine production by Th1 cells. J. Immunol. *146*, 3444–3451.

Flannagan, R.S., Jaumouillé, V., and Grinstein, S. (2012). The Cell Biology of Phagocytosis. Annu. Rev. Pathol. Mech. Dis. *7*, 61–98.

Flesch, I., Schwamberger, G., and Kauffman, C. (1989). Fungicidal activity of IFN-

gamma-activated macrophages. Extracellular killing of Cryptococcus neoformans. J. Immunol. *142*, 3219–3224.

Franzot, S.P., Salkin, I.F., and Casadevall, A. (1999). Cryptococcus neoformans var. grubii: Separate varietal status for Cryptococcus neoformans serotype A isolates. J. Clin. Microbiol. *37*, 838–840.

Fries, B.C., Taborda, C.P., Serfass, E., and Casadevall, A. (2001). Phenotypic switching of Cryptococcus neoformans occurs in vivo and influences the outcome of infection. J. Clin. Invest. *108*, 1639–1648.

Fusco, A.C., Salafsky, B., and Delbrook, K. (1986). Schistosoma mansoni: Production of Cercarial Eicosanoids as Correlates of Penetration and Transformation. J. Parasitol. *72*, 397–404.

Gaillard, J.-L., Berche, P., Mounier, J., Richard, S., and Sansonetti, P. (1987). In Vitro Model of Penetration and Intracellular Growth of Listeria monocytogenes in the Human Enterocyte-Like Cell Line Caco-2. Infect. Immun. *55*, 2822–2829.

Gajewski, T.F., and Fitch, F.W. (1988). Anti-proliferative effect of IFN-gamma in immune regulation. I. IFN-gamma inhibits the proliferation of Th2 but not Th1 murine helper T lymphocyte clones. J. Immunol. *140*, 4245–4252.

Galanis, E., and MacDougall, L. (2010). Epidemiology of Cryptococcus gattii, British Columbia, Canada, 1999–2007. Emerg. Infect. Dis. *16*, 251–257.

Gambello, M.J., and Iglewski, B.H. (1991). Cloning and characterization of the Pseudomonas aeruginosa lasR gene, a transcriptional activator of elastase expression. J. Bacteriol. *173*, 3000–3009.

Garcia-Hermoso, D., Janbon, G., and Dromer, F. (1999). Epidemiological Evidence for Dormant Cryptococcus neoformans Infection. *37*, 3204-3209.

Garelnabi, M., and May, R.C. (2018). Variability in innate host immune responses to cryptococcosis. Mem. Inst. Oswaldo Cruz *113*, e180060.

Garelnabi, M., Taylor-Smith, L.M., Bielska, E., Hall, R.A., Stones, D., and May, R.C. (2018). Quantifying donor-to-donor variation in macrophage responses to the human fungal pathogen Cryptococcus neoformans. PLoS One *13*, e0194615.

Garro, A.P., Chiapello, L.S., Baronetti, J.L., and Masih, D.T. (2010). Rat eosinophils stimulate the expansion of Cryptococcus neoformans-specific CD4+ and CD8+ T cells with a T-helper 1 profile. Immunology *132*, 174–187.

Garro, A.P., Chiapello, L.S., Baronetti, J.L., and Masih, D.T. (2011). Eosinophils elicit proliferation of naive and fungal-specific cells in vivo so enhancing a T helper type 1 cytokine profile in favour of a protective immune response against Cryptococcus

neoformans infection. Immunology *134*, 198–213.

Gassiep, I., McDougall, D., Douglas, J., Francis, R., and Playford, E.G. (2017). Cryptococcal infections in solid organ transplant recipients over a 15-year period at a state transplant center. Transpl. Infect. Dis. *19*, e12639.

George, E.A., and Muir, T.W. (2007). Molecular Mechanisms of agr Quorum Sensing in Virulent Staphylococci. ChemBioChem *8*, 847–855.

Gerstein, A.C., Fu, M.S., Mukaremera, L., Li, Z., Ormerod, K.L., Fraser, J.A., Berman, J., and Nielsen, K. (2015). Polyploid titan cells produce haploid and aneuploid progeny to promote stress adaptation. MBio *6*, e01340-15.

Geunes-Boyer, S., Oliver, T.N., Janbon, G., Lodge, J.K., Heitman, J., Perfect, J.R., and Wright, J.R. (2009). Surfactant protein D increases phagocytosis of hypocapsular Cryptococcus neoformans by murine macrophages and enhances fungal survival. Infect. Immunity *77*, 2783–2794.

Geunes-Boyer, S., Beers, M.F., Perfect, J.R., Heitman, J., and Wright, J.R. (2012). Surfactant protein D facilitates Cryptococcus neoformans infection. Infect. Immun. *80*, 2444–2453.

Gibson, J.F., and Johnston, S.A. (2015). Immunity to Cryptococcus neoformans and C. gattii during cryptococcosis. Fungal Genet. Biol. *78*, 76–86.

Gibson, J.F., Evans, R.J., Bojarczuk, A., Hotham, R., Lagendijk, A.K., Hogan, B.M., Ingham, P.W., Renshaw, S.A., and Johnston, S.A. (2017). Dissemination of Cryptococcus neoformans via localised proliferation and blockage of blood vessels. BioRxiv 184200.

Gideon, H.P., and Flynn, J.L. (2011). Latent tuberculosis: what the host “sees”? Immunol Res *50*, 202–212.

Giles, S.S., Dagenais, T.R.T., Botts, M.R., Keller, N.P., and Hull, C.M. (2009). Elucidating the pathogenesis of spores from the human fungal pathogen Cryptococcus neoformans. Infect. Immun. *77*, 3491–3500.

Gilroy, D., Colville-Nash, P., Willis, D., Chivers, J., Paul-Clark, M., and Willoughby, D. (1999). Inducible cyclooxygenase may have anti-inflammatory properties. Nat. Med. *5*, 698–701.

Goel, A., Deogaonkar, M., Nagpal, R.D., Deogaonk, M., and Agpal, R.D.N. (1996). Extra-axial clival blastomycosis granulom a: a case report. Br. J. Neurosurg. *10*, 97–98.

Gold, K., Weyand, C., and Goronzy, J. (1994). Modulation of helper T cell function by prostaglandins. Arthritis Rheum. *37*, 925–933.

Goldman, D., Cho, Y., Zhao, M.-L., Casadevall, A., and Lee, S.C. (1996). Expression of Inducible Nitric Oxide Synthase in Rat Pulmonary Cryptococcus neoformans Granulomas. *148*, 1275-1282.

Goldman, D.L., Lee, S.C., Mednick, A.J., Montella, L., and Casadevall, A. (2000). Persistent Cryptococcus neoformans Pulmonary Infection in the Rat Is Associated with Intracellular Parasitism, Decreased Inducible Nitric Oxide Synthase Expression, and Altered Antibody Responsiveness to Cryptococcal Polysaccharide. *68*, 832-838.

Goldman, D.L., Khine, H., Abadi, J., Lindenberg, D.J., Pirofski, L., Niang, R., and Casadevall, A. (2001). Serologic Evidence for Cryptococcus neoformans Infection in Early Childhood. Pediatrics *105*, e66–e66.

Gomez, P., Pillinger, M., Attur, M., Marjanovic, N., Dave, M., Park, J., Bingham III, C., Al-Mussawir, H., and Abramson, S. (2005). Resolution of Inflammation: Prostaglandin E 2 Dissociates Nuclear Trafficking of Individual NF- κB Subunits (p65, p50) in Stimulated Rheumatoid Synovial Fibroblasts. J. Immunol. *175*, 6924–6930.

Gordon, S. (2016). Phagocytosis: An Immunobiologic Process. Immunity *44*, 463–475.

Graf, B.A., Nazarenko, D.A., Borrello, M.A., Roberts, L.J., Morrow, J.D., Palis, J., and Phipps, R.P. (1999). Biphenotypic B / macrophage cells express COX-1 and up-regulate COX-2 expression and prostaglandin E2 production in response to pro-inflammatory signals. Eur. J. Immunol. *29*, 3793–3803.

Grant, A.J., Restif, O., McKinley, T.J., Sheppard, M., Maskell, D.J., and Mastroeni, P. (2008). Modelling within-Host Spatiotemporal Dynamics of Invasive Bacterial Disease. PLoS Biol. *6*, e74.

Grijpstra, J., Tefsen, B., Van Die, I., and De Cock, H. (2009). The Cryptococcus neoformans cap10 and cap59 mutant strains, affected in glucuronoxylomannan synthesis, dijerentially activate human dendritic cells. FEMS Immunol. Med. Microbiol. *57*, 142–150.

Grubmüller, S., Schauer, K., Goebel, W., Fuchs, T.M., and Eisenreich, W. (2014). Analysis of carbon substrates used by Listeria monocytogenes during growth in J774A.1 macrophages suggests a bipartite intracellular metabolism. Front. Cell. Infect. Microbiol. *4*, 156.

Guermonprez, P., Valladeau, J., Zitvogel, L., Théry, C., and Amigorena, S. (2002). Antigen Presentation and T Cell Stimulation by Dendritic Cells. Annu. Rev. Immunol. *20*, 621–667.

Gupta, S., Maurya, M., Stephens, D., Dennis, E., and Subramaniam, S. (2009). An integrated model of eicosanoid metabolism and signaling based on lipidomics flux

analysis. Biophys. J. *96*, 4542–4551.

Guttman, J.A., and Finlay, B.B. (2009). Tight junctions as targets of infectious agents. Biochim. Biophys. Acta *1788*, 832–841.

Hagen, F., Khayhan, K., Theelen, B., Kolecka, A., Polacheck, I., Sionov, E., Falk, R., Parnmen, S., Lumbsch, H.T., and Boekhout, T. (2015). Recognition of seven species in the Cryptococcus gattii/Cryptococcus neoformans species complex. Fungal Genet. Biol. *78*, 16–48.

Hagen, F., Lumbsch, H.T., Arsic Arsenijevic, V., Badali, H., Bertout, S., Billmyre, R.B., Bragulat, M.R., Cabañes, F.J., Carbia, M., Chakrabarti, A., et al. (2017). Importance of Resolving Fungal Nomenclature: the Case of Multiple Pathogenic Species in the Cryptococcus Genus. MSphere *2*, e00238-17.

Halle, S., Halle, O., and Förster, R. (2017). Mechanisms and Dynamics of T Cell-Mediated Cytotoxicity In Vivo. Trends Immunol. *38*, 432–443.

Hansakon, A., Mutthakalin, P., Ngamskulrungroj, P., Chayakulkeeree, M., and Angkasekwinai, P. (2019). Cryptococcus neoformans and Cryptococcus gattii clinical isolates from Thailand display diverse phenotypic interactions with macrophages. Virulence *10*, 26–36.

Hardison, S.E., Ravi, S., Wozniak, K.L., Young, M.L., Olszweski, M.A., and Wormley Jr., F.L. (2010). Pulmonary infection with an interferon-gamma-producing Cryptococcus neoformans strain results in classical macrophage activation and protection. Am. J. Pathol. *176*, 774–785.

Hardison, S.E., Herrera, G., Young, M.L., Hole, C.R., Wozniak, K., and Wormley, F. (2012). Protective Immunity against Pulmonary Cryptococcosis Is Associated with STAT1-Mediated Classical Macrophage Activation. J. Immunol. *189*, 4060–4068.

Harizi, H., and Gualde, N. (2004). Inhibition of IL-6, TNF-α, and cyclooxygenase-2 protein expression by prostaglandin E2-induced IL-10 in bone marrow-derived dendritic cells. Cell. Immunol. *228*, 99–109.

Harizi, H., Corcuff, J.-B., and Gualde, N. (2008). Arachidonic-acid-derived eicosanoids: roles in biology and immunopathology. Trends Mol. Med. *14*, 461–469.

Harrison, T.S., and Levitz, S.M. (1996). Role of IL-12 in peripheral blood mononuclear cell responses to fungi in persons with and without HIV infection. J. Immunol. *156*, 4492–4497.

Harrison, T.S., Griffin, G.E., and Levitz, S.M. (2000). Conditional Lethality of the Diprotic Weak Bases Chloroquine and Quinacrine against Cryptococcus neoformans. J. Infect. Dis. *182*, 283–289.

Harrison, T.S., Chen, J., Simons, E., and Levitz, S.M. (2002). Determination of the pH of the Cryptococcus neoformans vacuole. Med. Mycol. *40*, 329–332.

Hazan, R., and Engelberg-Kulka, H. (2004). Escherichia coli mazEF-mediated cell death as a defense mechanism that inhibits the spread of phage P1. Mol. Genet. Genomics *272*, 227–234.

He, Y., Reichow, S., Ramamoorthy, S., Ding, X., Lathigra, R., Craig, J.C., Sobral, B.W.S., Schurig, G.G., Sriranganathan, N., and Boyle, S.M. (2006). Brucella melitensis Triggers Time-Dependent Modulation of Apoptosis and Down-Regulation of Mitochondrion-Associated Gene Expression in Mouse Macrophages Downloaded from. Infect. Immun. *74*, 5035–5046.

Heesters, B.A., van der Poel, C.E., Das, A., and Carroll, M.C. (2016). Antigen Presentation to B Cells. Trends Immunol. *37*, 844–854.

Helaine, S., Cheverton, A.M., Watson, K.G., Faure, L.M., Matthews, S.A., and Holden, D.W. (2014). Internalization of Salmonella by macrophages induces formation of nonreplicating persisters. Science (80-.). *343*, 204–208.

Heninger, E., Hogan, L.H., Karman, J., Macvilay, S., Hill, B., Woods, J.P., and Sandor, M. (2006). Characterization of the Histoplasma capsulatum-induced granuloma. J. Immunol. *177*, 3303-3313.

Herbomel, P., Thisse, B., and Thisse, C. (1999). Ontogeny and behaviour of early macrophages in the zebrafish embryo. Development *126*, 3735–3745.

Herring, A.C., Lee, J., McDonald, R.A., Toews, G.B., and Huffnagle, G.B. (2002). Induction of interleukin-12 and gamma interferon requires tumor necrosis factor alpha for protective T1-cell-mediated immunity to pulmonary Cryptococcus neoformans infection. Infect. Immun. *70*, 2959–2964.

Hesse, M., Modolell, M., La Flamme, A.C., Schito, M., Fuentes, J.M., Cheever, A.W., Pearce, E.J., and Wynn, T.A. (2001). Differential regulation of nitric oxide synthase-2 and arginase-1 by type 1/type 2 cytokines in vivo: granulomatous pathology is shaped by the pattern of L-arginine metabolism. J. Immunol. *167*, 6533–6544.

Hidore, M.R., Nabavi, N., Sonleitner, F., and Murphy, J.W. (1991). Murine Natural Killer Cells Are Fungicidal to Cryptococcus neoformans. Infect. Immun. *59*, 1747–1754.

Higgs, G.A. (1986). The role of eicosanoids in inflammation. Prog. Lipid Res. *25*, 555–561.

Hilkens, C.M.U., Vermeulen, H., van Neerven, R.J.J., Snijdewint, F.G.M., Wierenga, E.A., and Kapsenber, M.L. (1995). Differential modulation of T helper type 1 (Th1) and T helper type 2 (Th2) cytokine secretion by prostaglandin E2 critically depends

on interleukin-2. Eur. J. Immunol. *25*, 59–63.

Hill, J.O., and Harmsen, A.G. (1991). Intrapulmonary Growth and Dissemination of an Avirulent Strain of Cryptococcus neoformans in Mice Depleted of CD4+ or CD8+ T Cells. J. Exp. Med. *173*, 755–758.

Hoag, K.A., Street, N.A., Huffnagle, G.B., and Lipscomb, M.F. (1995). Early cytokine production in pulmonary Cryptococcus neoformans infections distinguishes susceptible and resistant mice. Am. J. Respir. Cell Mol. Biol. *13*, 487-495.

Hoag, K.A., Lipscomb, M.F., Izzo, A.A., and Street, N.E. (1997). IL-12 and IFN-gamma are required for initiating the protective Th1 response to pulmonary cryptococcosis in resistant C.B-17 Mice. Am. J. Respir. Cell Mol. Biol. *17*, 733–739.

Hole, C.R., Bui, H., Wormley, F.L., and Wozniak, K.L. (2012). Mechanisms of Dendritic Cell Lysosomal Killing of Cryptococcus. Sci. Rep. *2*, 739.

Hornby, J.M., Jensen, E.C., Lisec, A.D., Tasto, J.J., Jahnke, B., Shoemaker, R., Dussault, P., and Nickerson, K.W. (2001). Quorum sensing in the dimorphic fungus Candida albicans is mediated by farnesol. Appl. Environ. Microbiol. *67*, 2982–2992.

Hu, G., Hacham, M., Waterman, S.R., Panepinto, J., Shin, S., Liu, X., Gibbons, J., Valyi-Nagy, T., Obara, K., Jaffe, H.A., et al. (2008). PI3K signaling of autophagy is required for starvation tolerance and virulence of Cryptococcus neoformans. J. Clin. Invest. *118*, 1186–1197.

Huffnagle, G., Boyd, M., Street, N., and Lipscomb, M. (1998). IL-5 Is Required for Eosinophil Recruitment, Crystal Deposition, and Mononuclear Cell Recruitment During a Pulmonary Cryptococcus neoformans Infection in Genetically Susceptible Mice (C57BL/6). J. Immunol. *160*, 2393–2400.

Huffnagle, G.B., Yates, J.L., and Lipscomb, M.F. (1991). Immunity to a pulmonary Cryptococcus neoformans infection requires both CD4+ and CD8+ T cells. J. Exp. Med. *173*, 793–800.

Huisman, G.W., and Kolter, R. (1995). Sensing Starvation: A Homoserine Lactone-Dependent Signaling Pathway in Escherichia coli. Science. *265*, 537–539.

Huston, S.M., Shun Li, S., Stack, D., Timm-McCann, M., Jones, G.J., Islam, A., Berenger, B.M., Xiang, R.F., Colarusso, P., and Mody, C.H. (2013). Cryptococcus gattii is killed by dendritic cells, but evades adaptaive immunity by failing to induce dendritic cell maturation. J. Immunol. *191*, 249–261.

Ingersoll, M.A., Spanbroek, R., Lottaz, C., Gautier, E.L., Frankenberger, M., Hoffmann, R., Lang, R., Haniffa, M., Collin, M., Tacke, F., et al. (2010). Comparison of gene expression profiles between human and mouse monocyte subsets. Blood *115*, e10–e19.

Islam, A., Li, S.S., Oykhman, P., Timm-McCann, M., Huston, S.M., Stack, D., Xiang, R.F., Kelly, M.M., and Mody, C.H. (2013). An acidic microenvironment increases NK cell killing of Cryptococcus neoformans and Cryptococcus gattii by enhancing perforin degranulation. PLoS Pathog. *9*, e1003439.

Izadpanah, A., and Gallo, R.L. (2005). Antimicrobial peptides. J. Am. Acad. Dermatol. *52*, 381–390.

James, P.G., Cherniak, R., Jones, R.G., and Stortz, C.A. (1990). Cell-wall glucans of Cryptococcus neoformans CAP 67. Carbohydr. Res. *198*, 23–38.

Janbon, G., Ormerod, K.L., Paulet, D., Byrnes, E.J., Yadav, V., Chatterjee, G., Mullapudi, N., Hon, C.-C., Billmyre, R.B., Brunel, F., et al. (2014). Analysis of the Genome and Transcriptome of Cryptococcus neoformans var. grubii Reveals Complex RNA Expression and Microevolution Leading to Virulence Attenuation. PLoS Genet. *10*, e1004261.

Jank, T., Giesemann, T., and Aktories, K. (2007). Rho-glucosylating Clostridium difficile toxins A and B: new insights into structure and function. Glycobiology *17*, 15R-22R.

Jarvis, J., Meintjes, G., Williams, A., Brown, Y., Crede, T., and Harrison, T.S. (2010). Adult meningitis in a setting of high HIV and TB prevalence : findings from 4961 suspected cases. BMC Infect. Dis. 67.

Jarvis, J., Meintjes, G., Bicanic, T., Buffa, V., Hogan, L., Mo, S., Tomlinson, G., Kropf, P., Noursadeghi, M., and Harrison, T.S. (2015). Cerebrospinal fluid cytokine profiles predict risk of early mortality and immune reconstitution inflammatory syndrome in HIV-associated cryptococcal meningitis. PLoS Pathog. *11*, e1004754.

Jarvis, J.N., Casazza, J.P., Stone, H.H., Meintjes, G., Lawn, S.D., Levitz, S.M., Harrison, T.S., and Koup, R.A. (2013). The phenotype of the cryptococcus-specific CD4+ memory T-cell response is associated with disease severity and outcome in HIV-associated cryptococcal meningitis. J. Infect. Dis. *207*, 1817–1828.

Jarvis, J.N., Bicanic, T., Loyse, A., Namarika, D., Jackson, A., Nussbaum, J.C., Longley, N., Muzoora, C., Phulusa, J., Taseera, K., et al. (2014). Determinants of Mortality in a Combined Cohort of 501 Patients With HIV-Associated Cryptococcal Meningitis: Implications for Improving Outcomes. Clin. Infect. Dis. *58*, 736–745.

Jazayeri, J.A., Nguyen, K., Kotsanas, D., Schneiders, F., Tan, C.-H., Jazayeri, M., and Armstrong, D. (2016). Comparison of Virulence Factors in Pseudomonas aeruginosa Strains Isolated from Cystic Fibrosis Patients. Journel Med. Microb. Diagnostics *5*, 1000242.

Jenkins, S.J., Ruckerl, D., Cook, P.C., Jones, L.H., Finkelman, F.D., van Rooijen, N.,

MacDonald, A.S., and Allen, J.E. (2011). Local macrophage proliferation, rather than recruitment from the blood, is a signature of TH2 inflammation. Science (80-.). *332*, 1284–1288.

Ji, G., Beavist, R.C., and Novick, R.P. (1995). Cell density control of staphylococcal virulence mediated by an octapeptide pheromone. *92*, 12055-12059.

Johnston, S.A., and May, R. (2010). The human fungal pathogen Cryptococcus neoformans escapes macrophages by a phagosome emptying mechanism that is inhibited by arp2/3 complex- mediated actin polymerisation. PLoS Pathog. *6*, 27–28.
Johnston, S.A., and May, R. (2013). Cryptococcus interactions with macrophages: Evasion and manipulation of the phagosome by a fungal pathogen. Cell. Microbiol. *15*, 403–411.

Johnston, S.A., Voelz, K., and May, R.C. (2016). Cryptococcus neoformans Thermotolerance to Avian Body Temperature Is Sufficient For Extracellular Growth But Not Intracellular Survival In Macrophages. Sci. Rep. *6*, 20977.

Józefowski, S., Bobek, M., and Marcinkiewicz, J. (2003). Exogenous but not endogenous prostanoids regulate cytokine secretion from murine bone marrow dendritic cells: EP2, DP, and IP but not EP1, EP3, and FP prostanoid receptors are involved. Int. Immunopharmacol. *3*, 865–878.

Jubrail, J., Morris, P., Bewley, M.A., Stoneham, S., Johnston, S.A., Foster, S.J., Peden, A.A., Read, R.C., Marriott, H.M., and Dockrell, D.H. (2016). Inability to sustain intraphagolysosomal killing of *Staphylococcus aureus* predisposes to bacterial persistence in macrophages. Cell. Microbiol. *18*, 80–96.

Jung, S.A., Chapman, C.A., and Ng, W.-L. (2015). Quadruple Quorum-Sensing Inputs Control Vibrio cholerae Virulence and Maintain System Robustness. PLOS Pathog. *11*, e1004837.

Kang, R., Freire-Moar, J., Sigal, E., and Chu, C. (1996). Expression of cyclooxygenase-2 in human and an animal model of rheumatoid arthritis. Br. J. Rheumatol. *35*, 711–718.

Kaplan, H.B., and Plamann, L. (1996). A Myxococcus xanthus cell density-sensing system required for multicellular development. *139*, 89-95.

Kawahito, Y., Hla, T., Sano, H., Kawahito, Y., Kondo, M., Tsubouchi, Y., Hashiramoto, A., Bishop-bailey, D., Inoue, K., Kohno, M., et al. (2000). 15-deoxy-Δ12,14-PGJ2 Induces Synoviocyte Apoptosis and Suppresses Adjuvant-Induced Arthritis in Rats. J. Clin. Invest. *106*, 189–197.

Kawakami, K., Kohno, S., Kadota, J.-I., Tohyama, M., Teruya, K., Kudeken, N., Saito, A., and Hara, K. (1995). T Cell-Dependent Activation of Macrophages and Enhancement of Their Phagocytic Activity in the Lungs of Mice Inoculated with Heat-

Killed Cryptococcus neoformans: Involvement of IFN-gamma and Its Protective Effect against Cryptococcal Infection. *39*, 135-143.

Kawakami, K., Qifent, X., Tohyama, M., Qureshi, M.H., and Saito, A. (1996a). Contribution of tumour necrosis factor-alpha in host defence mechanism against Cryptococcus neoformans. Clin. Exp. Immunol. *106*, 468–474.

Kawakami, K., Tohyama, M., Xie, Q., and Saito, A. (1996b). IL-12 protects mice against pulmonary and disseminated infection caused by Cryptococcus neoformans. Clin. Exp. Immunol. *104*, 208–214.

Kawakami, K., Koguchi, Y., Qureshi, H., Yara, S., Kinjo, Y., Uezu, K., and Saito, A. (2000). NK cells eliminate Cryptococcus neoformans by potentiating the fungicidal activity of macrophages rather than by direct killing them up on stimulation with IL-12 and IL-18. *44*, 1043-1050.

Kedzierska, K., and Crowe, S.M. (2001). Cytokines and HIV-1: interactions and clinical implications. Antivir. Chem. Chemother. *12*, 133–150.

Kelly, R.M., Chen, J., Yauch, L.E., and Levitz, S.M. (2005). Opsonic Requirements for Dendritic Cell-Mediated Responses to Cryptococcus neoformans. Infect. Immun. *73*, 592–598.

Kempner, E., and Hanson, F.E. (1968). Aspects of Light Production by Photobacterium fischeri. *95*, 975-979.

Kidd, S.E., Hagen, F., Tscharke, R.L., Huynh, M., Bartlett, K.H., Fyfe, M., Macdougall, L., Boekhout, T., Kwon-Chung, K.J., and Meyer, W. (2004). A rare genotype of Cryptococcus gattii caused the cryptococcosis outbreak on Vancouver Island (British Columbia, Canada). Proc. Natl. Acad. Sci. U. S. A. *101*, 17258–17263.

Kiertiburanakul, S., Wirojtananugoon, S., Pracharktam, R., and Sungkanuparph, S. (2006). Cryptococcosis in human immunodeficiency virus-negative patients. Int. J. Infect. Dis. *10*, 72–78.

Knodler, L.A., Helaine, S., García-Del Portillo, F., and Castanheira, S. (2017). Salmonella Populations inside Host Cells. Front. Cell. Infect. Microbiol. *7*, 432.

Knowles, M.R., and Boucher, R.C. (2002). Mucus clearance as a primary innate defense mechanism for mammalian airways. J. Clin. Invest. *109*, 571–577.

Kobayashi, M., Ito, M., Sano, K., and Koyama, M. (2001). Granulomatous and cytokine responses to pulmonary Cryptococcus neoformans in two strains of rats. Mycopathologia *151*, 121–130.

Koguchi, Y., and Kawakami, K. (2002). Cryptococcal Infection and Th1-Th2 Cytokine Balance. Int. Rev. Immunol. *21*, 423–428.

Kolodkin-Gal, I., Hazan, R., Gaathon, A., Carmeli, S., and Engelberg-Kulka, H. (2007). A linear pentapeptide is a quorum-sensing factor required for mazEF-mediated cell death in Escherichia coli. Science (80-.). *318*, 652–655.

Kozel, T.R. (1977). Non-encapsulated variant of Cryptococcus neoformans. II. Surface receptors for cryptococcal polysaccharide and their role in inhibition of phagocytosis by polysaccharide. Infect. Immun. *16*, 99–106.

Kozel, T., and Gotschlich, E. (1982). The capsule of cryptococcus neoformans passively inhibits phagocytosis of the yeast by macrophages. J. Immunol. *129*, 1675–1680.

Kretschmer, M., Wang, J., and Kronstad, J.W. (2012). Peroxisomal and mitochondrial β-oxidation pathways influence the virulence of the pathogenic fungus Cryptococcus neoformans. Eukaryot. Cell *11*, 1042–1054.

Kubata, B., Eguchi, N., Urade, Y., Yamashita, K., Mitamura, T., Tai, K., Hayaishi, O., and Horii, T. (1998). Plasmodium falciparum produces prostaglandins that are pyrogenic, somnogenic, and immunosuppressive substances in humans. J. Exp. Med. *188*, 1197–1202.

Kügler, S., Schurtz Sebghati, T., Groppe Eissenberg, L., and Goldman, W.E. (2000). Phenotypic variation and intracellular parasitism by histoplasma Capsulatum. Proc. Natl. Acad. Sci. *97*, 8794–8798.

Kumar, H., Kawai, T., and Akira, S. (2011). Pathogen recognition by the innate immune system. Int. Rev. Immunol. *30*, 16–34.

Kuspa, A., Plamann, L., and Kaiser, D. (1992). A-Signalling and the Cell Density Requirement for Myxococcus xanthus Development. J. Bacteriol. *174*, 7360–7369.

Kwon-Chung, K.J. (1975). A new genus, filobasidiella, the perfect state of Cryptococcus neoformans. Mycologia *67*, 1197–1200.

Kwon-Chung, K.J. (1976). A new species of Filobasidiella, the sexual state of Cryptococcus neoformans B and C serotypes. Mycologia *68*, 943–946.

Kwon-Chung, K.J.K., and Varma, A. (2006). Do major species concepts support one, two or more species within Cryptococcus neoformans? FEMS Yeast Res. *6*, 574–587.

Kwon-Chung, K.J., Bennett, J.E., and Rhodes, J.C. (1982). Taxonomic studies on Filobasidiella species and their anamorphs. Antonie Van Leeuwenhoek *48*, 25–38.

Kwon-Chung, K.J., Boekhout, T., Fell, J.W., and Diaz, M. (2002). Proposal to conserve the name Cryptococcus gattii against C. hondurianus and C. bacillisporus (Basidiomycota, Hymenomycetes, Tremellomycetidae). Taxon *51*, 804–806.

Kwon-Chung, K.J., Bennett, J.E., Wickes, B.L., Meyer, W., Cuomo, C.A., Wollenburg, K.R., Bicanic, T.A., Castañeda, E., Chang, Y.C., Chen, J., et al. (2017). The Case for Adopting the "Species Complex" Nomenclature for the Etiologic Agents of Cryptococcosis. MSphere *2*, 1–7.

Kyei, S.K., Ogbomo, H., Li, S., Timm-McCann, M., Xiang, R.F., Huston, S.M., Ganguly, A., Colarusso, P., John Gill, M., Mody, C.H., et al. (2016). Mechanisms by Which Interleukin-12 Corrects Defective NK Cell Anticryptococcal Activity in HIV-Infected Patients. MBio *7*, e00878-16.

Lacey, D., Achuthan, A., Fleetwood, A., Dinh, H., Roiniotis, J., Scholz, G., Chang, M., Beckman, S., Cook, A., and Hamilton, J. (2012). Defining GM-CSF- and macrophage-CSF-dependent macrophage responses by in vitro models. J. Immunol. *188*, 5752–5765.

Lam, R.S., O'Brien-Simpson, N.M., Holden, J.A., Lenzo, J.C., Fong, S.B., and Reynolds, E.C. (2016). Unprimed, M1 and M2 Macrophages Differentially Interact with Porphyromonas gingivalis. PLoS One *11*, e0158629.

Lam, S.., Chua, H.., Gong, Z., Lam, T.., and Sin, Y.. (2004). Development and maturation of the immune system in zebrafish, Danio rerio: a gene expression profiling, in situ hybridization and immunological study. Dev. Comp. Immunol. *28*, 9–28.

Lanier, L.L. (2005). NK Cell Recognition. Annu. Rev. Immunol. *23*, 225–274.

Lawley, T.D., Bouley, D.M., Hoy, Y.E., Gerke, C., Relman, D.A., and Monack, D.M. (2008). Host Transmission of Salmonella enterica Serovar Typhimurium Is Controlled by Virulence Factors and Indigenous Intestinal Microbiota. Infect. Immun. *76*, 403–416.

Lee, A.H.-Y., Flibotte, S., Sinha, S., Paiero, A., Ehrlich, R.L., Balashov, S., Ehrlich, G.D., Zlosnik, J.E.A., Mell, J.C., and Nislow, C. (2017). Phenotypic diversity and genotypic flexibility of Burkholderia cenocepacia during long-term chronic infection of cystic fibrosis lungs. Genome Res. *27*, 1–13.

Lee, H., Chang, Y.C., Nardone, G., and Kwon-Chung, K.J. (2007). TUP1 disruption in Cryptococcus neoformans uncovers a peptide-mediated density-dependent growth phenomenon that mimics quorum sensing. Mol. Microbiol. *64*, 591–601.

Lee, H., Chang, Y.C., Varma, A., and Kwon-Chung, K.J. (2009). Regulatory diversity of TUP1 in Cryptococcus neoformans. Eukaryot. Cell *8*, 1901–1908.

Lee, S.C., Kress, Y., Zhao, M.L., Dickson, D.W., and Casadevall, A. (1995). Cryptococcus neoformans survive and replicate in human microglia. Lab. Invest. *73*, 871–879.

Lee, Y.-C., Wang, J.-T., Sun, H.-Y., and Chen, Y.-C. (2011). Comparisons of clinical features and mortality of cryptococcal meningitis between patients with and without human immunodeficiency virus infection. J. Microbiol. Immunol. Infect. *44*, 338–345.

Lehnert, T., Timme, S., Pollmächer, J., Hünniger, K., Kurzai, O., and Figge, M.T. (2015). Bottom-up modeling approach for the quantitative estimation of parameters in pathogen-host interactions. Front. Microbiol. *6*, 608.

Lengeler, K.B., Cox, G.M., and Heitman, J. (2001). Serotype AD strains of Cryptococcus neoformans are diploid or aneuploid and are heterozygous at the mating-type locus. Infect. Immun. *69*, 115–122.

Leung, K.Y., and Finlay, B.B. (1991). Intracellular replication is essential for the virulence of Salmonella typhimurium.PNAS *88*, 11470-11474.

Levitz, S.M., and Dibenedetto, D.J. (1989). Paradoxical role of capsule in murine bronchoalveolar macrophage-mediated killing of Cryptococcus neoformans. J. Immunol. *142*, 659–669.

Levitz, S.M., and Farrell, T.P. (1990). Growth Inhibition of Cryptococcus neoformans by Cultured Human Monocytes: Role of the Capsule, Opsonins, the Culture Surface, and Cytokines. Infect. immun. *58*, 1201-1209.

Levitz, S.M., and Tabuni, A. (1991). Binding of Cryptococcus neoformans by Human Cultured Macrophages: Requirements for Multiple Complement Receptors and Actin. J. Clin. Invest. *87*, 528–535.

Levitz, S., Tabuni, A., Kornfeld, H., and Dolenbock, D. (1994). Production of tumor necrosis factor alpha in human leukocytes stimulated by *Cryptococcus neoformans*. Infect. Immun. *62*, 1975–1981.

Levitz, S.M., Harrison, T.S., Tabuni, A., and Liu, X. (1997). Chloroquine induces human mononuclear phagocytes to inhibit and kill Cryptococcus neoformans by a mechanism independent of iron deprivation. J. Clin. Invest. *100*, 1640–1646.

Levitz, S.M., Nong, S.H., Seetoo, K.F., Harrison, T.S., Speizer, R.A., and Simons, E.R. (1999). Cryptococcus neoformans resides in an acidic phagolysosome of human macrophages. Infect. Immun. *67*, 885–890.

Li, Z., and Nair, S.K. (2012). Quorum sensing: How bacteria can coordinate activity and synchronize their response to external signals? Protein Sci. *21*, 1403–1417.

Li, S.S., Kyei, S.K., Timm-Mccann, M., Ogbomo, H., Jones, G.J., Shi, M., Xiang, R.F., Oykhman, P., Huston, S.M., Islam, A., et al. (2013). The NK Receptor NKp30 Mediates Direct Fungal Recognition and Killing and Is Diminished in NK Cells from HIV-Infected Patients. Cell Host Microbe *14*, 387-397.

Lieschke, G.J., Oates, A.C., Crowhurst, M.O., Ward, A.C., and Layton, J.E. (2008). Morphologic and functional characterization of granulocytes and macrophages in embryonic and adult zebrafish. Phagocytes *98*, 3087–3096.

Lim, J., Coates, C.J., Seoane, P.I., Garelnabi, M., Taylor-Smith, L.M., Monteith, P., Macleod, C.L., Escaron, C.J., Brown, G.D., Hall, R.A., et al. (2018). Characterizing the Mechanisms of Nonopsonic Uptake of Cryptococci by Macrophages. J. Immunol. *200*, 3539–3546.

Lin, Y.-Y., Shiau, S., and Fang, C.-T. (2015). Risk Factors for Invasive Cryptococcus neoformans Diseases: A Case-Control Study. PLoS One *10*, e0119090.

Lipscomb, M.F., Alvarellos, T., Toews, G.B., Tompkins, R., Evans, Z., Koo, G., and Kumar, V. (1987). Role of natural killer cells in resistance to Cryptococcus neoformans infections in mice. Am. J. Pathol. *128*, 354–361.

Lister, J.A., Robertson, C.P., Lepage, T., Johnson, S.L., and Raible, D.W. (1999). nacre encodes a zebrafish microphthalmia-related protein that regulates neural-crest-derived pigment cell fate. Development *126*, 3757–3767.

Loynes, C.A., Lee, J.A., Robertson, A.L., Steel, M.J., Ellett, F., Feng, Y., Levy, B.D., Whyte, M.K.B., and Renshaw, S.A. (2018). PGE $_2$ production at sites of tissue injury promotes an anti-inflammatory neutrophil phenotype and determines the outcome of inflammation resolution in vivo. Sci. Adv. *4*, eaar8320.

Luther, K., Torosantucci, A., Brakhage, A.A., Heesemann, J., and Ebel, F. (2007). Phagocytosis of Aspergillus fumigatus conidia by murine macrophages involves recognition by the dectin-1 beta-glucan receptor and Toll-like receptor 2. Cell. Microbiol. *9*, 368–381.

Ma, H., Croudace, J.E., Lammas, D.A., and May, R. (2006). Expulsion of Live Pathogenic Yeast by Macrophages. Curr. Biol. *16*, 2156–2160.

Ma, H., Hagen, F., Stekel, D.J., Johnston, S.A., Sionov, E., Falk, R., Polacheck, I., Boekhout, T., and May, R. (2009). The fatal fungal outbreak on Vancouver Island is characterized by enhanced intracellular parasitism driven by mitochondrial regulation. Proc. Natl. Acad. Sci. U. S. A. *106*, 12980–12985.

Ma, L., Wang, C.L.C., Neely, G.G., Epelman, S., Krensky, A.M., and Ling, C.H.M. (2004). NK cells use perforin rather than granulysin for anticryptococcal activity. J. Immunol. *173*, 3357–3365.

Macatonia, S.E., Hosken, N.A., Litton, M., Vieira, P., Hsieh, C.S., Culpepper, J.A., Wysocka, M., Trinchieri, G., Murphy, K.M., and O'Garra, A. (1995). Dendritic cells produce IL-12 and direct the development of Th1 cells from naive CD4+ T cells. J. Immunol. *154*, 5071–5079.

MacDougall, L., Kidd, S., Galanis, E., and Mak, S. (2007). Spread of Cryptococcus gattii in British Columbia, Canada, and detection in the Pacific Northwest, USA. Emerg. Infect. Dis. *13*, 42–45.

Maggi, L., Sadeghi, H., Weigand, C., Scarim, A., Heitmeier, M., and Corbett, J. (2000). Anti-inflammatory actions of 15-deoxy-delta 12,14-prostaglandin J2 and troglitazone: evidence for heat shock-dependent and -independent inhibition of cytokine-induced inducible nitric oxide synthase expression. Diabetes *49*, 346–355.

Mahamed, D., Boulle, M., Ganga, Y., Mc Arthur, C., Skroch, S., Oom, L., Catinas, O., Pillay, K., Naicker, M., Rampersad, S., et al. (2017). Intracellular growth of Mycobacterium tuberculosis after macrophage cell death leads to serial killing of host cells. Elife *6*, e22028.

Mambula, S.S., Simons, E.R., Hastey, R., Selsted, M.E., and Levitz, S.M. (2000). Human Neutrophil-Mediated Nonoxidative Antifungal Activity against Cryptococcus neoformans. Infect. Immun. *68*, 6257–6264.

Mansour, M., Reedy, J.L., Tam, J.M., and Vyas, J.M. (2014). Macrophage Cryptococcus interactions: an update. Curr. Fungal Infect. Rep. *8*, 109–115.

Mansour, M.K., Latz, E., Levitz, S.M., and Levitz, S.M. (2006). *Cryptococcus neoformans* glycoantigens are captured by multiple lectin receptors and presented by dendritic cells. J. Immunol. *176*, 3053–3061.

Marr, K.J., Jones, G.J., Zheng, C., Huston, S.M., Timm-Mccann, M., Islam, A., Berenger, B.M., Ma, L.L., Wiseman, J.C.D., and Mody, C.H. (2009). Cryptococcus neoformans Directly Stimulates Perforin Production and Rearms NK Cells for Enhanced Anticryptococcal Microbicidal Activity. Infect. Immun. *77*, 2436–2446.

Martin, M.E., Dieter, J.A., Luo, Z., Baumgarth, N., and Solnick, J. V. (2012). Predicting the Outcome of Infectious Diseases: Variability among Inbred Mice as a New and Powerful Tool for Biomarker Discovery. MBio *3*, e00199-12.

Martinez-Gonzalez, I., Mathä, L., Steer, C.A., Ghaedi, M., Poon, G.F.T., and Takei, F. (2016). Allergen-Experienced Group 2 Innate Lymphoid Cells Acquire Memory-like Properties and Enhance Allergic Lung Inflammation. Immunity *45*, 198–208.

Martinez-Gonzalez, I., Mathä, L., Steer, C.A., and Takei, F. (2017). Immunological Memory of Group 2 Innate Lymphoid Cells. Trends Immunol. *38*, 423–431.

Martinez, F., Helming, L., and Gordon, S. (2009). Alternative Activation of Macrophages: An Immunologic Functional Perspective. Annu. Rev. Immunol. *27*, 451–483.

Mayer-Barber, K., Andrade, B., Oland, S., Amaral, E., Barber, D., Gonzalez, J., Derrick,

S., Shi, R., Kuman, N., Wei, W., et al. (2014). Host-directed therapy of tuberculosis based on interleukin-1 and type I interferon crosstalk. Nature *511*, 99–103.

McBride, W.H., Economou, J.S., Nayersina, R., Comora, S., and Essner, R. (1990). Influences of interleukins 2 and 4 on tumor necrosis factor production by murine mononuclear phagocytes. Cancer Res. *50*, 2949–2952.

McKenzie, A.N., Culpepper, J.A., de Waal Malefyt, R., Brière, F., Punnonen, J., Aversa, G., Sato, A., Dang, W., Cocks, B.G., and Menon, S. (1993). Interleukin 13, a T-cell-derived cytokine that regulates human monocyte and B-cell function. Proc. Natl. Acad. Sci. U. S. A. *90*, 3735–3739.

McQuiston, T.J., and Williamson, P.R. (2012). Paradoxical roles of alveolar macrophages in the host response to Cryptococcus neoformans. J. Infect. Chemother. *18*, 1–9.

Mednick, A.J., Feldmesser, M., Rivera, J., and Casadevall, A. (2003). Neutropenia alters lung cytokine production in mice and reduces their susceptibility to pulmonary cryptococcosis. Eur. J. Immunol. *33*, 1744–1753.

Mence Richaud, C., Chandesris, M.-O., Lanternier, F., Ne Benzaquen-Forner, H., Garcia-Hermoso, D., Picard, C., Catherinot, E., Bougnoux, M.-E., and Lortholary, O. (2014). Case Report: Imported African Histoplasmosis in an Immunocompetent Patient 40 Years after Staying in a Disease-Endemic Area. Am. J. Trop. Med. Hyg. *91*, 1011–1014.

Merle, N.S., Noe, R., Halbwachs-Mecarelli, L., Fremeaux-Bacchi, V., and Roumenina, L.T. (2015). Complement System Part II: Role in Immunity. Front. Immunol. *6*, 257.

Mielke, M.E.A., Niedobitek, G., Stein, H., and Hahn, H. (1989). Acquired resistence to Listeria monocytogenes is mediated by Lyt-2+ T cells indepependelty of the influx of monocytes into granulomatous lesion. J. Exp. Med. *170*, 589-594.

Mills, C.D., Kincaid, K., Alt, J.M., Heilman, M.J., and Hill, A.M. (2000). M-1/M-2 macrophages and the Th1/Th2 paradigm. J. Immunol. *164*, 6166–6173.

Mirkovich, A.M., Galelli, A., Allison, A.C., and Modabber, F.Z. (1986). Increased myelopoiesis during Leishmania major infection in mice: generation of “safe targets”, a possible way to evade the effector immune mechanism.Clin. Exp. Immunol. *64*, 1-7.

Mitchell, B.Y.G.F., and Miller, J.F.A.P. (1968). Cell to cell interaction in the immune response. II. The source of hemolysin- forming cells in irradiated mice given bone marrow and thymus or thoracic duct lymphocytes. J. Exp. Med. *128*, 821–837.

Mitchell, D.H., Sorrell, T.C., Allworth, A.M., Heath, C.H., McGregor, A.R., Papanaoum, K., Richards, M.J., and Gottlieb, T. (1995). Cryptococcal disease of the

CNS in immunocompetent hosts: Influence of cryptococcal variety on clinical manifestations and outcome. Clin. Infect. Dis. *20*, 611–616.

Mitchell, R.E., Hassan, M., Burton, B.R., Britton, G., Hill, E. V., Verhagen, J., and Wraith, D.C. (2017). IL-4 enhances IL-10 production in Th1 cells: implications for Th1 and Th2 regulation. Sci. Rep. *7*, 11315.

Mora, D.J., Fortunato, L.R., Andrade-Silva, L.E., Ferreira-Paim, K., Rocha, I.H., Vasconcelos, R.R., Silva-Teixeira, D.N., Nascentes, G.A.N., and Silva-Vergara, M.L. (2015). Cytokine Profiles at Admission Can Be Related to Outcome in AIDS Patients with Cryptococcal Meningitis. PLoS One *10*, e0120297.

Morrow, C.A., Lee, I.R., Chow, E.W.L., Ormerod, K.L., Goldinger, A., Byrnes, E.J., Nielsen, K., Heitman, J., Schirra, H.J., and Fraser, J.A. (2012). A unique chromosomal rearrangement in the Cryptococcus neoformans var. grubii type strain enhances key phenotypes associated with virulence. MBio *3*, e00310-11.

Moscoso, M., García, E., and López, R. (2006). Biofilm Formation by Streptococcus pneumoniae: Role of Choline, Extracellular DNA, and Capsular Polysaccharide in Microbial Accretion. J. Bacteriol. *188*, 7785–7795.

Mosmann, T.R., and Coffman, R.L. (1989). TH1 and TH2 cells: different patterns of lymphokine secretion lead to different functional properties. Annu. Rev. Immunol. *7*, 145–173.

Mosmann, T.R., Cherwinski, H., Bond, M.W., Giedlin, M.A., and Coffman, R.L. (1986). Two types of murine helper T cell clone. I. Definition according to profiles of lymphokine activities and secreted proteins. J. Immunol. *136*, 2348–2357.

Moulder, J.W. (1985). Comparative biology of intracellular parasitism. Microbiol. Rev. *49*, 298–337.

Mueller, D.L., Jenkins, M.K., and Schwartz, R.H. (1989). Clonal expansion versus functional clonal inactivation: A costimulatory signalling pathway determines the outcome of T cell antigen receptor occupancy. Annu. Rev. Immunol. *7*, 445–480.

Mukherjee, S., Feldmesser, M., and Casadevall, A. (1996). J774 Murine Macrophage-like Cell Interactions with Cryptococcus neoformans in the Presence and Absence of Opsonins. J. Infect. Dis. *173*, 1222–1231.

Müller, U., Stenzel, W., Kohler, G., Werner, C., Polte, T., Hansen, G., Schutze, N., Straubinger, R.K., Blessing, M., McKenzie, A.N., et al. (2007). IL-13 induces disease-promoting type 2 cytokines, alternatively activated macrophages and allergic inflammation during pulmonary infection of mice with Cryptococcus neoformans. J. Immunol. *179*, 5367–5377.

Müller, U., Stenzel, W., Piehler, D., Grahnert, A., Protschka, M., Köhler, G., Frey, O.,

Held, J., Richter, T., Eschke, M., et al. (2013). Abrogation of IL-4 receptor-α-dependent alternatively activated macrophages is sufficient to confer resistance against pulmonary cryptococcosis despite an ongoing Th2 response. Int. Immunol. *25*, 459–470.

Murdock, B.J., Huffnagle, G.B., Olszewski, M.A., and Osterholzer, J.J. (2014). Interleukin-17A Enhances Host Defense against Cryptococcal Lung Infection through Effects Mediated by Leukocyte Recruitment, Activation, and Gamma Interferon Production. Infect. Immun. *82*, 937–948.

Murphy, J.W., Zhou, A., and Wong, S.C. (1997). Direct Interactions of Human Natural Killer Cells with Cryptococcus neoformans Inhibit Granulocyte-Macrophage Colony-Stimulating Factor and Tumor Necrosis Factor Alpha Production. Infect. Immun. *65*, 4564–4571.

Murphy, K., Weaver, C., and Weaver, C. (2016). Janeway's Immunobiology (9th edition. | New York, NY : Garland Science/Taylor & Francis: Garland Science).

Nakamura, K., Miyazato, A., Xiao, G., Hatta, M., Aoyagi, T., Shiratori, K., Takeda, K., Akira, S., Saijo, S., Iwakura, Y., et al. (2008). Deoxynucleic Acids from Cryptococcus neoformans Activate Myeloid Dendritic Cells via a TLR9-Dependent Pathway. J. Immunol. *180*, 4067–4074.

Naranbhai, V., Chang, C.C., Durgiah, R., Omarjee, S., Lim, A., Moosa, M.-Y.S., Elliot, J.H., Ndung'u, T., Lewin, S.R., French, M.A., et al. (2014). Compartmentalisation of innate immune responses in the central nervous system during cryptococcal meningitis/HIV co-infection. AIDS *28*, 657–666.

Nathan, C., Murray, H., Wiebe, M., and Rubin, B. (1983). Identification of interferon-gamma as the lymphokine that activates human macrophage oxidative metabolism and antimicrobial activity. J. Exp. Med. *158*, 670–689.

Nau, G.J., Richmond, J.F.L., Schlesinger, A., Jennings, E.G., Lander, E.S., and Young, R.A. (2002). Human macrophage activation programs induced by bacterial pathogens. Proc. Natl. Acad. Sci. U. S. A. *99*, 1503–1508.

Neal, L.M., Xing, E., Xu, J., Kolbe, J.L., Osterholzer, J.J., Segal, B.M., Williamson, P.R., and Olszewski, M.A. (2017). CD4+ T cells orchestrate lethal immune pathology despite fungal clearance during Cryptococcus neoformans meningoencephalitis. MBio2 *8*, e01415-17.

Nealson, K.H., Platt, T., and Hastings, J.W. (1970). Cellular control of the synthesis and activity of the bacterial luminescent system. J. Bacteriol. *104*, 313–322.

Ngamskulrungroj, P., Chang, Y., Sionov, E., and Kwon-Chunga, K.J. (2012). The primary target organ of cryptococcus gattii is different from that of cryptococcus neoformans in a murine model. MBio *3*, 1–9.

Nicholson, S.E., Keating, N., and Belz, G.T. (2019). Natural killer cells and anti-tumor immunity. Mol. Immunol. *110*, 40–47.

Nolan, S.J., Fu, M.S., Coppens, I., and Casadevall, A. (2017). Lipids Affect the Cryptococcus neoformans-Macrophage Interaction and Promote Nonlytic Exocytosis. Infect. Immun. *85*, e00564-17.

Norris, P., Reichart, D., Dumlao, D., Glass, C., and Dennis, E. (2011). Specificity of eicosanoid production depends on the TLR-4-stimulated macrophage phenotype. J. Leukoc. Biol. *90*, 563–574.

Noverr, M., Phare, S., Toews, G., Coffey, M., and Huffnagle, G. (2001). Pathogenic yeasts Cryptococcus neoformans and Candida albicans produce immunomodulatory prostaglandins. Infect. Immun. *69*, 2957–2963.

Noverr, M., Toews, G., and Huffnagle, G. (2002). Production of prostaglandins and leukotrienes by pathogenic fungi. Infect. Immun. *70*, 400–402.

Noverr, M., Cox, G., Perfect, J., and Huffnagle, G. (2003a). Role of PLB1 in pulmonary inflammation and cryptococcal eicosanoid production. Infect. Immun. *71*, 1538–1547.

Noverr, M., Erb-Downward, J., and Huffnagle, G. (2003b). Production of eicosanoids and other oxylipins by pathogenic eukaryotic microbes. Clin. Microbiol. Rev. *16*, 517–533.

Novick, R.P. (2003). Autoinduction and signal transduction in the regulation of staphylococcal virulence. Mol. Microbiol. *48*, 1429–1449.

Novick, R.P., and Geisinger, E. (2008). Quorum Sensing in Staphylococci. Annu. Rev. Genet. *42*, 541–564.

Numazaki, K., Asanuma, H., and Chiba, S. (1995). Latent infection and reactivation of human cytomegalovirus. Serodiagn. Immunother. Infect. Dis. *7*, 70–74.

O'loughlin, C.T., Miller, L.C., Siryaporn, A., Drescher, K., Semmelhack, M.F., and Bassler, B.L. (2013). A quorum-sensing inhibitor blocks Pseudomonas aeruginosa virulence and biofilm formation. Proc. Natl. Acad. Sci. *110*, 17981–17986.

Okagaki, L.H., and Nielsen, K. (2012). Titan Cells Confer Protection from Phagocytosis in Cryptococcus neoformans Infections. Eukaryot. Cell *11*, 820–826.

Oliveira, D.L., Freire-de-Lima, C.G., Nosanchuk, J.D., Casadevall, A., Rodrigues, M.L., and Nimrichter, L. (2010). Extracellular vesicles from Cryptococcus neoformans modulate macrophage functions. Infect. Immun. *78*, 1601–1609.

Osterholzer, J.J., Curtis, J.L., Polak, T., Ames, T., Chen, G.-H., McDonald, R., Huffnagle, G.B., and Toews, G.B. (2008). CCR2 mediates conventional dendritic cell recruitment and the formation of bronchovascular mononuclear cell infiltrates in the lungs of mice infected with Cryptococcus neoformans. J. Immunol. *181*, 610–620.

Osterholzer, J.J., Milam, J.E., Chen, G.H., Toews, G.B., Huffnagle, G.B., and Olszewski, M.A. (2009). Role of dendritic cells and alveolar macrophages in regulating early host defense against pulmonary infection with Cryptococcus neoformans. Infect. Immun. *77*, 3749–3755.

Pagán, A.J., and Ramakrishnan, L. (2018). The Formation and Function of Granulomas. Annu. Rev. Immunol. *36*, 639–665.

Pappas, P., Perfect, J.R., Cloud, G. a, Larsen, R. a, Pankey, G. a, Lancaster, D.J., Henderson, H., Kauffman, C. a, Haas, D.W., Saccente, M., et al. (2001). Cryptococcosis in human immunodeficiency virus-negative patients in the era of effective azole therapy. Clin. Infect. Dis. *33*, 690–699.

Pappas, P., Alexander, B., Andes, D., Hadley, S., Kauffman, C., Freifeld, A., Anaissie, E.J., Brumble, L.M., Herwaldt, L., Ito, J., et al. (2010). Invasive fungal infections among organ transplant recipients: results of the Transplant-Associated Infection Surveillance Network (TRANSNET). Clin. Infect. Dis. *50*, 1101–1111.

Park, B.J., Wannemuehler, K.A., Marston, B.J., Govender, N., Pappas, P., and Chiller, T.M. (2009). Estimation of the current global burden of cryptococcal meningitis among persons living with HIV/AIDS. Aids *23*, 525–530.

Park, G.Y., Hu, N., Wang, X., Sadikot, R.T., Yull, F.E., Joo, M., Stokes Peebles, R., Blackwell, T.S., and Christman, J.W. (2007). Conditional regulation of cyclooxygenase-2 in tracheobronchial epithelial cells modulates pulmonary immunity. Clin. Exp. Immunol. *150*, 245–254.

Pascual, G., Fong, A.L., Ogawa, S., Gamliel, A., Li, A.C., Perissi, V., Rose, D.W., Willson, T.M., Rosenfeld, M.G., and Glass, C.K. (2005). A SUMOylation-dependent pathway mediates transrepression of inflammatory response genes by PPAR-γ. Nature *437*, 759–763.

Passador, L., Cook, J., Gambello, M., Rust, L., and Iglewski, B. (1993). Expression of Pseudomonas aeruginosa virulence genes requires cell-to-cell communication. Science (80-.). *260*, 1127–1130.

Pearson, J.P., Gray, K.M., Passador, L., Tucker, K.D., Eberhard, A., Iglewski, B.H., and Greenberg, E.P. (1994). Structure of the autoinducer required for expression of Pseudomonas aeruginosa virulence genes. Proc. Natl. Acad. Sci. USA *91*, 197–201.

Pearson, J.P., Passador, L., Iglewski, B.H., and Greenberg, E.P. (1995). A second N-

acylhomoserine lactone signal produced by Pseudomonas aeruginosa. Proc. Natl. Acad. Sci. U. S. A. *92*, 1490–1494.

Phaiboun, A., Zhang, Y., Park, B., and Kim, M. (2015). Survival Kinetics of Starving Bacteria Is Biphasic and Density-Dependent. PLOS Comput. Biol. *11*, e1004198.

Phillips, P., Galanis, E., Macdougall, L., Chong, M.Y., Balshaw, R., Cook, V.J., Bowie, W., Steiner, T., Hoang, L., Morshed, M., et al. (2015). Longitudinal clinical findings and outcome among patients with cryptococcus gattii infection in British Columbia. Clin. Infect. Dis. *60*, 1368–1376.

Piehler, D., Stenzel, W., Grahnert, A., Held, J., Richter, L., Köhler, G., Richter, T., Eschke, M., Alber, G., and Müller, U. (2011). Eosinophils Contribute to IL-4 Production and Shape the T-Helper Cytokine Profile and Inflammatory Response in Pulmonary Cryptococcosis. Am. J. Pathol. *179*, 733–744.

Pietrella, D., Corbucci, C., Perito, S., Bistoni, G., and Vecchiarelli, A. (2005). Mannoproteins from Cryptococcus neoformans Promote Dendritic Cell Maturation and Activation. Infect. Immun. *73*, 820–827.

Pollitt, E.J.G., West, S.A., Crusz, S.A., Burton-Chellew, M.N., and Diggle, S.P. (2014). Cooperation, Quorum Sensing, and Evolution of Virulence in Staphylococcus aureus. Infect. Immun. *82*, 1045–1051.

Pollmächer, J., Timme, S., Schuster, S., Brakhage, A.A., Zipfel, P.F., and Figge, M.T. (2016). Deciphering the Counterplay of Aspergillus fumigatus Infection and Host Inflammation by Evolutionary Games on Graphs. Sci. Rep. *6*, 27807.

Porcheray, F., Viaud, S., Rimaniol, A.C., Léone, C., Samah, B., Dereuddre-Bosquet, N., Dormont, D., and Gras, G. (2005). Macrophage activation switching: An asset for the resolution of inflammation. Clin. Exp. Immunol. *142*, 481–489.

Portnoy, D.A., Chakraborty, T., Goebel, W., and Cossart, P. (1992). Molecular Determinants of Listeria monocytogenes Pathogenesis. Infect. Immun. *60*, 1263–1267.

Prajsnar, T.K., Hamilton, R., Garcia-Lara, J., McVicker, G., Williams, A., Boots, M., Foster, S.J., and Renshaw, S.A. (2012). A privileged intraphagocyte niche is responsible for disseminated infection of *Staphylococcus aureus* in a zebrafish model. Cell. Microbiol. *14*, 1600–1619.

Preston, J.A., Bewley, M.A., Marriott, H.M., McGarry Houghton, A., Mohasin, M., Jubrail, J., Morris, L., Stephenson, Y.L., Cross, S., Greaves, D.R., et al. (2019). Alveolar macrophage apoptosis-associated bacterial killing helps prevent murine pneumonia. Am. J. Respir. Crit. Care Med. *200*, 84–97.

Price, J.V., and Vance, R.E. (2014). The Macrophage Paradox. Immunity *41*, 685–693.

Qiang, L., Wang, J., Zhang, Y., Ge, P., Chai, Q., Li, B., Shi, Y., Zhang, L., Gao, G.F., and Liu, C.H. (2019). Mycobacterium tuberculosis Mce2E suppresses the macrophage innate immune response and promotes epithelial cell proliferation. Cell. Mol. Immunol. *16*, 380–391.

Qiu, Y., Davis, M., Dayrit, J., Hadd, Z., Meister, D., Osterholzer, J., Williamson, P., and Olszewski, M. (2012a). Immune Modulation Mediated by Cryptococcal Laccase Promotes Pulmonary Growth and Brain Dissemination of Virulent Cryptococcus neoformans in Mice. PLoS One *7*, e47853.

Qiu, Y., Zeltzer, S., Zhang, Y., Wang, F., Chen, G.-H., Dayrit, J., Murdock, B.J., Bhan, U., Toews, G.B., Osterholzer, J.J., et al. (2012b). Infection of Robust Immunity to Cryptococcal TLR9 Signaling Promotes the Development Early Induction of CCL7 Downstream of. J. Immunol. *188*, 3940–3948.

Qureshi, A., Subathra, M., Grey, A., Schey, K., Del Poeta, M., and Luberto, C. (2010). Role of Sphingomyelin Synthase in Controlling the Antimicrobial Activity of Neutrophils against Cryptococcus neoformans. PLoS One *5*, e15587.

Qureshi, A., Grey, A., Rose, K.L., Schey, K.L., and Del Poeta, M. (2011). Cryptococcus Neoformans Modulates Extracellular Killing by Neutrophils. Front. Microbiol. *2*, 193.

Rabadi, S.M., Sanchez, B.C., Varanat, M., Ma, Z., Catlett, S. V, Andres Melendez, J., Malik, M., and Shekhar Bakshi, C. (2015). Antioxidant Defenses of Francisella tularensis Modulate Macrophage Function and Production of Proinflammatory Cytokines. J. Biol. Chem. *291*, 5009–5021.

Rajakariar, R., Hilliard, M., Lawrence, T., Trivedi, S., Colville-Nash, P., Bellingan, G., Fitzgerald, D., Yaqoob, M., and Gilroy, D. (2007). Hematopoietic prostaglandin D2 synthase controls the onset and resolution of acute inflammation through PGD2 and 15-deoxyΔ12–14 PGJ2. Proc. Natl. Acad. Sci. *104*, 20979–20984.

Rajaram, M.V.S., Brooks, M.N., Morris, J.D., Torrelles, J.B., Azad, A.K., and Schlesinger, L.S. (2010). Mycobacterium tuberculosis activates human macrophage peroxisome proliferator-activated receptor gamma linking mannose receptor recognition to regulation of immune responses. J. Immunol. *185*, 929–942.

Rajasingham, R., Smith, R.M., Park, B.J., Jarvis, J.N., Govender, N.P., Chiller, T.M., Denning, D.W., Loyse, A., and Boulware, D.R. (2017). Global burden of disease of HIV-associated cryptococcal meningitis: An updated analysis. Lancet Infect. Dis. *3099*, 1–9.

Ramage, G., Saville, S.P., Wickes, B.L., and López-Ribot, J.L. (2002). Inhibition of Candida albicans biofilm formation by farnesol, a quorum-sensing molecule. Appl. Environ. Microbiol. *68*, 5459–5463.

Raphael, I., Nalawade, S., Eagar, T.N., and Forsthuber, T.G. (2015). T cell subsets and

their signature cytokines in autoimmune and inflammatory diseases. Cytokine *74*, 5–17.

Rappleye, C.A., Eissenberg, L.G., and Goldman, W.E. (2007). Histoplasma capsulatum alpha-(1,3)-glucan blocks innate immune recognition by the beta-glucan receptor. Proc. Natl. Acad. Sci. *104*, 1366–1370.

Rath, M., Müller, I., Kropf, P., Closs, E.I., and Munder, M. (2014). Metabolism via Arginase or Nitric Oxide Synthase: Two Competing Arginine Pathways in Macrophages. Front. Immunol. *5*, 532.

Redfield, R. (2002). Is quorum sensing a side effect of diffusion sensing? Trends Microbiol. *10*, 365–370.

Retini, C., Vecchiarelli, A., Monari, C., Tascini, C., Bistoni, F., and Kozel, T.R. (1996). Capsular polysaccharide of Cryptococcus neoformans induces proinflammatory cytokine release by human neutrophils. Infect. Immun. *64*, 2897–2903.

Ricciotti, E., and Fitzgerald, G.A. (2011). Prostaglandins and inflammation. Arterioscler. Thromb. Vasc. Biol. *31*, 986–1000.

Rice, K.C., Mann, E.E., Endres, J.L., Weiss, E.C., Cassat, J.E., Smeltzer, M.S., Bayles, K.W., and Greenberg, E.P. (2007). The cidA murein hydrolase regulator contributes to DNA release and biofilm development in Staphylococcus aureus. Proc. Natl. Acad. Sci. *104*, 8113–8118.

Ricote, M., Li, A., Willson, T., Kelly, C., and Glass, C. (1998). The peroxisome proliferator-activated receptor-γ is a negative regulator of macrophage activation. Nature *391*, 79–82.

Rooijakkers, S.H.M., van Wamel, W.J.B., Ruyken, M., van Kessel, K.P.M., and van Strijp, J.A.G. (2005). Anti-opsonic properties of staphylokinase. Microbes Infect. *7*, 476–484.

Rose-John, S. (2012). IL-6 trans-signaling via the soluble IL-6 receptor: importance for the pro-inflammatory activities of IL-6. Int. J. Biol. Sci. *8*, 1237–1247.

Rose-John, S., and Heinrich, P.C. (1994). Soluble receptors for cytokines and growth factors: generation and biological function. Biochem. J. *300*, 281–290.

Rouzer, C., Kingsley, P., Wang, H., Zhang, H., Morrow, J., Dey, S., and Marnett, L. (2004). Cyclooxygenase-1-dependent prostaglandin synthesis modulates tumor necrosis factor-α secretion in lipopolysaccharide-challenged murine resident peritoneal. J. Biol. Chem. *279*, 34256–34268.

Rudkin, F.M., Bain, J.M., Walls, C., Lewis, L.E., Gow, N.A.R., and Erwig, L.P. (2013). Altered Dynamics of Candida albicans Phagocytosis by Macrophages and PMNs

When Both Phagocyte Subsets Are Present. MBio *4*, e00810-13.

Rudman, J., Evans, R.J., and Johnston, S.A. (2019). Are macrophages the heroes or villains during cryptococcosis? Fungal Genet. Biol. *132*, 103261.

Ryan, E., Pollack, S., Murant, T., Bernstein, S., Felgar, R., and Phipps, R. (2005). Inhibitors Attenuate Antibody Production Cyclooxygenase-2 and Cyclooxygenase Activated Human B Lymphocytes Express. J. Immunol. *174*, 2619–2626.

Sabiiti, W., Robertson, E., Beale, M.A., Johnston, S.A., Brouwer, A.E., Loyse, A., Jarvis, J., Gilbert, A.S., Fisher, M.C., Harrison, T.S., et al. (2014). Efficient phagocytosis and laccase activity affect the outcome of HIV-associated cryptococcosis. J. Clin. Invest. *124*, 2000–2008.

Sadikot, R.T., Zeng, H., Azim, A.C., Joo, M., Dey, S.K., Breyer, R.M., Peebles, R.S., Blackwell, T.S., and Christman, J.W. (2007). Bacterial clearance of Pseudomonas aeruginosa is enhanced by the inhibition of COX-2. Eur. J. Immunol. *37*, 1001–1009.

Santangelo, R., Zoellner, H., Sorrell, T., Wilson, C., Donald, C., Djordjevic, J., Shounan, Y., and Wright, L. (2004). Role of Extracellular Phospholipases and Mononuclear Phagocytes in Dissemination of Cryptococcosis in a Murine Model. Infect. Immun. *72*, 2229–2239.

Santiago-Tirado, F.H., Onken, M.D., Cooper, J.A., Klein, R.S., and Doering, T.L. (2017). Trojan Horse Transit Contributes to Blood-Brain Barrier Crossing of a Eukaryotic Pathogen. MBio *8*, e02183-16.

Schmalzle, S.A., Buchwald, U.K., Gilliam, B.L., and Riedel, D.J. (2016). Cryptococcus neoformans infection in malignancy. Mycoses *59*, 542–552.

Seider, K., Brunke, S., Schild, L., Jablonowski, N., Wilson, D., Majer, O., Barz, D., Haas, A., Kuchler, K., Schaller, M., et al. (2011). The Facultative Intracellular Pathogen Candida glabrata Subverts Macrophage Cytokine Production and Phagolysosome Maturation. J. Immunol. *187*, 3072–3086.

Shalek, A.K., Satija, R., Shuga, J., Trombetta, J.J., Gennert, D., Lu, D., Chen, P., Gertner, R.S., Gaublomme, J.T., Yosef, N., et al. (2014). Single-cell RNA-seq reveals dynamic paracrine control of cellular variation. Nature *510*, 363–369.

Shao, X., Mednick, A., and Alvarez, M. (2005). An innate immune system cell is a major determinant of species-related susceptibility differences to fungal pneumonia. J. Immunol. *175*, 3244–3241.

Sheldon, K.E., Shandilya, H., Kepka-Lenhart, D., Poljakovic, M., Ghosh, A., Morris, S.M., and Jr. (2013). Shaping the murine macrophage phenotype: IL-4 and cyclic AMP synergistically activate the arginase I promoter. J. Immunol. *191*, 2290–2298.

Shen, L., and Liu, Y. (2015). Prostaglandin E2 blockade enhances the pulmonary anti-Cryptococcus neoformans immune reaction via the induction of TLR-4. Int. Immunopharmacol. *28*, 376–381.

Sheppe, A.E.F., Kummari, E., Walker, A., Richards, A., Hui, W.W., Lee, J.H., Mangum, L., Borazjani, A., Ross, M.K., and Edelmann, M.J. (2018). PGE2 Augments Inflammasome Activation and M1 Polarization in Macrophages Infected With Salmonella Typhimurium and Yersinia enterocolitica. Front. Microbiol. *9*, 2447.

Shi, M., Li, S.S., Zheng, C., Jones, G.J., Kim, K.S., Zhou, H., Kubes, P., and Mody, C.H. (2010). Real-time imaging of trapping and urease-dependent transmigration of Cryptococcus neoformans in mouse brain. J. Clin. Invest. *120*, 1683–1693.

Shibuya, K., Coulson, W.F., and Naoe, S. (2002). Histopathology of Deep-Seated Fungal Infections and Detailed Examination of Granulomatous Response Against Cryptococci in Patients with Acquired Immunodeficiency Syndrome. Jpn. J. Med. Mycol *43*, 143–151.

Shibuya, K., Hirata, A., Omuta, J., Sugamata, M., Katori, S., Saito, N., Murata, N., Morita, A., Takahashi, K., Hasegawa, C., et al. (2005). Granuloma and cryptococcosis. J. Infect. Chemother. *11*, 115–122.

Shirey, K.A., Cole, L.E., Keegan, A.D., and Vogel, S.N. (2008). Francisella tularensis live vaccine strain induces macrophage alternative activation as a survival mechanism. J. Immunol. *181*, 4159–4167.

Shirtliff, M.E., Krom, B.P., Meijering, R.A.M., Peters, B.M., Zhu, J., Scheper, M.A., Harris, M.L., and Jabra-Rizk, M.A. (2009). Farnesol-induced apoptosis in Candida albicans. Antimicrob. Agents Chemother. *53*, 2392–2401.

Shompole, S., Henon, K.T., Liou, L.E., Dziewanowska, K., Bohach, G.A., and Bayles, K.W. (2003). Biphasic intracellular expression of Staphylococcus aureus virulence factors and evidence for Agr-mediated diffusion sensing. Mol. Microbiol. *49*, 919–927.

Siafakas, A.R., Sorrell, T.C., Wright, L.C., Wilson, C., Larsen, M., Boadle, R., Williamson, P.R., and Djordjevic, J.T. (2007). Cell wall-linked cryptococcal phospholipase B1 is a source of secreted enzyme and a determinant of cell wall integrity. J. Biol. Chem. *282*, 37508–37514.

Siddiqui, A.A., Shattock, R.J., and Harrison, T.S. (2006). Role of capsule and interleukin-6 in long-term immune control of Cryptococcus neoformans infection by specifically activated human peripheral blood mononuclear cells. Infect. Immun. *74*, 5302–5310.

Sigve Havarstein, L., Coomaraswamyt, G., and Morrisont, D.A. (1995). An unmodified heptadecapeptide pheromone induces competence for genetic

transformation in Streptococcus pneumoniae (ABC transporter/bacteriocin/peptide signal/comC gene). PNAS. *92*, 11140-11144.

Silva, M.T. (2012). Classical labeling of bacterial pathogens according to their lifestyle in the host: inconsistencies and alternatives. Front. Microbiol. *3*.

da Silva, M.B., Marques, A.F., Nosanchuk, J.D., Casadevall, A., Travassos, L.R., and Taborda, C.P. (2006). Melanin in the dimorphic fungal pathogen Paracoccidioides brasiliensis: effects on phagocytosis, intracellular resistance and drug susceptibility. Microbes Infect. *8*, 197–205.

Sim, R.B., and Tsiftsoglou, S.A. (2004). Proteases of the complement system. Biochem. Soc. Trans. *32*, 21–27.

Singh, N., Gayowski, T., Wagener, M.M., and Marino, I. (1997). Clinical spectrum of invasive cryptococcosis in liver transplant recipients receiving tacrolimus. Clin. Transplant. *11*, 66–70.

Singh, N., Kumar, R., Chauhan, S.B., Engwerda, C., and Sundar, S. (2018). Peripheral Blood Monocytes With an Antiinflammatory Phenotype Display Limited Phagocytosis and Oxidative Burst in Patients With Visceral Leishmaniasis. J. Infect. Dis. *218*, 1130–1141.

Smith, K.M., Pottage, L., Thomas, E.R., Leishman, A.J., Doig, T.N., Xu, D., Liew, F.Y., and Garside, P. (2000). Th1 and Th2 CD4 + T Cells Provide Help for B Cell Clonal Expansion and Antibody Synthesis in a Similar Manner In Vivo . J. Immunol. *165*, 3136–3144.

Smith, L.M., Dixon, E.F., and May, R.C. (2015). The fungal pathogen Cryptococcus neoformans manipulates macrophage phagosome maturation. Cell. Microbiol. *17*, 702-713.

Smyth, E.M., Grosser, T., Wang, M., Yu, Y., and FitzGerald, G.A. (2009). Prostanoids in health and disease. J. Lipid Res. *Supplement*, S423–S428.

Snijder, B., Sacher, R., Rämö, P., Damm, E.-M., Liberali, P., and Pelkmans, L. (2009). Population context determines cell-to-cell variability in endocytosis and virus infection. Nat. Lett. *461*, 520–523.

Soares, A.M.V.C., Calvi, S.A., Peraçoli, M.T.S., Fernandez, A.C., Dias, L.A., and Dos Anjos, A.R. (2001). Modulatory effect of prostaglandins on human monocyte activation for killing of high- and low-virulence strains of Paracoccidioides brasiliensis. Immunology *102*, 480–485.

Sonnenberg, G.F., and Hepworth, M.R. (2019). Functional interactions between innate lymphoid cells and adaptive immunity. Nat. Rev. Immunol. *19*, 599–613.

Sorrell, T.C., Juillard, P.-G., Djordjevic, J.T., Kaufman-Francis, K., Dietmann, A., Milonig, A., Combes, V., and Grau, G.E.R. (2016). Cryptococcal transmigration across a model brain blood-barrier: evidence of the Trojan horse mechanism and differences between Cryptococcus neoformans var. grubii strain H99 and Cryptococcus gattii strain R265. Microbes Infect. *18*, 57–67.

Spits, H., Artis, D., Colonna, M., Diefenbach, A., Di Santo, J.P., Eberl, G., Koyasu, S., Locksley, R.M., McKenzie, A.N.J., Mebius, R.E., et al. (2013). Innate lymphoid cells — a proposal for uniform nomenclature. Nat. Rev. Immunol. *13*, 145–149.

Squizani, E.D., Oliveira, N.K., Reuwsaat, J.C.V., Marques, B.M., Lopes, W., Gerber, A.L., de Vasconcelos, A.T.R., Lev, S., Djordjevic, J.T., Schrank, A., et al. (2018). Cryptococcal dissemination to the central nervous system requires the vacuolar calcium transporter Pmc1. Cell. Microbiol. *20*, 1–13.

Sreeramkumar, V., Hons, M., Punzón, C., Stein, J. V, Sancho, D., Fresno, M., and Cuesta, N. (2016). Efficient T-cell priming and activation requires signaling through prostaglandin E2 (EP) receptors. Immunol. Cell Biol. *94*, 39–51.

Stafford, J.B., and Marnett, L.J. (2008). Prostaglandin E2 inhibits tumor necrosis factor-alpha RNA through PKA type I. Biochem. Biophys. Res. Commun. *366*, 104–109.

Stano, P., Williams, V., Villani, M., Cymbalyuk, E.S., Qureshi, A., Huang, Y., Morace, G., Luberto, C., Tomlinson, S., and Del Poeta, M. (2009). App1: an antiphagocytic protein that binds to complement receptors 3 and 2. J. Immunol. *182*, 84–91.

Steeb, B., Claudi, B., Burton, N.A., Tienz, P., Schmidt, A., Farhan, H., Mazé, A., and Bumann, D. (2013). Parallel Exploitation of Diverse Host Nutrients Enhances Salmonella Virulence. PLoS Pathog. *9*, e1003301.

Stein, M., Keshav, S., Harris, N., and Gordon, S. (1992). Interleukin 4 potently enhances murine macrophage mannose receptor activity: a marker of alternative immunologic macrophage activation. J. Exp. Med. *176*, 287–292.

Steinmoen, H., Knutsen, E., and Håvarstein, L.S. (2002). Induction of natural competence in Streptococcus pneumoniae triggers lysis and DNA release from a subfraction of the cell population. Proc. Natl. Acad. Sci. U. S. A. *99*, 7681–7686.

Stenzel, W., Müller, U., Köhler, G., Heppner, F.L., Blessing, M., McKenzie, A.N.J., Brombacher, F., and Alber, G. (2009). IL-4/IL-13-Dependent Alternative Activation of Macrophages but Not Microglial Cells Is Associated with Uncontrolled Cerebral Cryptococcosis. Am. J. Pathol. *174*, 486–496.

Stout, R.D., Jiang, C., Matta, B., Tietzel, I., Watkins, S.K., and Suttles, J. (2005). Macrophages Sequentially Change Their Functional Phenotype in Response to Changes in Microenvironmental Influences. J. Immunol. *175*, 342–349.

Sturgill-Koszycki, S., Schlesinger, P., Chakraborty, P., Haddix, P., Collins, H., Fok, A., Allen, R., Gluck, S., Heuser, J., and Russell, D. (1994). Lack of acidification in Mycobacterium phagosomes produced by exclusion of the vesicular proton-ATPase. Science. *263*, 678–671.

Sugimoto, Y., and Narumiya, S. (2007). Prostaglandin E Receptors. J. Biol. Chem. *282*, 11613–11617.

Surette, M.G., and Bassler, B.L. (1998). Quorum sensing in Escherichia coli and Salmonella typhimurium. Proc. Natl. Acad. Sci. *95*, 7046–7050.

Swain, S.L., Weinberg, A.D., English, M., and Huston, G. (1990). IL-4 directs the development of Th2-like helper effectors. J. Immunol. *145*, 3796–3806.

Taborda, C.P., and Casadevall, A. (2002). CR3 (CD11b/CD18) and CR4 (CD11c/CD18) Are Involved in Complement-Independent Antibody-Mediated Phagocytosis of Cryptococcus neoformans. Immunity *16*, 791–802.

Tada, T., Takemori, T., Okumura, K., Nonaka, M., and Tokuhisa, T. (1978). Two distinct types of helper T cells involved in the secondary antibody response: independent and synergistic effects of Ia- and Ia+ helper T cells. J. Exp. Med. *147*, 446–458.

Tadrowski, A.C., Evans, M.R., and Waclaw, B. (2018). Phenotypic Switching Can Speed up Microbial Evolution. Sci. Rep. *8*, 8941.

Takano, S., Pawlowska, B.J., Gudelj, I., Yomo, T., and Tsuru, S. (2017). Density-Dependent Recycling Promotes the Long-Term Survival of Bacterial Populations during Periods of Starvation. MBio *8*, e02336-16.

Tanaka, M., Ishii, K., Nakamura, Y., Miyazato, A., Maki, A., Abe, Y., Miyasaka, T., Yamamoto, H., Akahori, Y., Fue, M., et al. (2012). Toll-Like Receptor 9-Dependent Activation of Bone Marrow-Derived Dendritic Cells by URA5 DNA from Cryptococcus neoformans. Infect. Immun. *80*, 778–786.

Telepnev, M., Golovliov, I., Grundstrom, T., Tarnvik, A., and Sjostedt, A. (2003). Francisella tularensis inhibits Toll-like receptor-mediated activation of intracellular signalling and secretion of TNF-alpha and IL-1 from murine macrophages. Cell. Microbiol. *5*, 41–51.

Tenor, J.L., Oehlers, S.H., Yang, J.L., Tobin, D.M., and Perfect, J.R. (2015). Live imaging of host-parasite interactions in a zebrafish infection model reveals cryptococcal determinants of virulence and central nervous system invasion. MBio *6*, 1–11.

Thron, A., and Wiethtilter, H. (1982). Cerebral Candidiasis: Studies in a Case of Brain

Abscess and Granuloma Due to Candida albicans. Neuroradiology. *23*, 223-225.

Thywißen, A., Heinekamp, T., Dahse, H.-M., Schmaler-Ripcke, J., Nietzsche, S., Zipfel, P.F., and Brakhage, A.A. (2011). Conidial Dihydroxynaphthalene Melanin of the Human Pathogenic Fungus Aspergillus fumigatus Interferes with the Host Endocytosis Pathway. Front. Microbiol. *2*, 96.

Tian, X., He, G.-J., Hu, P., Chen, L., Tao, C., Cui, Y.-L., Shen, L., Ke, W., Xu, H., Zhao, Y., et al. (2018). Cryptococcus neoformans sexual reproduction is controlled by a quorum sensing peptide. Nat. Microbiol. *3*, 698–707.

Tiefenbach, J., Moll, P.R., Nelson, M.R., Hu, C., Baev, L., Kislinger, T., and Krause, H.M. (2010). A Live Zebrafish-Based Screening System for Human Nuclear Receptor Ligand and Cofactor Discovery. PLoS One *5*, e9797.

Tierney, L., Linde, J., Müller, S., Brunke, S., Molina, J.C., Hube, B., Schöck, U., Guthke, R., and Kuchler, K. (2012). An Interspecies Regulatory Network Inferred from Simultaneous RNA-seq of Candida albicans Invading Innate Immune Cells. Front. Microbiol. *3*, 85.

Tilley, A.E., Walters, M.S., Shaykhiev, R., and Crystal, R.G. (2015). Cilia dysfunction in lung disease. Annu. Rev. Physiol. *77*, 379–406.

Tomasz, A. (1965). Control of the Competent State in Pneumococcus by a Hormone-Like Cell Product: An Example for a New Type of Regulatory Mechanism in Bacteria. Nature *208*, 155–159.

Tomasz, A., and Hotchkiss, R.D. (1964). Regulation of the transformability of pneumococcal cultures by macromolecular cell products. PNAS. *51*, 480-487.

Tsitsigiannis, D.I., Bok, J.-W., Andes, D., Fog Nielsen, K., Frisvad, J.C., and Keller, N.P. (2005). Aspergillus Cyclooxygenase-Like Enzymes Are Associated with Prostaglandin Production and Virulence. Infect. Immun. *73*, 4548–4559.

Tucker, S.C., and Casadevall, A. (2002). Replication of Cryptococcus neoformans in macrophages is accompanied by phagosomal permeabilization and accumulation of vesicles containing polysaccharide in the cytoplasm. Proc. Natl. Acad. Sci. U. S. A. *99*, 3165–3170.

Uicker, W., Doyle, H. a, McCracken, J.P., Langlois, M., and Buchanan, K.L. (2005). Cytokine and chemokine expression in the central nervous system associated with protective cell-mediated immunity against Cryptococcus neoformans. Med. Mycol. *43*, 27–38.

Uicker, W., McCracken, J., and Buchanan, K. (2006). Role of CD4+ T cells in a protective immune response against Cryptococcus neoformans in the central nervous system. Med. Mycol. *44*, 1-11.

Uribe-Querol, E., and Rosales, C. (2017). Control of Phagocytosis by Microbial Pathogens. Front. Immunol. *8*, 1368.

Vane, J. (1971). Inhibition of Prostaglandin Synthesis as a Mechanism of Action for Aspirin-like Drugs. Nat. New Biol. *231*, 232–235.

Van Dyke, M.C.C., Chaturvedi, A.K., Hardison, S.E., Leopold Wager, C.M., Castro-Lopez, N., Hole, C.R., Wozniak, K.L., and Wormley Jr., F.L. (2017). Induction of Broad-Spectrum Protective Immunity against Disparate Cryptococcus Serotypes. Front. Immunol. *8*, 1359.

Vanherp, L., Ristani, A., Poelmans, J., Hillen, A., Lagrou, K., Janbon, G., Brock, M., Himmelreich, U., and Vande Velde, G. (2019). Sensitive bioluminescence imaging of fungal dissemination to the brain in mouse models of cryptococcosis. Dis. Model. Mech. *12*, dmm039123.

Vecchiarelli, A., Pietrella, D., Lupo, P., Bistoni, F., McFadden, D.C., and Casadevall, A. (2003). The polysaccharide capsule of *Cryptococcus neoformans* interferes with human dendritic cell maturation and activation. J. Leukoc. Biol. *74*, 370–378.

Velagapudi, R., Hsueh, Y.-P., Geunes-Boyer, S., Wright, J.R., and Heitman, J. (2009). Spores as infectious propagules of Cryptococcus neoformans. Infect. Immun. *77*, 4345–4355.

Vidotto, V., Sinicco, A., Fraia, D., Cardaropoli, S., Aoki, S., and Ito-Kuwa, S. (1996). Phospholipase activity in Cryptococcus neoformans. Mycopathologia *136*, 119–123.

Vikström, E., Magnusson, K.-E., and Pivoriūnas, A. (2005). The Pseudomonas aeruginosa quorum-sensing molecule N-(3-oxododecanoyl)-l-homoserine lactone stimulates phagocytic activity in human macrophages through the p38 MAPK pathway. Microbes Infect. *7*, 1512–1518.

Vilani-Moreno, F.R., Silva, L.M., and Opromolla, D.V.A. (2004). Evaluation of the phagocytic activity of peripheral blood monocytes of patients with Jorge Lobo's disease. Rev. Soc. Bras. Med. Trop. *37*, 165–168.

Voelz, K., and May, R. (2010). Cryptococcal interactions with the host immune system. Eukaryot. Cell *9*, 835–846.

Voelz, K., Lammas, D.A., and May, R. (2009). Cytokine signaling regulates the outcome of intracellular macrophage parasitism by Cryptococcus neoformans. Infect. Immun. *77*, 3450–3457.

Voelz, K., Johnston, S.A., Rutherford, J.C., May, R., and Perfect, J. (2010). Automated Analysis of Cryptococcal Macrophage Parasitism Using GFP-Tagged Cryptococci. PLoS One *5*, e15968.

Voelz, K., Johnston, S.A., Smith, L.M., Hall, R.A., Idnurm, A., and May, R.C. (2014). 'Division of labour' in response to host oxidative burst drives a fatal Cryptococcus gattii outbreak. Nat. Commun. *5*, 5194.

Volkman, H.E., Clay, H., Beery, D., Chang, J.C.W., Sherman, D.R., and Ramakrishnan, L. (2004). Tuberculous Granuloma Formation Is Enhanced by a Mycobacterium Virulence Determinant. PLoS Biol. *2*, e367.

Wagner, C., Zimmermann, S., Brenner-Weiss, G., Hug, F., Prior, B., Obst, U., and Hänsch, G.M. (2007). The quorum-sensing molecule N-3-oxododecanoyl homoserine lactone (3OC12-HSL) enhances the host defence by activating human polymorphonuclear neutrophils (PMN). Anal. Bioanal. Chem. *387*, 481–487.

Walker, J.A., Barlow, J.L., and McKenzie, A.N.J. (2013). Innate lymphoid cells — how did we miss them? Nat. Rev. Immunol. *13*, 75–87.

Walsh, N.M., Botts, M.R., McDermott, A.J., Ortiz, S.C., Wüthrich, M., Klein, B., and Hull, C.M. (2019). Infectious particle identity determines dissemination and disease outcome for the inhaled human fungal pathogen Cryptococcus. PLOS Pathog. *15*, e1007777.

Wang, Y., Aisen, P., and Casadevall, A. (1995). Cryptococcus neoformans Melanin and Virulence: Mechanism of Action. Infect. Immun. *63*, 3131-3136.

Wang, Z.A., Li, L.X., and Doering, T.L. (2018). Unraveling synthesis of the cryptococcal cell wall and capsule. Glycobiology *28*, 719–730.

Waterman, S.R., Hacham, M., Hu, G., Zhu, X., Park, Y.-D., Shin, S., Panepinto, J., Valyi-Nagy, T., Beam, C., Husain, S., et al. (2007). Role of a CUF1/CTR4 copper regulatory axis in the virulence of Cryptococcus neoformans. J. Clin. Invest. *117*, 794–802.

Werz, O., Gerstmeier, J., Libreros, S., De La Rosa, X., Werner, M., Norris, P.C., Chiang, N., and Serhan, C.N. (2018). Human macrophages differentially produce specific resolvin or leukotriene signals that depend on bacterial pathogenicity. Nat. Commun. *9*, 1–12.

Westwater, C., Balish, E., and Schofield, D.A. (2005). Candida albicans-conditioned medium protects yeast cells from oxidative stress: a possible link between quorum sensing and oxidative stress resistance. Eukaryot. Cell *4*, 1654–1661.

Wheeler, R.T., Kombe, D., Agarwala, S.D., and Fink, G.R. (2008). Dynamic, Morphotype-Specific Candida albicans β-Glucan Exposure during Infection and Drug Treatment. PLoS Pathog. *4*, e1000227.

Whiteley, M., Lee, K.M., and Greenberg, E.P. (1999). Identification of genes controlled by quorum sensing in Pseudomonas aeruginosa. Proc. Natl. Acad. Sci. U.

S. A. *96*, 13904–13909.

Wiesner, D.L., Specht, C.A., Lee, C.K., Smith, K.D., Mukaremera, L., Lee, S.T., Lee, C.G., Elias, J.A., Nielsen, J.N., Boulware, D.R., et al. (2015). Chitin Recognition via Chitotriosidase Promotes Pathologic Type-2 Helper T Cell Responses to Cryptococcal Infection. PLOS Pathog. *11*, e1004701.

Williams, V., and Del Poeta, M. (2011). Role of glucose in the expression of Cryptococcus neoformans antiphagocytic protein 1, App1. Eukaryot. Cell *10*, 293–301.

Williamson, P., Wakamatsu, K., and Ito, S. (1998). Melanin biosynthesis in Cryptococcus neoformans. J. Bacteriol. *180*, 1570–1572.

Wozniak, K.L. (2018). Interactions of Cryptococcus with Dendritic Cells. J. Fungi *4*.

Wozniak, K.L., and Levitz, S.M. (2008). Cryptococcus neoformans enters the endolysosomal pathway of dendritic cells and Is killed by lysosomal components. Infect. Immun. *76*, 4764–4771.

Wozniak, K., Ravi, S., Macias, S., Young, M.L., Olszewski, M.A., Steele, C., and Wormley, F. (2009). Insights into the Mechanisms of Protective Immunity against Cryptococcus neoformans Infection Using a Mouse Model of Pulmonary Cryptococcosis. PLoS One *4*, e6854.

Wozniak, K., Kolls, J.K., and Wormley, F. (2012). Depletion of neutrophils in a protective model of pulmonary cryptococcosis results in increased IL-17A production by gamma/delta T cells. BMC Immunol. *13*, 65.

Wozniak, K.L., Vyas, J.M., and Levitz, S.M. (2006). In Vivo Role of Dendritic Cells in a Murine Model of Pulmonary Cryptococcosis. Infect. Immun. *74*, 3817–3824.

Wright, A., and Douglas, S.R. (1903). An Experimental Investigation of the Role of the Blood Fluids in Phagocytosis. Proc. R. Soc. *72*, 357–370.

Yao, C., Sakata, D., Esaki, Y., Li, Y., Matsuoka, T., Kuroiwa, K., Sugimoto, Y., and Narumiya, S. (2009). Prostaglandin E2–EP4 signaling promotes immune inflammation through TH1 cell differentiation and TH17 cell expansion. Nat. Med. *15*, 633–640.

Yao, H.-W., Ling, P., Tung, Y.-Y., Hsu, S.-M., and Chen, S.-H. (2014). In vivo reactivation of latent herpes simplex virus 1 in mice can occur in the brain before occurring in the trigeminal ganglion. J. Virol. *88*, 11264–11270.

Yauch, L.E., Lam, J.S., and Levitz, S.M. (2006). Direct Inhibition of T-Cell Responses by the Cryptococcus Capsular Polysaccharide Glucuronoxylomannan. PLoS Pathog. *2*, e120.

Yu, L.-H., Wei, X., Ma, M., Chen, X.-J., and Xu, S.-B. (2012). Possible Inhibitory Molecular Mechanism of Farnesol on the Development of Fluconazole Resistance in Candida albicans Biofilm. Antimicrob. Agents Chemother. *56*, 770–775.

Zaragoza, O., Chrisman, C.J., Castelli, M.V., Frases, S., Cuenca-Estrella, M., Luis Rodríguez-Tudela, J., and Casadevall, A. (2008). Capsule enlargement in Cryptococcus neoformans confers resistance to oxidative stress suggesting a mechanism for intracellular survival. Cell. Microbiol. *10*, 2043–2057.

Zaragoza, O., Rodrigues, M.L., De Jesus, M., Frases, S., Dadachova, E., and Casadevall, A. (2009). Chapter 4 The Capsule of the Fungal Pathogen Cryptococcus neoformans. Adv. Appl. Microbiol. *68*, 133–216.

Zaragoza, O., García-Rodas, R., Nosanchuk, J.D., Cuenca-Estrella, M., Rodríguez-Tudela, J.L., and Casadevall, A. (2010). Fungal Cell Gigantism during Mammalian Infection. PLoS Pathog. *6*, e1000945.

Zhang, T., Kawakami, K., Qureshi, M.H., Okamura, H., Kurimoto, M., and Saito, A. (1997). Interleukin-12 (IL-12) and IL-18 Synergistically Induce the Fungicidal Activity of Murine Peritoneal Exudate Cells against Cryptococcus neoformans through Production of Gamma Interferon by Natural Killer Cells. Infect. Immun. *65*, 3594-3599.

Zhang, Y., Wang, F., Tompkins, K.C., McNamara, A., Jain, A. V, Moore, B.B., Toews, G.B., Huffnagle, G.B., and Olszewski, M.A. (2009). Robust Th1 and Th17 Immunity Supports Pulmonary Clearance but Cannot Prevent Systemic Dissemination of Highly Virulent Cryptococcus neoformans H99. Am. J. Pathol. *175*, 2489–2500.

Zhang, Y., Wang, F., Bhan, U., Huffnagle, G.B., Toews, G.B., Standiford, T.J., and Olszewski, M.A. (2010). TLR9 Signaling Is Required for Generation of the Adaptive Immune Protection in Cryptococcus neoformans-Infected Lungs. Am. J. Pathol. *177*, 754–765.

Zhou, X., and Ballou, E.R. (2018). The Cryptococcus neoformans Titan Cell: From In Vivo Phenomenon to In Vitro Model. Curr. Clin. Microbiol. Reports *5*, 252–260.

Zhu, J., and Mekalanos, J.J. (2003). Quorum Sensing-Dependent Biofilms Enhance Colonization in Vibrio cholerae. Dev. Cell *5*, 647–656.

Zimmermann, S., Wagner, C., Müller, W., Brenner-Weiss, G., Hug, F., Prior, B., Obst, U., and Hänsch, G.M. (2006). Induction of Neutrophil Chemotaxis by the Quorum-Sensing Molecule N-(3-Oxododecanoyl)-L-Homoserine Lactone. Infect. Immun. *74*, 5687–5692.